The Spatio-temporal Organization of DNA-repair: A live cell study

De organisatie van DNA herstel in ruimte en tijd:
een studie in levende cellen

Proefschrift

ter verkrijging van de graad van doctor
aan de Erasmus Universiteit Rotterdam
op gezag van de
Rector Magnificus
Prof.dr.ir. J. H. van Bemmel
en volgens besluit van het College voor Promoties

De openbare verdediging zal plaatsvinden op
woensdag 7 mei 2003 om 15:30 uur

door

Deborah Hoogstraten
Geboren te Stadskanaal

Promotiecommissie

Promotor:	Prof.dr. J.H.J. Hoeijmakers
Overige leden:	Prof.dr. B. Oostra Dr. J. Trapman Prof.dr. A.A. van Zeeland
Copromotor:	Dr. W. Vermeulen

Dit proefschrift kwam tot stand binnen de vakgroep Celbiologie en Genetica van de faculteit der Geneeskunde en Gezondheidswetenschappen van de Erasmus Universiteit Rotterdam. De vakgroep maakt deel uit van het Medisch Genetisch Centrum Zuid-West Nederland. Het onderzoek is financieel ondersteund door de Nederlandse Organisatie voor Wetenschappelijk Onderzoek (NWO).

Voor mijn ouders

Voor Jan

Contents

List of abbreviations

ATP	adenosine triphosphate
AR	androgen receptor
BER	base excision repair
CAK	cyclin-activating kinase complex
CDK7	cyclin-dependent kinase 7
CEN2	centrin 2/ caltractin 1
CSA/CSB	Cockayne syndrome A/B protein
CPD	cyclobutane pyrimidine dimer
CTD	C-terminal domain of the large subunit of RNA polymerase 2
ds/ssDNA	double stranded/single stranded DNA
DNA	deoxyribonucleic acid
DRB	5,6-dichloro-1β-D-ribofuranosyl benzimidazole
ER	estrogen receptor
ERCC1	human excision repair cross complementing gene 1
FLIP	fluorescence loss in photobleaching
FRAP	fluorescence recovery after photobleaching
FRAP-FIM	FRAP for immobilization measurements
FRP	fluorescence ratio profile
GFP	green fluorescent protein
GG-NER	global genome NER
HA	histidine- hemagglutinin
hHR23B	human homolog of *S.cerevisiae* repair protein RAD23B
HR	homologous recombination
kDa	kilodalton
MAT1	menage-à-trios 1
MEF	mouse embryonic fibroblast
m/rRNA	messenger/ribosomal ribonucleic acid
MMR	mismatch repair
NER	nucleotide excision repair
NHEJ	non-homologous end-joining
PCNA	proliferating cell nuclear factor
Pol δ/ε	polymerase δ/ε
(6-4) PP	(6-4) pyrimidine –pyrimidone photoproduct
PRR	post-replication repair
RAD	radiation sensitive
RAR	retinoic acid receptor
RNAP1	RNA polymerase I
RNAP2	RNA polymerase II
RPA	replication factor A
TC-NER	transcription-coupled NER
TFIIH	transcription factor IIH
TTD	trichothiodystrophy
UDS	unscheduled DNA synthesis
(UV)DDB	(UV- light) DNA damage binding protein
XAB2	XPA binding protein 2
XPA to –G	xeroderma pigmentosum group A to –G protein

Chapter 1

General introduction and aim of the thesis

General introduction and aim of the thesis

1.1 Nucleotide excision repair

DNA, the carrier of genetic information, is continuously challenged. It is under attack of numerous environmental agents, including UV-light, ionizing radiation and chemicals, and genotoxic compounds derived from endogenous sources during common metabolic processes [1]. An intrinsic network of DNA repair mechanisms and cell cycle checkpoints safeguards the integrity of DNA [2]. Various repair pathways exist that can counteract the deleterious effects of DNA injuries. Accumulation of DNA damages can induce permanent changes in the DNA or cell death, which might lead to cancer and aging respectively [2, 3]. One of the most versatile repair mechanisms is nucleotide excision repair (NER) that can remove a variety of helix-distorting injuries from the DNA, including the main UV-light induced lesions. The importance of NER is illustrated by the severe clinical consequences present in the three inherited NER-associated human disorders: xeroderma pigmentosum (XP), Cockayne syndrome (CS) and trichothiodystrophy (TTD) [4]. NER is a multistep process that requires the action of at least 30 polypeptides. Two sub-pathways exist within NER; global genome NER (GG-NER) and transcription coupled NER (TC-NER). These sub-pathways use different modes of lesion detection. In GG-NER a specialized damage-sensing complex, XPC-hHR23B is employed to survey the entire genome for helix-distorting injuries [5]. Within TC-NER, an elongating RNA polymerase II (RNAP2) blocked at a lesion in the transcribed strand, triggers the repair by NER [6]. Subsequent steps of these sub-pathways are identical and include local unwinding of the DNA around the damage, dual incision on both sites of the lesion and mending of the residual single stranded gap [7].

1.2 Transcription factor IIH

The local unwinding within NER is performed by the transcription factor IIH (TFIIH). TFIIH consists of nine subunits, of which five (XPB, p62, p52, p44 and p34) form a tight "core"-complex. The XPD protein is less tightly associated and anchors the ternary cyclin-activating kinase (CAK) complex, consisting of cyclin-dependent kinase 7 (CDK7), MAT1 and cyclinH into the core of TFIIH [8]. Within the complex three enzymatic polypeptides are identified; XPB and XPD are DNA-dependent ATPase/helicases [9-11] and the CDK7 subunit encompasses kinase activity [12].

TFIIH was originally identified as one of the five basal transcription factors essential for RNAP2 transcription [10]. In the initiation reaction, TFIIH is required for the formation of melted regions around the transcription start site and in addition, for promoter escape [13, 14]. CDK7 is able to phosphorylate the carboxy-terminal domain of the largest subunit of the RNAP2 *in vitro*, an essential event in promoter escape [15]. Recently, an additional function for TFIIH was uncovered, the complex was shown to

be required for RNAP1 transcription ([16] and chapter 5). The role of TFIIH within RNAP1 transcription is still unclear, since it does not require the enzymatic properties of the complex. In both GG-NER and TC-NER pathways, TFIIH plays a crucial role. The two ATPase/helicases activities of the XPB and XPD subunits are required for locally opening a 25-30 nt. region of the DNA-duplex around the lesion [17]. The role for CDK7 activity within NER is unclear.

Mutations in *XPB* and *XPD* are associated with two NER related disorders XP combined with CS and TTD, in addition defects in XPD can also lead to classical XP [18]. It was hypothesized that malfunctioning of XPB and XPD may not only affect NER, causing XP and UV-sensitivity. In addition, they might also impair the transcription function of TFIIH. This could account for the additional non-NER related features seen in XP/CS and TTD, like the neurodevelopmental abnormalities [19].

1.3 Aim of the thesis

The aim of the work outlined in this thesis is to gain more insight into the organization, dynamic properties and differential reaction kinetics of NER factors within living mammalian cell nuclei. To accomplish this, we made use of the green fluorescent protein technology to study TFIIH and XPC in living cells. We mainly focused on: (i) nuclear distribution of the multifunctional TFIIH and the GG-NER sensor XPC-hHR23B under various conditions, (ii) dynamic interactions of TFIIH with NER, RNAP1 and RNAP2 transcription, (iii) the understanding of how TFIIH accomplishes its multiple engagements, (iv) the functional requirement for CAK in NER, and (v) involvement of XPC-hHR23B with NER.

In **chapter 2**, the importance of genome stability and the role of the multiple DNA repair pathways in maintenance of the DNA integrity is discussed. In addition, the connection of the repair mechanisms to other DNA transacting pathways and the crosstalk between these processes are described. In **chapter 3**, the various functions of TFIIH are presented. **Chapter 4** focuses on the nuclear organization of DNA transacting processes and the current views on the dynamical aspects of these processes are discussed. The experimental work described in **chapter 5** deals with the nuclear organization and dynamic interplay of TFIIH with NER, RNAP1 and RNAP2 transcription under various conditions. The differential involvement of TFIIH in GG-NER and TC-NER is described in **chapter 6**. In **chapter 7**, the presence of the CAK-complex at TC-NER and GG-NER sites is presented. In addition, the requirement of the CAK-complex for the repair of (6-4)PPs and CPDs is discussed. Moreover, the presence of the CAK complex at NER sites of various XPD and XPB mutant cell lines is outlined. In **chapter 8**, the nuclear organization and dynamics of XPC in the NER process are studied. **Chapter 9** describes the dynamic interaction of the core NER factor, XPA, in NER. The major implications of the experimental work are summarized and discussed in light of the recent literature in **chapter 10**. Also potential future directions of this work are presented.

Chapter 2

Genome stability and

DNA repair mechanisms

Genome stability and DNA repair mechanisms

2.1 Genome stability

Survival of all species depends on the translation of accurate genetic information into functional proteins and in addition, passing on of the correct genetic code to progeny. This requires precise replication of the DNA and distribution of the chromosomes, but also calls for a battery of reliable repair machinery's to correct adventitious damages to the genetic material.

Cellular DNA is susceptible to multiple damage-inducing agents both from within the cell and external sources. Active oxygen species are released into cells during essential metabolic processes and cause oxidative modifications to the DNA, despite the presence of antioxidants. Also spontaneous hydrolysis of nucleotide residues, leaving non-informative abasic sites are not uncommon in the nucleus and need to be dealt with [20]. Furthermore, environmental agents, such as UV-light, ionizing radiation and genotoxic components found in, for instance, cigarette smoke can alter the DNA structure. UV-light induces the dimerization of two adjacent pyrimidines leading to the formation of 6-4 photoproducts ((6-4)PP) or cyclobutane pyrimidine dimers (CPD). Ionizing radiation will generate hydroxyl radicals along the track of the beam yielding in clustered sites of base damages. These damaged bases can result in single stranded breaks and depending on the position of these breaks, in double stranded breaks within the DNA (Fig. 1) [20].

Immediate consequences of injuries to the DNA include the rapid blockage of crucial ongoing DNA-transacting processes, like transcription and replication. Lesions located in the transcribed strand of active genes interfere with elongation of RNA polymerase II transcription. This stalling of the transcription machinery at a damage will inactivate the injured gene and could eventually result in the death of the affected cell [21, 22]. DNA lesions also interfere with DNA replication. The replication machinery can misinterpret the damaged bases during replication and as a result incorporation of an incorrect nucleotide occurs, leading to a mutation in the genetic information. The long-term effects of DNA damages, include mutations or chromosome aberrations, which in time might lead to cancer, inborn diseases or aging [2, 3]. Mutations in proto-onco genes or tumor suppressor genes are considered to underlie the initiation and progression from a normal to a cancer cell. When mutations arise in essential genes of reproductive cells, offspring may inherit a serious disorder. Aging is believed to be caused by the accumulation of mutations in the DNA in time, resulting in a decline of physiological functions of cells. The DNA damage-induced cell death will affect the functioning of specific organs and consequently an organism.

During evolution multiple interwoven DNA repair systems have evolved, which safeguard our genetic material [2]. Mammals have an intrinsic multifaceted DNA network of cell cycle checkpoints and various DNA repair mechanisms. It is known that the *ataxia telangiectasia mutated* gene (*ATM*) plays a crucial role in the initial

phosphorylation of multiple key players of the cell cycle regulation like p53, Mdm2 and Chk2 in response to ionizing radiation. As a result the cell cycle is arrested. Depending on the type of injury induced to the DNA, the cell cycle can be blocked at different checkpoints, that is before replication of the genome (G1-S arrest), during replication (S-arrest) or before segregation into daughter cells (G2-M arrest) [23]. Blockage of the cell cycle provides the cell with the essential time required for the repair of the damages in the DNA and to resume vital processes like transcription. If the damage to the DNA cannot be repaired and might pose a threat for the organism as a whole, a cell may go into programmed cell death [24].

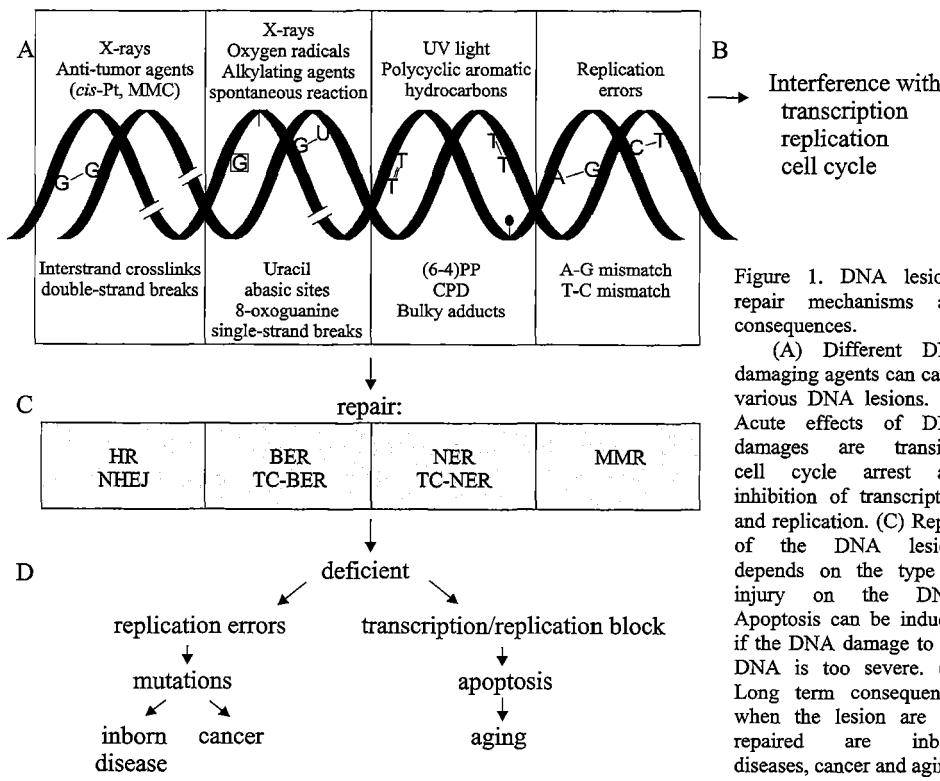

Figure 1. DNA lesions, repair mechanisms and consequences.

(A) Different DNA damaging agents can cause various DNA lesions. (B) Acute effects of DNA damages are transient cell cycle arrest and inhibition of transcription and replication. (C) Repair of the DNA lesions depends on the type of injury on the DNA. Apoptosis can be induced if the DNA damage to the DNA is too severe. (D) Long term consequences when the lesion are not repaired are inborn diseases, cancer and aging.

2.2 DNA repair pathways

In virtually all organisms from the unicellular bacteria to higher eukaryotes, different DNA repair pathways prevent the deleterious consequences of DNA damages [2]. The biological significance of functional DNA damage repair is apparent from the severe clinical features seen in individuals with repair-related disorders, such as xeroderma pigmentosum (XP), Cockayne syndrome (CS), trichothiodystrophy (TTD), ataxia telangiectasia (AT), fanconi anemia (FA), Bloom syndrome (BS) and hereditary nonpolyposis colon cancer (HNPPC) [18, 25, 26]. These patients have a mutation in a DNA repair-associated gene, leading to malfunctioning of a DNA repair pathway. The dysfunctional protein is either involved in the actual repair process or in the regulation of DNA repair. The highly conserved DNA repair pathways are able to remove the vast majority of injuries from the DNA. In mammals multiple partly overlapping DNA repair mechanisms exist, each with their own damage specificity. These repair systems utilize different modes of damages recognition, which in most cases depends on the effect the damage poses on the DNA in terms of helix distortion, obstruction of DNA probing, or blockage of DNA replication or transcription [2].

2.2.1 Nucleotide excision repair

Helix-distorting lesions that interfere with proper base pairing are substrate to nucleotide excision repair (NER) (see box 2 for detailed information, [7, 27]). In mammals, NER is the most important repair pathway to remove the major UV-light induced damages, (6-4)PPs and CPDs. NER comprises the following steps: (i) damage recognition, (ii) open complex formation by melting of the DNA around the lesion and lesion demarcation, (iii) dual incision of the damaged strand on both sides of the lesion, leaving a single stranded gap of 24-32 nucleotides, and (iv) gap-filling by DNA synthesis and ligation. In NER two sub-pathways exist, global genome NER (GG-NER) and transcription-coupled NER (TC-NER), each with a different approach to detect DNA damages. In GG-NER, XPC-hHR23B surveys the entire genome for helix-distorting injuries. In vitro, this heterodimer specifically binds a small bubble structure with or without a damaged base, however, dual incision only takes place when a damage is present in the bubble [28]. This indicates that XPC-hHR23B first binds a helix distortion, after which the presence of an injured base is verified prior to incision. This multistep mechanism of damage recognition for GG-NER ensures a high level of damage discrimination, and prevents illegitimate cutting at non-NER lesions or non-damaged DNA.

Within TC-NER, the actual lesion sensing is performed by an elongating RNAP2 which is blocked at a lesion in the transcribed strand of an active gene [6]. Specific TC-NER factors, such as Cockayne syndrome group A and B proteins (CSA and CSB) and the XPA binding protein 2 (XAB2) are implicated in the processing of the stalled RNAP2, thereby making the lesion accessible for repair. The subsequent steps of GG-NER and TC-NER are identical. After damage recognition, the basal transcription

factor IIH (TFIIH) is recruited to the NER site, where it induces strand separation. XPA and replication protein A (RPA) are required for damage verification, stabilization of the open complex and permit the proper orientation of the two structure-specific endonucleases XPG and ERCC1-XPF for the dual incision [7].

2.2.2 Base excision repair

The base excision repair machinery (BER) mainly removes bases with small chemical alterations, like oxidative and alkylated damages from the DNA [29]. In contrast to NER, no universal recognition mechanism is employed within the BER pathway. A set of distinct DNA glycosylases are utilized, each with a specific affinity for a subset of related lesions, functioning thereby as a sensor for base damages. These glycosylases release the damaged base from the deoxyribose-phosphate chain, resulting in an abasic site. A strand specific incision adjacent to the abasic site opens the deoxyribose-phosphate backbone and the base-less sugar is removed. This is followed by either one-nucleotide gap filling (short patch repair) or a short stretch of DNA next to the damage is removed and subsequently renewed (long patch repair) and sealing of the nick [20].

2.2.3 Mismatch repair

The mismatch repair pathway (MMR) can recognize and repair all base-base mismatches as well as small (up to 5 nucleotides) insertion/deletion mismatches generated by erroneous insertion and slippage respectively of the DNA polymerases during replication [30]. A unique feature within this pathway is the ability to distinguish between the correct nucleotide on the original template strand and the incorrect nucleotide within the newly synthesized strand. This capacity enables this process to remove the erroneous nucleotide and replace it by a correct nucleotide. The MMR pathway involves the following activities: (i) identification of the incorrect nucleotide (ii) degradation of a long stretch of the error containing strand (iii) DNA re-synthesis and ligation of the nick.

2.2.4 Double stranded break repair

Homologous recombination (HR) and non-homologous end-joining (NHEJ) both can repair double stranded DNA breaks [31]. HR requires the presence of homologous DNA (sister chromosome), as the intact DNA strand can be used as a template for DNA repair synthesis, so no genetic information will be lost. This pathway comprises (i) nucleolytic processing of the DNA ends to create single-stranded regions, (ii) after the search for homologous duplex DNA, (iii) DNA strand exchange generates a joint molecule between the homologous damaged and undamaged duplex, (iv) DNA synthesis and ligation, and (v) resolution of the recombination intermediates. The most

prominent repair process in somatic cells to cope with double stranded DNA breaks is NHEJ. This process requires limited processing of the ends, *i.e.* removal or addition of a few base pair. This is followed by joining and ligation of the ends. In contrast to HR, NHEJ does not require homologous DNA to repair the double stranded breaks and is therefore error-prone.

2.2.5 Lesion bypass synthesis

When a damage is not removed by one of the above described repair mechanisms, it will interfere with DNA replication. To avoid replication blockage, lesions in the DNA template can be bypassed by the replication machinery in two different ways: translesion synthesis or recombination-dependent daughter-strand gap repair [2]. Both lesion bypass mechanisms do not repair the lesions, but serve as a temporal resolution for a stalled replicative DNA polymerase. During translesion synthesis, the regular DNA polymerase (polδ/ε or α) is temporarily switched for a specific translesion polymerase (pol ζ-κ), that takes over the synthesis to bypass the injured site. After which the regular DNA polymerase continues the replication process. These translesion polymerases are less accurate than the regular DNA polymerases, rendering translesion synthesis generally an error-prone process. The recombination-dependent daughter-strand gap repair is not well understood. This mechanism is based on re-initiation of replication downstream of the blocking injury. The regular DNA polymerase uses the newly synthesized DNA via recombinational strand exchange as a template, to fill in the gaps. This lesion bypass process is essentially error-free.

2.3 Interwoven DNA-transacting pathways

Previously, the above described repair procedures were perceived as separate pathways. However, recent findings suggest that most of these genome surveillance mechanisms are part of an intrinsic network of damage response processes. In fact, most repair pathways are in part overlapping and connected to other DNA-transacting pathways, often due to the usage of shared factors.

2.3.1 Transcription and Transcription-coupled repair

A prime example of such interwoven nuclear processes, is the tight connection between NER and transcription, which is evident from both the existence of the specialized transcription-coupled NER pathway (TC-NER) and the dual functionality of TFIIH and CSB in the two processes.

2.3.1.1 Dual functionality of TFIIH and CSB

TFIIH was originally identified as a basal transcription factor essential for RNAP2 transcription initiation [32, 33]. The repair function of TFIIH was apparent after the

identification of the two largest subunits of TFIIH, XPB and XPD, as gene products defective in NER-deficient individuals [10, 34]. In both processes the two DNA-dependent ATPase and helicases, XPB and XPD, are required for unwinding of the duplex DNA [13, 35] (see chapter 3 for more details). The TC-NER specific protein CSB, is another factor coupling transcription to NER [36]. This protein is a member of the SWI2/SNF2 family of DNA-dependent ATPases. The SWI2/SNF2-like proteins are implicated in chromatin remodeling during transcription. Purified recombinant CSB is able to remodel chromatin structure in an ATP-dependent fashion [37]. This property of CSB is unique for an NER-factor, since it is the first repair protein found to play a direct role in chromatin remodeling. A possible role for CSB in transcription was suggested, after co-immunoprecipitation studies revealed that a significant fraction of the protein resided in an RNAP2-containing complex and CSB could stimulate the rate of RNAP2 elongation *in vitro* [36, 38]. Very recently, *in vivo* evidence for a direct role of CSB in RNAP2 transcription has been found in live-cell protein dynamic studies (Van den Boom, *et al.*, in prep). CSB was shown to be transiently engaged in RNAP2 transcription elongation. These studies further reveal that this protein is constantly probing the elongation process. After DNA damage induction the CSB protein was bound for a longer period, suggesting that when the RNAP2 is stalled at a lesion CSB could aid in the displacement of the RNAP2 from the damage, and subsequently promote the removal of the damage by recruiting the repair machinery.

2.3.1.2 Transcription-coupled repair

Within TC-NER, UV-induced lesions present in actively transcribed genes are repaired at a faster rate compared to those present in inactive DNA [6]. This increased repair rate of transcribed genes is mainly due to the preferential repair of the transcribed strand, by the TC-NER pathway. The TC-NER pathway is dependent on most NER-factors, except for the XPC-hHR23B heterodimer [5] and the damaged-DNA binding complex (DDB) [39]. Next to RNAP2, additional factors, like CSA, CSB and XAB2 are essential for this TC-NER process [36, 40, 41]. Deficiency in CSA or CSB will lead to the rare clinical disorder Cockayne syndrome. No obvious gene-specific differences are apparent between CSA and CSB patients. Like CSB, also CSA was shown to reside in a multiprotein complex [36]. The CSA protein has been reported to interact with CSB and the p44 subunit of TFIIH *in vitro* [40]. XAB2 was shown to associate with XPA, CSA, CSB and RNAP2. In addition, microinjection of antibodies against this protein inhibited transcription and TC-NER *in vivo*. The role of CSA and XAB2 within TC-NER is unknown, however, the sequence characteristics of both proteins are consistent with a structural rather a catalytic function.

Le Page and others have found evidence that the functional link with transcription might not be unique for NER but also exists for BER [42, 43] (see box 2 for additional information). Recently, it was shown that cells from CS-B patients were not only defective in removing the NER-specific CPD lesions from the transcribed strand, but

also oxidated nucleotides were not eliminated [44]. Similarly, also TFIIH and XPG were shown to be required for the repair of these BER-lesions from actively transcribed genes [42]. A provocative idea was put forward that a general TCR pathway might exist that requires factors like CSB, TFIIH, XPG and possibly others for the initial step of displacing the stalled RNAP2 from the lesion, thereby making the damage accessible for the repair machinery, after which the damage can be repaired by one of the specialized repair pathways or by the NER core part that might process the lesion independent from its nature [42, 43]. This general TCR pathway would take care of any type of transcription-stalling injury. In this way, the blockage of transcription can quickly be overcome by recruiting the appropriate repair pathway and moreover, it ensures efficient progression of transcription elongation.

The TC-NER factors, CSA and XAB2, are likely to play a role in this general TCR pathway [45]. But also several other nuclear proteins, such as BRCA1, p53 and the MMR-associated hMSH2, seem to be required for TCR [42, 46, 47]. However, the role for these factors in TCR is not yet understood.

2.3.2 Replication and repair

The functional connection between transcription and repair is not exceptional, since also replication is linked to genome surveillance processes like MMR, lesion bypass synthesis, and homologous recombination. The error-rate of the three already high fidelity mammalian DNA polymerases, polδ/ε and pol α, in DNA replication is reduced by a factor 2 to 3 as a result of the correcting activities of the MMR pathway [30]. Due to the ability of the MMR pathway to distinguish between the newly synthesized strand and the original template strand, the erroneous nucleotide can be replaced by a correct one. The process of MMR is directly coupled and in most cases strictly dependent on replication.

2.3.3 Non-homologous end joining and homologous recombination

Non-homologous end joining (NHEJ) is a multifunctional pathway, since it is not only used to repair double stranded breaks generated by exogenous DNA-damaging agents, but is also required to process the double stranded break intermediates that are generated during V(D)J recombination, a natural process involved in generation of unique mature Ig heavy chains genes in B-cells [31]. In both processes DNA-ends are joined together, with no or limited sequence homology requirements. The NHEJ pathway shares one important heterotrimeric complex with the other more elaborate double stranded break repair process, HR. A clear function for this Nijmegen breakage syndrome 1 (NBS1), Rad50 and meiotic recombination 11 (Mre11) containing complex has not yet been identified. The architecture of the Rad50-Mre11 complex obtained by scanning force microscopy suggests a role for this complex in tethering of the two DNA ends of the same sister chromatid in both HR and NHEJ [48]. In addition, during

HR it could provide a tether between a broken end and the intact sister chromatid. Due to the exonuclease activity of the Mre11 protein, this complex is also implicated in the nucleolytic processing of the broken ends of DNA into 3'-end single stranded DNA extensions in both recombination repair processes [49].

2.4 Multifunctional DNA trans-acting factors

The basis for a connection between vital nuclear mechanisms is usually sharing of essential components. A range of proteins and proteincomplexes are known that execute similar activities in multiple processes, such as replication protein A (RPA), proliferating cell nuclear antigen (PCNA), p53 and TFIIH.

2.4.1 Replication protein A

The heterotrimeric RPA is a single stranded binding protein complex essential for DNA replication [50] and several repair pathways, like HR [51], NER [52] and possibly BER [53]. The involvement of RPA within these repair processes is coordinated by a series of RPA-ssDNA and RPA-protein interactions. These interactions are thought to assist in the assembly of repair complexes. A specific domain of the RPA32 subunit was shown to interact with the HR-associated factor Rad52, the NER-related component XPA and the major uracil-DNA glycosylase UNG2 involved in BER [54]. RPA is involved in both early and later steps of DNA repair. In the early steps, RPA binds to the ssDNA opposite or adjacent to the DNA damage and subsequently interacts with other repair factors. In a later stage, RPA is known to be required for DNA polymerization, where it is associated with the repair DNA polymerases [55]. RPA is thought to play an architectural role in the early stages of NER, since it binds with high affinity to ssDNA in a defined orientation with respect to its 5' and 3' polarity [56]. The positioning of XPA and the two endonucleases XPG and ERCC1/XPF within the repair complex are facilitated by direct protein-protein interactions with RPA [57]. It is suggested that during progression of the NER process the RPA32 domain is involved in a "handing-off" mechanism, where binding of RPA32 to XPA is replaced by its binding to ERCC1/XPF. In later stages of the NER reaction RPA might substitute its interaction with the endonuclease for one with DNA polymerase δ/ε to complete the repair process [54]. RPA32 might thus serve as an anchor and exchange point for various NER factors. Moreover, since RPA32 similarly interacts with XPA, Rad52 and UNG2, the interaction of RPA32 with the NER, HR and BER machinery are mutually exclusive and thus, competitive. This exclusion property of RPA32 interaction, where only one of the repair components is able to bind to it, might provide a mechanistic basis for the decision of a specific repair pathway, but this will also be determined by the previous repair events [54].

2.4.2 Proliferating cell nuclear antigen

Another multifunctional protein is PCNA. It is involved in DNA replication, various repair pathways, cell cycle arrest and chromatin assembly coupled to DNA synthesis. PCNA is essential for the following repair pathways: NER, BER, MMR, error-free recombination-dependent daughter-strand gap repair and error-prone translesion synthesis [58, 59]. PCNA assembles into a trimeric ring that encircles the DNA. The PCNA clamp can slide freely along the duplex. In its replicative function, PCNA directly interacts with various DNA polymerases and as a sliding clamp can stimulate accurate and processive DNA synthesis. In addition, PCNA functions as a platform for accessory factors of replication-linked functions [60]. Similarly to RPA, a hydrophobic pocket formed by PCNA is responsible for the competitive binding of various proteins, like DNA polymerase δ, the cell-cycle inhibitor p21, DNA ligase I and the endonucleases XPG and FEN1 associated with NER and BER respectively [61]. Recently, Hoege and co-workers showed how the error-free and error-prone lesion bypass synthesis processes could be integrated with replication [62]. The activity of PCNA depends on the attachment of proteins, like ubiquitin and the small-ubiquitin-related modifier (SUMO). It was shown that (poly)ubiquitination and SUMO modification of PCNA affects the same amino acid, and are therefore competitive. SUMO conjugation inhibits the role of PCNA in the recombination-dependent daughter-strand gap repair and suggests a function for the SUMO conjugation in normal DNA replication [62]. However, when DNA damage is present, the Rad6-Rad18 complex catalyses the mono-ubiquitination of PCNA. This mono-ubiquitinated PCNA is active in translesion synthesis. In addition, DNA damage induces the transport of proteins into the nucleus, which are capable of extending the ubiquitin-chain (poly-ubiquitination) of PCNA [63]. This polyubiquitinated PCNA is not functional in replication, but is fully functional in the recombination-dependent daughter-strand gap repair pathway [62]. This suggests that the blocked replication machinery may be switched to different modes of repair through distinct modification of PCNA.

2.4.3 p53

The p53 tumor-suppressor gene product is a real centipede, involved in various processes. It is essential for the integration of numerous signals within the cell that control life and death. Its functions include cell-cycle inhibition, induction of apoptosis and maintenance of genome stability (reviewed in [64]). The biological importance of the p53 protein was evident after the finding that the p53 protein is dysfunctional in most human cancers. In about half of these tumors, p53 was inactivated indirectly, whereas in the other cases the inactivation was a direct result of mutations in the *p53* gene [65]. The p53 network is activated when cells are damaged or stressed. The p53 level in the cell is increased due to stabilization of the protein and inhibition of its

degradation [66]. The best-documented biochemical function of p53 is its ability to bind specific sequences in the DNA and activate the transcription of adjacent genes [67]. One of the first effects of increased levels of p53 is blockage of the cell cycle. The p53 protein directly stimulates the expression of p21, an inhibitor of key cell cycle regulators, the cyclin-dependent kinases. The p21 protein inhibits both G1-S and G2-M transitions [64, 68].

Depending on the severity of DNA damage, p53 can either stimulate various repair pathways or inhibit them and induce apoptosis [24]. The involvement of the p53 protein in DNA damage repair is unclear, but it may involve the induction of genes that regulate NER, HR and PRR [64]. Also a direct involvement of the p53 protein in repair has been described. The p53 protein binds with high specificity to a HR-intermediate, the Holiday junction and facilitates its cleavage [69]. Similarly, the p53 protein directly interacts with two proteins, BRCA2 and Rad51, involved in the HR pathway [70, 71]. In addition, p53 also exhibits a 3' to 5' exonuclease activity suggesting a direct role in DNA repair. Direct interactions with p53 have also been reported for the BER specific Ref-1 and DNA polymerase β, where binding of p53 to the latter stabilizes its interaction with an abasic site [72, 73]. Moreover, both GG-NER and TC-NER depend on p53 *in vivo* [74, 75].

The underlying process of DNA repair blockage and apoptosis is not well understood. After a high lethal dose of UV-irradiation, p53 can directly interact with the XPB, XPD and p62 components of TFIIH, an essential factor of NER. These interactions inhibit the helicase activity of TFIIH without affecting its ATPase activity and thereby blocking the function of TFIIH in NER [76-78]. There are several potential mediators of p53-induced apoptosis, including specialized proteins, like Bax and NOXA proteins. These proteins are located in mitochondria and can induce apoptosis when overexpressed [67].

In addition, many different interactions with proteins and genome surveillance mechanisms have been reported. This is just a brief summary of the most relevant ones.

Model for global genome nucleotide excision repair.

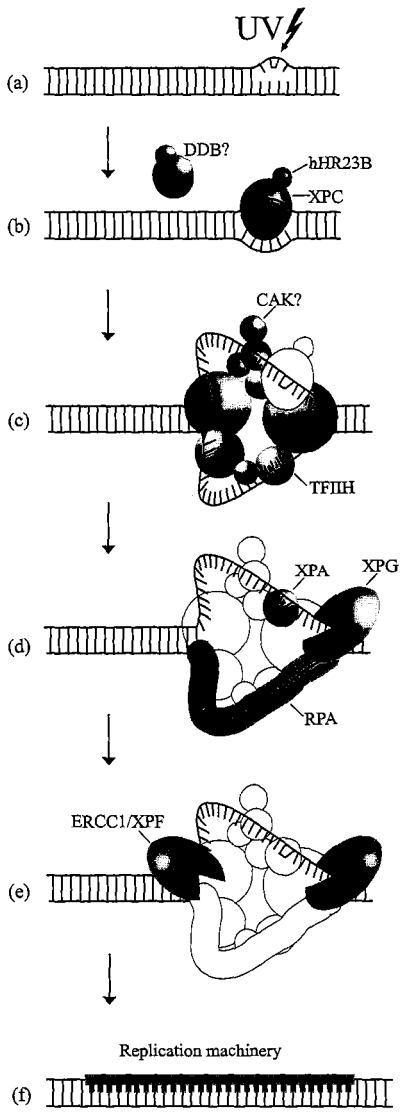

(a) NER mainly removes helix distorting lesions from the genome, including UV-induced (6-4)PPs and CPDs. (b) The initiator of this pathway is XPC, which is stabilized by hHR23B [152]. The XPC-hHR23B is thought to inspect the DNA by constantly probing it for injuries. The precise damage sensing mechanism of XPC-hHR23B is not well understood. This heterodimer has an intrinsic high DNA binding affinity, both for single and double stranded DNA [153, 154]. However, the affinity for damaged DNA and helix-distortions in general is even greater [28, 155]. A possible mechanism for lesion detection by XPC-hHR23B is either scanning the genome for lesions or by constantly binding and releasing DNA, where a lesion is possibly identified by a higher binding capacity of the heterodimer to a helix-distortion. The exact role for the UV-damaged DNA binding protein (DDB) in the NER reaction is not clear. DDB was shown to stimulate an *in vitro* excision reaction for CPD lesion, but hardly for (6-4)PP damages [156]. Since the p127 subunit of DDB binds p300 protein, a histone acetyltransferase, it has been suggested that this complex could play a role in recruiting chromatin remodeling factors to the site of damaged DNA [157]. Thus, XPC-hHR23B might be aided by DDB in the recognition of lesions that are

difficult to detect, such as CPDs. (c) Next, TFIIH is recruited to the site of the damage [93, 94]. The helicase activities of XPB and XPD, imbedded into the TFIIH complex, are required for local unwinding of the DNA around the lesion to create an open complex [17]. Biochemical studies have shown that the ATPase activity of the two helicases might be regulated by the XPC-hHR23B, since the heterodimer is able to e stimulate this activity [98]. Additional roles for TFIIH within the NER process are not excluded, since in *in vitro* assays the TFIIH requirement can not be bypassed by using pre-melted substrates [158]. (d) The assembly of XPG in the incision complex might be mediated by its interaction with TFIIH, as several subunits of the complex interact with the 3' endonuclease [159]. However, XPG might be incorporated prior to or simultaneously with TFIIH. XPG was not essential for open complex formation, however, it could facilitate the process by binding and stabilizing the complex [158]. RPA and XPA are subsequently recruited to the NER site for protection of the non-damaged single stranded region of about 30 nucleotides and lesion demarcation respectively [94]. (e) After open complex formation, ERCC1/XPF is required for the 5' incision. A 24-32 nucleotide patch containing the lesion is removed from the DNA [17]. Kinetic experiments showed that the incisions are closely coupled in time, the 3' incision by XPG precedes the 5' incision by ERCC1/XPF [17, 100]. Moreover, ERCC1/XPF requires the physical presence of XPG in order to perform the nuclease activity [100]. The regulation of the XPG and ERCC1/XPF activity seem to be governed by TFIIH and RPA [57, 160]. RPA appeared to play an important role in proper positioning of both endonucleases. It stimulates the cleavage activity of ERCC1/XPF after binding to the 3' oriented end of RPA, whereas the 5' oriented end will inhibited this activity [57]. TFIIH was shown to be able to inhibit the endonuclease activity of both XPG and ERCC1/XPF *in vitro* [98]. Further evidence for the regulatory role of TFIIH came from the isolation of this complex from cells of XP11BE individuals with a splice mutation at the C-terminus. TFIIH of these individuals was not capable of governing the 5' incision, even though open complex formation was observed [17]. (f) The replication factors, PCNA, RFC, RPA, and DNA polymerase δ/ε fill in the resulting gap of about 30 nucleotides. DNA synthesis is followed by sealing of the nick by ligation of the newly synthesized DNA by DNA ligase I [161].

Transcription-coupled repair

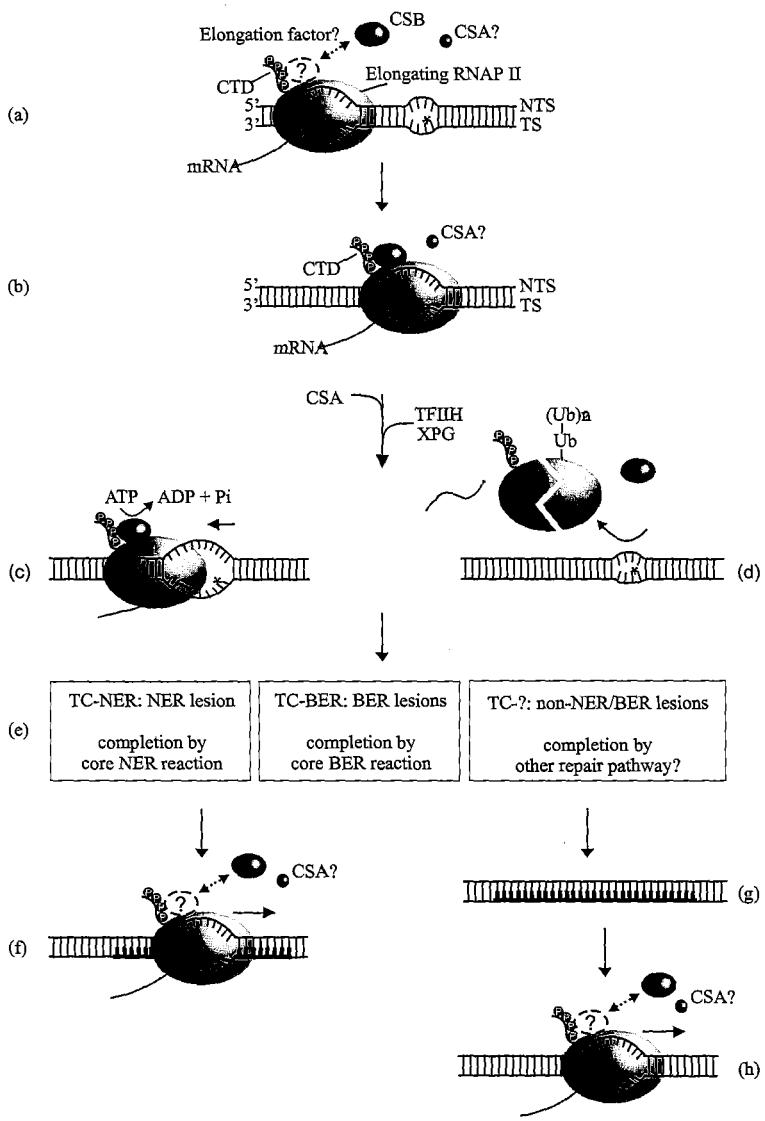

In recent years a model is emerging for a general transcription coupled repair pathway [42, 43]. Evidence for a TC-NER pathway have existed for more than a decade [6], however, the possible existence of a TC-BER pathway utilizing NER-factors like TFIIH and XPG, was suggested recently [42]. It has been extensively shown that mainly UV-induced CPDs are removed from the transcribed strand by the NER pathway that is not dependent on the XPC-hHR23B and DDB heterodimers [6]. Instead, TC-NER dependents on at least three additional proteins, Cockayne syndrome complementation group A (CSA) [40] and CSB [162], and XPA binding protein 2 (XAB2) [41].

(a) During transcription an elongating RNAP2 is stalled at a DNA lesion and is thereby acting as the damage sensor. The roles of CSA and XAB2 are unknown, however, the role of CSB is becoming clearer. It was suggested that CSB is constantly probing the RNAP2 transcription elongation process and when the RNAP2 machinery is stalled at a lesion, the protein becomes more stably bound and could recruit other repair factors (Van den Boom, *et al.*, in prep) (b). (c) In addition, the chromatin remodeling properties of CSB, suggests that this protein might be involved in the conformational changes of chromatin surrounding the stalled RNAP2 [37]. This might allow displacement of the RNAP2 machinery and may facilitate access for other repair factors. The role of TFIIH and XPG in a general TCR pathway suited for all types of transcription blocking injuries is largely unknown [42, 43]. Both factors might be involved in the displacement of the RNAP2 from the lesion, but there is no experimental evidence supporting this hypothesis. (e) Depending on the injury that was inflicted on the DNA, one of the repair pathways is triggered to remove the lesion. (f) This permits DNA repair without aborting transcription.

(d) Alternatively, the largest subunit of the stalled RNAP2 is polyubiquitinated and subsequently degraded [163]. (e and g) Depending on the lesion, repair is completed by NER, BER, or by a possible other repair pathways. (h) The unfinished mRNA is discarded and reinitiation of transcription can occur.

Chapter 3

Transcription factor IIH

Transcription factor IIH

3.1 TFIIH

A prime example of a multifunctional component in the nucleus is the transcription factor IIH (TFIIH, see box 3 for detailed information). It is involved in at least five distinct pathways, RNAP2 transcription initiation [32], transactivation of hormone-responsive genes [79, 80], RNAP1 transcription [16], NER [10] and TCR [42]. TFIIH consists of nine subunits, of which five (XPB, p62, p52, p44 and p34) form a tight "core"-complex. The XPD protein is less tightly associated and serves as a bridge between the core and the ternary cyclin-activating kinase (CAK) complex, consisting of CDK7, MAT1 and cyclinH (Table 1) [8]. The complex encompasses three subunits with enzymatic properties. The two largest subunits, XPB and XPD, are DNA-dependent ATPase and helicases with opposite polarities [9-11]. It was shown that XPD interacts specifically with the p44 subunit and this contact serves a dual function: (i) this interaction results in the stimulation of the 5'→3' helicase activity of XPD and (ii) addition through the interaction between XPD and MAT1 the CAK complex is anchored into the TFIIH complex [81]. Similarly, the p52 subunit is required to incorporate XPB into TFIIH and this binding regulates the function of the XPB helicase [82]. The third subunit of TFIIH with enzymatic properties is the kinase activity of CDK7, as part of the CAK-complex [12]. As well as being part of TFIIH, the CAK-complex is also present in 3-5 fold excess as an autonomous entity in the nucleus. It has been shown that the substrate specificity of CDK7 is altered upon association with TFIIH [83].

Table 1. TFIIH components

Subunit	Complex			Properties
	Holo	Core	CAK	
p34	+	+	-	Zn-finger protein
p44	+	+	-	Zn-finger protein; putative DNA-binding
p52	+	+	-	
p62	+	+	-	
XPB (p89)	+	+	-	DNA-dependent ATPase, 3'-5' helicase
XPD (p80)	+	-	-	DNA-dependent ATPase, 5'-3' helicase
CDK7 (p40)	+	-	+	kinase catalytic subunit
cyclin H (p36)	+	-	+	cyclin-like structure
MAT1 (p32)	+	-	+	RING finger

3.2 Function of TFIIH in RNAP2 transcription

TFIIH was originally identified as one of the five basal transcription factors required for optimal RNA polymerase II (RNAP2) transcription [10, 34]. A considerable amount of biochemical data is published concerning the role of TFIIH within transcription initiation. The helicase activity of the XPB subunit, necessary for opening the promoter distal to the start site, appeared to be absolutely essential for RNAP2 transcription [84]. In contrast to XPB, the helicase activity of XPD is not essential for transcription, but the protein serves rather a structural function [85, 86]. The other enzymatic activity displayed by CDK7, is capable of phosphorylating the tandem heptapeptide repeat of the carboxy-terminal domain (CTD) of the largest subunit of RNAP2 *in vitro*, in the presence of all basal transcription factors. However, CAK is dispensable for transcription initiation *in vitro*, but can stimulate the reaction depending on the nature of the promoter. Hyper-phosphorylation of the CTD is essential for the transition from initiation to elongation of RNAP2 machinery *in vivo* [87]. The requirement for CTD phosphorylation by CDK7 in transcription initiation *in vivo* is still unclear [84]. Recent studies on MAT1$^{-/-}$ mouse cells provided some clues on the requirement for the MAT1 component of CAK in CTD phosphorylation *in vivo*. Even though these cells exhibited a diminished phosphorylation of the CTD domain of RNAP2, a functional de novo transcription could be observed. This suggests that MAT1 is not essential for RNAP2 transcription, but might have a stimulatory function or alternatively, be required for a subset of genes [88].

The importance of CDK7 activity in RNAP2 transcription became obvious when an additional function for TFIIH within this process was identified. TFIIH was shown to be able to phosphorylate and thereby activate the transactivator, retinoic acid receptor [79]. Further studies revealed that CDK7 targets and phosphorylates several transcriptional activators including the nuclear receptors retinoic acid receptor (RAR), the estrogen receptor (ER) and androgen receptor (AR) both *in vitro* and *in vivo* [80, 89]. This indicates that TFIIH also has a regulatory role in the ligand-dependent activation of hormone-responsive genes.

In addition, it was recently shown that via the interaction of gene-specific activators with TFIIH, this complex is involved in another level of transcriptional regulation. A complicated series of interactions of gene-specific regulators with TFIIH, modulates TFIIH's helicase activity and thereby controlling transcript extension during the transition from initiation to promoter escape. The FUSE binding protein (FBP) facilitates transcription of *c-myc* genes until promoter escape via TFIIH interaction. Whereas after initiation, FBP interacting repressor (FIR) binds to XPB of TFIIH to delay promoter escape from the *c-myc* genes [90]. Together these opposing factors regulate *c-myc* expression through their interaction with TFIIH.

3.3 Involvement of TFIIH in RNAP1 transcription

Very recently, it was shown that TFIIH is involved in RNA polymerase I transcription as well. Highly purified TFIIH can stimulate an *in vitro* RNAP1 transcription reaction. In addition, a subpopulation of TFIIH appeared to be associated with RNAP1 and the basal transcription factor TIF-1B during purification of RNAP1 [16]. The mechanism underlying the activation of RNAPI transcription by TFIIH is still unclear. However, it seems different from the role of TFIIH in RNAP2 transcription initiation, since the enzymatic activities of TFIIH are not required, neither the DNA-dependent ATPase and helicase activities nor the kinase activity. The involvement in multiple transcription processes is not unique for TFIIH, given that the TATA-binding protein (TBP) is required for transcription of class I, II and III genes [91]. Recently, it was shown that purified CSB can stimulate RNAP1 transcription *in vitro* [92]. Also, CSB was found in a complex containing RNAP1, TFIIH, and the RNAP1 transcription factor TIF-1B.

3.4 TFIIH activity in NER

TFIIH was shown to be recruited to the repair site after recognition of the lesion by the XPC-hHR23B heterodimer [93, 94]. The main role for TFIIH in GG-NER and TC-NER is to open the DNA template around the lesion. The concerted action of the XPB and XPD helicases are needed for the local unwinding of the DNA duplex [35]. The melted DNA structure is stabilized by XPA and RPA and is necessary for further assembly of the NER pre-incision complex [7]. A number of distinct interactions between TFIIH and various components of the NER machinery have been observed, including XPC [93, 95], XPA [96] and XPG [97]. An additional function for TFIIH within NER might be the regulation of endonucleolytic activity of XPG and ERCC1/XPF [98].

Reversible phosphorylation of NER factors is important for dual incision *in vitro* [99]. However, the kinase involved has not been identified. A likely candidate to catalyze the phosphorylation of NER factors, is the CDK7 subunit of TFIIH, but experimental data so far have not been conclusive about the requirement of this kinase in NER. The CAK complex is not required in an *in vitro* NER reaction [100] and under ATP-regenerating condition can even inhibit the reaction [101]. However, microinjection of antibodies against CDK7 inhibits NER *in vivo* [12].

3.5 Function of TFIIH in TCR

As described previously, TFIIH is implicated in a general TCR pathway [42, 43]. Besides its function in TC-NER, it was shown that TFIIH is required for the removal of BER-lesions from the transcribed strand and not the non-transcribed strand [6, 42]. TFIIH, together with CSA, CSB, XAB2 and XPG have been proposed to be components of a general TCR pathway [43]. These factors may participate in

processing of the stalled RNAP2 making the damage more accessible to repair and subsequent resumption of transcription. This step could involve conformational changes or backward movement of RNAP2, release of RNAP2, or by-pass of the lesion [43].

3.6 TFIIH in cell cycle regulation

Progression through the cell cycle is mediated by the sequential activation of cyclin-dependent kinases (cdk), which phosphorylate substrates critical for advancing the cell cycle. Generally it is believed that the CAK-complex is a regulator of the cell cycle (reviewed in [102]). This CAK-complex is found in 3-5 fold excess over CAK incorporated into TFIIH. Free-CAK is capable of phosphorylating several key components of the cell-cycle regulation machinery, including CDK1-cyclin B (G2-M transition), CDK4-cyclin D (G1-S transition) and CDK2-cyclin A (S-phase) *in vitro* (reviewed in [103]), next to the kinating of the C-terminal domain of the large subunit of RNAP2. Recently, the first *in vivo* data was published, indicating that the CAK complex might be involved in cell cycle regulation. A mouse with loss-of-function allele of *MAT1* was generated to study the function of the ternary complex in cell cycle regulation, *in vivo* [88]. The disruption of the gene lead to embryonic lethality. It was shown that although the $MAT1^{-/-}$ mouse trophoblast cells had entered cycles of endoreduplication, they were nonetheless comprised in some aspects of the endocycle, consisting of only G and S-phase. These $MAT1^{-/-}$ mouse trophoblast cells rapidly displayed an arrest of the endocycle, due to an inability to enter S-phase [88].

No evidence has been found proving that TFIIH in addition to the autonomous CAK-complex is also involved in cell-cycle control. However, it has been shown that the transcriptional activity of TFIIH is regulated by factors that control progression through the cell cycle. Key components of the transcriptional machinery are inhibited when the cell enters into mitosis. CDK7 is a substrate for cdc2/cyclinB during mitosis, the phosphorylation of CDK7 renders the TFIIH inactive in transcription [104]. In addition, the cdk-inhibitor p16/Ink4A can influence the transcriptional activity of TFIIH by binding to the XPB and CDK7 subunits *in vitro* [105]. It is unknown if the cell cycle dependent phosphorylation of CDK7 influences the function of TFIIH in repair.

3.7 Clinical consequence of inherited TFIIH mutations

Mutations in genes coding for TFIIH subunits have only been found in the genes encoding for the XPB and XPD helicases. Malfunctioning of either subunit can lead to the genetic clinical disorders XP, combined XP/CS or TTD. A summary of the clinical symptoms are listed in Table 2 (adapted from [18]). The sun-induced pigmentation abnormalities and skin cancer predisposition seen in XP patients and the UV-sensitivity seen in all three syndromes can be explained on the basis of a NER defect. However, many mutations in *XPB* and *XPD* give rise to additional symptoms associated with CS

or TTD, like severe physical and neurological defects, premature aging and the TTD-associated brittle hair and nails. Given the multifunctionality of TFIIH in NER and transcription, it has been proposed that the non-repair related features found in XP/CS and TTD patient might be related to a transcription defect rather than a repair impairment [19, 106]. Currently, a number of reports have been published supporting this hypothesis. An *in vitro* transcription defect was shown for TFIIH purified from cells of XP-B/CS individuals, likely due to an impeded promoter opening by the decreased helicase activity of the mutated XPB protein [107, 108]. A mouse model of TTD was created by mutating the *XPD* gene at the same position as found in several TTD individuals. The TTD mouse displayed multiple typical features also found in TTD patients, like reduction of hair specific cysteine-rich matrix proteins resulting in brittle hair, growth delay, reduced fertility, UV-sensitivity and skin abnormalities. And indeed, a reduced level of mRNA derived from a skin-specific gene was found in terminally differentiated keratinocytes isolated from the skin of the TTD mouse [109]. Recently, it was shown that some TTD individuals have the β-thalassaemia trait caused by reduced levels of β-globin mRNA, due to a decrease in transcription of the *β-globin* gene [110]. Reduced *in vivo* stability of TFIIH is perhaps the prime cause of the subtle transcription defect observed in some TTD patients. This has been shown for a sub-class of TTD patients (TTD-A) that have no mutation in any of the TFIIH subunits, whereas the total amount of TFIIH appeared severely reduced. This decreased level mainly affects its functioning in repair and mildly in transcription [111]. Reduced levels of TFIIH are common among TTD individuals [112, 113].

Two patients with a mutation in the *XPD* gene are identified having both XP and CS symptoms. Cells of these individuals are much more sensitive to UV-light than XP-D cells, however, the level of repair, measured as unscheduled DNA synthesis (UDS) was 30-40% of that in wild type cells, which is close to the maximum levels found in XP-D cells [114, 115]. These XP/CS cells were unable to restore transcriptional activity within 24 hours after UV-irradiation, in contrast to XP-D cells that revealed a moderate recovery of UV-inhibited RNA synthesis [116]. Despite their extreme UV sensitivity, these cells appeared to incise their DNA as efficiently as wild type cells in response to UV damage [117]. However, in the XP/CS cells the incisions were not introduced at the site of damage, and were not part of the repair process. When irradiated plasmid DNA was introduced into these cells, breakage of the cells' undamaged genomic DNA could be observed. The introduction of breaks into the DNA distant from the damage, might account for the extreme UV sensitivity of XP/CS cells [117]. Apart from their abnormal UV response, XP/CS cells were also shown to be deficient in repair of oxidative damages from transcribed genes of active cells [42]. 8-oxoguanine is normally repaired by the base excision repair (BER).

Several mutations found in the *XPD* gene can lead to a weakened interaction between the gene product and p44, thereby generating an instable incorporation of XPD into TFIIH. This will not only result in a reduced 5'→3' helicase activity of XPD but also a weakened incorporation of the CAK-complex into TFIIH [118]. Mutations

that weaken the p44-XPD interaction have been found in individuals with XP, XP/CS and TTD [108, 118, 119].

Table 2. Clinical features of TFIIH related syndromes

Feature	XP	XP/CS	TTD
Skin abnormalities			
Photosensitivity	++	++	+[a]
Pigmentation abnormalities	++	+	-
Skin cancer	++	+	-
Brittle hair and nails	-	-	+
Ichtyosis	-	-	+
Developmental			
Growth defect	-	+	+
Hypogonadism	-	+	+
Neurologic			
Progressive mental Degeneration	+/-	+	+
Wizened face	-	+	+
Primary defect:			
Neuronal loss	+	-	-
Neurodysmyelination	-	+	+
Aging	-	+	+

[a] Also TTD patients exist without photosensitivity
Table adapted from Bootsma *et al.*, 2001

It was recently shown that the activity of several nuclear hormone receptors (NHR) is reduced in XP cells, carrying a R683W mutation in the *XPD* gene [89]. The retonic acid receptor (RARα) was hypophosphorylated in these XP-D cells, which could be restored by exogenous expression of wild-type XPD protein. Defective RARα function was observed in XP-D (R683W) and TTD (R722W) cell lines. Isolation and characterization of the R683WXPD mutant TFIIH complex indicated that its *in vitro* basal transcription function was not affected. Rather the CAK association to the core of TFIIH was shown to be sensitive to moderate ionic strength treatment. This suggests that due to a weakened CAK incorporation NHR are not phophorylated correctly in these cells. Although these findings offer an explanation for the developmental problems in XP/CS and TTD patients, it should be noted that patients with a R683W mutation in the *XPD* gene display a classical XP phenotype with no additional abnormalities.

3.8 Aging phenotype in TTD mice

Accumulation of DNA damage, was one of the factors postulated to drive the aging process. This hypothesis was supported by recent studies on the TTD mouse [109, 120]. Apart from the recognized TTD features, such as growth and neurological abnormalities and brittle hair and nails, the mice have a range of symptoms associated with premature aging. These include reduced lifespan, cachexia, osteoporosis and osteosclerosis [120]. Interestingly, crossing of the TTD mice with mice carrying an *XPA* null allele enhanced the aging features dramatically, and the double-mutant mice died within three weeks. This suggests that unrepaired lesions of endogenous origin aggravate the TTD symptoms in the double-mutant mice. When the TTD mice were crossed with either CSB or XPC mice, the enhancement of the TTD features was less pronounced, suggesting that the residual repair activity in these mice is sufficient to repair most endogenous damages [120]. The authors proposed that the underlying mechanism for aging in TTD mice is not only the accumulation of damages in time. In addition, the persistence of stalled RNAP2 complexes [43] can cause gene inactivation and trigger apoptosis [21, 22], leading to functional decline and depletion of cell renewal capacity. Thus, both cell death and impaired cell functioning may underlie the aging phenotype in TTD mice.

Five functions of TFIIH

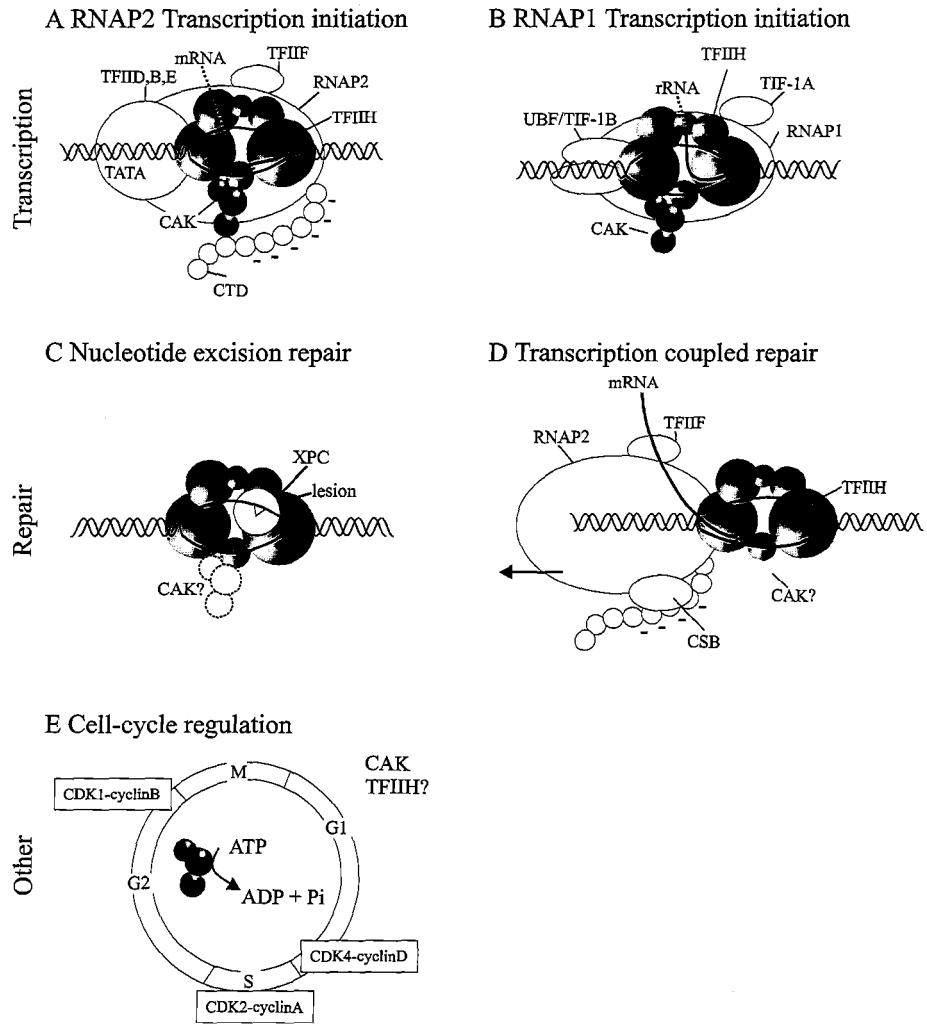

(A) TFIIH is one of the five basal transcription factors required for proper RNAP2 transcription initiation of class II genes [164]. Formation of the pre-initiation complex (PIC), starts by binding of TFIID to the TATA-element [165], after which TFIIB will bind a small sequence located upstream from the TATA box [166]. TFIIF conducts the binding of RNAP2 to the PIC and TFIIE can bind (reviewed in [164]). Subsequently, TFIIH is recruited to the PIC by TFIIE [167] and an open-complex is formed by melting the DNA helix around the transcription site [168]. *In vitro* and *in vivo* studies with active-site mutants of XPB and XPD, revealed that the enzymatic activity of XPB is required for transcription initiation, whereas XPD is only structurally needed [84, 86]. TFIIH is also required for maintaining the open complex during the synthesis of the initial phosphodiester bonds of the nascent mRNA [169] and for promoter clearance [170, 171]. A second important event in the transition from initiation to elongation is the phosphorylation of the C-terminal domain (CTD) of the largest subunit of RNAP2 (reviewed in [87]). The cyclin-dependent kinase (CDK7), as part of the trimeric CAK sub-complex of TFIIH, is one of the kinases involved in phosphorylation of the CTD *in vitro* [15]. Rossi *et al*, provided some evidence on the requirement for the MAT1 component of CAK in CTD phosphorylation *in vivo*. Despite a decreased level of phosphorylation of the CTD of the largest subunit of RNAP2, a functional de novo transcription could be observed in MAT1$^{-/-}$ mouse cells. This suggests that MAT1 is not essential for RNAP2 transcription, but might have a stimulatory function or alternatively, be required for a subset of genes [88].

Before the synthesis of tenth nucleotide most basal transcription factors have dissociated from the transcribing RNAP2 (TFIIB and TFIIE) or remain bound to the promoter (TFIID). TFIIH was shown to be released from the elongating RNAP2 after synthesis of a ~30 nucleotide transcript [172].

(B) Recently, it was shown that TFIIH is an important transcription factor for RNAP1 transcription initiation, since addition of purified TFIIH enhances RNAP1 transcription *in vitro* [16]. In addition, TFIIH was shown to interact with RNAP1 transcription in living cells [142]. In contrast to RNAP2 transcription initiation, TFIIH is not required for open complex formation and synthesis of the first phosphodiester bond [16]. This implies a role for TFIIH in a post-initiation step. In addition, ATP hydrolysis is not required for RNAP1 transcription initiation suggesting that neither the helicase or kinase activity is essential for rDNA transcription. The mechanism underlying activation of RNAP1 transcription by TFIIH is still obscure.

(C) NER is one of the most versatile repair pathways able to remove a large variety of lesions, including the UV-induced (6-4)PPs and CPDs (also see box 1). After detection of the DNA lesion by XPC-hHR23B, TFIIH is recruited to the NER site [94].

The two DNA-dependent ATPase and helicase activities of TFIIH are required for unwinding of the DNA helix around the lesion [84, 86]. An additional function of TFIIH within the NER pathway is the correct positioning of the 5' endonuclease ERCC1/XPF [57]. A role for the CAK complex in NER is still ambiguous, since it is not required for an *in vitro* NER reaction and in the presence of an ATP-regenerating system can even inhibit the process [100, 101]. However, microinjection of antibodies directed against CDK7 inhibit NER *in vivo* [12]. It has been shown that multiple components of NER (XPC and XPG) are phosphorylated during the repair process, but no other kinase activity besides CDK7 has been implicated in NER [98].

(D) TFIIH is required for the repair of UV-induced damages in template strands of genes transcribed by RNAP2 by the TC-NER process [6]. It was recently shown that TFIIH is also essential for the removal of BER-lesions from the transcribed strand, but not the non-transcribed strand [42]. It was proposed that a general a general TCR pathway might exist, which would take care of any type of transcription-stalling injury. TFIIH, together with CSA, CSB, XAB2 and XPG have been implicated in this pathway, although the role of these factors is largely unknown [43]. However, they may participate in processing of the stalled RNAP2 making the damage more accessible to repair by one of the specialized repair pathways and subsequent resumption of transcription. This step could involve conformational changes or backward movement of RNAP2, release of RNAP2, or by-pass of the lesion [43].

(E) In addition to being incorporated into TFIIH, the CAK complex is autonomously present in the nucleus in 3-5 fold excess [83]. It has been shown that the substrate specificity of the autonomous CAK-complex is different from the CAK-complex integrated into TFIIH. Autonomous CAK has been implicated in cell cycle regulation, since it is capable of phosphorylating other cyclin-dependent kinases. Some substrates are CDK1-cyclin B essential for G2-M transition, CDK4-cyclin D required for G1-S transition and CDK2-cyclin A, which triggers DNA and histone synthesis in S-phase (reviewed in [103]). Recently, the first *in vivo* evidence for a role of the CAK complex in cell cycle regulation has been published [88]. The disruption of the *MAT1* gene leads to peri-implantation lethality, which coincides with depletion of maternal MAT1 protein. In culture, MAT$^{-/-}$ blastocysts gave rise to viable post-mitotic trophoblast giant cells, while mitotic lineages failed to grow. MAT$^{-/-}$ cells rapidly displayed an arrest in endoreduplication, due to an inability to enter S-phase [88]. However, no evidence exists for a potential role of TFIIH in cell-cycle control.

Chapter 4

Nuclear organization of DNA trans-acting processes and chromatin

Nuclear organization of DNA trans-acting processes and chromatin

4.1 Classical view on the organization of DNA trans-acting processes

Mammalian nuclei are complex organelles that contain high concentrations of proteins and nucleic acids. Human DNA has a contour length of approximately 2 meters, which has to fit into a nucleus with a diameter of roughly 10 μm. Association with histones and non-histone proteins allows the packaging of genomic DNA into a highly compact and organized structure, known as chromatin. Chromatin is a heterogeneous structure that undergoes reversible local rearrangements during DNA metabolizing processes, such as replication, transcription and repair as well as chromosome condensation for mitosis and meiosis. Remodeling of the chromatin structure is required to increase the accessibility of DNA processing factors to chromosomal DNA.

The mechanism how DNA transacting processes regulate the loading of the necessary components and how nuclear factors act on their specific targets, is still largely unknown. Various models have been suggested: (i) all necessary proteins are incorporated into a factory fixed at certain positions in the nucleus where DNA can be received for metabolization, (ii) a large pre-assembled complex, which contains all required components, is roaming the nucleus, or (ii) all proteins are recruited individually into transient assemblies when required.

4.1.1 Replication

During the DNA replication-stage of the cell cycle (S-phase), a focal pattern of replication sites has been observed microscopically. These foci are small spots, which contain besides the required replication factors, such as DNA polymerases and PCNA, also newly synthesized DNA. In early S-phase small discrete replication foci appear scattered all over the nucleus, in mid S-phase these foci are located at the periphery of the nucleus and nucleolus, and then in late S-phase these foci are larger and less numerous. It is still not clear whether within the replication foci active DNA polymerases track along the DNA or remain static by being attached to a larger structure and reel the templates as they extrude newly made nucleic acids. Replication occurs in stretches scattered along a DNA duplex. These stretches initiate and elongate synchronously, presumably through the coordinated action of adjacent polymerases. So the idea is that many replication forks must be active in each replication focus, in other words each focus can be considered as a 'factory' containing many polymerizing machines working on different templates (see for review, [121]).

4.1.2 RNAP1 and RNAP2 transcription

RNAP2 transcription could work in a similar fashion as replication. But, the evidence for transcription is less compelling than for replication. Focal patterns have been described for nascent RNAP2 transcripts. In contrast to replication foci these small foci are spread throughout the nucleoplasm [122]. One important question is, do these foci represent one transcription unit or multiple units clustered into a transcription factory, like suggested for replication factories. Thus far, no data has been published that could solve this issue. Unlike RNAP2 transcription, the transcription of ribosomal genes by RNAP1 is organized into transcription units that form one transcription factory (fibrillar center) in the nucleolus (see for review, [121]). Each fibrillar center contains numerous RNAP1 molecules and about four active genes at or close to its surface. It was calculated that each gene is associated with ~125 engaged RNAP1 molecules [123].

4.1.3 Repair processes

Some genome surveillance proteins linked to replication, such as RAD18 and Polε, involved in lesion bypass synthesis [124, 125], are localized in replication sites. This indicates that these repair pathways work side by side with the replication machinery, during S-phase. Surprisingly, many of the Rad52 group proteins involved in homologous recombination re-localize into nuclear foci upon induction of DNA damage by ionizing radiation [126-128]. Since the complicated task of bringing the two DNA ends and template together can only be accomplished by close coordination and cooperation of several proteins, a replication-like mechanism might be employed where 'immobilized' proteins reel in the different pieces of DNA. However, it is far from clear what process occurs in these foci.

NER seems to have a different nuclear organization from other repair pathways, like MMR, lesion bypass synthesis and HR. Immunofluorescent studies, using an antibody against the 3' endonuclease XPG revealed that the NER protein was not evenly distributed throughout the nucleus, but concentrated in large foci. These foci disappeared after UV-irradiation and in time (8 h) the XPG antigenic signal reappeared in foci again [129]. However, these distribution patterns were not seen in immunofluorescent studies using antibodies against XPB [130], XPA [131] or XPC [132]. In fact, no difference in distribution could be observed for these proteins before and after UV-irradiation. By locally UV-irradiating a small part of the nucleus and subsequent immunofluorescence, it was shown that the NER factors relocalized to the damaged site without a distinct distribution pattern, but rather in a large bright spot [94]. Similar studies performed in various NER-deficient cell lines, revealed that assembly of NER factors (XPA, TFIIH, ERCC1/XPF and XPG) at a local damaged area is dependent on the presence of XPC. Moreover, these studies revealed that NER factors are recruited sequentially to a NER site [94]. This shows that NER is an ordered process, where all factors assemble onto the damaged DNA when required.

4.2 Dynamic organization of the nucleus

The above-described nuclear organization of DNA-transacting mechanisms reflects the classical view based on a steady state situation of frozen processes in chemically fixed cells. In the last few years it was shown that most DNA-transacting processes are highly dynamic and less static than suggested from *in vitro* studies. The recent insight into how nuclear processes are organized, was mostly obtained by using the life-cell marker green fluorescent protein (GFP) [133]. GFP is a small stable rod-shaped protein containing a chromophore with an excitation wavelength of 488nm and emission at 507 nm. When the *GFP* gene is fused to a coding gene, the hybrid protein (GFP-tagged protein) is expressed in living cells, where it can be localized by the GFP-fluorescence. This creates the possibility of using time-lapse imaging to determine the behavior of GFP-tagged proteins in living cells in time under various conditions. The adverse property of fluorescence-loss during imaging of GFP, is used in quantitative fluorescence methods such as fluorescence redistribution after photobleaching (FRAP) [134-136]. These photobleaching techniques can be used to study the dynamic behavior of GFP-tagged proteins involved in several cellular processes. In FRAP experiments part of the GFP-signal is bleached and the redistribution of bleached and non-bleached GFP-molecules in time can be used as a measure for the dynamics of a GFP-tagged protein in living cells [134]. One crucial condition for these type of experiments is that the tagged protein should remain functional, properly located, and expressed at physiological. Only after obeying these critical parameters, the hybrid protein can be considered as a bonafide tool to study the dynamic properties under physiological conditions. The usage of GFP-fused proteins in combination with time-lapse studies as well as quantitative fluorescence methods like FRAP have revolutionized the field and has provided spectacular new insight into the regulation and organization of cellular processes.

4.2.1 Chromatin

In eukaryotic cells, DNA is packaged into nucleosomes, where ~146 basepairs are wrapped around an octamer containing two copies of the four core-histones, H2A, H2B, H3 and H4 and this octomer is stabilized by the linker histone H1 [137]. To determine if these histones are statically bound to chromatin or are exchanging frequently with non-bound histones from the nucleoplasm, photobleaching studies were performed on GFP-tagged histones. It was shown that most H1-GFP is bound to chromatin at any given time and the residence time of individual GFP-tagged H1 molecules at chromatin was in the order of minutes in both active (euchromatin) and inactive condensed parts (heterochromatin) of chromatin [138]. This suggests that H1-GFP was continuously exchanging between chromatin regions. Hyperacetylation of the core histones changes the chromatin structure, resulting in a more open chromatin conformation, and thereby increasing the accessibility of DNA to remodeling factors. This is a naturally occurring process during transcription. After hyperactetylation of the

core histones, the residence time of GFP tagged H1 was reduced, suggesting that chromatin remodeling increases the exchange rate of H1-GFP on chromatin [138]. Similar FRAP experiment were also performed on GFP-tagged core-histones. Unlike H1, the core histones H3-GFP and H4-GFP were shown to be assembled into chromatin when DNA is replicated and bound permanently. On the other hand, H2B-GFP had a slowly exchanging fraction, with a residence time on chromatin in the order of hours and a small rapid exchanging fraction in the order of minutes [139]. The latter fraction was transcription-dependent and so may represent H2B in transcriptionally active chromatin. These FRAP experiments on GFP-tagged histones indicate that although H2A, H2B, H3 and H4 are part of the same nucleosomal structure, their individual stability in chromatin is very different. H3 and H4 were more stably bound to the chromatin structure, as compared to histone H2B. The linker histone H1 seemed to be continuously exchanging between chromatin areas, rather than being a stable component of chromatin.

4.2.2 Replication

Even though replication occurs at specific locations (replication foci) in the nucleus, a model in which the replication factors continuously exchange with the surroundings can be envisaged. Evidence for such a model was provided by Leonhardt and colleagues [140]. In this manuscript the authors describe the tagging of PCNA with GFP and the expression of the hybrid protein in mouse myoblast cells. Photo-bleaching experiments revealed a dynamic behavior for PCNA-GFP in replication foci, indicating that the involvement of PCNA in replication is a transient event. The replication of DNA is not performed in a static factory, but is at least for some part a dynamic process.

4.2.3 RNAP2 transcription

The dynamical aspects of the multifaceted process, RNAP2 transcription, have been a topic of research in many different laboratories. Both basal transcription factors, like RNAP2 [141], TFIIH [142], TFIIB and TBP [143], and transcription activators, like the glucocorticoid receptor (GR, [144]) have been tagged with GFP. FRAP analysis on GFP-tagged TFIIH and RNAP2 revealed that these transcription factors are not incorporated into larger holoenzymes, pre-initiation complexes, or 'factories'. Also TFIIB-GFP is most likely to diffuse through the nucleus as an autonomous protein, unlike TBP-GFP that seems to remain promoter-bound for multiple rounds of transcription [143]. These data suggest a step-wise assembly where TFIID (TBP) is bound to a promoter, followed successively by TFIIB, RNAP2/TFIIF, TFIIE and TFIIH.

TFIIH-GFP was shown to be engaged in transcription in the order of seconds [142], whereas RNAP2 is engaged in the order of minutes ($t_{½}$ ~14min) [141]. This is not unexpected, since it is known that TFIIH enters the pre-initiation complex to

initiate transcription and dissociates from the complex after promoter escape, whereas RNAP2 is the key player involved in transcription elongation. Only a small percentage of the RNAP2 molecules were found to be involved in the transcription process [141]. This in contrast to TFIIH that was shown to be engaged in much more ongoing transcription initiation events each given time. It was calculated that only a fraction of TFIIH interactions with promoters lead to the successful completion of a transcription initiation event [142]. These data suggest that in general transcription factors collide with promoters at random, to bind and dissociate immediately. Only occasionally collisions occur in the appropriate sequence which permits the rapid assembly of a pre-initiation complex and the initiation of transcription. This sequential assembly of transcription factors provides the opportunity for regulation of an important process like transcription.

Steroid receptors modulate the rate of transcription of target genes through protein-protein interactions with basal transcription factors and through recruitment of a variety of coactivators or corepressors. The classic view is that the receptor binds to a recognition site and remains for as long as the ligand is present. Alternatively, the receptor binds transiently to a responsive element in the target gene and thereby recruits secondary factors to initiate transcription. Photobleaching experiments revealed that the GFP-tagged GR undergoes rapid exchange between a target site and the nucleoplasm, with a residence time of a few seconds at a binding site [144]. This type of mechanism has been referred to as 'hit and run', and was also shown for the co-activator, GR interacting protein 1 (GRIP-1) [145] and the basal transcription factor TFIIH [142].

4.2.4 RNAP1 transcription

This 'on the spot assembly' of all factors required, is not unique for RNAP2 transcription, but also seems to be employed by the RNAP1 transcription machinery. It was shown that components required for rRNA synthesis are rapidly exchanged between nucleoplasm and ribosomal transcription sites in the nucleolus [146]. A short retention time in rRNA synthesis of about 25 seconds was found for TFIIH, which was recently shown to play a role in RNAP1 transcription [16, 142]. Similar residence times were observed for the pre-initiation factors of RNAP1 transcription, UBF1-GFP, UBF2-GFP and TAF_I48-GFP. Interestingly, these studies further revealed that the four RNAP1 subunits enter the nucleolus as distinct subunits rather than as a pre-assembled protein complex. This indicates that all these RNAP1 factors, including the subunits of the RNAP1 protein complex, assemble onto an RNAP1 promoter and dissociate when their requirement has ended.

Chen and colleagues showed that proteins in different steps of ribosome biogenesis have different dynamics in living cells [147]. Like factors involved in rRNA transcription, also proteins involved in processing, such as nucleolin and fibrillarin, and ribosome assembly, such as B23, exchange rapidly between nucleoplasm and

nucleolus. In contrast, ribosomal subunit proteins, such as S5 and L9, exchange at a much lower rate.

4.2.5 Repair processes

Repair mechanisms also appear to recruit the required factors transiently to the damaged DNA. Several studies have shown that both HR and NER are far from static processes. Upon treatment with ionizing radiation, GFP tagged Rad51, Rad52 and Rad54 accumulated into foci [148]. Photobleaching experiments revealed that these foci are dynamic structures of which Rad51 was a stably associated core component. In contrast, Rad52 and Rad54 only transiently interact with the foci structures. Moreover, these proteins are not pre-assembled into a large 'holo'-complex but rather diffuse in small molecular weight entities and all three GFP-tagged proteins revealed a different residence time at these repair foci [148].

GFP based studies were also performed on multiple components of the NER pathway. The NER-specific 5'-endonuclease ERCC1/XPF tagged with a GFP was not incorporated into a large 'holo'-complex, but rather diffused autonomously to find a NER site where it was immobilized for 4 minutes [149]. Similar results were also found for GFP tagged XPA (Rademakers *et al.*, in prep) and the multifunctional TFIIH complex [142]. In contrast to ERCC1/XPF, XPA and TFIIH, high resolution imaging and FRAP studies on XPC-GFP expressing cells suggest that the GG-NER damage sensor has a high probability to be associated with chromatin. After damage detection XPC-GFP is present for ~90 seconds at a NER site (this thesis, chapter 8). All these NER components, except for XPC-hHR23B display comparable binding times to NER sites. This NER binding time of ~4 minutes corresponds very well with the average time of a single NER event calculated from the number of lesions induced, the number of repair protein molecules actually engaged in NER and the time required to remove all induced lesions [149]. This suggests that these NER components, except for XPC-hHR23B form one stable assembly on the damaged DNA in a relatively short time and after the repair process has been completed, all factors are simultaneously released. It has been reported previously that XPC-hHR23B is not present in the pre-incision complex that contains TFIIH, XPG, XPA, RPA, and ERCC1/XPF [150].

All above described processes, replication, transcription and repair, benefit from ordered temporal assembly over large pre-assembled 'holo'-complexes. Sequential assembly provides a process flexibility and the prospect of utilizing multifunctional protein(complex)s [151]. TFIIH is a prime example of this. Free diffusion of this complex allows it to function in and rapidly exchange between multiple processes. In addition, sequential assembly brings about the opportunity to optimize regulation by controlling each step of the process and the option for premature abortion of the reaction when necessary. Moreover, the dynamic nature of small freely diffusing constituents guarantees a quick response to stress conditions, like induction of DNA

damages, since they are omnipresent and have more efficient access to sites in condensed chromatin than bulky 'holo'-complexes. In the case of TFIIH the observed homogeneous distribution permits this factor to be always in the vicinity of DNA lesions or promoters.

References

1. **Lindahl, T.**, *Instability and decay of the primary structure of DNA.* Nature, 1993. 362: p. 709-715.
2. **Hoeijmakers, J.H.**, *Genome maintenance mechanisms for preventing cancer.* Nature, 2001. 411(6835): p. 366-74.
3. **Friedberg, E.C., G.C. Walker, and W. Siede**, *DNA repair and mutagenesis.* 1995, Washington D.C.: ASM Press.
4. **Bootsma, D., et al.**, *Nucleotide excision repair syndromes: xeroderma pigmentosum, Cockayne syndrome and trichothiodystrophy.*, in *The metabolic basis of inherited disease. Eight edition*, C.R. Scriver, et al., Editors. 1997, McGraw-Hill Book Co.: New York.
5. **Sugasawa, K., et al.**, *Xeroderma pigmentosum group C protein complex is the initiator of global genome nucleotide excision repair.* Mol. Cell, 1998. 2(2): p. 223-232.
6. **Hanawalt, P. and G. Spivak**, *Transcription-coupled DNA repair*, in *Advances in DNA damage and repair*, Dizdaroglu and Karakaya, Editors. 1999, Kluwer Academic/Plenum Publishers: New York.
7. **de Laat, W.L., N.G. Jaspers, and J.H. Hoeijmakers**, *Molecular mechanism of nucleotide excision repair.* Genes Dev., 1999. 13(7): p. 768-785.
8. **Egly, J.M.**, *The 14th Datta Lecture. TFIIH: from transcription to clinic.* FEBS Lett, 2001. 4 98(2-3): p. 124-8.
9. **Schaeffer, L., et al.**, *The ERCC2/DNA repair protein is associated with the class II BTF2/TFIIH transcription factor.* EMBO J., 1994. 13(10): p. 2388-2392.
10. **Schaeffer, L., et al.**, *DNA repair helicase: a component of BTF2 (TFIIH) basic transcription factor.* Science, 1993. 260: p. 58-63.
11. **Drapkin, R., et al.**, *Dual role of TFIIH in DNA excision repair and in transcription by RNA polymerase II.* Nature, 1994. 368: p. 769-772.
12. **Roy, R., et al.**, *The MO15 cell cycle kinase is associated with the TFIIH transcription-DNA repair factor.* Cell, 1994. 79: p. 1093-1101.
13. **Holstege, F.C.P., P.C. Van der Vliet, and H.T.M. Timmers**, *Opening of an RNA polymerase II promoter occurs in two distinct steps and requires the basal transcription factors TFIIE and TFIIH.* EMBO J., 1996. **15**(7): p. 1666-1677.
14. **Dvir, A., R.C. Conaway, and J.W. Conaway**, *A role for TFIIH in controlling the activity of early RNA polymerase II elongation complexes.* Proc Natl Acad Sci U S A, 1997. 94(17): p. 9006-10.
15. **Lu, H., et al.**, *Human general transcription factor IIH phosphorylates the C-terminal domain of RNA polymerase II.* Nature, 1992. 358: p. 641-645.
16. **Iben, S., et al.**, *TFIIH Plays an Essential Role in RNA Polymerase I Transcription.* Cell, 2002. 109(3): p. 297-306.
17. **Evans, E., et al.**, *Mechanism of open complex and dual incision formation by human nucleotide excision repair factors.* EMBO J., 1997. 16(21): p. 6559-6573.
18. **Bootsma, D., et al.**, *Nucleotide excision repair syndromes: xeroderma pigmentosum, Cockayne syndrome and trichothiodystrophy.*, in *The genetic basis of human cancer*, B. Vogelstein and K.W. Kinzler, Editors. 2001, McGraw-Hill: New York. p. 677-703.
19. **Vermeulen, W., et al.**, *Three unusual repair deficiencies associated with transcription factor BTF2(TFIIH): evidence for the existence of a transcription syndrome.*, in *Cold-Spring-Harb-Symp-Quant-Biol.* 1994. p. 317-329.

20. **Lindahl, T. and R.D. Wood**, *Quality control by DNA repair.* Science, 1999. 286(5446): p. 1897-905.
21. **Yamaizumi, M. and T. Sugano**, *U.v.-induced nuclear accumulation of p53 is evoked through DNA damage of actively transcribed genes independent of the cell cycle.* Oncogene, 1994. 9(10): p. 2775-84.
22. **Ljungman, M. and F. Zhang**, *Blockage of RNA polymerase as a possible trigger for u.v. light-induced apoptosis.* Oncogene, 1996. 13(4): p. 823-831.
23. **Zhou, B.B. and S.J. Elledge**, *The DNA damage response: putting checkpoints in perspective.* Nature, 2000. 408(6811): p. 433-9.
24. **Bernstein, C., et al.**, *DNA repair/pro-apoptotic dual-role proteins in five major DNA repair pathways: fail-safe protection against carcinogenesis.* Mutat Res, 2002. 511(2): p. 145-78.
25. **Rotman, G. and Y. Shiloh**, *ATM: from gene to function.* Hum Mol Genet, 1998. 7(10): p. 1555-63.
26. **Thompson, L.H. and D. Schild**, *Recombinational DNA repair and human disease.* Mutat Res, 2002. 509(1-2): p. 49-78.
27. **Batty, D.P. and R.D. Wood**, *Damage recognition in nucleotide excision repair of DNA.* Gene, 2000. 241(2): p. 193-204.
28. **Sugasawa, K., et al.**, *A multistep damage recognition mechanism for global genomic nucleotide excision repair.* Genes Dev, 2001. 15(5): p. 507-21.
29. **Lu, A.L., et al.**, *Repair of oxidative DNA damage: mechanisms and functions.* Cell Biochem Biophys, 2001. 35(2): p. 141-70.
30. **Aquilina, G. and M. Bignami**, *Mismatch repair in correction of replication errors and processing of DNA damage.* J Cell Physiol, 2001. 187(2): p. 145-54.
31. **van Gent, D.C., J.H. Hoeijmakers, and R. Kanaar**, *Chromosomal stability and the DNA double-stranded break connection.* Nat Rev Genet, 2001. 2(3): p. 196-206.
32. **Gerard, M., et al.**, *Purification and interaction properties of the human RNA polymerase B(II) general transcription factor BTF2.* J. Biol. Chem., 1991. **266**(31): p. 20940-20945.
33. **Flores, O., H. Lu, and D. Reinberg**, *Factors involved in specific transcription by mammalian RNA polymerase II.* J.Biol.Chem., 1992. 267: p. 2786-2790.
34. **Drapkin, R. and D. Reinberg**, *The multifunctional TFIIH complex and transcriptional controle.* Trends in Biochem. Sci., 1994. 19: p. 504-508.
35. **Evans, E., et al.**, *Open complex formation around a lesion during nucleotide excision repair provides a structure for cleavage by human XPG protein.* EMBO J., 1997. 16(3): p. 6625-6238.
36. **van Gool, A.J., et al.**, *The Cockayne syndrome B protein, involved in transcription-coupled DNA repair, resides in a RNA polymerase II containing complex.* EMBO J., 1997. 16(19): p. 5955-5965.
37. **Citterio, E., et al.**, *ATP-Dependent Chromatin Remodeling by the Cockayne Syndrome B DNA Repair-Transcription-Coupling Factor.* Mol Cell Biol, 2000. 20(20): p. 7643-7653.
38. **Selby, C.P. and A. Sancar**, *Cockayne syndrome group B protein enhances elongation by RNA polymerase II.* Proc. Natl. Acad. Sci. USA, 1997. 94(21): p. 11205-11209.
39. **Tang, J.Y., et al.**, *Xeroderma pigmentosum p48 gene enhances global genomic repair and suppresses UV-induced mutagenesis.* Mol Cell, 2000. 5(4): p. 737-44.

40. **Henning, K.A., et al.**, *The Cockayne syndrome group A gene encodes a WD repeat protein that interacts with CSB protein and a subunit of RNA polymerase II TFIIH.* Cell, 1995. 82: p. 555-564.
41. **Nakatsu, Y., et al.**, *XAB2, a novel tetratricopeptide repeat protein involved in transcription-coupled DNA repair and transcription.* J Biol Chem, 2000. 275(45): p. 34931-7.
42. **Le Page, F., et al.**, *Transcription-coupled repair of 8-oxoguanine: requirement for XPG, TFIIH, and CSB and implications for Cockayne syndrome.* Cell, 2000. 101(2): p. 159-171.
43. **Citterio, E., W. Vermeulen, and J.H.J. Hoeijmakers**, *Transcriptional healing.* Cell, 2000. 101: p. 447-450.
44. **Cooper, P.K., et al.**, *Defective transcription-coupled repair of oxidative base damage in Cockayne syndrome patients from XP group G.* Science, 1997. 275(5302): p. 990-993.
45. **Leadon, S.A. and P.K. Cooper**, *Preferential repair of ionizing-radiation induced damage in the transcribed strand of an active human gene is defective in Cockayne syndrome.* Proc.Natl.Acad.Sci.USA, 1993. 90: p. 10499-10503.
46. **Yu, A., et al.**, *Activation of p53 or Loss of the Cockayne Syndrome Group B Repair Protein Causes Metaphase Fragility of Human U1, U2, and 5S Genes.* Molecular Cell, 2000. 5: p. 801-810.
47. **Leadon, S.A.**, *Transcription-coupled repair of DNA damage: unanticipated players, unexpected complexities.* Am. J. Hum. Genet., 1999. 64(5): p. 1259-1263.
48. **de Jager, M., et al.**, *Human Rad50/Mre11 is a flexible complex that can tether DNA ends.* Mol Cell, 2001. 8(5): p. 1129-35.
49. **Paull, T.T. and M. Gellert**, *The 3' to 5' exonuclease activity of Mre 11 facilitates repair of DNA double-strand breaks.* Mol Cell, 1998. 1(7): p. 969-79.
50. **MacNeill, S.A.**, *DNA replication: partners in the Okazaki two-step.* Curr Biol, 2001. 11(20): p. R842-4.
51. **Park, M.S., et al.**, *Physical interaction between human RAD52 and RPA is required for homologous recombination in mammalian cells.* J Biol Chem, 1996. 271(31): p. 18996-9000.
52. **Coverley, D., et al.**, *Requirement for the replication protein SSB in human DNA excision repair.* Nature, 1991. 349(6309): p. 538-541.
53. **DeMott, M.S., S. Zigman, and R.A. Bambara**, *Replication protein A stimulates long patch DNA base excision repair.* J Biol Chem, 1998. **273**(42): p. 27492-8.
54. **Mer, G., et al.**, *Structural basis for the recognition of DNA repair proteins UNG2, XPA, and RAD52 by replication factor RPA.* Cell, 2000. 103(3): p. 449-56.
55. **Longhese, M.P., P. Plevani, and G. Lucchini**, *Replication factor A is required in vivo for DNA replication, repair, and recombination.* Molecular and cellular Biology, 1994. 14: p. 7884-7890.
56. **Bochkarev, A., et al.**, *Structure of the single-stranded-DNA-binding domain of replication protein A bound to DNA.* Nature, 1997. 385(6612): p. 176-81.
57. **de Laat, W.L., et al.**, *DNA-binding polarity of human replication protein A positions nucleases in nucleotide excision repair.* Genes Dev., 1998. 12(16): p. 2598-2609.
58. **Tsurimoto, T.**, *PCNA binding proteins.* Front Biosci, 1999. 4: p. D849-58.
59. **Warbrick, E.**, *The puzzle of PCNA's many partners.* Bioessays, 2000. 22(11): p. 997-1006.
60. **Hingorani**, M.M. and M. O'Donnell, *Sliding clamps: a (tail)ored fit.* Curr Biol, 2000. 10(1): p. R25-9.

61. **Warbrick, E.**, *PCNA binding through a conserved motif.* Bioessays, 1998. 20(3): p. 195-9.
62. **Hoege, C., et al.**, *RAD6-dependent DNA repair is linked to modification of PCNA by ubiquitin and SUMO.* Nature, 2002. 419(6903): p. 135-41.
63. **Ulrich, H.D. and S. Jentsch**, *Two RING finger proteins mediate cooperation between ubiquitin- conjugating enzymes in DNA repair.* Embo J, 2000. 19(13): p. 3388-97.
64. **Vogelstein, B., D. Lane, and A.J. Levine**, *Surfing the p53 network.* Nature, 2000. 408(6810): p. 307-10.
65. **Hollstein, M., et al.**, *New approaches to understanding p53 gene tumor mutation spectra.* Mutat Res, 1999. 431(2): p. 199-209.
66. **Momand, J., H.H. Wu, and G. Dasgupta**, *MDM2--master regulator of the p53 tumor suppressor protein.* Gene, 2000. 242(1-2): p. 15-29.
67. **el-Deiry, W.S.**, *Regulation of p53 downstream genes.* Semin Cancer Biol, 1998. 8(5): p. 345-57.
68. **Boulaire, J., A. Fotedar, and R. Fotedar**, *The functions of the cdk-cyclin kinase inhibitor p21WAF1.* Pathol Biol (Paris), 2000. 48(3): p. 190-202.
69. **Lee, S., L. Cavallo, and J. Griffith**, *Human p53 binds Holliday junctions strongly and facilitates their cleavage.* J Biol Chem, 1997. 272(11): p. 7532-9.
70. **Welcsh, P.L., K.N. Owens**, and M.C. King, *Insights into the functions of BRCA1 and BRCA2.* Trends Genet, 2000. 16(2): p. 69-74.
71. **Sturzbecher, H.W., et al.**, *p53 is linked directly to homologous recombination processes via RAD51/RecA protein interaction.* Embo J, 1996. 15(8): p. 1992-2002.
72. **Offer, H., et al.**, *Structural and functional involvement of p53 in BER in vitro and in vivo.* Oncogene, 2001. 20(5): p. 581-9.
73. **Zhou, J., et al.**, *A role for p53 in base excision repair.* Embo J, 2001. 20(4): p. 914-23.
74. **Li, G. and V.C. Ho**, *p53-dependent DNA repair and apoptosis respond differently to high- and low-dose ultraviolet radiation.* Br J Dermatol, 1998. 139(1): p. 3-10.
75. **Therrien, J.P., et al.**, *Human cells compromised for p53 function exhibit defective global and transcription-coupled nucleotide excision repair, whereas cells compromised for pRb function are defective only in global repair.* Proc Natl Acad Sci U S A, 1999. 96(26): p. 15038-43.
76. **Wang, X.W., et al.**, *The XPB and XPD DNA helicases are components of the p53-mediated apoptosis pathway.* Genes Dev, 1996. 10(10): p. 1219-32.
77. **Wang, X.W., et al.**, *p53 modulation of TFIIH-associated nucleotide excision repair activity.* Nat Genet, 1995. 10(2): p. 188-95.
78. **Frit, P., E. Bergmann, and J.M. Egly**, *Transcription factor IIH: a key player in the cellular response to DNA damage.* Biochimie, 1999. 81(1-2): p. 27-38.
79. **Rochette-Egly, C., et al.**, *Stimulation of RAR alpha activation function AF-1 through binding to the general transcription factor TFIIH and phosphorylation by CDK7.* Cell, 1997. 90(1): p. 97-107.
80. **Bastien, J., et al.**, *TFIIH interacts with the retinoic acid receptor gamma and phosphorylates its AF-1-activating domain through cdk7.* J Biol Chem, 2000. 275(29): p. 21896-904.
81. **Coin, F., J.C. Marinoni, and J.M. Egly**, *Mutations in XPD helicase prevent its interaction and regulation by p44, another subunit of TFIIH, resulting in Xeroderma pigmentosum (XP) and trichothiodystrophy (TTD) phenotypes.* Pathol Biol (Paris), 1998. 46(9): p. 679-80.

82. **Jawhari, A., et al.**, *p52 Mediates XPB function within the transcription/repair factor TFIIH.* J Biol Chem, 2002. 277(35): p. 31761-7.
83. **Rossignol, M., I. Kolb-Cheynel, and J.M. Egly**, *Substrate specificity of the cdk-activating kinase (CAK) is altered upon association with TFIIH.* Embo J, 1997. 16(7): p. 1628-37.
84. **Tirode, F., et al.**, *Reconstitution of the transcription factor TFIIH: assignment of functions for the three enzymatic subunits, XPB, XPD, and cdk7.* Mol. Cell, 1999. 3(1): p. 87-95.
85. **de Boer, J., et al.**, *Disruption of the mouse xeroderma pigmentosum group D DNA repair/basal transcription gene results in preimplantation lethality.* Cancer Res, 1998. 58(1): p. 89-94.
86. **Winkler, G.S., et al.**, *TFIIH with inactive XPD helicase functions in transcription initiation but is defective in DNA repair.* J. Biol. Chem., 2000. 275(6): p. 4258-4266.
87. **Dahmus, M.E.**, *Phosphorylation of C-terminal domain of RNA polymerase II.* Biochemica et Biophysica Acta, 1995. 1261: p. 71-82.
88. **Rossi, D.J., et al.**, *Inability to enter S phase and defective RNA polymerase II CTD phosphorylation in mice lacking Mat1.* Embo J, 2001. 20(11): p. 2844-56.
89. **Keriel, A., et al.**, *XPD mutations prevent TFIIH-dependent transactivation by nuclear receptors and phosphorylation of RARalpha.* Cell, 2002. 109(1): p. 125-35.
90. **Liu, J., et al.**, *Defective interplay of activators and repressors with TFIH in xeroderma pigmentosum.* Cell, 2001. 104(3): p. 353-63.
91. **Hernandez, N.**, *TBP, a universal eukaryotic transcription factor?* Genes Dev, 1993. 7(7B): p. 1291-308.
92. **Bradsher, J.**, et al., *CSB Is a Component of RNA Pol I Transcription.* Mol Cell, 2002. **10**(4): p. 819-29.
93. **Yokoi, M., et al.**, *The xeroderma pigmentosum group C protein complex XPC-HR23B plays an important role in the recruitment of transcription factor IIH to damaged DNA.* J Biol Chem, 2000. 275(13): p. 9870-5.
94. **Volker, M., et al.**, *Sequential Assembly of the Nucleotide Excision Repair Factors In Vivo.* Molecular Cell, 2001. 8(1): p. 213-224.
95. **Araujo, S.J., E.A. Nigg, and R.D. Wood**, *Strong functional interactions of TFIIH with XPC and XPG in human DNA nucleotide excision repair, without a preassembled repairosome.* Molecular and Cellular Biology, 2001. 21(7): p. 2281-2291.
96. **Park, C.-H., et al.**, *The general transcription-repair factor TFIIH is recruited to the excision repair complex by the XPA protein independent of the TFIIE transcription factor.* J. Biol. Chem., 1995. 270: p. 4896-4902.
97. **Mu, D., et al.**, *Reconstitution of human DNA repair excision nuclease in a highly defined system.* J. Biol. Chem., 1995. 270(6): p. 2415-8.
98. **Winkler, G.S., et al.**, *Novel functional interactions between nucleotide excision DNA repair proteins influencing the enzymatic activities of TFIIH, XPG, and ERCC1- XPF.* Biochemistry, 2001. 40(1): p. 160-5.
99. **Ariza, R.R., et al.**, *Reversible protein phosphorylation modulates nucleotide excision repair of damaged DNA by human cell extracts.* Nucleic Acids Res, 1996. 24(3): p. 433-40.
100. .**Mu, D., D.S. Hsu, and A. Sancar**, *Reaction mechanism of human DNA repair excision nuclease.* J. Biol. Chem., 1996. 271(14): p. 8285-8294.
101. **Araujo, S.J., et al.**, *Nucleotide excision repair of DNA with recombinant human proteins: definition of the minimal set of factors, active forms of TFIIH, and modulation by CAK.* Genes Dev., 2000. 14(3): p. 349-359.

102. **Harper, J.W. and S.J. Elledge**, *The role of Cdk7 in CAK function, a retro-retrospective.* Genes Dev, 1998. 12(3): p. 285-9.
103. **Kaldis, P.**, *The cdk-activating kinase (CAK): from yeast to mammals.* Cell Mol Life Sci, 1999. 55(2): p. 284-96.
104. **Akoulitchev, S. and D. Reinberg**, *The molecular mechanism of mitotic inhibition of TFIIH is mediated by phosphorylation of CDK7.* Genes Dev, 1998. 12(22): p. 3541-50.
105. **Serizawa, H.**, *Cyclin-dependent kinase inhibitor p16INK4A inhibits phosphorylation of RNA polymerase II by general transcription factor TFIIH.* J Biol Chem, 1998. 273(10): p. 5427-30.
106. **Bootsma, D. and J.H.J. Hoeijmakers**, *Engagement with transcription.* Nature, 1993. 363: p. 114-115.
107. **Hwang, J.R., et al.**, *A 3' to 5' XPB helicase defect in repair/transcription factor TFIIH of xeroderma pigmentosum group B affects both DNA repair and transcription.* The Journal of Biological Chemistry, 1996. 271: p. 15898-15904.
108. **Coin, F., et al.**, *Mutations in XPB and XPD helicases found in xeroderma pigmentosum patients impair the transcription function of TFIIH.* EMBO J., 1999. 18(5): p. 1357-1366.
109. **de Boer, J., et al.**, *A mouse model for the basal transcription/DNA repair syndrome trichothiodystrophy.* Mol. Cell, 1998. 1(7): p. 981-990.
110. **Viprakasit, V., et al.**, *Mutations in the general transcription factor TFIIH result in beta-thalassaemia in individuals with trichothiodystrophy.* Hum Mol Genet, 2001. 10(24): p. 2797-802.
111. **Vermeulen, W., et al.**, *A temperature-sensitive disorder in basal transcription and DNA repair in humans.* Nat Genet, 2001. 27(3): p. 299-303.
112. **Vermeulen, W., et al.**, *Sublimiting concentration of TFIIH transcription/DNA repair factor causes TTD-A trichothiodystrophy disorder.* Nat Genet, 2000. 26: p. 307-313.
113. **Botta, E., et al.**, *Reduced level of the repair/transcription factor TFIIH in trichothiodystrophy.* Hum Mol Genet, 2002. 11(23): p. 2919-2928.
114. **Broughton, B.C., et al.**, *Molecular and cellular analysis of the DNA repair defect in a patient in xeroderma pigmentosum complementation group D who has the clinical features of xeroderma pigmentosum and cockayne syndrome.* American Journal of Human Genetics, 1995. 56: p. 167-174.
115. **Takayama, K., et al.**, *Defects in the DNA repair and transcription gene ERCC2 in the cancer- prone disorder xeroderma pigmentosum group D.* Cancer Res, 1995. 55(23): p. 5656-63.
116. **van Hoffen, A., et al.**, *Cells from XP-D and XP-D-CS patients exhibit equally inefficient repair of UV-induced damage in transcribed genes but different capacity to recover UV-inhibited transcription.* Nucleic Acids Res, 1999. **27**(14): p. 2898-904.
117. **Berneburg, M., et al.**, *UV damage causes uncontrolled DNA breakage in cells from patients with combined features of XP-D and Cockayne syndrome.* Embo J, 2000. **19**(5): p. 1157-66.
118. **Coin, F., et al.**, *Mutations in the XPD helicase gene result in XP and TTD phenotypes, preventing interaction between XPD and the p44 subunit of TFIIH [see comments].* Nat Genet, 1998. 20(2): p. 184-8.
119. **Sandrock, B. and J.M. Egly**, *A yeast four-hybrid system identifies Cdk-activating kinase as a regulator of the XPD helicase, a subunit of transcription factor IIH.* J Biol Chem, 2001. 276(38): p. 35328-33.

120. **de Boer, J., et al.**, *Premature aging in mice deficient in DNA repair and transcription.* Science, 2002. 296(5571): p. 1276-9.
121. **Cook, P.R.**, *The organization of replication and transcription.* Science, 1999. 284(5421): p. 1790-5.
122. **Jackson, D.A., et al.**, *Visualization of focal sites of transcription within human nuclei.* Embo J., 1993. 12(3): p. 1059-1065.
123. **Miller, O.L., Jr.**, *The nucleolus, chromosomes, and visualization of genetic activity.* J Cell Biol, 1981. 91(3 Pt 2): p. 15s-27s.
124. **Svetlova, M.P., et al.**, *Staurosporine-sensitive protein phosphorylation is required for postreplication DNA repair in human cells.* FEBS Lett, 1998. 428(1-2): p. 23-6.
125. **Kannouche, P., et al.**, *Domain structure, localization, and function of DNA polymerase eta, defective in xeroderma pigmentosum variant cells.* Genes Dev, 2001. 15(2): p. 158-72.
126. **Haaf, T., et al.**, *Nuclear foci of mammalian Rad51 recombination protein in somatic cells after DNA damage and its localization in synaptonemal complexes.* Proc Natl Acad Sci U S A, 1995. 92(6): p. 2298-302.
127. **Tan, T.L., et al.**, *Mouse Rad54 affects DNA conformation and DNA-damage-induced Rad51 foci formation.* Curr. Biol., 1999. 9(6): p. 325-328.
128. **Liu, Y., et al.**, *Localization and dynamic relocalization of mammalian Rad52 during the cell cycle and in response to DNA damage.* Curr Biol, 1999. 9(17): p. 975-8.
129. **Park, M.S., et al.**, *Ultraviolet-induced movement of the human DNA repair protein, Xeroderma pigmentosum type G, in the nucleus.* Proc Natl Acad Sci U S A, 1996. 93(16): p. 8368-73.
130. **Grande, M.A., et al.**, *Nuclear distribution of transcription factors in relation to sites of transcription and RNA polymerase II.* J. Cell. Sci., 1997. 110(Pt 15): p. 1781-1791.
131. **Miura, N., et al.**, *Identification and characterization of XPAC protein, the gene product of the human XPAC (xeroderma pigmentosum group A complementing) gene.* Journal of Biological Chemistry, 1991. 266: p. 19786-19789.
132. **Van der Spek, P.J., et al.**, *XPC and human homologs of RAD23: intracellular localization and relationship to other nucleotide excision repair complexes.* Nucleic Acids Res., 1996. 24(13): p. 2551-2559.
133. **Tsien, R.Y.**, *The green fluorescent protein.* Annu Rev Biochem, 1998. 67: p. 509-44.
134. **Houtsmuller, A.B. and W. Vermeulen**, *Macromolecular dynamics in living cell nuclei revealed by fluorescence redistribution after photobleaching.* Histochem Cell Biol, 2001. 115(1): p. 13-21.
135. **White, J. and E. Stelzer**, *Photobleaching GFP reveals protein dynamics inside live cells.* Trends Cell Biol., 1999. 9(2): p. 61-65.
136. **Phair, R.D. and T. Misteli**, *High mobility of proteins in the mammalian cell nucleus.* Nature, 2000. 404(6778): p. 604-9.
137. **Luger, K., et al.**, *Crystal structure of the nucleosome core particle at 2.8 A resolution.* Nature, 1997. 389(6648): p. 251-60.
138. **Misteli, T., et al.**, *Dynamic binding of histone H1 to chromatin in living cells.* Nature, 2000. 408(6814): p. 877-81.
139. **Kimura, H. and P.R. Cook**, *Kinetics of core histones in living human cells: little exchange of H3 and H4 and some rapid exchange of H2B.* J Cell Biol, 2001. 153(7): p. 1341-53.

140. **Leonhardt, H., et al.**, *Dynamics of DNA replication factories in living cells.* J Cell Biol, 2000. 149(2): p. 271-80.
141. **Kimura, H., K. Sugaya, and P.R. Cook**, *The transcription cycle of RNA polymerase II in living cells.* J Cell Biol, 2002. 159(5): p. 777-82.
142. **Hoogstraten, D., et al.**, *Rapid Switching of TFIIH between RNA Polymerase I and II Transcription and DNA Repair In Vivo.* Mol Cell, 2002. 10(5): p. 1163-74.
143. **Chen, D., et al.**, *TBP dynamics in living human cells: constitutive association of TBP with mitotic chromosomes.* Mol Biol Cell, 2002. 13(1): p. 276-84.
144. **McNally, J.G., et al.**, *The glucocorticoid receptor: rapid exchange with regulatory sites in living cells.* Science, 2000. 287(5456): p. 1262-5.
145. **Becker, M., et al.**, *Dynamic behavior of transcription factors on a natural promoter in living cells.* EMBO Rep, 2002. 3(12): p. 1188-94.
146. **Dundr, M., et al.**, *A kinetic framework for a mammalian RNA polymerase in vivo.* Science, 2002. 298(5598): p. 1623-6.
147. **Chen, D. and S. Huang**, *Nucleolar components involved in ribosome biogenesis cycle between the nucleolus and nucleoplasm in interphase cells.* J Cell Biol, 2001. 153(1): p. 169-76.
148. **Essers, J., et al.**, *Nuclear dynamics of RAD52 group homologous recombination proteins in response to DNA damage.* EMBO j, 2002. 21(8):2030-7.
149. **Houtsmuller, A.B., et al.**, *Action of DNA repair endonuclease ERCC1/XPF in living cells.* Science, 1999. 284(5416): p. 958-961.
150. **Wakasugi, M. and A. Sancar**, *Assembly, subunit composition, and footprint of human DNA repair excision nuclease.* Proc Natl Acad Sci U S A, 1998. 95(12): p. 6669-74.
151. **Kowalczykowski, S.C.**, *Some assembly required.* Nat Struct Biol, 2000. 7(12): p. 1087-9.
152. **Sugasawa, K., et al.**, *HHR23b, a human RAD23 homolog, stimulates XPC protein in nucleotide excision repair in vitro.* Mol. Cell. Biol., 1996. 16(9): p. 4852-4861.
153. **Masutani, C., et al.**, *Purification and cloning of a nucleotide excision repair complex involving the xeroderma pigmentosum group C protein and a human homolog of yeast RAD23.* EMBO J., 1994. 13(8): p. 1831-1843.
154. **Shivji, M.K., A.P. Eker, and R.D. Wood**, *DNA repair defect in xeroderma pigmentosum group C and complementing factor from HeLa cells.* J Biol Chem, 1994. 269(36): p. 22749-57.
155. **Reardon, J.T., D. Mu, and A. Sancar**, *Overproduction, purification, and characterization of the XPC subunit of the human DNA repair excision nuclease.* J Biol Chem, 1996. 271(32): p. 19451-6.
156. **Wakasugi, M., et al.**, *DDB accumulates at DNA damage sites immediately after UV irradiation and directly stimulates nucleotide excision repair.* J Biol Chem, 2002. 277(3): p. 1637-40.
157. **Rapic-Otrin, V., et al.**, *Sequential binding of UV DNA damage binding factor and degradation of the p48 subunit as early events after UV irradiation.* Nucleic Acids Res, 2002. 30(11): p. 2588-98.
158. **Mu, D., et al.**, *Characterization of reaction intermediates of human excision repair nuclease.* J. Biol. Chem., 1997. 272(46): p. 28971-28979.
159. **Iyer, N., et al.**, *Interactions involving the human RNA polymerase II transcription/nucleotide excision repair complex TFIIH, the nucleotide excision repair*

protein XPG, and Cockayne syndrome group B (CSB) protein. Biochemistry, 1996. 35: p. 2157-2167.

160. **Matsunaga, T., et al.**, *Replication protein A confers structure-specific endonuclease activities to the XPF-ERCC1 and XPG subunits of human DNA repair excision nuclease.* J Biol Chem, 1996. 271(19): p. 11047-50.
161. **Shivji, M.K., et al.**, *Nucleotide excision repair DNA synthesis by DNA polymerase epsilon in the presence of PCNA, RFC, and RPA.* Biochemistry, 1995. 34(15): p. 5011-5017.
162. **Troelstra, C., et al.**, *ERCC6, a member of a subfamily of putative helicases, is involved in Cockaynes syndrome and preferential repair of active genes.* Cell, 1992. 71(6): p. 939-953.
163. **Ratner, J.N., et al.**, *Ultraviolet radiation-induced ubiquitination and proteasomal degradation of the large subunit of RNA polymerase II. Implications for transcription-coupled DNA repair.* J. Biol. Chem., 1998. 273(9): p. 5184-5189.
164. **Orphanides, G., T. Lagrange, and D. Reinberg**, *The general transcription factors of RNA polymerase II.* Genes Dev., 1996. 10(21): p. 2657-2683.
165. **Burley, S.K. and R.G. Roeder**, *Biochemistry and structural biology of transcription factor IID (TFIID).* Annu Rev Biochem, 1996. 65: p. 769-99.
166. **Lagrange, T., et al.**, *New core promoter element in RNA polymerase II-dependent transcription: sequence-specific DNA binding by transcription factor IIB.* Genes Dev, 1998. 12(1): p. 34-44.
167. **Flores, O., H. Lu, and D. Reinberg**, *Factors involved in specific transcription by mammalian RNA polymerase II. Identification and characterization of factor IIH.* J Biol Chem, 1992. 267(4): p. 2786-93.
168. **Wang, W., M. Carey, and J.D. Gralla**, *Polymerase II promoter activation: closed complex formation and ATP- driven start site opening.* Science, 1992. 255(5043): p. 450-3.
169. **Kumar, K.P., S. Akoulitchev, and D. Reinberg**, *Promoter-proximal stalling results from the inability to recruit transcription factor IIH to the transcription complex and is a regulated event.* Proc Natl Acad Sci U S A, 1998. 95(17): p. 9767-72.
170. **Goodrich, J.A. and R. Tjian**, *Transcription factors IIE and IIH and ATP hydrolysis direct promoter clearance by RNA polymerase II.* Cell, 1994. 77: p. 145-156.
171. **Holstege, F.C., U. Fiedler, and H.T. Timmers**, *Three transitions in the RNA polymerase II transcription complex during initiation.* Embo J., 1997. 16(24): p. 7468-7480.
172. **Zawel, L., K.P. Kumar, and D. Reinberg**, *Recycling of the general transcription factors during RNA polymerase II transcription.* Genes Dev, 1995. 9(12): p. 1479-90.

Chapter 5

Rapid Switching of TFIIH between RNA polymerase I and II Transcription and DNA Repair *in vivo*

Adapted from Molecular Cell. 10(5):1163-74 (2002)

Rapid Switching of TFIIH between RNA polymerase I and II Transcription and DNA Repair *in vivo*

Deborah Hoogstraten[1], Alex L. Nigg[2], Helen Heath[1], Leon H.F.Mullenders[3], Roel van Driel[4], Jan H. J. Hoeijmakers[1], Wim Vermeulen[1*+] and Adriaan B. Houtsmuller[2*]

[1]Department of Cell Biology and Genetics (Medical Genetics Center, CBG), Erasmus University, P.O.Box 1738, 3000 DR Rotterdam, the Netherlands,
[2]Department of Pathology (Josephine Nefkens Institute), Erasmus University, the Netherlands,
[3]Department of Radiation Genetics and Chemical Mutagenesis, (Medical Genetics Center, CBG), University of Leiden, Leiden, the Netherlands.
[4]Swammerdam Institute for Life Sciences, University of Amsterdam, the Netherlands

[*]These authors contributed equally to this work.
[+]To whom correspondence should be addressed. E-mail vermeulen@gen.fgg.eur.nl

Summary

The transcription/repair factor TFIIH operates as DNA helix opener in RNA polymerase II (RNAP2) transcription and nucleotide excision repair. To study TFIIH *in vivo* we generated cell lines expressing functional GFP-tagged TFIIH. TFIIH was homogeneously distributed throughout the nucleus with nucleolar accumulations. We provide *in vivo* evidence for involvement of TFIIH in RNA polymerase I (RNAP1) transcription. Photobleaching revealed that TFIIH moves freely and gets engaged in RNAP1 and RNAP2 transcription for ~25 and ~6 seconds respectively. TFIIH readily switches between transcription and repair sites (where it is immobilised for ~4 minutes) without large-scale alterations in composition. Our findings support a model of diffusion and random collision of individual components which permits a quick and versatile response to changing conditions.

Introduction

DNA is continuously damaged by endogenous reactive metabolites and exogenous chemicals and irradiation (Lindahl and Wood, 1999). A dedicated network of DNA repair mechanisms and cell cycle checkpoints safeguards DNA integrity to prevent the deleterious consequences of genetic degeneration notably mutations and cell death leading to cancer and aging respectively (Friedberg et al., 1995; Hoeijmakers, 2001; Wood et al., 2001). One of these DNA repair pathways, nucleotide excision repair (NER) removes a broad range of helix-distorting injuries e.g. UV-light induced pyrimidine dimers and bulky chemical adducts. The multi-step NER process requires the coordinated action of at least 25-30 polypeptides (Wood et al., 2001). Two modes of DNA damage detection exist: one by transcription-coupled repair (TC-NER) the other by global genome repair (GG-NER). In TC-NER an elongating RNA polymerase II (RNAP2) stalled by a lesion in the transcribed strand triggers efficient repair to allow quick resumption of the very cytotoxic blockage of transcription (Hanawalt and Spivak, 1999). Lesions anywhere in the genome are targets for the GG-NER pathway, primarily initiated by the XPC/hHR23B complex (Sugasawa et al., 1998), aided (for some types of damage) by the UV-DDB heterodimeric complex (Tang et al., 2000; Wakasugi et al., 2002). Subsequently transcription factor IIH (TFIIH) (Volker et al., 2001; Yokoi et al., 2000) locally opens a 25-30 nt. region of the DNA-duplex around the lesion (Evans et al., 1997). XPA verifies the damage, replication protein A (RPA) stabilizes the melted region and both properly position the 3' and 5' scissors, respectively, XPG and the heterodimer ERCC1/XPF (Hoeijmakers, 2001). After dual incision of the damaged strand and removal of the injury containing oligonucleotide the reaction is completed by gap-filling DNA synthesis and ligation (Araujo et al., 2000).
The nine-subunit TFIIH complex containing the XPB and XPD helicases (Egly, 2001), was initially identified as an essential component of the transcription initiation machinery of RNAP2 (Drapkin and Reinberg, 1994). After the assembly of the transcription pre-initiation complex (including TFIIB, D, E, F and RNAP2) on a promoter TFIIH opens the DNA helix (Holstege et al., 1996), like in NER, enabling promoter escape of the transcribing RNAP2 complex template (Dvir et al., 2001; Moreland et al., 1999).

Biochemical analysis of individual components and *in vitro* reconstitution has provided scenarios for the consecutive steps within transcription initiation and NER (Aboussekhra et al., 1995; Orphanides et al., 1996). These studies have strongly contributed to our understanding on each of these processes separately. However, it is becoming increasingly evident that NER and transcription are tightly linked both by the dual functionality of TFIIH and the existence of TC-NER. In addition, intimate connections exist between NER and other repair pathways, replication, recombination and cell cycle control, which have largely escaped experimental investigation (Citterio et al., 2000; Le Page et al., 2000). Holo-complexes for NER and transcription have been proposed and several models have been put forward to explain the differential

behavior of TFIIH in transcription and repair, such as: (i) distinct complex composition for each process (Svejstrup et al., 1995) (ii) specific modification of subunits (van Oosterwijk et al., 1998), and (iii) completely assembled transcription 'holo-complexes' containing also most of the repair constituents that roam the nuclear space in search for either promoters or DNA damage (Maldonado et al., 1996; Ossipow et al., 1995).
To examine the crosstalk between NER, TC-NER and transcription, to study the organization of these processes in living cells and to understand how TFIIH accomplishes its multiple engagements, we have tagged one of the core subunits of TFIIH, the xeroderma pigmentosum group B (XPB) 3'->5' helicase with enhanced green fluorescent protein (GFP). The fusion protein was stably expressed in human XPB mutant fibroblasts. Expressing cells were carefully selected for physiological expression levels and functionality in repair and transcription. Here we report on the dynamic *in vivo* nuclear distribution including preferential localization of TFIIH in nucleoli as well as protein mobility and kinetics of the differential engagements of TFIIH disentangled using photobleaching techniques, computer modeling and local DNA damage induction.

Results

Experimental Design

In a previous study we have determined *in vivo* protein dynamics and kinetics of engagement in NER of GFP-tagged ERCC1 expressed in CHO cells. The ERCC1/XPF complex is a core NER factor responsible for the incision 5' to the lesion. Protein immobilization, as a result of engagement in NER after UV-irradiation, was determined by applying a variant of fluorescence recovery after photobleaching (FRAP) (Houtsmuller et al., 1999). However, in contrast to the ERCC1/XPF complex, which is specifically involved in DNA repair, TFIIH has an intriguing dual engagement: NER and transcription initiation. Both engagements are expected to influence its overall nuclear mobility and behavior. In order to investigate this we applied several variants of FRAP.

GFP-tagged XPB is Expressed at Physiological Levels in Stably Transfected Cells

To visualize TFIIH in living cells we tagged one of the core-subunits, the XPB (xeroderma pigmentosum group B, 3'-> 5' helicase) with the live cell protein marker, green fluorescent protein (GFP). Since XPB is highly conserved in size and sequence from yeast to man and has to act in a complex with 8 other partners it was important to verify whether addition of a 27kD GFP tag did not influence its function. The functionality of the fusion construct (XPB-GFP) was first checked by microinjecting the XPB-GFP cDNA into XPB-mutated primary fibroblasts (that have a severe defect in DNA repair synthesis after UV-irradiation). One day after injection, cells with green fluorescent nuclei were clearly visible and they had regained wild type levels of DNA

repair synthesis (data not shown). Since the microinjection experiments suggested that the *XPB-GFP*, was functional in NER when transiently expressed, we generated a stably expressing cell line. NER-deficient, UV-sensitive human fibroblasts with an endogenous mutated *XPB* (Vermeulen et al., 1994) (XPCS2BA-SV40) were transfected with the XPB-GFP cDNA. Stably XPB-GFP expressing subpopulations were isolated after UV-selection and further selected on the basis of the expression level of the fusion protein. As shown by immunoblot analysis (Figure 1A), the total cellular content of GFP-tagged and endogenous XPB in different clones remained strikingly constant: a relatively high level of XPB-GFP coincides with low expression of endogenous mutated XPB and *vice versa* (Figure 1A). The total amount of XPB protein (GFP-tagged plus endogenous) did not exceed wild type expression levels, as previously noticed using HA-tagged XPB (Winkler et al., 1998).

To verify whether the GFP-tagged version of XPB was able to fit into the TFIIH immunoprecipitation experiments were performed, using antibodies against p62 (another core TFIIH subunit). As demonstrated in Figure 1B, the XPB-GFP was as efficiently incorporated into the complex as endogenous mutant XPB. Since the fusion protein appeared to be an integral component of the core TFIIH complex, we hereafter refer to it as TFIIH-GFP.

TFIIH-GFP is Functional in Repair and Transcription

To verify whether physiological levels of GFP-tagged TFIIH are functional in DNA repair, the stably expressing cells were tested for their UV-sensitivity. UV-survival experiments revealed that XPB-GFP completely corrected the severe UV-sensitivity of XPCS2BA-SV40 cells (Figure 1C). Moreover, cells with a high proportion of XPB-GFP (Figure 1A, lane 4) and consequently low quantities of endogenous mutant XPB, have levels of RNA synthesis comparable to wild-type cells: 107 % of wild-type (MRC5) whereas the recipient (XPCS2BA-SV) cells have 91 % of the level of MRC5 (as determined by ^{3}H-uridine incorporation). This strongly suggests that GFP-tagged TFIIH is also active in transcription. This generated cell line is a bonafide tool to study the spatio-temporal distribution of TFIIH *in vivo* since TFIIH-GFP expression is at physiological levels and the tagged complex is functional in repair and transcription.

TFIIH-GFP is Homogeneously Distributed in the Nucleoplasm but is Enriched in Nucleoli

As expected TFIIH-GFP was located in the nucleus. However, unexpected for a factor engaged in RNAP2 transcription we observed a focal accumulation of TFIIH-GFP in nucleoli (hereafter referred to as nucleolar clusters or NCs), on top of an overall homogeneous distribution over the entire nucleus (Figure 1D). This localization is in concordance with the recently described role for TFIIH in RNAP1 transcription *in vitro*

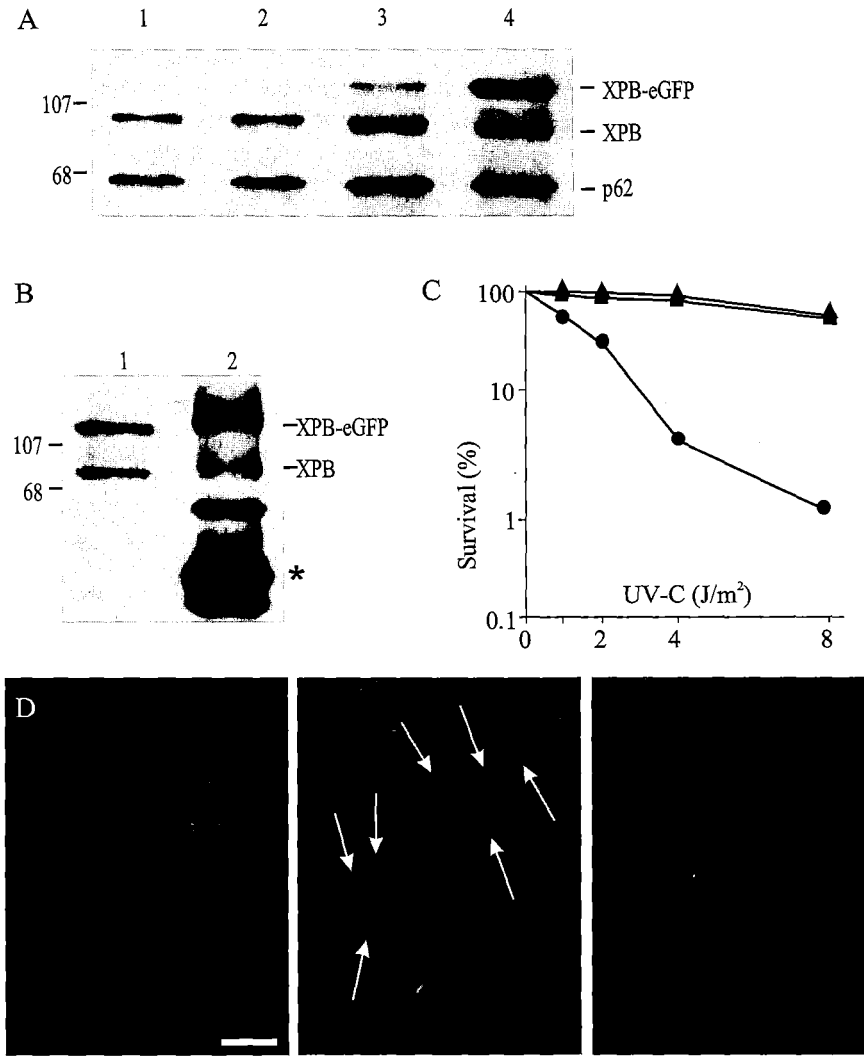

Figure 1. Characterization of XPB-GFP Expressing Cells
(A) Immunoblot probed with anti-XPB and anti-p62 monoclonals of WCE of MRC5 (repair-proficient), and XPCS2BA (lanes 1 and 2) and two FACS-sorted populations of XPCS2BA cells stably expressing XPB-GFP (XPB-GFP cells) at a relatively low and high level respectively (lanes 3 and 4). Note that the total XPB content is similar in low and high expressing cells. Molecular weight markers indicated at the left are in kDa. (B) Immunoblot of anti-p62 immunoprecipitated WCE of XPB-GFP expressing cells probed with an anti-XPB antibody ,lane 1 WCE and lane 2 precipitated TFIIH. Band marked with (*) represents the heavy IgG chains of anti-p62. (C) Survival after UV irradiation of MRC5 (squares), XPCS2BA (circles), and XPB-GFP cells (triangles). The percentage of surviving cells is plotted against the applied UV-C dose. (D) Confocal and transmitted light image of two XPB-GFP cells. White arrows indicate nucleoli. Left panel: GFP-fluorescence, middle: phase-contrast, right: merged image. Scale bar is 5 μm.

(Iben et al., 2002). In addition, we clearly observed co-localization of TFIIH nucleolar accumulations with RNA polymerase I (RNAP1) (Figure 2A). Moreover, microinjection of different antibodies, against three distinct subunits of TFIIH, induced a strong, rapid reduction of rRNA transcription, as determined by in situ ^{3}H-uridine incorporation and autoradiography. The number of grains above nucleoli was clearly diminished in nuclei of cells injected with polyclonal Rabbit anti-XPB serum (red arrows in Figure 2B), as compared to non-injected neighboring cells (dark areas containing numerous grains, green arrows in Figure 2B). In fact inhibition of nucleolar transcription in general was more pronounced than that in the remainder of the nucleus. These findings are consistent with an *in vivo* involvement of TFIIH in RNAP1 transcription.

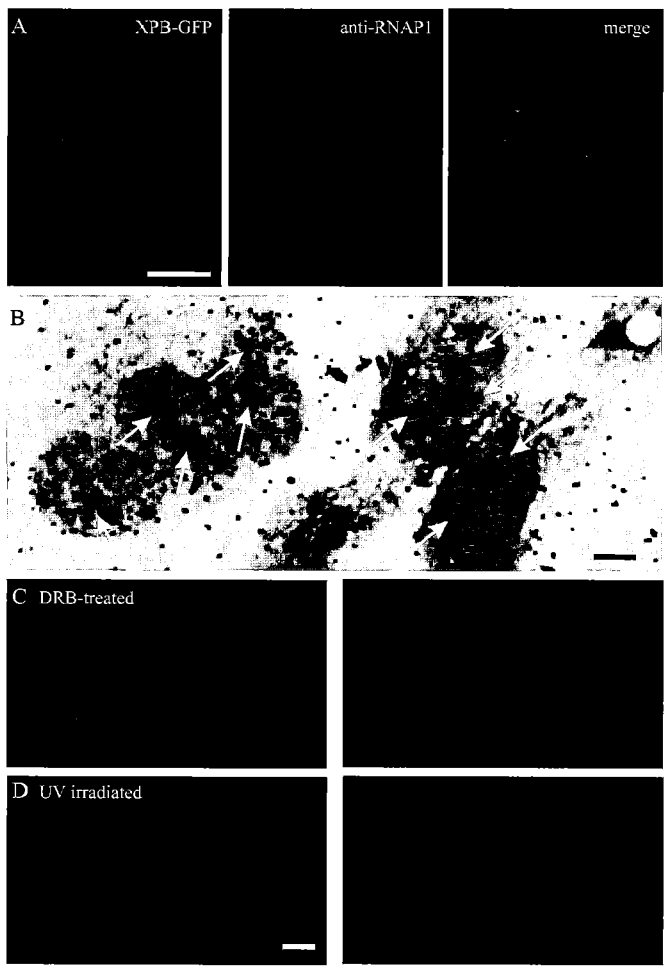

Figure 2. Characterization of the Nucleolar Accumulation in XPB-GFP Expressing Cells under Different Conditions.
(A) Confocal image of a fixed XPB-GFP cell. Left panel: GFP-fluorescence, middle: anti-RNAP1 immunofluorescence, right: merged image. (B) Transcription after microinjection of a polyclonal antibody directed against XPB visualized by auto-radiographic grains after in situ 3H-uridine incorporation. Left arrows indicate nucleoli in microinjected cells and right arrows nucleoli of non-injected neighboring cells. Note that the nucleoli are much darker in non-injected cells because they are covered by grains. (C) Cells 3 hours after incubation with transcription inhibitor DRB (100 μM). (D) cells 5 minutes after irradiation with 8 J/m2 UV. Confocal images, left: GFP-fluorescence, right: GFP-fluorescence merged with phase-contrast image. Scale bars are 5 μm.

Transcription Inhibition and UV-irradiation Abrogate Nucleolar Localization of TFIIH-GFP

The *in vivo* evidence for a role of TFIIH in nucleolar RNA synthesis was further corroborated by studies involving different types of transcription inhibitors. Inhibition of transcription using 5,6-dichloro-1β-D-ribofuranosyl benzimidazole (DRB) induced a dramatic change in TFIIH nucleolar distribution from NCs to discrete foci around the nucleolus (Figure 1D, 2C). These structures also contained RNAP1 and resembled the 'nucleolar necklace' previously observed after DRB treatment (Granick, 1975), in which ribosomal transcripts and various transcription factors of the RNAP1 machinery are found. After DRB removal, both TFIIH and RNAP1 relocalized into NCs within ~4 hrs (data not shown). Importantly, within a few minutes after UV-irradiation (16 J/m^2), causing DNA damage and consequently transcriptional arrest of RNAP2 and possibly RNAP1, the nuclear distribution of TFIIH-GFP was completely homogeneous, also in the nucleoli where no accumulation was present (Figure 2D). The localization of TFIIH in nucleoli of living cells, its co-localization and co-behavior with RNAP1 upon transcriptional interference and the observed inhibition of nucleolar transcription after injection of TFIIH antisera, provide *in vivo* evidence for involvement of TFIIH in RNAP1 transcription.

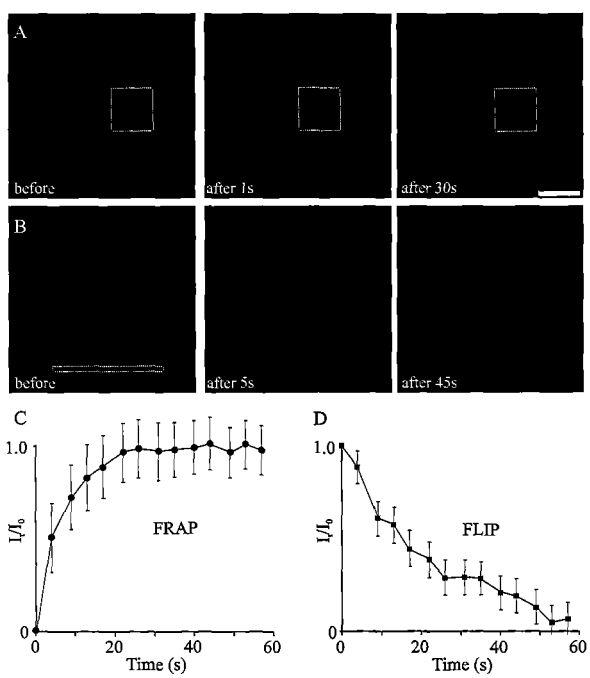

Figure 3. FRAP Analysis of the Dynamics of Nucleolar Stuctures by Photobleaching. (A) FRAP of a nucleolar cluster. The nucleolar accumulation in the square is bleached. Left: before bleaching, middle: 1 second after bleaching, right: 30 seconds after bleaching. (B) FLIP of a nucleolar cluster. The region within the strip is bleached. Left: before bleaching, middle: 5 second after bleaching, right: 45 seconds after bleaching. (C) FRAP curve of a nucleolar cluster. Relative fluorescence is plotted against time. (D) FLIP curve of a nucleolar cluster. The time until complete recovery is longer in the FLIP than in the FRAP experiment since in FLIP bleached molecules have to diffuse from the bleached area to the nucleolar clusters. Scale bar is 5 μm.

Association of TFIIH with Nucleoli is Highly Dynamic

To investigate whether TFIIH is stably associated with the observed nucleolar structures or whether it is in a dynamic equilibrium with the freely mobile pool we applied standard variants of photobleaching (Essers et al., 2002). Fluorescence recovery after photobleaching (FRAP) of NCs (Figure 3A) revealed a dynamic interaction of TFIIH with nucleoli: within 20 to 30 seconds fluorescence was fully regained in previously bleached nucleoli (Figure 3C), indicating a quick exchange of bleached TFIIH molecules from the nucleoli with fluorescent molecules outside. The observed decay of fluorescence in nucleoli, after bleaching of a distant region in FLIP (fluorescence loss in photobleaching) experiments, suggested a similar rate of exchange between nucleoli and nucleoplasm (Figure 3B, D) as detected by FRAP. This swift replacement suggests that the pool of non-nucleolar TFIIH moves through the nucleus with a relative high mobility. In conclusion, the bleaching studies indicated that individual TFIIH molecules are transiently associated with RNAP1 transcriptional machinery.

TFIIH is Transiently Engaged in Transcription

To study the mechanism of action of TFIIH in RNAP2 transcription initiation we used different variants of FRAP, FLIP and a combination of both (see below). Overall nuclear mobility was determined using FRAP with a high temporal resolution (100 ms) (Ellenberg et al., 1997; Essers et al., 2002; Houtsmuller and Vermeulen, 2001) (Figure 4A). Briefly, a narrow strip spanning the entire nucleus is bleached for 100 ms at high laser power and recovery of fluorescence in the strip by influx of non-bleached TFIIH-GFP was monitored at 100 ms intervals with low laser power. The effective diffusion coefficient (D_{eff}) determined in untreated cells appeared significantly lower than in transcription-inhibited cells using DRB (5.1 ± 1.0 and 6.2 ± 1.0 $\mu m^2/s$, respectively; $p = 0.022$) (Figure 4B). However, the shape of the fluorescence recovery curve of untreated cells suggested a biphasic process: an initial rapid recovery (in the first seconds) similar to the one determined in DRB-treated cells, and a secondary slower component absent in DRB-treated cells. The initial recovery is probably due to a freely diffusing TFIIH pool, whereas the latter may be due to a shortly (< 10 s) immobilized fraction released during monitoring. Indeed, the diffusion coefficient of the fast component ($D_{eff} = 5.9 \pm 0.9$ $\mu m^2/s$), determined on the basis of the first two seconds of recovery, is not significantly different ($p = 0.48$) from the one found in transcription-inhibited cells, suggesting that transcription inhibition abolished the transient immobilization events. Curves obtained by computer simulation fitted best to the experimental plots when the transient immobility parameters were in the range of 20-40% of TFIIH bound for 2-10 seconds. The scenario in which TFIIH freely diffuses and a fraction is shortly bound in a transcription-dependent manner was further investigated with a different photobleaching procedure in which we simultaneously determine FRAP and FLIP in the same nucleus (Figure 4C).

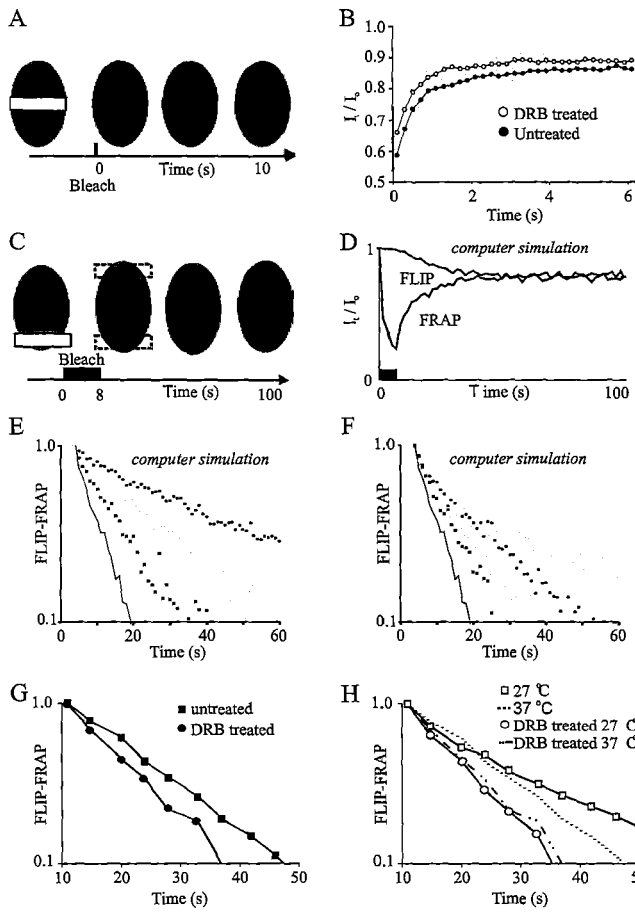

Figure 4. FRAP Analysis of TFIIH Engagement in Transcription Initiation.
(A) Scheme of temporal strip-FRAP analysis to determine effective diffusion coefficients. Green ellipses represent confocal images of cell nuclei, where darker regions contain fluorophores bleached by a focused laser beam; grey bars represent bleach pulses. A strip spanning the entire nucleus is photobleached for 100 ms at high laser intensity. The recovery of fluorescence in the strip is monitored at low laser intensity. (B) Temporal FRAP analysis of untreated (n=90, closed circles) and transcription inhibited (DRB) cells (n=70, open circles). (C) Scheme of simultaneous FRAP/FLIP analysis used to determine the TFIIH-GFP mobility. A small area at one side of a nucleus is bleached at relatively low laser intensity for a relatively long period of time (8 s). Subsequently fluorescence is monitored at regular time intervals in the bleached area and in a region at the other side of the nucleus. (D) Computer simulation curves of the (log) of fluorescence redistribution difference between FRAP and FLIP determined in the two areas indicated in (C). (E) Simulations of molecules with different diffusion coefficients (D = 10 (black line), 5 (closed squares), 2.5 (open squares) and 1.25 (closed circles) $\mu m^2/s$, respectively. (F) Computer simulations of molecules with constant diffusion rates (10 $\mu m^2/s$) and an immobile fraction of 40% with increasing binding times of 7 s (closed squares), 14 s (open squares), 28 s (closed circles) and 56 s (open circles), black line as in (E). Note that in this method correction should be made if nuclei have different size. (G) Simultaneous FRAP/FLIP analysis of untreated and transcription inhibited (DRB treated) cells at 37 °C (closed squares and circles respectively). (H) Simultaneous FRAP/FLIP analysis of untreated and transcription inhibited cells at 32 °C (open squares and circles respectively). The curves of untreated cells and DRB treated cells at 37 °C (dotted lines) as a reference.

Briefly, a strip at one pole of the nucleus is bleached and subsequently fluorescence is monitored in both the bleached strip (FRAP) and at the opposite pole of the nucleus (FLIP) (Figure 4D). The kinetics for both regions to reach equal fluorescence intensity (*i.e.* complete mixing of bleached and non-bleached molecules) initially depends on the

diffusion of free molecules and later on molecules that are delayed by transient binding (see computer simulation curves in Figure 4E, F). We observed a significant shorter redistribution time in transcriptionally inhibited cells (37 s, including bleach time, to reach >90% homogeneous redistribution of fluorescence) compared to active cells (47 s) (Figure 4G). This confirms that the delay in reaching complete fluorescence distribution was due to short-lived interactions of TFIIH with the transcription machinery. The notion that the overall mobility of TFIIH was delayed by transient, transcription-dependent, immobilization events was further supported by the finding that complete redistribution took significantly longer in transcriptionally active cells cultured at 27 °C (65 s) than at 37 °C (47 s). However, redistribution times in transcription-inhibited cells were similar at both temperatures (36 s versus 37 s) (Figure 4H). A decrease in temperature (here 10 K) has only a marginal effect on diffusion (as passive diffusion is linear with temperature), but strongly influences the duration of enzymatic processes (Phair and Misteli, 2000). Together these data support the idea that in transcriptionally active cells TFIIH is present in different kinetic pools: (i) a freely diffusing fraction, (ii) a (temperature-sensitive) fraction of 20-40% that is transiently immobilized when engaged in RNAP2 transcription initiation (2 to 10 s, based on computer simulation) and (iii) a fraction transiently associated with nucleoli most likely involved in RNAP1 transcription. The residence time in nucleolar clusters was longer than the estimated binding time in RNAP2 transcription (~ 25 s versus 2-10 seconds).

Residence Time of TFIIH at DNA Lesions is in the Order of Minutes

To investigate the engagement of TFIIH in NER and the effect on the mobility properties induced by NER-specific lesions we exploited the ability to instantaneously introduce DNA damage in the nucleus by UV irradiation and follow the response of TFIIH FRAP analysis. A relatively high dose of UV-light is expected to present suddenly a high concentration of potential binding sites for TFIIH that may drastically influence the equilibrium between the different dynamic pools.

Strip-FRAP analysis of UV-damaged cells (16 J/m^2, a repair-saturating UV dose) revealed a severe reduction in the amount of fluorescence recovery (blue line, Figure 5A) when compared to non-UV-damaged cells (green line). This incomplete recovery indicates that a significant (~40%, at 16 J/m^2) fraction of TFIIH molecules is immobilized for a relatively long period of time. The fact that non-NER factors (such as GFP and androgen receptor-GFP) were not immobilized upon UV exposure (Houtsmuller et al., 1999), suggests that this binding is NER-specific. The magnitude of the immobile fraction was directly related to the amount of induced DNA damage (UV-dose) up to the saturation point of repair (Figure 5B). The immobilized fraction gradually decreased to background levels within a few hours after damage induction, similar in kinetics to the decline of DNA repair activity in time (data not shown).

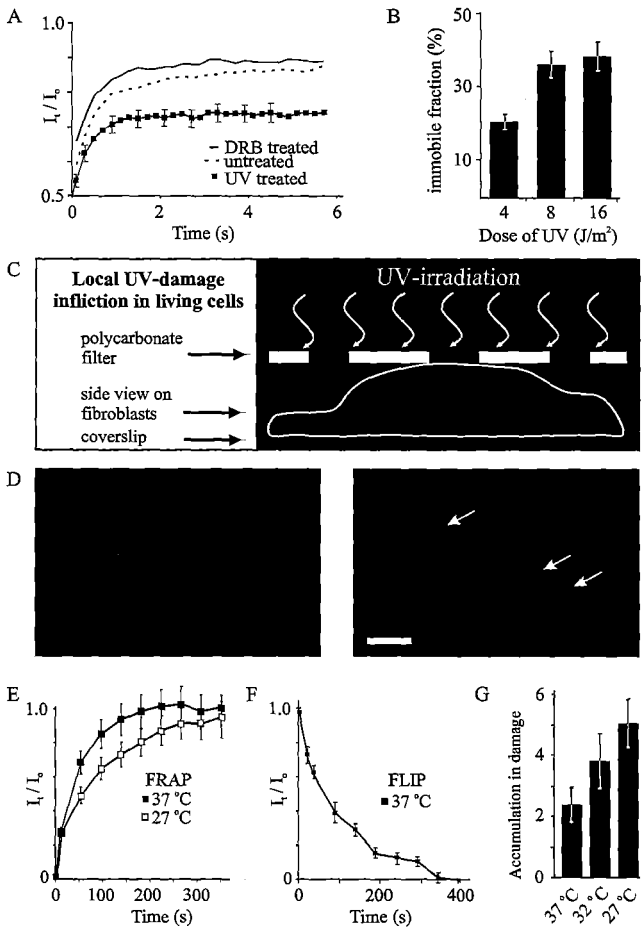

Figure 5. FRAP Analysis of DNA Damage Induced TFIIH Immobilization.
(A) Temporal FRAP analysis of UV-irradiated cells (squares). DRB treated (black curve) and untreated cells (dotted curve) (Figure 4B) are shown as references. (B) UV-dose dependent immobilization of TFIIH. Percentage of immobilization is plotted against UV-dose. (C) Scheme of the procedure to locally irradiate living cell nuclei showing a confocal XZ-scan of a TFIIH-GFP expressing cell covered by a UV-blocking membrane (white) containing 5 μm-wide pores. (D) Confocal images of locally UV-irradiated TFIIH-GFP cells 5 minutes after irradiation (UV-dose applied to the membrane: 48 J/m^2). Left panel: GFP-fluorescence, right: merged image together with phase-contrast. Black arrows indicate the accumulation of TFIIH at the sites of local UV-damage. White arrows indicate the accumulation of TFIIH in the nucleoli. Scale bar is 5 μm. (E) FRAP curves of the UV-damaged area of cells cultured at 27 and 37 °C (open and closed squares, respectively). (F) FLIP curve of the locally damaged-area. (G) Ratio between fluorescence in the damaged area and fluorescence in the remainder of the nucleoplasm at different temperatures (n=35 for each temperature), showing that at lower temperature the amount of accumulated TFIIH is considerably increased.

Together these results suggest that the observed binding is a consequence of active DNA repair, and indicate that ERCC1/XPF is not exceptional in its behavior after UV exposure (Houtsmuller et al., 1999). Moreover, UV-light did not largely affect the mobility (D_{eff} = 6.0 ± 0.2 μm^2/s) of the remaining non-bound fraction of TFIIH molecules. This suggests that the presence of lesions does not lead to formation of mobile repair precursor complexes or the dissociation of mobile transcription precursor complexes.

To further study the behavior of TFIIH in NER we utilized a protocol that permits induction of DNA damage at restricted areas of the nucleus. To that aim, cells were

covered with a UV-blocking membrane containing randomly distributed pores with a diameter of ~5 μm (Figure 5C) resulting in nuclei with local UV damage. Very soon after UV-irradiation (within ~2 minutes) TFIIH-GFP accumulated in bright fluorescent regions in most cell nuclei (Figure 5D). This fluorescence accumulation in UV-damaged regions is specific for TFIIH, since free GFP as well as hRAD52-GFP (J. Essers, personal communication) do not accumulate. Immunofluorescent studies on fixed cells already showed that most NER factors, including TFIIH, concentrate to areas containing large amounts of UV-damage (Mone et al., 2001; Volker et al., 2001). Here we show in living cells that the recruitment of TFIIH is very fast and reaches a steady-state situation within only few minutes after damage induction, further illustrating the high mobility of this complex in the nucleoplasm.

Local damage has the important advantage that residence times of proteins in these regions can be directly determined using photobleaching techniques. Both FRAP and FLIP analysis (similar to the study of nucleoli) revealed that TFIIH-GFP molecules reside in the damaged area in the order of ~4 minutes (Figure 5E,F). Comparable DNA repair-dependent immobilization times were previously determined for ERCC1-GFP/XPF, albeit in a more indirect way in cells that were completely irradiated (not locally) (Houtsmuller et al., 1999). Interestingly, the residence time was ~1.5 fold longer when temperature was decreased from 37 °C to 27 °C (Figure 5E). This indicates that TFIIH immobilization is due to the participation in a temperature-dependent process, entirely consistent with enzymatic engagement in the NER reaction. Interestingly, at lower temperatures the number of accumulated molecules in the damaged area appeared significantly increased (Figure 5G). This observation suggests that TFIIH reaches damaged sites by passive diffusion and binding of TFIIH *per se* to these sites is not a temperature-dependent step.

TFIIH Rapidly Switches between Transcription and Repair

It has been reported previously that transcription is still active in areas outside locally UV-irradiated regions (Mone et al., 2001). To investigate whether transcription kinetics were influenced by the presence of damage elsewhere in the same nucleus (Figure 6A), we applied the combined FRAP-FLIP method on the non-irradiated area of locally irradiated cells. The mobility and binding characteristics of TFIIH-GFP in those areas appeared unaffected by the presence of damage elsewhere (compare Figure 6B with Figure 4G), suggesting that transcription kinetics outside the damaged area are similar to that in non-irradiated cells. This was confirmed by the fact that a decrease in temperature led to a significant reduction of TFIIH mobility (Figure 6C, green line open squares) similar to that observed in unirradiated cells. Temperature-dependent reduction was completely abolished when cells were pretreated with the RNAP2 inhibitor α-amanitin (Figure 6C, red line open circles). These data argue against a trans-acting effect of UV-lesions on the involvement of TFIIH in transcription and provides *in vivo* evidence for previously published data (Mone et al., 2001). In

addition, the nucleolar accumulations of TFIIH are still present when cells contain UV-damaged DNA in a restricted area, suggesting that the role of TFIIH in rRNA synthesis is also not affected *in trans* by the presence of DNA lesions. The observation that involvement of TFIIH in NER does not affect its kinetics in RNAP1 or RNAP2 transcription and *vice versa*, and that the mobility of free TFIIH is unaltered by participation in either of these processes suggests that TFIIH divides its attention in a stochastic manner, by random collision and diffusion, rather than by some regulated process. Moreover, it suggests that TFIIH does not require large-scale modification that would affect its effective diffusion to switch from one to another process.

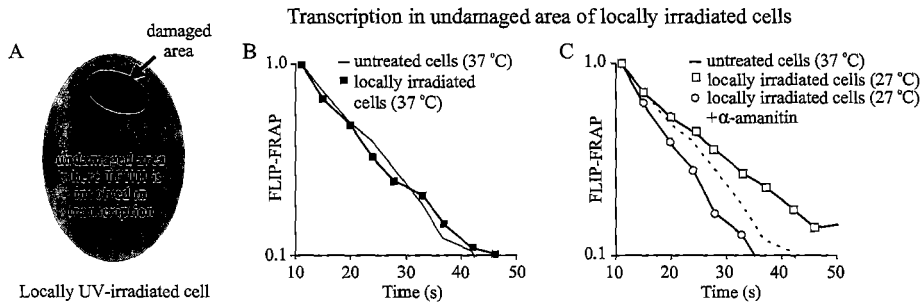

Figure 6. Simultaneous FRAP/FLIP Analysis in Unirradiated Areas of Locally Damaged Cells.
(A) Scheme to show where transcription is measured in locally irradiated cells. Dark gray is the locally irradiated area and light gray where transcription initiation is measured. (B) Difference in fluorescence intensity in the FRAP and FLIP areas after bleaching plotted against time (see also figure 4C and D). Closed squares represent mobility measurements in the undamaged area of locally irradiated nuclei. Black line represents undamaged nuclei at 37 °C (n=20). (C) Similar graphs as in (B) of cells cultured at 27 °C in presence (open circles) and absence (open squares) of transcription inhibitors (α-amanitin) (n=20). Dotted line: untreated cells at 37 °C.

Discussion

The most striking feature of TFIIH is its multifunctionality, particularly its versatile engagement in completely distinct processes: promoter opening and phosphorylation of the carboxy-terminal domain of RNAP2 in the context of transcription and DNA opening in the setting of nucleotide excision and transcription-coupled repair. Very recently, evidence has been obtained for an additional involvement in RNAP1 transcription initiation (Iben et al., 2002). Hitherto these functions have mainly been studied using *in vitro* assays. Here we have explored the function of transcription/repair factor TFIIH in its most relevant context: the living cell nucleus. Our results support a stochastic principle for the participation of TFIIH in NER and RNAP1 and RNAP2 transcription. The complex is omnipresent in the nucleus, moves freely by diffusion and in this random fashion gets access to sites of activity where it becomes transiently engaged in one of its transactions (Figure 7). When little or no damage is present, both

RNAP1 and RNAP2 transcription are the major activities of TFIIH. Under these conditions the complex was homogeneously distributed, arguing against the formation of stable immobile transcription factories (for a review see (Cook, 1999). When cells are UV-irradiated, the equilibrium of bound and unbound TFIIH quickly shifts towards TFIIH bound in DNA repair events. This explains the rapid change in subnuclear distribution of TFIIH upon UV-irradiation (Figure 1D and 2D).

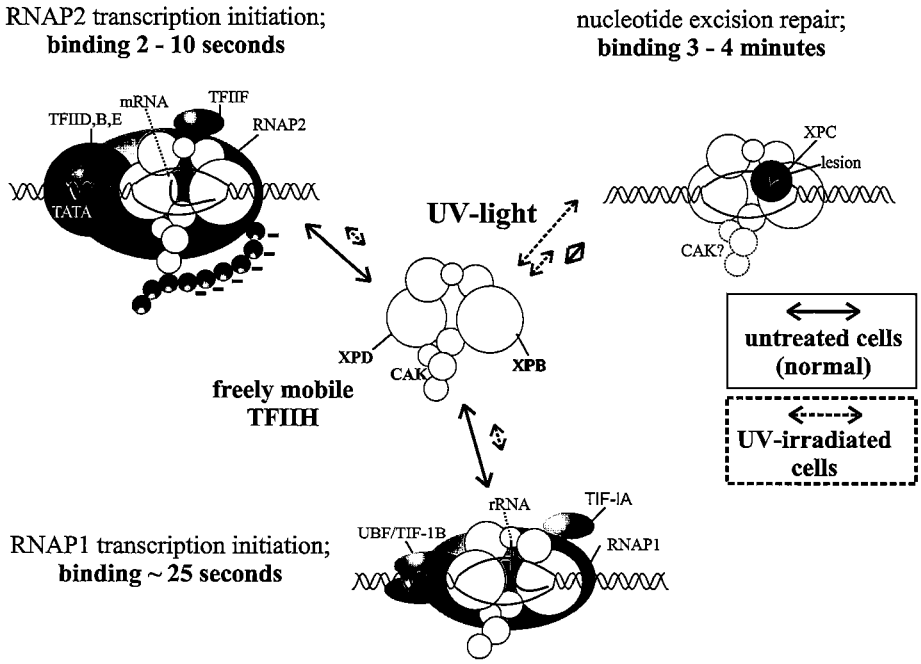

Figure 7. Model for the Dynamic Switching of TFIIH between RNAP1, RNAP2 Transcription Initiation and NER.
The arrows represented the equilibrium between the different kinetic pools under unchallenged (normal) conditions. After induction of UV-lesions a rapid shift in the equilibrium towards association in NER occurs (as indicated by the dotted arrows), in which TFIIH is engaged for a significantly longer period of time.

This model is based on several observations: (i) in living cells, the majority of TFIIH is freely mobile. The effective diffusion coefficient of free TFIIH (6.2 $\mu m^2/s$), as determined by FRAP is consistent with its molecular size (when compared with a number of other GFP-tagged proteins, assayed in the same manner (Houtsmuller et al., 1999)) and appears unaltered in UV-irradiated cells. (ii) TFIIH interacts with both RNAP1 and RNAP2 transcription machineries in a highly dynamic manner. Using various FRAP assays, we found no evidence for the existence of significant amounts of a long-lived immobilized fraction in transcriptionally active cells, indicating that TFIIH

is not present in permanent transcription assemblies. However, in transcription-inhibited cells TFIIH mobility was significantly higher than in transcriptionally active cells. Comparison of the FRAP mobility data with computer simulation suggests that the observed mobility increase is caused by absence of transient immobilizations (residence times 2-10 sec), rather than by overall faster diffusion. These transient immobilizations are likely due to engagement in transcription initiation. (iii) The residence times of TFIIH were significantly increased at lower temperatures in transcriptionally active, but not in inhibited cells. This strongly supports the idea that the observed TFIIH immobilization is due to involvement in transcription, since the energy-dependent steps in this process are temperature sensitive. Interestingly, the relative increase in residence time for TFIIH when implicated in NER (Figure 5E, G) was in the same range as found in transcription (Figure 4H). (iv) Immediately after damage induction by UV-irradiation the short-lived binding events of TFIIH in transcription were abolished, including association with the nucleolar clusters. Instead, a significant fraction of TFIIH molecules was now immobilized in NER complexes with an average residence time for individual molecules of ~ 4 minutes (Figure 5E, F). (v) Measurements in nuclei containing local damage support the idea that TFIIH operates simultaneously in repair, RNAP1 and RNAP2 transcription. Moreover, the presence of damage does not affect the binding behavior of TFIIH in transcription in undamaged regions (Figure 4H; 6B,C), nor its effective rate of diffusion. This indicates that multifunctional TFIIH can interact with and rapidly exchange between transcription sites and damage without large-scale modifications.

TFIIH in Transcription

TFIIH appeared homogeneously distributed through the nucleoplasm with disperse clusters co-localizing with RNAP1 in nucleoli. This remarkable observation provides *in vivo* support for recently published results indicating that TFIIH is involved in RNAP1 transcription (Iben et al., 2002). This was further corroborated by the observation that microinjection of monospecific antisera against TFIIH components predominantly inhibited nucleolar (rRNA) transcription and by co-behavior of TFIIH and RNAP1 in response to various treatments (Figure 1D and 2C, D). Nucleolar accumulation of TFIIH can be explained by a longer retention time of individual TFIIH complexes in these structures, or by a higher concentration of binding sites or a combination of both. This is likely related to the high frequency of successive RNAP1 transcription initiation events at clustered ribosomal genes. In the presented bleaching studies we determined an average residence time of ~25 seconds (as compared to the estimated immobilization time in RNAP2 transcription of 2-10 seconds). This suggests that transient binding of individual TFIIH complexes in RNAP1 promoters has a longer duration than its engagement in RNAP2 transcription initiation. Regardless the differences in binding or action times we presume that the principal function of this complex in both systems is similar. TFIIH may induce or stimulate the formation of an

open structure in the template to allow processive transcription. In view of the longer retention time in rRNA transcription one binding event of TFIIH may allow multiple rounds of transcription initiation.

The dynamic, short-term association of TFIIH in RNAP2 transcription initiation, is in accordance with previous experiments (Dvir et al., 1996; Timmers, 1994). In these *in vitro* studies it was reported that TFIIH is the last factor to enter the pre-initiation complex and the first one to leave. A similar type of short term 'hit-and-run' association has been described for the glucocorticoid receptor with the transcriptional machinery (McNally et al., 2000). However, when not only the time of interaction is considered, but also the frequency at which events take place (20-40% of TFIIH is immobilized based on computer simulation), the presented model suggests a rather large number of transcription initiation events at a given moment. It has been estimated that within mammalian cells ~1.1 x 10^5 TFIIH molecules reside (Kimura et al., 1999), with ~30% of these bound to RNAP2 promoters this would suggest ~3 x 10^4 ongoing transcription initiation events each time. This figure equals the total number of human genes. Therefore, it is likely that only a fraction of interactions lead to the successful completion of a transcription initiation event providing at the same time a window of opportunities for regulation.

TFIIH in NER

In striking contrast to transcription the engagement of TFIIH in NER events takes minutes in stead of seconds. As we found for different GFP-tagged NER factors different effective diffusion rates, each consistent with the molecular size of the specific factor or stable complex, we anticipate that each factor migrates separately in the nucleoplasm. Several options can be envisaged for their actual involvement in NER: i) a hand-over model in which every factor participates sequentially; ii) each NER factor is engaged in NER for a different time (open house model) or iii) all factors rapidly assemble in a sequential order at the site of the damage, forming a large complex that after completion of the reaction dissociates. Interestingly, in the case of photobleaching of the ERCC1-GFP/XPF NER complex (Houtsmuller et al., 1999) and XPA-GFP (manuscript in preparation) we obtained very similar values as observed for TFIIH (residence time ~4 minutes). The fact that all these NER components display comparable binding times suggests that they form one stable assembly in a relatively short time and that after a relatively long period all factors are simultaneously released. As argued before the NER binding time of ~4 minutes corresponds very well with the average time of a single NER event calculated from the number of lesions induced, the number of repair protein molecules actually engaged in NER and the time required to remove all induced lesions (Houtsmuller et al., 1999). Another interesting observation in the case of local DNA damage is the continuation of TFIIH participation with the same kinetics in transcription despite the presence of a high level of DNA injury

elsewhere in the nucleus. This illustrates the independence and versatility of the system and the ability of TFIIH to rapidly switch from one engagement to another.

Free Diffusion, Random Collision and Affinity Determine TFIIH Activity and Involvement in Various DNA Transactions

All our data support a scenario, in which repair and transcription proteins diffuse in relatively small complexes and assemble in a sequential order at the sites of action. For several reasons such a principle may be favourable to a design in which large, preassembled 'holo-complexes' are involved. Free diffusion of small subunits allows them to function in and rapidly exchange between multiple processes and warrants a quick response to changing conditions within or outside the cellular environment, *e.g.* regulatory signals or DNA damaging agents. TFIIH provides a prime example of this. Investigations of S.cereviseae suggested the presence of a preassembled 'repairosome' (Svejstrup et al., 1995). In yeast however, such a holo-complex could be favorable, since these rapidly dividing cells may require a quicker response to DNA damage. In addition, the organization of nuclear processes in yeast may differ from mammalians due to its smaller and less complex genome.

In addition to facilitation of multi-functionality and versatility, small constituents have more efficient access to DNA damage or specific sequences in condensed chromatin than bulky holo-complexes. In the case of TFIIH the observed homogeneous distribution permits this factor to be always in the vicinity of DNA lesions or promoters. Sequential assembly enables also refined regulation and options for premature abortion of the reaction when necessary (Kowalczykowski, 2000). These features are more difficult to realize with inert, massive holo-complexes. Probably similar scenario's hold for *RAD52* group proteins (Essers et al., 2002), messenger RNA processing factors (Phair and Misteli, 2000), and transcription factors (McNally et al., 2000) which show rapid exchange and histones (Misteli et al., 2000) which form more stable complexes. Thus, the principles deduced here may have more general validity.

Experimental procedures

Construction and Expression of XPB-GFP Fusion Protein

EGFP (Clontech) was cloned in frame to the C-terminus of XPB and transfected to XPCS2BA SV cells. Transfectants were selected with 250 μg/ml G418 (Sigma). An UV-resistant population that survived three UV-exposures (4 J/m^2) was isolated. All cell strains were cultured in RPMI + hepes (Life technologies) supplemented with 10% fetal calf serum, and maintained in a humidified 5% CO_2, 37 °C incubator. Whole-cell extracts (WCE) prepared by sonication were separated on 11% SDS-PAGE and transferred to Nitro-cellulose membranes. Expression of the fusion gene was analyzed by hybridizing the membranes with a monoclonal anti-XPB antibody (J.M. Egly), followed by a secondary antibody rabbit anti mouse conjugated with Horseradish

peroxidase (DAKO) and detected using enhanced chemoluminescence (ECL; Amersham). WCE were prepared by using a lysisbuffer containing 20 mM TEA, 0.7 M NaCl, 0.5% NP40, 0.2% DOC and 400 µg/ml CLAP. After 15 min 10000 rpm 4 °C, 2 µl p62 anti-serum (J.M. Egly) was added and incubated for 2 hours at 4 °C. 50 µl of protein A sepharose was added overnight. The beads were washed twice with lysisbuffer and boiled in the presence of loading buffer. The endogenous XPB and fusion protein were visualized as described above.

Microinjection

Polyclonal XPB-antibodies were microinjected into homo-polykarions of C5RO. After 15 hours the RNA synthesis was visualized by 1 hour pulse-labeling with ^{3}H-uridine as described in (Vermeulen et al., 1994).

UV-Survival Assay

For UV-survival experiments, cells were exposed to different UV doses 2 days after plating. Survival was determined 3 days after UV-irradiation by incubation at 37°C with [^{3}H]thymidine pulse labeling as described elsewhere (Hamel et al., 1996).

Confocal Microscopy

Three days prior to microscopic experiments, cells were seeded onto 24 mm coverslips. Imaging and FRAP were performed on a Zeiss confocal laser scanning microscope LSM 410 (Zeiss, Oberkochen, FRG). Images were recorded with a 488nm Ar-laser and a 515-540 nm bandpass filter. Lateral resolution was 104 nm.

Fluorescence Recovery after Photobleaching

Diffusion measurements were performed by FRAP analysis at high time resolution (strip-FRAP). A strip spanning the nucleus was photobleached for 200 ms at 100% laser intensity. Recovery of fluorescence in the strip was monitored with 100 ms intervals at 1% laser intensity (Figure 4A). The effective diffusion coefficient (D_{eff}) of TFIIH-GFP was obtained by calculating relative intensity $FR_{diff}(t) = (I_t-I_0)/(I_\infty-I_0)$, where I_∞ is fluorescence intensity (FI) after complete recovery, I_0 is FI immediately after bleaching, and I_t is FI during monitoring. D_{eff} was estimated by minimizing $\sum[FR_{diff}(t)- FT(t)]$, where FT is a theoretical equation for one-dimensional diffusion: $FT(t) = 1 - (w^2 * [w^2 + 4\pi t D_{\text{eff}}]^{-1})^{-½}$. Immobile fractions were calculated as $N_{\text{immobile}}/N_{\text{tot}} = 1 - FR_{imm}(\infty) * (1-N_{\text{mobile, bleached}}/N_{\text{tot}})^{-1}$, where $FR_{imm} = (I_t-I_0)/(I_{t<0}-I_0)$ and $I_{t<0}$ is fluorescence before bleaching and $N_{\text{mobile, bleached}}/N_{\text{tot}}$ is the fraction of mobile molecules bleached by the pulse. The latter is ~30% in our set-up as determined by bleaching experiments on free GFP. In simultaneous FRAP/FLIP experiments a strip at one side of a nucleus was bleached at 20% laser intensity for 8 s. Fluorescence was then

monitored in the bleached and unbleached side of the nucleus and the difference was plotted against time (Figure 4C-F).

Acknowledgements

We thank Drs. A.A. van Zeeland, J. Essers, K. Mattern and R. Kanaar for helpful suggestions and discussion and J.M. Egly for antibodies against TFIIH . This work was supported by the Dutch Scientific Organization (NWO-ALW, and Spinoza award), the EC contract (DNA repair disorders) and the Dutch Cancer Society (KWF).

References

Aboussekhra, A., Biggerstaff, M., Shivji, M. K. K., Vilpo, J. A., Moncollin, V., Podust, V. N., Protic, M., Hubscher, U., Egly, J.-M., and Wood, R. D. (1995). Mammalian DNA nucleotide excision repair reconstituted with purified components., Cell *80*, 859-868.

Araujo, S. J., Tirode, F., Coin, F., Pospiech, H., Syvaoja, J. E., Stucki, M., Hubscher, U., Egly, J. M., and Wood, R. D. (2000). Nucleotide excision repair of DNA with recombinant human proteins: definition of the minimal set of factors, active forms of TFIIH, and modulation by CAK, Genes Dev *14*, 349-359.

Citterio, E., Vermeulen, W., and Hoeijmakers, J. H. J. (2000). Transcriptional healing, Cell *101*, 447-450.

Cook, P. R. (1999). The organization of replication and transcription, Science *284*, 1790-5.

Drapkin, R., and Reinberg, D. (1994). The multifunctional TFIIH complex and transcriptional controle., Trends in Biochem Sci *19*, 504-508.

Dvir, A., Conaway, J. W., and Conaway, R. C. (2001). Mechanism of transcription initiation and promoter escape by RNA polymerase II, Curr Opin Genet Dev *11*, 209-14.

Dvir, A., Garrett, K. P., Chalut, C., Egly, J. M., Conaway, J. W., and Conaway, R. C. (1996). A role for ATP and TFIIH in activation of the RNA polymerase II preinitiation complex prior to transcription initiation, J Biol Chem *271*, 7245-8.

Egly, J. M. (2001). The 14th Datta Lecture. TFIIH: from transcription to clinic, FEBS Lett *498*, 124-8.

Ellenberg, J., Siggia, E. D., Moreira, J. E., Smith, C. L., Presley, J. F., Worman, H. J., and Lippincott-Schwartz, J. (1997). Nuclear membrane dynamics and reassembly in living cells: targeting of an inner nuclear membrane protein in interphase and mitosis, J Cell Biol *138*, 1193-1206.

Essers, J., Houtsmuller, A. B., van Veelen, L., Paulusma, C., Nigg, A. L., Pastink, A., Vermeulen, W., Hoeijmakers, J. H. J., and Kanaar, R. (2002). Nuclear dynamics of RAD52 group homologous recombination proteins in response to DNA damage., EMBO J. 21(8):2030-7.

Evans, E., Moggs, J. G., Hwang, J. R., Egly, J. M., and Wood, R. D. (1997). Mechanism of open complex and dual incision formation by human nucleotide excision repair factors, EMBO J *16*, 6559-6573.

Friedberg, E. C., Walker, G. C., and Siede, W. (1995). DNA repair and mutagenesis (Washington D.C., ASM Press).

Granick, D. (1975). Nucleolar necklaces in chick embryo fibroblast cells. I. Formation of necklaces by dichlororibobenzimidazole and other adenosine analogues that decrease RNA synthesis and degrade preribosomes, J Cell Biol *65*, 398-417.

Hamel, B. C., Raams, A., Schuitema-Dijkstra, A. R., Simons, P., van der Burgt, I., Jaspers, N. G., and Kleijer, W. J. (1996). Xeroderma pigmentosum--Cockayne syndrome complex: a further case, J Med Genet *33*, 607-10.

Hanawalt, P., and Spivak, G. (1999). Transcription-coupled DNA repair. In Advances in DNA damage and repair, Dizdaroglu, and Karakaya, eds. (New York, Kluwer Academic/Plenum Publishers).

Hoeijmakers, J. H. (2001). Genome maintenance mechanisms for preventing cancer, Nature *411*, 366-74.

Holstege, F. C. P., Van der Vliet, P. C., and Timmers, H. T. M. (1996). Opening of an RNA polymerase II promoter occurs in two distinct steps and requires the basal transcription factors TFIIE and TFIIH., EMBO J *15*, 1666-1677.

Houtsmuller, A. B., Rademakers, S., Nigg, A. L., Hoogstraten, D., Hoeijmakers, J. H. J., and Vermeulen, W. (1999). Action of DNA repair endonuclease ERCC1/XPF in living cells, Science *284*, 958-961.

Houtsmuller, A. B., and Vermeulen, W. (2001). Macromolecular dynamics in living cell nuclei revealed by fluorescence redistribution after photobleaching, Histochem Cell Biol *115*, 13-21.

Iben, S., Tschochner, H., Bier, M., Hoogstraten, D., Hozak, P., Egly, J. M., and Grummt, I. (2002). TFIIH Plays an Essential Role in RNA Polymerase I Transcription, Cell *109*, 297-306.

Kimura, H., Tao, Y., Roeder, R. G., and Cook, P. R. (1999). Quantitation of RNA polymerase II and its transcription factors in an HeLa cell: little soluble holoenzyme but significant amounts of polymerases attached to the nuclear substructure, Mol Cell Biol *19*, 5383-92.

Kowalczykowski, S. C. (2000). Some assembly required, Nat Struct Biol *7*, 1087-9.

Le Page, F., Kwoh, E. E., Avrutskaya, A., Gentil, A., Leadon, S. A., Sarasin, A., and Cooper, P. K. (2000). Transcription-coupled repair of 8-oxoguanine: requirement for XPG, TFIIH, and CSB and implications for Cockayne syndrome, Cell *101*, 159-171.

Lindahl, T., and Wood, R. D. (1999). Quality control by DNA repair, Science *286*, 1897-905.

Maldonado, E., Shiekhattar, R., Sheldon, M., Cho, H., Drapkin, R., Rickert, P., Lees, E., Anderson, C. W., Linn, S., and Reinberg, D. (1996). A human RNA polymerase II complex associated with SRB and DNA-repair proteins., Nature *381*, 86-89.

McNally, J. G., Muller, W. G., Walker, D., Wolford, R., and Hager, G. L. (2000). The glucocorticoid receptor: rapid exchange with regulatory sites in living cells, Science *287*, 1262-5.

Misteli, T., Gunjan, A., Hock, R., Bustin, M., and Brown, D. T. (2000). Dynamic binding of histone H1 to chromatin in living cells, Nature *408*, 877-81.

Mone, M. J., Volker, M., Nikaido, O., Mullenders, L. H., van Zeeland, A. A., Verschure, P. J., Manders, E. M., and van Driel, R. (2001). Local UV-induced DNA damage in cell nuclei results in local transcription inhibition, EMBO Rep *2*, 1013-1017.

Moreland, R. J., Tirode, F., Yan, Q., Conaway, J. W., Egly, J. M., and Conaway, R. C. (1999). A role for the TFIIH XPB DNA helicase in promoter escape by RNA polymerase II, J Biol Chem *274*, 22127-30.

Orphanides, G., Lagrange, T., and Reinberg, D. (1996). The general transcription factors of RNA polymerase II, Genes Dev *10*, 2657-2683.

Ossipow, V., Tassan, J.-P., Nigg, E. A., and Schibler, U. (1995). A mammalian RNA polymerase II holoenzyme containing all components required for promotor-specific transcription initiation., Cell *83*, 137-146.

Phair, R. D., and Misteli, T. (2000). High mobility of proteins in the mammalian cell nucleus, Nature *404*, 604-9.

Sugasawa, K., Ng, J. M., Masutani, C., Iwai, S., van der Spek, P. J., Eker, A. P., Hanaoka, F., Bootsma, D., and Hoeijmakers, J. H. (1998). Xeroderma pigmentosum group C protein complex is the initiator of global genome nucleotide excision repair, Mol Cell *2*, 223-232.

Svejstrup, J. Q., Wang, Z. G., Feaver, W. J., Wu, X. H., Bushnell, D. A., Donahue, T. F., Friedberg, E. C., and Kornberg, R. D. (1995). Different forms of TFIIH for transcription and DNA repair: holo-TFIIH and a nucleotide excision repairosome, Cell *80*, 21-28.

Tang, J. Y., Hwang, B. J., Ford, J. M., Hanawalt, P. C., and Chu, G. (2000). Xeroderma pigmentosum p48 gene enhances global genomic repair and suppresses UV-induced mutagenesis, Mol Cell *5*, 737-44.

Timmers, H. T. (1994). Transcription initiation by RNA polymerase II does not require hydrolysis of the beta-gamma phosphoanhydride bond of ATP, Embo J *13*, 391-9.

van Oosterwijk, M. F., Filon, R., de Groot, A. J., van Zeeland, A. A., and Mullenders, L. H. (1998). Lack of transcription-coupled repair of acetylaminofluorene DNA adducts in human fibroblasts contrasts their efficient inhibition of transcription, J Biol Chem *273*, 13599-13604.

Vermeulen, W., Van Vuuren, A. J., Chipoulet, M., Schaeffer, L., Appeldoorn, E., Weeda, G., Jaspers, N. G., Priestley, A., Arlett, C. F., Lehmann, A. R., *et al.* (1994). Three unusual repair deficiencies associated with transcription factor BTF2(TFIIH): evidence for the existence of a transcription syndrome. In Cold-Spring-Harb-Symp-Quant-Biol., pp. 317-329.

Volker, M., Moné, M. J., Karmakar, P., Hoffen, A., Schul, W., Vermeulen, W., Hoeijmakers, J. H. J., van Driel, R., Zeeland, A. A., and Mullenders, L. H. F. (2001). Sequential Assembly of the Nucleotide Excision Repair Factors In Vivo, Molecular Cell *8*, 213-224.

Wakasugi, M., Kawashima, A., Morioka, H., Linn, S., Sancar, A., Mori, T., Nikaido, O., and Matsunaga, T. (2002). DDB accumulates at DNA damage sites immediately after UV irradiation and directly stimulates nucleotide excision repair, J Biol Chem *277*, 1637-40.

Winkler, G. S., Vermeulen, W., Coin, F., Egly, J. M., Hoeijmakers, J. H., and Weeda, G. (1998). Affinity purification of human DNA repair/transcription factor TFIIH using epitope-tagged xeroderma pigmentosum B protein, J Biol Chem *273*, 1092-1098.

Wood, R. D., Mitchell, M., Sgouros, J., and Lindahl, T. (2001). Human DNA repair genes, Science *291*, 1284-9.

Yokoi, M., Masutani, C., Maekawa, T., Sugasawa, K., Ohkuma, Y., and Hanaoka, F. (2000). The xeroderma pigmentosum group C protein complex XPC-HR23B plays an important role in the recruitment of transcription factor IIH to damaged DNA, J Biol Chem *275*, 9870-5.

Chapter 6

Kinetics of TFIIH in the TC-NER and GG-NER pathways

Manuscript in preparation

Kinetics of TFIIH in the TC-NER and GG-NER pathways

Deborah Hoogstraten[1], Jérôme Auriol[2], Alex L. Nigg[3], Jan H. J. Hoeijmakers[1], Jean-Marc Egly[2], Adriaan B. Houtsmuller[3] and Wim Vermeulen[1]

[1]Department of Cell Biology and Genetics (Medical Genetics Center, CBG), Erasmus University, P.O.Box 1738, 3000 DR Rotterdam, the Netherlands,
[2]Institut de Génétique et de Biologie Moléculaire et Cellulaire, CNRS/INSERM/Université Louis Pasteur, Strasbourg, France,
[3]Department of Pathology (Josephine Nefkens Institute), Erasmus University, the Netherlands

Summary

Nucleotide excision repair is an essential process for the removal of UV-induced lesions from the genome. Within NER two sub-pathways exist, GG-NER that surveys the entire genome and TC-NER, which repairs the injured transcribed strand of active genes. The transcription factor IIH is required for both NER sub-pathways. To study the reaction kinetics of TFIIH in both processes, we used GFP tagged TFIIH and various photobleaching techniques in transcriptionally active and inhibited cells. We show that the involvement of TFIIH-GFP in TC-NER and GG-NER is similar with respect to the quick response to UV-treatment and the dynamic involvement of TFIIH-GFP in TC-NER and GG-NER. Immediately after UV-irradiation the predominant pathway is GG-NER.

Introduction

During evolution multiple interwoven DNA repair systems have evolved, which safeguard our genetic material [1]. One of these DNA repair mechanisms is the versatile nucleotide-excision repair (NER) pathway, which removes a variety of helix-distorting lesions such as the UV-induced cyclobutane pyrimidine dimers (CPD) and 6-4 photoproducts (6-4 PP) [2]. Three rare genetically heterogeneous NER-associated syndromes are known: xeroderma pigmentosum (XP), the neuro-developmental disorder Cockayne syndrome (CS), or trichothiodystrophy (TTD), a CS-like condition with characteristic brittle hair and nails [3].

In NER two sub-pathways exist, global genome NER (GG-NER) and transcription-coupled NER (TC-NER), each with a different mode of damage detection. In GG-NER the xeroderma pigmentosum group C protein (XPC) in complex with the hHR23B screens the overall genome for helix-distortions [4], supported by the UV-DDB complex for specific lesions [5]. In contrast, TC-NER is specialized in the repair of lesions located in the transcribed strand of active genes, which are detected by a transcribing RNA polymerase II (RNAP2) [6]. Two TC-NER specific proteins

Cockayne syndrome A protein (CSA) and CSB are thought to be involved in the displacement of the stalled RNAP2 from the DNA damage, allowing access of the NER machinery. Both sub-pathways funnel into a core NER process to complete the reactions [7]. After damage detection the nine-subunit complex TFIIH, containing the XPB and XPD ATPase/helicases, is needed for locally unwinding the DNA double helix around the lesion [8]. Most likely, the 5' endonuclease XPG is next to enter the reaction, after which replication protein A and XPA are required for respectively stabilization and damage validation [9]. When the 3' endonuclease ERCC1/XPF is present dual incision can occur on opposite sites of the damage, leaving a 24 nucleotides single stranded gap [7]. The NER reaction is completed by DNA polymerase δ/ε and Ligase I, which are needed for DNA re-synthesis and sealing of the nick [10]. In contrast to mammals, rodents only remove CPD lesions from the transcribed strand [11], due to a deficiency of the UV-DDB complex in the cells [5], while (6-4)PP damages are removed genome-wide.

An intimate link between NER and basal transcription of RNAP2 is evident from the existence of TC-NER, which assures quick resumption of transcription after UV damage, but also from the involvement of the multifunctional TFIIH complex in both pathways. TFIIH is composed of nine subunits and possesses several enzymatic activities. The subunits XPB and XPD are DNA-dependent ATPases and helicases [12, 13], whereas CDK7 encompasses a kinase activity, which is capable of phosphorylating several substrates, including the C-terminal domain of the largest subunit of RNAP2 [14]. TFIIH was originally identified as one of the five basal transcription factors required for transcription initiation by RNAP2 [12, 15]. In the initiation reaction TFIIH is required for the ATP-dependent melting of the region around the transcription start site [16], enabling promoter escape of the transcribing RNAP2 complex [17, 18]. Recently, it was shown that TFIIH has a role in RNAP1 transcription initiation, an additional function for this transcription/repair factor [19].

In a previous study we have determined the *in vivo* dynamics of TFIIH tagged with the green fluorescent protein (GFP) [20]. We analyzed the kinetics of TFIIH-GFP in both RNAP1 and RNAP2 transcription, as well as in NER. Different fluorescence recovery after photobleaching (FRAP) techniques revealed that TFIIH-GFP moves freely through the nucleus, rather than being incorporated into a "transcription factory" or a "repairosome". This was also shown for ERCC1-GFP/XPF [21] and XPA-GFP (Rademakers *et al.*, submitted). Live cell studies on RNAP1 and RNAP2 transcription factors indicated that also transcription complexes are assembled in a stochastic fashion from freely diffusible subunits [22-26]. TFIIH-GFP was shown to be alternating between the three different DNA metabolic processes. The involvement of TFIIH with the multiple processes was ~25 seconds for RNAP1 transcription, ~6 seconds for RNAP2 transcription and ~4 minutes for NER. Moreover, we demonstrated that the RNAP1 and RNAP2 transcription kinetics of TFIIH are unaltered upon infliction of DNA damage elsewhere in the nucleus, indicating that TFIIH readily switches between transcription and repair sites without large-scale alterations.

In this study we examined the behavior of TFIIH in NER in more detail. Using photobleaching techniques we studied the dynamics of TFIIH-GFP in the sub-pathway GG-NER. We were able to block the TC-NER pathway, by inhibiting RNAP2 transcription. A quick response of TFIIH-GFP in both pathways can be observed after UV-treatment. Immediately after UV-irradiation the predominant pathway is GG-NER. We found a dynamic interaction of ~4 minutes for TFIIH-GFP in GG-NER pathway. A similar residence time of TFIIH-GFP at a NER site was also determined for general NER. However, GG-NER specific substrates are repaired at a much faster rate than those removed by TC-NER.

Results

Characterization of XPB-GFP

To study TFIIH in living cells, *GFP* was fused to the C-terminus of the *XPB* gene and the XPB-GFP fusion protein was expressed in XPB-deficient cells (XPCS2BA SV). We have previously shown that the fusion protein was expressed at physiological levels, efficiently incorporated into the TFIIH complex and fully functional in repair [20]. Moreover, the GFP tag did not appear to interfere with the transcriptional function of TFIIH, since XPB-GFP expressing cells had levels of RNA synthesis comparable to wild-type cells [20]. To further study the functionality of the fusion protein in transcription initiation, we examined TFIIH-GFP in an *in vitro* transcription assay. TFIIH-GFP was (partly) purified from a whole cell extract (WCE) of TFIIH-GFP expressing cells as described in Marinoni, *et al.* (1997) (Figure 1A) [27]. First a heparin column was used to concentrate TFIIH-GFP in the WCE. The fusion protein was eluted from the column at 400 mM KCl (data not shown). TFIIH-GFP was isolated from the 400 mM KCl fraction via immunoprecipitation with a polyclonal GFP antibody. As seen in Figure 1B (compare lane 1 with lane 3 and 4), only TFIIH containing the GFP tagged XPB was precipitated and not the endogenous XPB protein. Subsequently, an *in vitro* transcription assay as described in Marinoni, *et al.* (1997), was performed on the immunoprecipitated TFIIH-GFP. Note that in the assay, the fusion protein was attached to the polyclonal antibodies, which were retained on sepharose beads. In Figure 1C, lanes 3 to 5 clearly show that TFIIH-GFP was capable of initiating RNAP2 transcription and producing the 309 nucleotides transcript. This corroborates earlier findings that TFIIH tagging with GFP does not interfere with the transcription initiation function of this complex [20].

UV-irradiation alters the nuclear localization of TFIIH-GFP

As described previously, TFIIH-GFP was shown to have an overall homogeneous nuclear distribution with in addition focal accumulations in nucleoli (nucleolar clusters or NCs, (Figure 2A)). A clear co-localization of TFIIH with RNAP1 was observed in these nucleolar accumulations. These NCs were shown to be very sensitive to RNAP2

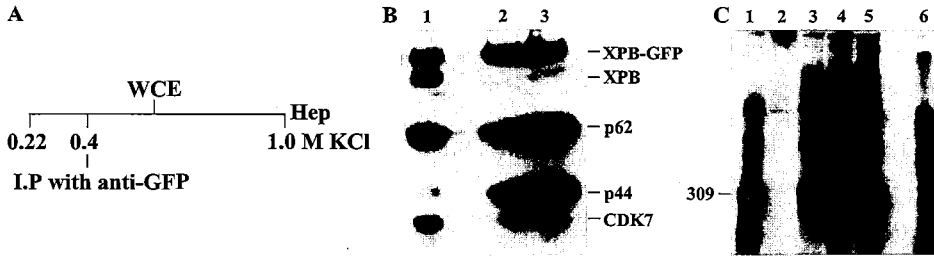

Figure 1. Characterization of the transcriptional functionality of TFIIH-GFP.
(A) Purification scheme of TFIIH-GFP from TFIIH-GFP expressing cells. (B) Immunoblot of anti-GFP immunoprecipitated TFIIH-GFP from the 400 mM KCl fraction of the heparin column, probed with an anti-XPB, anti-p62, anti-p44 and anti-CDK7 antibodies, lane 1 400 mM KCl fraction of the heparin column, lane 2 and 3 respectively 5 and 10 µl of beads. (C) *In vitro* transcription assay. In lane 1 highly purified (HAP fraction) TFIIH from HeLa cells, lane 2 negative control without TFIIH addition, lane 3 trough 5 respectively 5, 10 and 15 µl of beads added to the reaction, lane 6 marker.

inhibition and UV-irradiation [20]. Within five minutes after UV-treatment of 4 J/m^2 the NCs disappeared in the majority (~80%) of the cells and TFIIH-GFP was homogenously distributed in the nucleus (Figure 2B and E). Upon UV-irradiation, the available affinity sites is quickly changed and as a consequence the equilibrium of TFIIH bound in transcription is altered, since TFIIH is recruited into NER complexes. This withdrawal of TFIIH from the transcription processes explains the rapid abolishment of nucleolar accumulation of the TFIIH complex. Unlike TFIIH, immunofluorescent studies revealed that RNAP1 is still accumulated in the nucleolus 15 minutes after UV-irradiation (Figure 2B). It has been shown that RNAP1 is blocked at CPD lesions on the transcribed strand *in vitro* [28] and that RNAP1 transcription is inhibited after UV-irradiation [29] in human fibroblasts, which might explain the persistent nucleolar accumulation of RNAP1. NER of mammalian rDNA exhibits no strand bias and thus appears not to be coupled to RNAP1 transcription [30, 31]. In contrast, yeast *Saccharomyces cerevisiae* was shown preferential repair of the transcribed genes of active genes [32, 33].

Four hours after UV-irradiation (4 J/m^2) TFIIH-GFP appeared to be localized in large bright foci at the periphery of the nucleolus in a majority of cells (~90%) (Figure 2C and F). Since repair has been completed at this time, the available affinity sites have changed and a fraction of TFIIH was bound to these large nucleolar foci. A Similar distribution pattern of TFIIH-GFP was also observed after treatment with low concentrations of the RNAP1 inhibitor, actinomycin D (Figure 2D). Interestingly, in both instances the large nucleolar foci of TFIIH-GFP colocalize with RNAP1. These data suggest that the relocalization of TFIIH-GFP after UV-irradiation into bright nucleolar foci might be related to the inhibited state of RNAP1.

Twenty-four hours after UV-irradiation (4 J/m^2), when DNA repair is completed and both RNAP1 and RNAP2 transcription have been resumed [29, 34], TFIIH-GFP

has regained its original distribution pattern (Figure 2E). Note that the percentage of cells with a TFIIH-GFP distribution as in unchallenged cells 24 hours after UV-irradiation (4 and 16 J/m^2) is similar to the fraction of cells surviving such UV treatment [20]. This suggests that the fraction of cells that can not make the transition from accumulation of TFIIH-GFP and possibly RNAP1 in large bright nucleolar foci to NCs are prone to cell death.

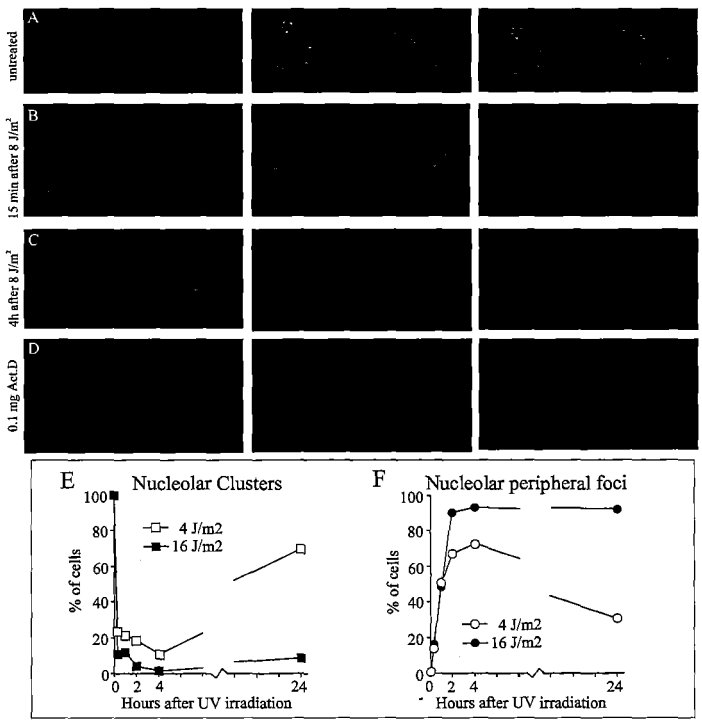

Figure 2. Nucleolar accumulation in XPB-GFP expressing cells under different conditions. Confocal images of fixed XPB-GFP cells. Left panel: GFP - fluorescence, middle panel: anti-RNAP1 immunofluorescence and right panel: merged image. (A) Untreated cells. (B) 5 minutes after irradiation with 8J/m^2 of UV-light. (C) 4 hours after UV-irradiation (8J/m^2) (D) 2 hours after Actinomycin D treatment. (E) Kinetics of nucleolar clusters after UV-irradiation. Percentage of cells containing NCs is plotted against time (hours). (F) Kinetics of nucleolar peripheral foci after UV-irradiation. Percentage of cells containing foci is plotted against time (hours).

DNA damage dependent immobilization of TFIIH

The nuclear redistribution of TFIIH-GFP as a response to DNA damage induction underscores the previously described dynamic behavior of TFIIH [20]. Furthermore, we have described a long-term transient immobilization of TFIIH, as compared to transcriptional involvement, in UV-dose dependent fashion. In addition, we have shown that other NER-factors like ERCC1-GFP/XPF [21] and XPA-GFP (Rademakers, *et al.*, submitted) are immobilized in an NER-specific manner. To further

investigate the kinetics of the engagement in NER we applied FRAP-FIM (FRAP for immobilization measurements) after different UV-doses [35]. This technique is specifically suited to quantify a possible immobilized fraction of GFP-tagged proteins in cell nuclei.

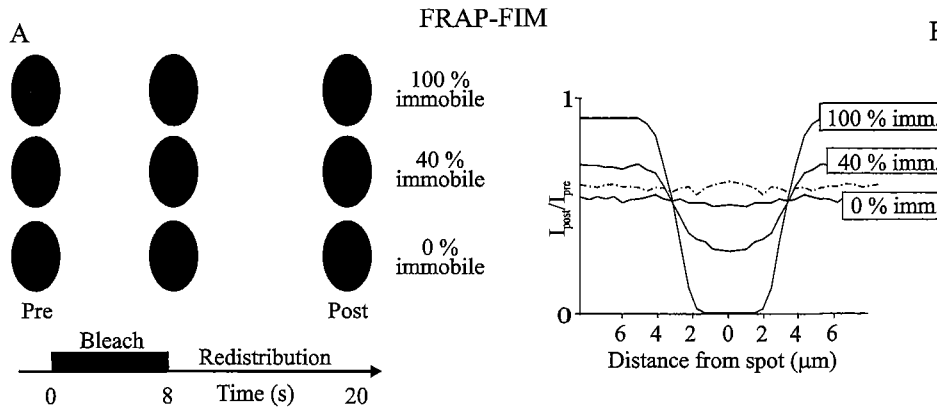

Figure 3. FRAP-FIM method.
(A) Scheme of FRAP-FIM analysis to determine immobilized fraction. Green ellipses represent confocal images of cell nuclei, where darker regions contain fluorophores bleached by a focused laser beam; grey bars represent bleach pulses. A laser beam (circle, left column) is focused in the center of the nucleus for a relatively long period (8 s) at relatively low laser intensity. After an additional 12 seconds, the post bleach image is taken. (B) The fluorescence ratio (I_{before}/I_{after}) is plotted as a function of distance from the laser-spot, generating a "fluorescence ratio profile (FRP).

In FRAP-FIM, a considerable portion of TFIIH-GFP molecules are bleached by focusing the laser in the center of the nucleus for a period of 8 seconds (Figure 3A). To allow the mobile GFP tagged proteins to redistribute through the nucleus, an additional 12 seconds is included before the post-bleach image is recorded. The pre-bleach images were compared with the post-bleach images at the same confocal plane. A fluorescence ratio profile (FRP) was generated by plotting the relative fluorescence (I_{post}/I_{pre}) against the distance to the bleach spot (Figure 3B). In Figure 4, typical pre- and post-image examples and their corresponding FRP's are shown. As expected, in chemically fixed cells bleaching of GFP molecules is only observed in the spot, since in these cells bleached and non-bleached molecules could not redistribute (Figure 4A). In untreated cells an overall bleaching is seen, suggesting that all GFP tagged molecules were mobile and able to redistribute over the entire nucleus (Figure 4B). Since in untreated cells not all TFIIH-GFP molecules are mobile, but rather involved in transcription process, we performed the FRAP-FIM analysis on transcription-inhibited cells (DRB-treated). The FRP of these cells is also flat (Figure 4D), but when compared to transcriptionally active (untreated) cells a significant larger fraction was photobleached in the transcriptionally inhibited cells (Figure 4C). This indicates that the overall

mobility of TFIIH-GFP is increased when transcription is inhibited and TFIIH is unhindered in its transcriptional function. These data correspond with previously obtained data where 20-40% of TFIIH is involved in transcription initiation for 2-10 seconds in untreated cells [20].

An intermediate FRP curve between the two extreme situations (fixed and DRB-treated) was apparent in UV-treated cells (Figure 4D). The FRP observed in UV-irradiated cells (8 J/m^2) was an intermediate of the FRP fixed cells (100% immobile) and of transcription inhibited cells (100% mobile). This indicates that a part of the TFIIH-GFP molecules were immobilized (Figure 5A). The immobilization of TFIIH-GFP after UV-irradiation is UV-dose-dependent and a maximum of ~35% was found at 16 J/m^2 (Figure 5B). The involvement of TFIIH-GFP in repair of lesions was mainly observed within the first four hours after an almost saturating UV-dose of 8 J/m^2 (Table 1). After two hours 40% of the initial fraction of TFIIH-GFP was still engaged in repair and within four hours the immobilized fraction dropped to background levels (that is <5%). This indicates that the vast majority of lesions have been repaired within four hours after DNA damage induction at an almost saturating dose of 8 J/m^2.

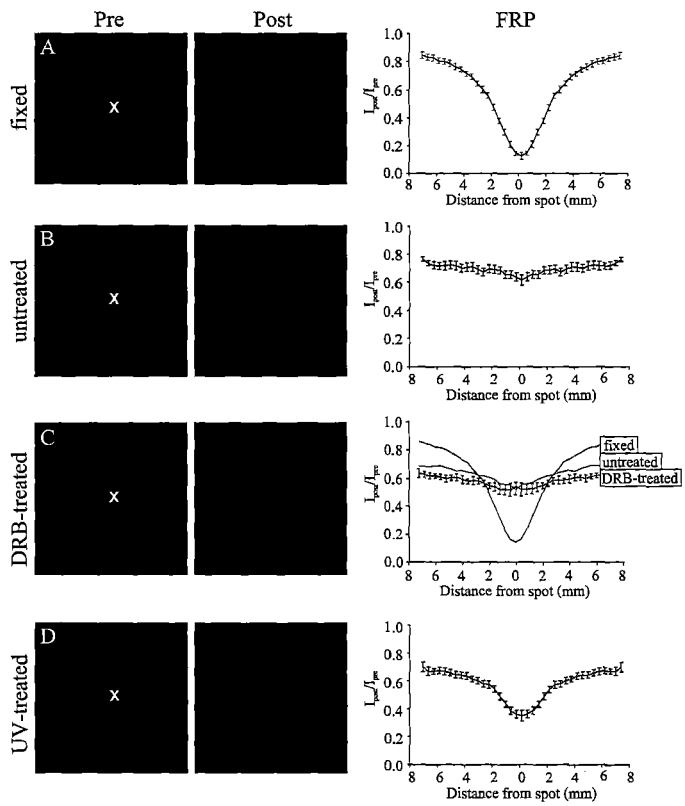

Figure 4. FRAP-FIM method applied on XPB-GFP expressing cells.
Left and middle panels, typical examples of cells before (pre-bleach) and after bleaching (postbleach) respectively, under different (indicated) experimental conditions. Right panel, corresponding fluorescence ratio profiles (FRP), the mean of 75 measured cells. (A) Cells fixed with 2% paraformaldehyde. (B) Untreated cells. (C) DRB treated cells. (D) UV-irradiated cells.

Repair kinetics for TFIIH in the GG-NER pathway

Since UV-irradiation causes both inhibition of transcription and induction of NER, two different sub-pathways get activated: global genome repair and the process of transcription-coupled repair that is directly linked to RNAP2 transcription. All together a complex and competitive situation for different involvement of TFIIH will occur. These multiple engagements complicate the kinetic analysis of the processes. To distinguish between the TFIIH actions in TC-NER, GG-NER and transcription, we investigated NER kinetics in transcriptionally arrested cells and compared this with transcription competent cells. To investigate the inhibition of transcription on the UV-induced alteration in mobility of TFIIH-GFP, we performed FRAP-FIM experiments on DRB treated TFIIH-GFP cells exposed to different doses of UV-C light. FRAP-FIM measurements revealed that in the absence of transcription, a significant part of the TFIIH-GFP molecules become immobilized also in an UV-dose dependent manner (Figure 5D). However, the amount of immobilized TFIIH-GFP due to UV-irradiation is lower (~70 ± 10%) than observed in transcription proficient cells (compare Figure 5B and 5C). Also in transcriptionally inhibited cells the NER-saturating dose was observed around 8 J/m^2. These results indicate that the number of transiently immobilized TFIIH-GFP molecules due to UV-damage induction depends on the number of lesions in both TC-NER and GG-NER. Moreover, the involvement of TFIIH-GFP in TC-NER and GG-NER is equal the first 30 minutes after UV-irradiation.

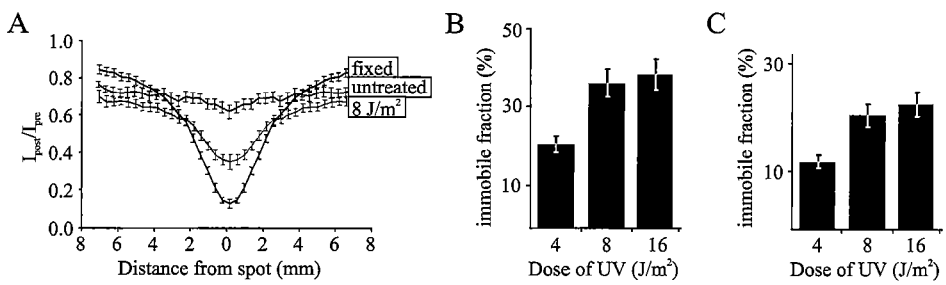

Figure 5. FRAP analysis of TFIIH engagement in NER in transcription-active and inactive cells.
(A) FRPs of fixed, untreated and UV-irradiated cells (8 J/m^2) (B) UV-dose dependent immobilization of TFIIH in transcription-proficient cells. Percentage of immobilization is plotted against UV-dose. (C) UV-dose dependent immobilization of TFIIH in transcription-deficient cells. Percentage of immobilization is plotted against UV-dose.

In transcription inhibited cells the fraction of bound TFIIH-GFP molecules gradually decreased to background levels within 2 hours after 8 J/m^2 of UV-irradiation (Table 1). This suggests that the vast majority of UV-induced lesions, which are substrate to the GG-NER pathway, have been removed within 2 hours after damage induction. In addition, at a dose of 8 J/m^2 the TC-NER pathway requires more time to

remove the bulk of lesions from the transcribed strand of active genes. Note that, this contrasts the a priori expectations that TC-NER is a more fast process GG-NER [36].

Table 1. Percentage of TFIIH-GFP molecules immobilized after UV-irradiation ($8J/m^2$) in time. The percentage compared to the immediate immobile fraction are given in brackets.

Transcription	Time after UV-damage induction		
	15 min	2 h	4h
active	35% (100%)	14% (40%)	background (<5%)
inhibited	25% (70%)	background (<5%)	background (<5%)

Residence time of TFIIH at a NER site in transcription-deficient cells

To further determine the reaction kinetics of TFIIH-GFP engaged in GG-NER, we measured the residence time of the complex at a GG-NER site. We covered DRB-treated cells with a filter containing 5 μm sized pores before UV-irradiation and thereby introducing UV-damage to a restricted area of the nucleus. Shortly after UV irradiation (< 5 min.) an accumulation of TFIIH-GFP molecules was observed in restricted parts of the nuclei. Albeit, the amount of accumulation was lower in transcriptionally inhibited cells than observed in transcription proficient cells (~70%, as calculated from the ratio $I_{localdamage}$:$I_{nucleoplasm}$) [20]. This is in agreement with the lower fraction of immobilized TFIIH-GFP molecules found in transcription deficient cells after total UV irradiation (Figure 5B and 5C).

The equilibrium at the steady-state situation of the NER reaction, in which the influx and the efflux of molecules in and from the localized NER region, is constant and can be conveyed as the time single molecules reside at a single repair event (residence time). To determine the residence time of TFIIH-GFP molecules within these locally damaged areas in transcription-deficient cells, we applied FLIP (fluorescence loss in photobleaching). Briefly, at a position at the opposite pole of the nucleus as where the damaged area is located, a small strip spanning the entire nucleus is bleached (FRAP) (Figure 6A). The bleached molecules will distribute over the entire nucleus and mix with the non-bleached proteins, resulting in an overall decrease in fluorescence intensity (FLIP). The relative fluorescence of the bleached (FRAP), locally damaged area and a region at the same distance from the bleaching spot without damage (FLIP) are plotted against time (Figure 6B). The delay in regaining the pre-bleach fluorescence ratio between damaged and nucleoplasm, is a measure for the residence time of molecules in the locally damaged area (I_t/I_o(local damage) – (I_t/I_o(FLIP - FRAP)), which is corrected for the diffusion of bleached molecules to the

other site of the nucleus and mix with non-bleached (I_t/I_o(FLIP) - I_t/I_o(FRAP)). In transcription inhibited cells the residence time for TFIIH-GFP was determined to be approximately 4 minutes (Figure 6D). The time, during which TFIIH-GFP molecules reside within these locally damaged areas (GG-NER) was prolonged to 8-10 minutes when these cells were incubated at 27°C, indicating that GG-NER is a temperature sensitive process. Comparable residence times were also found for TFIIH in general NER [20], suggesting that the interaction of TFIIH with both TC-NER and GG-NER are similar.

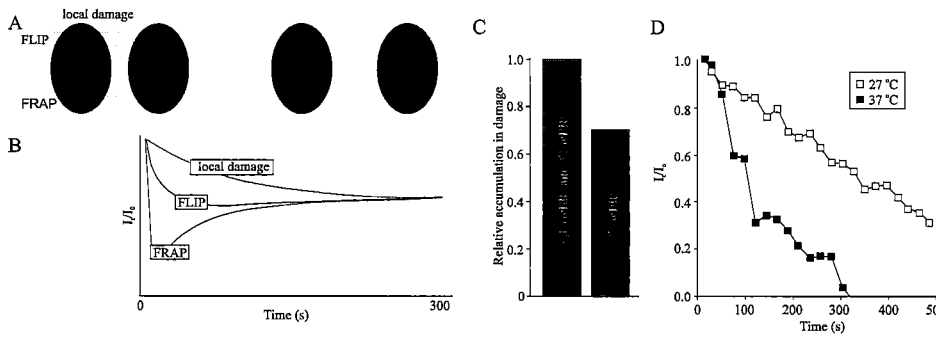

Figure 6. FLIP analysis of UV-induced local accumulation of TFIIH in transcription-deficient cells.
(A and B) Scheme of the FLIP procedure on local damaged area. A strip at the opposite pole of the nucleus than the local damage is bleached. Subsequently, the fluorescence intensity is monitored in regular time intervals in the bleach strip (FRAP), the local damage and in an undamaged region at the same distance from the bleach strip as the local damage (FLIP). (C) Relative accumulation of TFIIH-GFP at locally damaged site in transcription active and inhibited cells. The relative accumulation of TFIIH-GFP is set to 100%. (D) FLIP curve of the locally damaged-area in transcription-inhibited cells. The difference between fluorescence intensity in the locally damaged area and undamaged control region (FLIP) is plotted against time (I_t/I_o(local damage-I_t/I_o(FLIP).

Discussion

n this report we studied the reaction kinetics of the multifunctional complex TFIIH in TC-NER and GG-NER in living cells. Using the live cell marker GFP and different photobleaching techniques, we examined the behavior of TFIIH in response to DNA damage in transcriptionally active and (chemically) transcription-inhibited cells. This approach allowed the dissection between the kinetics of GG-NER and TC-NER. In addition to the kinetic study, we investigated the interaction of TFIIH with the nucleolus and the effect of UV-damage on this association.

Interaction of TFIIH with the nucleolus

The dispersed focal accumulation of TFIIH-GFP within the nucleolus was shown to be related to its recently uncovered function in RNAP1 transcription [19, 20]. It was shown that after UV-irradiation TFIIH redistributes homogeneously throughout the

nucleus. However, within 4 hours after UV-irradiation TFIIH accumulated again, but now into large bright foci located at the periphery of the nucleolus where it co-localized with RNAP1. Low concentrations of actinomycin-D, which specifically inhibited RNAP1 transcription, had a similar effect on the distribution of TFIIH-GFP and RNAP1. Since both have an inhibitory effect on RNAP1 transcription, these data suggest that the localization of TFIIH and RNAP1 are related to the inhibited state of the latter. Although the exact function of these larger RNAP1and TFIIH accumulations remains elusive, we speculate that they may play a role in resumption of RNAP1 transcription. Another explanation, for the existence of these peripheral foci is that they are early precursors in the process of DNA damage-induced cell death, since the percentage of cells still containing the large bright foci rather than dispersed nucleolar accumulations (NCs) after 24 hours is similar to the fraction of cells that do not survive the UV-treatment (Figure 2E and F).

TFIIH binding in global genome repair and transcription-coupled repair

The analysis on transcriptional active and transcription-inhibited cells (thus also TC-NER is inhibited) revealed that a significant amount of TFIIH-GFP was promptly engaged in both NER sub-pathways immediately after UV-irradiation. Shortly after UV-damage induction we observed with FRAP analysis that under both circumstance a considerable fraction of TFIIH became immobilized, that is however significantly smaller in transcription inhibited cells. Similarly, a rapid recruitment of TFIIH-GFP to locally UV-damaged areas could be observed within less then 5 minutes after UV-irradiation in nuclei of transcription inhibited and active cells. In addition, the fraction of immobilized TFIIH-GFP within transcriptionally active and inhibited cells appeared to depend on the number of lesions induced by UV irradiation. This further suggests that the observed immobilization reflects transient entrapment of TFIIH molecules in active DNA-lesion/NER complexes. Moreover, in both locally (Figure 6C) and overall irradiated cells (Figure 5C) we observed that directly after UV damage induction ~70% of all immobilized TFIIH-GFP molecules are involved in GG-NER. This indicates that directly after UV-irradiation the majority of TFIIH-GFP molecules were recruited to GG-NER. Our findings further imply that the initial damage recognition step in GG-NER performed by the hetero-dimeric complex XPC/hHR23B, which precedes TFIIH loading, should also be fast. Moreover, binding of TFIIH to XPC/DNA-lesion complexes in this pathway appeared to efficiently compete with the withdrawal of TFIIH-GFP by TC-NER. However, when the chance of a lesion being located in the transcribed strand of a gene, roughly estimated as ~ 1- 4 % compared to the rest of the genome (see footnote, [37]), is taken into consideration the sequestration of TFIIH by TC-NER appeared to significantly prevail over GG-NER. In a stochastic model that describes the different nuclear functions of TFIIH, as we have previously proposed [20], this would suggest that: (*i*) lesion sensing by TC-NER is much faster than translocation of XPC/hHR23B to injuries; (*ii*) TFIIH has a much higher affinity for

lesion-stalled RNAP2 than for XPC bound to a lesion, resulting in higher chance of binding; (*iii*) TFIIH binds longer to TC-NER complexes; (*iv*) or a combination of the above possibilities. Future live cell protein dynamic experiments on the crucial lesion recognition step(s) are required to gain more insight in the overall kinetic mechanism of NER.

Kinetics of GG-NER and TC-NER

FRAP experiments revealed that the amount of immobilized TFIIH-GFP molecules both in GG-NER and TC-NER was dependent on the (repair) time after damage infliction. The amount of bound TFIIH-GFP molecules after a saturating UV-dose of 8 J/m^2 in transcription-inhibited cells reduced to background levels within 2 hours, whereas in transcription-proficient cells it took more than 4 hours to reach the point that no significant immobilization was observed (Table 1). This remarkably relative slow decrease of immobilized fraction in transcriptionally active cells, suggests that lesions that are induced in actively transcribed genes (which are not present in transcription inhibited cells) are removed slower than those occurring in non-transcribed chromatin. Note that these findings contrast to the generally accepted model [38], in which TC-NER removes lesions more efficient than GG-NER. However, in these comparisons of lesion removal from the transcribed strand versus non-transcribed strand usually only CPD removal is examined from relatively highly expressed genes. Since it has been shown that the removal of (6-4)PPs by GG-NER is that efficient that hardly no preferential repair by the TC-NER pathway is detected for this lesion, it is suggested that the increased repair rate by TC-NER mainly holds for CPDs [39]. In addition, it is also known that (6-4)PP are repaired within the first few hours after damage induction, and that CPD lesions in general are poorly removed [40]. In summary, early after damage induction the majority of the repair, and by inference TFIIH immobilization is mainly focussed on (6-4)PPs (see Table 2). At later time points after UV-irradiation, when most (6-4)PP lesion are removed, mainly the TC-NER acting on CPDs is operational. It is likely that CPDs located in lowly transcribed and or long genes are poorly repaired, even by TC-NER, since it can take quiet a while before RNAP2 reaches a lesion in these genes. Therefor we suggest that the observed relatively long-lasting immobilization of TFIIH only when TC-NER is active (Table 1) is due to low level of CPD repair by TC-NER. The removal of CPDs by GG-NER might have escaped our attention within this experimental setup, because the immobilized fraction of TFIIH-GFP engaged in CPD repair is too small to detect.

Given that CPD lesions can be positioned anywhere, including within nucleosomes, as opposed to (6-4)PPs which were predominantly located in the inter-nucleosome linker DNA [41], it has been suggested the repair of CPDs by GG-NER might need additional factors for efficient recognition, such as chromatin relaxation and/or remodeling activities [42]. As a likely candidate for the assistance of CPD recognition the hetero-dimeric UV-DDB complex was suggested [5, 43].

FLIP measurements on locally damaged cells, both in transcription inhibited and transcriptionally active cells, showed a more or less similar mean residence time of TFIIH of ~4 minutes in both cases. This indicates that although the mechanism of initiation via TC-NER and GG-NER are quite different, the involvement of TFIIH in both processes follows comparable kinetics.

Conclusion

Also for other NER factors XPA-GFP (Rademakers *et al.*, submitted) and ERCC1-GFP/XPF [21] it was found that they diffuse according to their molecular size and in addition, reside in a NER complex for 4-6 minutes only when actively engaged in repair. This corroborates the notion put forward before [20] that within both TC-NER and GG-NER, these repair factors successively assemble into DNAdamage/repair complexes by random diffusion and collision. However, it has been shown that the initial DNA damage detection step in TC-NER occurs by a different mechanism, where transcribing RNAP2 travelling along the DNA contour will be stalled at an injury. Lesion detection by XPC-hHR23B in the GG-NER pathway may employ a similar scanning process, or alternatively a free diffusing heterodimer could probe the DNA for lesions by random associations to DNA. When the quick period in which a steady-state equilibrium (<4minutes) between NER-bound and free factors is established is considered it is unlikely that the rate-limiting step within NER is neither lesion detection nor complex assembly. The more or less similar residence times of ERCC1/XPF, XPA and TFIIH, rather suggest that the subsequent dissociation of the NER complex is the delaying step in the process.

Material and Methods

Cell lines

Cell line used in this study is the SV40-immortalized fibroblasts XPCS2BA stably expressing the XPB-eGFP fusion protein as described in Hoogstraten *et al.*, 2002. All cells were cultured on RPMI$^+$-Hepes medium, supplemented with antibiotics and 10% fetal calf serum at 37°C and 5% CO_2. Before UV irradiation cells were rinsed with PBS and UV-irradiated with a Philips TUV lamp (254 nm) at a dose rate of ~ 0.8 J.m^2/s. In the cases when cells are locally damaged, an isopore polycarbonate filter (Millipore) containing 5 μm diameter pores was used to cover the cells before UV-irradiation [9, 44]. After irradiation cells were put back into medium and microscopically examined. For DRB treatment cells were incubated with 100 μM DRB for 3 hours. For actinomycin D treatment cells were incubated with 0.1 μg/ml actinomycin D for 2 hours.

Immunofluorescence

Where stated cells were labeled with latex beads as described by [45]. Cells were fixed with 2% paraformaldehyde and 0.2% Triton X-100 and subsequently washed twice with PBS containing 0.1% Triton X-100. Antibodies were incubated in PBS^+ (containing 0.15% glycine and 0.5% BSA) for 90 minutes at room temperature at the following concentrations: α-RNAP1 (1:400) (kindly provided by H. Heath, Erasmus MC, Rotterdam). Afterwards cells were washed twice with PBS containing 0.1% Triton X-100. The secondary antibodies goat-anti-rabbit Alexa-594-conjugated (Molecular Probes) was diluted 800 times in PBS^+ and incubated for 1 hour at room temperature. After two washing steps with PBS containing 0.1% Triton X-100 the coverslip was mounted in Vectashield mounting medium (Vector Laboratory) containing 1.5 μg/μl DAPI. Epifluorescent and phase-contrast images were generated on a Leica DMRBE microscope.

Immunoprecipitation of TFIIH-GFP

WCE of TFIIH-GFP expressing cells was prepared as described in Marinoni et al. (1997) and the WCE was loaded onto a heparin column. After washing with 220 mM KCl TFIIH-GFP was eluated from the column with 400 mM KCl [27]. TFIIH-GFP was immunoprecipitated from the eluate using GFP polyclonal antibodies (abcam, Cambridge) cross-linked to protein A sepharose beads.

In vitro transcription

An reconstituted transcription reaction was performed as described in Marinoni et al. (1997), using purified basal transcription factors, RNAP2, TFIIB, TFIIEα, TFIIEβ, TFIIF, TBP and 5, 10 or 15 μl of TFIIH-GFP precipitated beads [27]. All basal transcription factors were preincubated with AdML promoter template, before RNA synthesis of the 309 nt transcript in the presence of ATP, UTP, GTP, [α-^{32}P]CTP and cold CTP.

UV irradiation

Cells were rinsed with PBS and UV-irradiated with a Philips TUV lamp (254 nm) at a dose rate of ~ 0.8 $J.m^2/s$. In the cases when fibroblasts are locally damaged, an isopore polycarbonate filter (Millipore) containing 5 μm diameter pores was used to cover the cells before UV-irradiation [9, 44]. After irradiation cells were put back into medium and microscopically examined.

Confocal Microscopy

Three days prior to microscopic experiments, cells were seeded onto 24 mm diameter coverslips. Imaging and FRAP were performed on a Zeiss confocal laser

scanning microscope LSM 410 (Zeiss, Oberkochen, FRG), equipped with a heatable scan stage (37 °C). Images were recorded with a 488nm Ar-laser and a 515-540 nm bandpass filter. Lateral resolution was 104 nm.

Fluorescence recovery after photobleaching for immobility measurement (FRAP-FIM)

FRAP-FIM can be used to measure the fraction of immobilization of GFP-tagged proteins [35]. In this procedure a laser beam (circle, left column) is focused in the center of the nucleus for a relatively long period (8 s) at relatively low laser intensity, causing bleaching of GFP molecules within and passing through this region (middle column), as shown in Figure 3A and B. Subsequently, after an additional 12 seconds, in order for the mobile proteins to redistribute through the nucleus a post-image is made (Figure 3A). Right column, top row shows theoretical redistribution patterns when all GFP-tagged molecules are immobile and all the GFP molecules were bleached within bleach spot. In the situation where all GFP molecules are mobile (bottom row) we only find an allover bleaching of the nucleus, since during and between the time of bleaching the bleached and non-bleached molecules have redistributed completely. When only a fraction is immobile and the remainder of the molecules moves freely (middle row), a combination of the latter described situation has occurred. An allover bleaching of the nucleus due to the mobile GFP molecules and a bleached spot in the center of the nucleus because of the immobile proteins. To quantify the immobile fraction the intensity of fluorescence at different distances from the bleach spot are determined in the pre- and post-bleach images. The fluorescence ratio (I_{before}/I_{after}) is plotted as a function of distance from the laser-spot, generating a "fluorescence ratio profile (FRP). In Figure 3B FRPs are shown as determined by computer simulation. Red line: all molecules are freely mobile ($D_{simulated}$ = 10 $\mu m^2/s$), blue line: a fraction (40%) of the molecules is immobile; green line: immobilization is transient (40% bound for 7 s), and the majority of molecules are released during the period of measurement.

Fluorescence loss in photobleaching (FLIP) of local damage

A second technique to determine the residence time of the fusion-protein at the locally damaged site is FLIP [20]. For this, a strip at the opposite pole of the nucleus than the local damage was bleached with a high laser intensity for 5 seconds (Figure 6A). Subsequently, 20 times the fluorescence intensity is monitored with an interval of 20 seconds in the bleach strip (FRAP), the local damage and in an undamaged region at the same distance from the bleach strip as the local damage (FLIP) (Figure 6B). The difference between fluorescence intensity in the locally damaged area and undamaged control region (FLIP) is plotted against time (I_t/I_0(local damage-I_t/I_0(FLIP). The time at which the initial (pre-bleach image) fluorescence contrast is reached is taken as an estimate for the residence time of individual proteins associated with the damaged DNA.

References

1. **Hoeijmakers, J.H.,** *Genome maintenance mechanisms for preventing cancer.* Nature, 2001. 411(6835): p. 366-74.
2. **Wood, R.D., et al.,** *Human DNA repair genes.* Science, 2001. 291(5507): p. 1284-9.
3. **Bootsma, D., et al.,** *Nucleotide excision repair syndromes: xeroderma pigmentosum, Cockayne syndrome and trichothiodystrophy.*, in *The genetic basis of human cancer*, B. Vogelstein and K.W. Kinzler, Editors. 2001, McGraw-Hill: New York. p. 677-703.
4. **Sugasawa, K., et al.,** *Xeroderma pigmentosum group C protein complex is the initiator of global genome nucleotide excision repair.* Mol. Cell, 1998. 2(2): p. 223-232.
5. **Tang, J.Y., et al.,** *Xeroderma pigmentosum p48 gene enhances global genomic repair and suppresses UV-induced mutagenesis.* Mol Cell, 2000. 5(4): p. 737-44.
6. **Hanawalt, P. and G. Spivak,** *Transcription-coupled DNA repair*, in *Advances in DNA damage and repair*, Dizdaroglu and Karakaya, Editors. 1999, Kluwer Academic/Plenum Publishers: New York.
7. **de Laat, W.L., N.G. Jaspers, and J.H. Hoeijmakers,** *Molecular mechanism of nucleotide excision repair.* Genes Dev., 1999. 13(7): p. 768-785.
8. **Egly, J.M.,** *The 14th Datta Lecture. TFIIH: from transcription to clinic.* FEBS Lett, 2001. 498(2-3): p. 124-8.
9. **Volker, M., et al.,** *Sequential Assembly of the Nucleotide Excision Repair Factors In Vivo.* Molecular Cell, 2001. 8(1): p. 213-224.
10. **Araujo, S.J., et al.,** *Nucleotide excision repair of DNA with recombinant human proteins: definition of the minimal set of factors, active forms of TFIIH, and modulation by CAK.* Genes Dev., 2000. 14(3): p. 349-359.
11. **Ruven, H.J.T., et al.,** *Ultrviolet-induced cyclobutane pyrimidine dimers are selectively removed from transcriptionally active genes in the epidermis of the hairless mouse.* Cancer Research, 1993. 53: p. 1642-1645.
12. **Schaeffer, L., et al.,** *DNA repair helicase: a component of BTF2 (TFIIH) basic transcription factor.* Science, 1993. 260: p. 58-63.
13. **Schaeffer, L., et al.,** *The ERCC2/DNA repair protein is associated with the class II BTF2/TFIIH transcription factor.* EMBO J., 1994. 13(10): p. 2388-2392.
14. **Roy, R., et al.,** *The MO15 cell cycle kinase is associated with the TFIIH transcription-DNA repair factor.* Cell, 1994. 79: p. 1093-1101.
15. **Drapkin, R. and D. Reinberg,** *The multifunctional TFIIH complex and transcriptional controle.* Trends in Biochem. Sci., 1994. 19: p. 504-508.
16. **Holstege, F.C.P., P.C. Van der Vliet, and H.T.M. Timmers,** *Opening of an RNA polymerase II promoter occurs in two distinct steps and requires the basal transcription factors TFIIE and TFIIH.* EMBO J., 1996. 15(7): p. 1666-1677.
17. **Dvir, A., J.W. Conaway, and R.C. Conaway,** *Mechanism of transcription initiation and promoter escape by RNA polymerase II.* Curr Opin Genet Dev, 2001. 11(2): p. 209-14.
18. **Moreland, R.J., et al.,** *A role for the TFIIH XPB DNA helicase in promoter escape by RNA polymerase II.* J Biol Chem, 1999. 274(32): p. 22127-30.
19. **Iben, S., et al.,** *TFIIH Plays an Essential Role in RNA Polymerase I Transcription.* Cell, 2002. 109(3): p. 297-306.

20. **Hoogstraten, D., et al.**, *Rapid Switching of TFIIH between RNA Polymerase I and II Transcription and DNA Repair In Vivo.* Mol Cell, 2002. 10(5): p. 1163-74.
21. **Houtsmuller, A.B., et al.**, *Action of DNA repair endonuclease ERCC1/XPF in living cells.* Science, 1999. 284(5416): p. 958-961.
22. **McNally, J.G., et al.**, *The glucocorticoid receptor: rapid exchange with regulatory sites in living cells.* Science, 2000. 287(5456): p. 1262-5.
23. **Kimura, H., K. Sugaya, and P.R. Cook**, *The transcription cycle of RNA polymerase II in living cells.* J Cell Biol, 2002. 159(5): p. 777-82.
24. **Dundr, M., et al.**, *A kinetic framework for a mammalian RNA polymerase in vivo.* Science, 2002. 298(5598): p. 1623-6.
25. **Becker, M., et al.**, *Dynamic behavior of transcription factors on a natural promoter in living cells.* EMBO Rep, 2002. 3(12): p. 1188-94.
26. Vermeulen, W. and A.B. Houtsmuller, *The transcription cycle in vivo. A blind watchmaker at work.* Mol Cell, 2002. 10(6): p. 1264-6.
27. **Marinoni, J.C., M. Rossignol, and J.M. Egly**, *Purification of the transcription/repair factor TFIIH and evaluation of its associated activities in vitro.* Methods, 1997. 12(3): p. 235-53.
28. **Hara, R., et al.**, *Human transcription release factor 2 dissociates RNA polymerases I and II stalled at a cyclobutane thymine dimer.* J. Biol. Chem., 1999. 274(35): p. 24779-24786.
29. **Ayaki, H., R. Hara, and M. Ikenaga**, *Recovery from ultraviolet tight-induced depression of ribosomal RNA synthesis in normal human, xeroderma pigmentosum and Cockayne syndrome cells.* J Radiat Res (Tokyo), 1996. 37(2): p. 107-16.
30. **Christians, F.C. and P.C. Hanawalt**, *Lack of transcription-coupled repair in mammalian ribosomal RNA genes.* Biochem., 1993. 32(39): p. 10512-10518.
31. **Fritz, L.K. and M.J. Smerdon**, *Repair of UV damage in actively transcribed ribosomal genes.* Biochemistry, 1995. 34(40): p. 13117-24.
32. **Verhage, R.A., P. Van de Putte, and J. Brouwer**, *Repair of rDNA in Saccharomyces cerevisiae: RAD4-independent strand-specific nucleotide excision repair of RNA polymerase I transcribed genes.* Nucl. Acids Res., 1996. 24(6): p. 1020-1025.
33. **Meier, A., M. Livingstone-Zatchej, and F. Thoma**, *Repair of active and silenced rDNA in yeast: the contributions of photolyase and transcription-couples nucleotide excision repair.* J Biol Chem, 2002. 277(14): p. 11845-52.
34. **Kantor, G.J. and D.R. Hull**, *An effect of ultraviolet light on RNA and protein synthesis in nondividing human diploid fibroblasts.* Biophys J, 1979. 27(3): p. 359-70.
35. **Houtsmuller, A.B. and W. Vermeulen**, *Macromolecular dynamics in living cell nuclei revealed by fluorescence redistribution after photobleaching.* Histochem Cell Biol, 2001. 115(1): p. 13-21.
36. **Bohr, V.A., et al.**, *DNA repair in an active gene: removal of pyrimidine dimers from the DHFR gene of CHO cells is much more efficient than in the genome overall.* Cell, 1985. 40(2): p. 359-369.
37. **Deloukas, P., et al.**, *A physical map of 30,000 human genes.* Science, 1998. 282(5389): p. 744-6.
38. **Hanawalt, P.C.**, *Controlling the efficiency of excision repair.* Mutat Res, 2001. 485(1): p. 3-13.

39. **Van Hoffen, A., et al.**, *Transcription-coupled repair removes both cyclobutane pyrimidine dimers and 6-4 photoproducts with equal efficiency and in a sequential way from transcribed DNA in xeroderma pigmentosum group C fibroblasts.* EMBO J., 1995. 14(2): p. 360-367.
40. **Mitchell, D.L. and R.S. Nairn**, *The biology of the (6-4) photoproduct.* Photochem. Photobiol., 1989. 49(6): p. 805-819.
41. **Thoma, F.**, *Light and dark in chromatin repair: repair of UV-induced DNA lesions by photolyase and nucleotide excision repair.* EMBO J., 1999. 18(23): p. 6585-6598.
42. **Green, C.M. and G. Almouzni**, *When repair meets chromatin. First in series on chromatin dynamics.* EMBO Rep, 2002. 3(1): p. 28-33.
43. **Wakasugi, M., et al.**, *DDB accumulates at DNA damage sites immediately after UV irradiation and directly stimulates nucleotide excision repair.* J Biol Chem, 2002. 277(3): p. 1637-40.
44. **Mone, M.J., et al.**, *Local UV-induced DNA damage in cell nuclei results in local transcription inhibition.* EMBO Rep, 2001. 2(11): p. 1013-1017.
45. **Vermeulen, W., et al.**, *Sublimiting concentration of TFIIH transcription/DNA repair factor causes TTD-A trichothiodystrophy disorder.* Nat Genet, 2000. 26: p. 307-313.

Footnote:

Average gene size ~ 14 kbp (3 x 10^4 bp), with 3.5 x 10^4 genes per genome gives ~ 5 x 10^8 b/genome occupied by genes, of which 50% located in the transcribed strand, resulting into ~ 2.5 x 10^8 b out of 6 x 10^9 per diploid mammalian genome, consequently maximally 1-4% of the base content is transcribed. Note that certainly not all genes are being transcribed at any time within an average cell, suggesting that this percentage is certainly an overestimation.

Chapter 7

A role for the cyclin-activating kinase complex in mammalian nucleotide excision repair

A role for the cyclin-activating kinase complex in mammalian nucleotide excision repair

Deborah Hoogstraten, Nils Wijgers, Jan H. J. Hoeijmakers and Wim Vermeulen

Department of Cell Biology and Genetics (Medical Genetics Center, CBG), Erasmus University, P.O.Box 1738, 3000 DR Rotterdam, the Netherlands

Summary

The basal transcription factor IIH (TFIIH), is required for both RNA polymerase II transcription and nucleotide excision repair (NER). The trimeric cyclin-activating-kinase complex (CAK) is associated with TFIIH and comprises a kinase activity. It is however not exactly known whether CAK functions in NER. Within NER two sub-pathways exist; global genome (GG-NER), which surveys the entire genome and transcription-coupled (TC-NER), which focuses on the transcribed strand of active genes. In this study, we demonstrate that the CAK complex appeared to be loaded at UV damaged areas. Surprisingly, CAK is absent from a NER site in a TC-NER deficient background, suggesting that CAK is not associated with GG-NER. In addition, in cells from trichothiodystrophy patients CAK is not or hardly present at locally damaged parts of nuclei. However, these cells are deficient in CPD repair, but proficient in (6-4)PP repair. This indicates that the CAK complex is not required for the removal of (6-4)PPs from the genome, and possibly GG-NER.

Introduction

The basal transcription factor IIH (TFIIH) is one of the most versatile nuclear components, harboring different enzymatic activities and playing a pivotal role in distinct nuclear processes. The complex was originally identified as one of the five basal transcription factors aiding the RNA polymerase II (RNAP2) in transcription initiation [1, 2]. TFIIH consists of nine subunits, of which five (XPB, p62, p52, p44 and p34) form a tight "core"-complex. The XPD protein is less tightly associated and serves as a bridge between the core via p44 and the ternary cyclin-activating kinase (CAK) complex, consisting of CDK7, MAT1 and cyclinH [3]. Both XPB and XPD subunits were shown to be DNA-dependent ATPases and helicases [4, 5] and the CDK7 subunit displayed a protein phosphorylating activity, such as kinating the C-terminal domain (CTD) of the largest subunit of the RNAP2 [6]. Recently, TFIIH was also shown to be involved in RNAP1 transcription *in vitro* [7] and *in vivo* [8]. In addition to its requirement in basal transcription, TFIIH is essential for nucleotide excision repair (NER) [9, 10]. NER is one of the main DNA repair pathways, crucial

for the removal of UV-induced photoproducts from the DNA [11]. NER consists of two sub-pathways, transcription-coupled NER (TC-NER), that is specialized in removal of transcription blocking lesions [12] and global genome NER (GG-NER), that employs a specialized sensor (XPC-hHR23B) to inspect the entire genome for lesions [13]. For efficient repair by NER about 30 proteins are involved in the recognition, dual incision and restoration steps [14]. TFIIH is one of the first factors required, for DNA unwinding around the lesion in order for the NER machinery to gain access [15]. The significance of a functional NER is apparent from the severe clinical features associated with three clinical disorders; xeroderma pigmentosum group D (XP), trichothiodystrophy (TTD), or the rare combination of XP with Cockayne syndrome (XP/CS).

Rossignol and colleagues have isolated four different TFIIH sub-complexes from cells, core-TFIIH with or without XPD, holo-TFIIH and in excess the ternary CAK-complex, that has an additional function in cell-cycle regulation [16]. It is still debated whether the CAK-complex is required for NER. It was suggested that in yeast core TFIIH lacking KIN28, the yeast CDK7 homologue plays a role in NER, since core-TFIIH was found in a pre-assembled 'repairosome' [17]. In addition, the minimal set of mammalian polypeptides required for an *in vitro* NER reaction, does not include CAK [18]. The CAK complex can even inhibit an *in vitro* NER assay in the presence of an ATP-regenerating system [19]. However, microinjection of antibodies against CDK7 inhibits NER *in vivo*, suggesting a role for CDK7 in NER [6]. Moreover, a defective Kin28 was shown to impair TC-NER, but not GG-NER in yeast [20].
The binding of XPD to p44 is bipartite, the 5'-3' helicase activity of XPD is stimulated through this interaction [21]. In addition, the attachment of XPD to p44 anchors the CAK-complex into the TFIIH complex. The binding of XPD to p44 was shown to be mediated through the C-terminal domain of XPD and a number mutations in *XPD* were identified to have a weakened p44-XPD interaction and thus a disturbed architecture of TFIIH [22, 23]. These mutations will not only result in the abrogation of the stimulatory function of p44 towards the XPD helicase, leading to a NER defect in these patients, but might also have additional consequences for the CDK7 activity. A reduced activity of CDK7 could influence optimal transcription activity, as a consequence of a modification in the phosphorylation of the CTD of the large subunit of RNAP2 or of DNA binding proteins such as nuclear receptors [24]. It was recently shown that in the XP-D (R683W) cell line the nuclear hormone receptors, retonic acid receptor, estrogen receptor and androgen receptor are not phosphorylated correctly, possibly due to a weakened CAK incorporation into TFIIH [24]. These findings were shown in cells of a classical XP-D patient with no severe additional abnormalities, so the situation might even be worse in XP/CS and TTD patients, which have further developmental problems.

Here we report, the presence of the CAK complex at the site of UV damage. The occurrence of CAK at an UV-damaged site is absent in a TC-NER deficient background, suggesting that the complex is not present at GG-NER sites. In addition,

in cells from TTD patients CAK is not or hardly accumulating at locally damaged area in nuclei. These cells are deficient in CPD repair, but proficient in (6-4)PP repair, suggesting that CAK is not required for (6-4)PPs removal and possibly GG-NER.

Results

Presence of CAK-complex at the site of local damage

To study the behavior of the CAK-complex after UV-irradiation and the possible involvement in NER, we visualized the NER process by applying local damage to cells and subsequently labeling the various proteins via immunofluorescence [25, 26]. Shortly after local UV-irradiation (within 15 minutes) the main NER factors, including TFIIH appear to accumulate at the site where local damage was inflicted, as was previously shown [26]. In these studies the core TFIIH component XPB was probed. Here, we used also specific antibodies raised against CDK7 and cyclinH. To detect the position of the local UV- damage we used an antibody directed against the XPC protein, the initial damage sensor, which turned out to be a sensitive marker for local UV damage. Surprisingly, in NER-proficient cells both these CAK-components appeared to accumulate at these damaged areas with the same kinetics as the core components (Figure 1A). Albeit, the accumulation was less pronounced than for core-TFIIH components (p62) (Figure1A), compare left panel with middle and right panel). This is not unexpected, since the autonomous CAK-complex is present in excess in the nucleus as compared to the CAK-complex incorporated into TFIIH [16]. This shows that the CAK-complex, as part of TFIIH is targeted to the NER sites simultaneously with core TFIIH, suggesting a possible role for CAK in NER *in vivo*. Remarkably, this local CAK accumulation cannot be observed in CS-B cells (CS1AN), whereas core TFIIH is accumulated at these sites (Figure 1C). CS-B cells have a specific TC-NER defect and a proficient GG-NER. In these cells both PX and p62 (core TFIIH) accumulate and co-localize. However, no visible accumulation of CAK-components, cyclin H (Figure 1C) nor CDK7 (data not shown) co-localize at damaged areas. This suggests that CAK is only targeted to TC-NER sites and is not implicated in GG-NER. However, low levels of accumulation, *i.e.* below detection level, can not excluded.

Kinetics of CAK-accumulation at a NER site is similar to core-TFIIH accumulations

In order to compare the kinetic behavior of the CAK-complex in NER with core-TFIIH, we locally irradiated wild-type cells and fixed them after 15 minutes, four and eight hours. Four hours post UV, the majority of XPC has redistributed throughout the nucleus, as local accumulations were almost not detectable above the background staining. This suggests that the GG-NER pathway has removed the vast majority of its substrates (likely (6-4)PPs) from the genome. Also the greater part of core-TFIIH has relocated throughout the nucleus and the CAK-components were hardly detectable anymore at this stage, indicating that both TFIIH sub-complexes follow similar

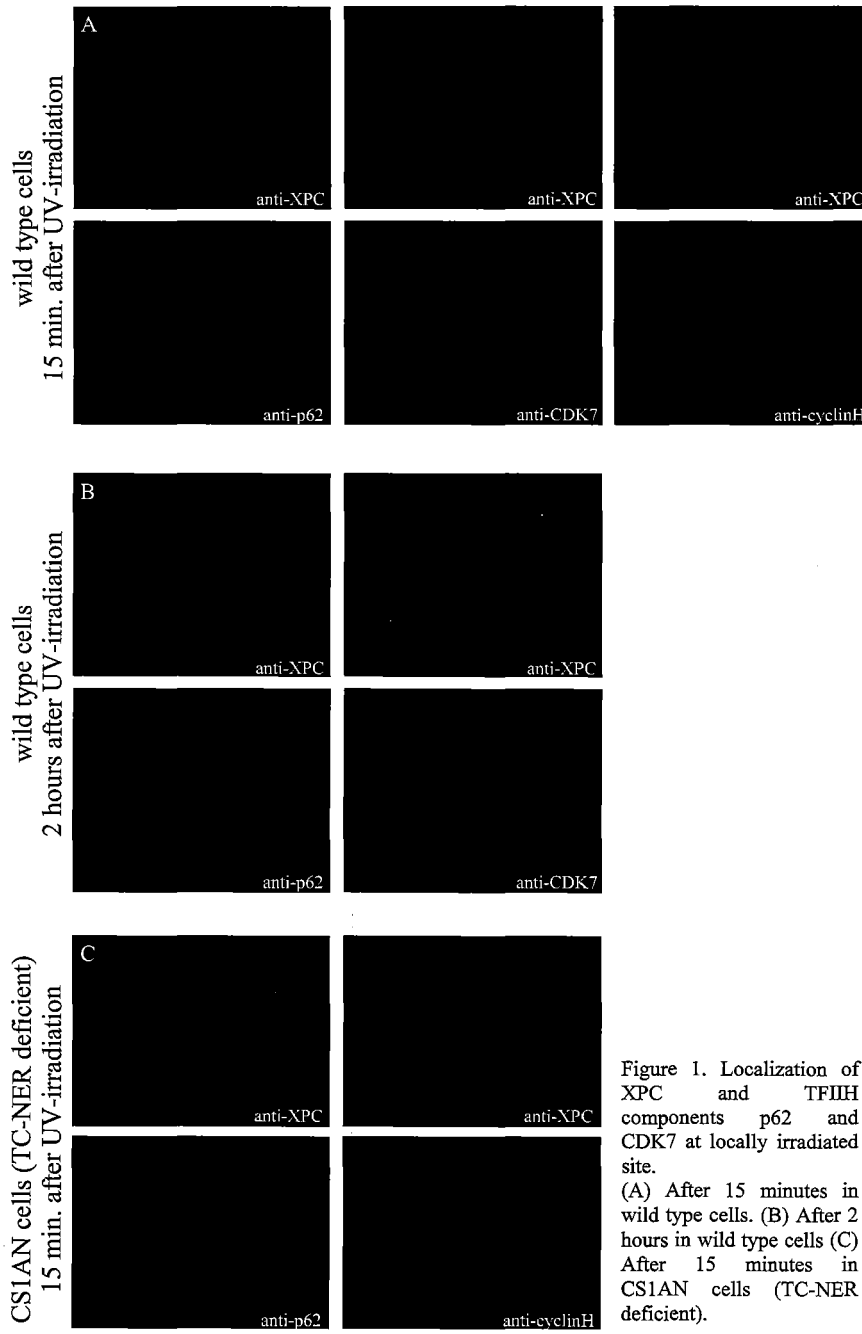

Figure 1. Localization of XPC and TFIIH components p62 and CDK7 at locally irradiated site.
(A) After 15 minutes in wild type cells. (B) After 2 hours in wild type cells (C) After 15 minutes in CS1AN cells (TC-NER deficient).

accumulation kinetics in NER (Table 2). To verify whether the reduction of XPC, core-TFIIH and CAK-complex accumulation in time after local damage induction, is due to the actual repair, we studied the removal of the (6-4)PP and CPD lesions at these sites 4 and 8 hours after UV-irradiation (Table 2). In wild type cells, (6-4)PPs were not detected 8 hours after applying local UV-irradiation, which is in line with previously observed relative fast removal of these lesions [27]. Removal of the CPDs was not completed even 24 hours after local damage induction. This indicates that the fading of the accumulation of NER factors within the first four hours is due to the removal of (6-4)PPs and that the observed NER-factor accumulation mainly monitors (6-4)PP repair. The removal of CPDs is relatively inefficient as compared to (6-4)PP repair and does not attribute to a large extent to the accumulation of NER factors. In conclusion, the trimeric CAK complex was shown to be targeted to NER-sites with the same kinetics as core TFIIH, where it appeared to be specifically involved in TC-NER.

Table 1. Used cell lines and characteristics

cell strain	gene	mutation	domain	syndrome
XP6BE	XPD	R683W	p44 interaction	XP-D
XP1NE	XPD	G47R	helicase	XP-D
XPCS2	XPD	G602D	helicase	XP-D/CS
TTD1BEL	XPD	R722W	p44 interaction	TTD
TTD1RO	XPD	R658C	p44 interaction	TTD
TTD6VI	XPB	T119P	p34 interaction	TTD
XP131MA	XPB	frameshift 742	5' incision	XP-B/CS
TTD1BR	unknown	unknown	unknown	TTD-A

Accumulation of TFIIH in various XPD mutant cells

To further analyze the targeting of CAK to UV-lesions we examined an assortment of cells from XP, XP /CS and TTD individuals for accumulation of various TFIIH components at the site of local damage (Table 1). First we focussed on cells with different disease causing mutations in the *XPD* gene, encoding one of the two DNA helicases in TFIIH. Previous *in vitro* studies have shown that mutations in the C-terminal coding part of XPD negatively influence the anchoring of this polypeptide into the core TFIIH part, via its reduced interaction with the p44 core component. Since the

CAK trimer is attached via XPD to TFIIH, a concomitant decreased association of CAK to TFIIH containing these mutant XPD proteins was noted [21, 23]. We

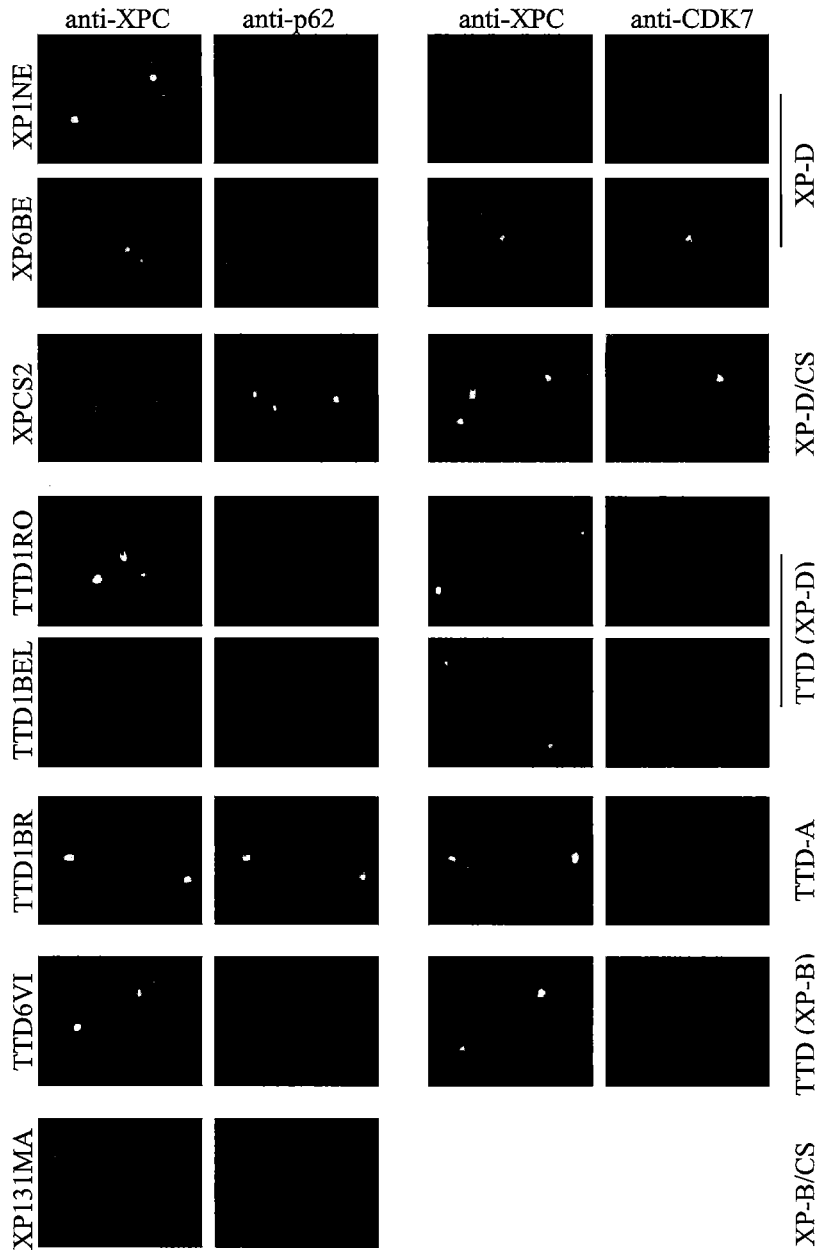

Figure 2. Localization of XPC and TFIIH components p62 and CDK7 at locally irradiated site in various TFIIH mutant cells.
(A) XP1NE cells (B) XP6BE cells (C) XPCS2 cells (D) TTD1RO cells (E) TTD1BEL cells (F) TTD1BR cells (G) TTD6VI cells (H) XP131MA cells.

wondered whether the enfeebled XPD-p44 interaction would result in a detachment of the CAK-complex from core TFIIH *in vivo* and consequently altered targeting to NER sites. Again we used the local damage technique to visualize the different subunits of TFIIH at NER sites. In all XP-D, XP-D/CS, and TTD cell lines tested, the two core components p62 (Figure 2) and XPB (data not shown) accumulated at the site of UV damage. Interestingly, core-TFIIH accumulated even to a higher extent in both XP-D and XP-D/CS cells compared to wild-type (Table 2). While p62 and XPB accumulation at local damaged site in TTD cell lines was either similar (TTD1RO) or slightly lower than wild-type cells (TTD1BEL) (Table 2 and Figure 2). Accumulation of the CAK components was similar to core TFIIH, in both XP-D and XP-D/CS cells more CDK7 (Figure 2) and cyclinH (data not shown) accumulated at the locally damaged sites as compared to wild-type cells. In contrast, in TTD1BEL cells the accumulation of CAK components was hardly visible (Figure 2). Surprisingly, in the TTD1RO cells no accumulation of any of the CAK components was observed (Figure 2 and Table 2), suggesting that the mutation G713R in *XPD* gene leads to the detachment of the CAK complex at a NER site *in vivo*.

For all these mutant cells, we examined the accumulation of the other NER factors, XPA and ERCC1 at the locally damaged sites (Table 2). In all these mutant cells accumulation of these two NER factors at NER sites could be detected. Despite the specific NER defect in cells carrying a mutation in the XPD component of TFIIH, NER factors which have been suggested to load late in the assembly (after TFIIH) appeared to be recruited normally and independent of TFIIH malfunctioning. In XP-D and XP-D/CS mutants a similar higher accumulation of XPA and ERCC1 as for TFIIH was noted.

Table 2. Accumulation of XPC, p62 and CDK7, and presence of (6-4)PP and CPD at local damaged site at different time points after irradiation in various cell lines

cell line	anti-XPC			anti-p62			anti-CDK7			anti-XPA and anti-ERCC1			anti-(6-4)PP		anti-CPD	
	15'	4h	8h	15'	4h	8h	15'	4h	8h	15'	4h	8h	15'	8h	15'	24h
C5RO	+	-	-	+	-	-	+	-	-	+	-	-	+++	-	+++	+
XP6BE	++	++	++	++	++	++	++	++	++	++	++	++	+++	+++	+++	+++
XP1NE	++	++	++	++	++	++	++	++	++	++	++	++	+++	+++	+++	+++
XPCS2	+++	+++	+++	+++	+++	+++	++	++	++	+++	+++	+++	+++	++	+++	++
TTD1BEL	+	+	+/-	+	+	+/-	+/-	+/-	+/-	+	+	+/-	+++	-	+++	++
TTD1RO	+	+/-	-	+	+/-	-	-	-	-	+	+/-	-	+++	-	+++	++
TTD6VI	+	+	+/-	+	+	+/-	+/-	+/-	+/-	+	+	+/-				
XP131MA	++	++	++	++	++	++	++	++	++	++	++	++	+++	+++	+++	+++
TTD1BR	+	+	+/-	+	+	+/-	+/-	+/-	+/-	+	+	+/-	+++	-	+++	++

Accumulation of TFIIH in TTD-A group and XPB mutant cells

We wondered if similar TFIIH accumulation behavior could be found in cells of patients with similar syndromes but with mutations in different genes, the *XPB* gene and the unidentified TTD-A gene. In both XP-B/CS and TTD(XP-B) cells the core-TFIIH components p62 and XPB accumulated at a local NER site. Similar to XPD mutant cells, p62 and XPB accumulated to a higher extent in XP131MA (XP-B/CS) and both components were less concentrated at the damaged site in TTD6VI (XP-B) and TTD1BR (TTD-A) cells. In addition, CDK7 was also more accumulated in the XP-B/CS cells compared to wild-type, whereas it was hardly visible in both TTD cells. This indicates that in general holo-TFIIH accumulates more in XP and XP/CS type cells and less in TTD type cells compared to wild-type cells. This suggests a correlation between phenotype and the dynamic behavior of TFIIH in NER. It is however not known how this increased accumulation of TFIIH can be explained in relation to the mutations. Two distinct models can be envisaged; (i) a permanent (steady) entrapment of TFIIH at repair sites that due to the mutation cannot be released or (ii) TFIIH continuously binding and dissociating NER sites.

Kinetics of the TFIIH accumulation in TFIIH mutant cell lines

In order to study the kinetic behavior of the malfunctioning TFIIH complex at NER sites in the above described mutant cell lines, we locally irradiated the cells and fixed them after four and eight hours. Immunofluorescence revealed that the accumulation of XPC and TFIIH remained at similar levels in XP and XP/CS type of cells up to eight hours after UV-irradiation in contrast to wild-type cells (Table 2), whereas in the TTD cell lines the accumulation of the two NER factors was strongly reduced at that time (Table 2). To examine if these cell lines had any kind of repair we used the (6-4)PP and CPD antibodies on the locally damaged cells. The immunofluorescence studies showed that the XP and XP/CS cells were not able to repair either one of the lesions, as was previously shown [28]. However, the TTD cell lines were capable of removing the (6-4)PPs within 8 hours, whereas the CPDs were hardly removed even after 24 hours (Table 2). This is in line with previously published data of Eveno, *et al.* (1995) [29, 30]. This indicates that XP and XP/CS individuals have a general NER defect, whereas TTD individuals are able to repair (6-4)PPs possibly by GG-NER.

Discussion

CDK activating complex targets to NER sites

In this report we studied the effect of UV-induced DNA damage on the location of the TFIIH-associated ternary CAK complex and its possible involvement in NER in the context of intact cellular nuclei. By inflicting local UV-damage to nuclei of cultured fibroblasts we were able to visualize the accumulation of NER factors at these sites [25,

26]. In addition, the dynamic interactions of repair factors with damaged DNA and the NER reaction kinetics can be monitored at these locally damaged spots. The in this way determined reaction kinetics reflect the situation of totally UV-irradiated cells ([8, 31], Rademakers, *et al.*, submitted, Hoogstraten, *et al.*, submitted). Here we used this method to monitor CAK participation in NER. We observed a remarkable accumulation of the CAK complex components at the site of local damage. The amount of CAK complex accumulation at UV-damaged nuclear areas is nevertheless less pronounced than observed with core TFIIH subunits. This difference in quantity of loading to NER spots can be easily explained by the fact that there exist an almost four times molar excess of free ternary CAK complex than TFIIH bound CAK [16]. These data suggest that the entire (holo)complex is targeted to lesions and contrasts to earlier observations in yeast [17]. In these studies two different pools of TFIIH were identified, a 'core-TFIIH' complex functional in NER (either as a free component or as part of an NER-holo-complex) and one, containing the CAK-orthologs, dedicated to transcription initiation. Moreover, other studies showed that the (mammalian) CAK hetero-trimeric complex was dispensable for *in vitro* NER [18, 19].

CAK is only involved in TC-NER

This apparent contradiction between our cellular studies and previous test-tube experiments might be explained by the fact that in these studies the involvement of TFIIH in both NER and transcription was examined on each of the isolated processes and on naked DNA. Under these experimental conditions, the complex interplay between both processes and a possible influence of higher-order structure (chromatin) of the template DNA cannot be monitored. The fact that CAK components do not accumulate at locally damaged sites in CSB-defective cells (Figure 1C) suggests that the presence of CAK is required for TC-NER and not GG-NER. This specific requirement for TC-NER to obtain a detectable CAK accumulation is in line with the above reasoning, since this part of the NER reaction cannot be reconstituted *in vitro* so far. In addition, the *Saccharomyces cerevisiae* CDK7 ortholog, KIN28 was shown to be specifically involved in TC-NER [20]. At non-permissive temperatures the temperature-sensitive KIN28 mutants were shown to be defective in TC-NER, while the GG-NER pathway was not affected.

Local CAK accumulation in TFIIH mutant cells

Interestingly, CAK appeared not to be significantly accumulated at locally damaged sites in cells derived from different photosensitive TTD (with mutated TFIIH) patients. This is in sharp contrast to cells harboring other disease-causing TFIIH mutations that show even increased accumulation at local damage (Table 2). It was previously shown that TTD cells exhibit an almost normal level of (6-4)PP repair, but a nearly complete deficient removal of CPDs [29, 30]. Repair kinetics of the specific lesions, as observed here by immunofluorescence studies at locally damaged areas in the different mutants

matched with published results. These data further indicate that TTD cells might have a proficient GG-NER and deficient TC-NER, since (6-4)PPs are mainly repaired via GG-NER, which is less efficient in removing CPDs from the genome. By the absence of locally CAK accumulation at lesions in TTD cells in combination with their proficient (6-4)PP removal we can conclude that the CAK complex is not required for the removal of (6-4)PPs.

Both cells derived from XP-type and XP/CS patients were deficient in removal of both (6-4)PPs and CPDs from the genome, suggesting an overall NER defect. Within these cells we observed a surprisingly higher accumulation of all tested TFIIH components (core as well as CAK) as compared to wild type cells. These robust accumulations remain high, even up to 8 h. after irradiation, with a concomitant absence of both (6-4)PP and CPD repair (Table 2). In addition, also the accumulation of XPC, a factor proceeding TFIIH action, remained strong long after damage induction. This suggests that not the entrance rate of NER factors at lesions is affected by the mutations, but rather the release of them from NER/DNA complexes. Whether factors as XPC and TFIIH are permanently bound to lesions or continuously assemble to a disassemble from abortive NER precursor complexes stuck in repair progression has to be established in future experiments.

CAK accumulation depends on anchoring to core TFIIH

How can the TTD-specific absence of CAK accumulation on locally damaged areas be rationalized? We found a seemingly complete lack of CAK incorporation into NER precursor complexes in TTD1RO cells and a severely weakened CAK interaction with core TFIIH in TTD1BEL (both mutated in *XPD*), TTD6VI (*XPB*) and TTD1BR (unknown gene). Whereas, all non-TTD TFIIH-mutated cells (from patients exhibiting XP and XP/CS features) revealed a relative high accumulation of the CAK complex at locally damaged sites. These observations suggest that within TTD the ternary CAK complex is more loosely attached to core TFIIH and provide further *in vivo* evidence of previous *in vitro* studies [21]. Using immunoprecipitation experiments, Coin and coworkers have shown that within TFIIH complexes carrying the XPD/R722W mutated protein (as in TTD1BEL patients) the interaction between XPD and one of the core components, p44 was strongly declined. As a consequence of this fragile interaction also the CAK trimer is less firmly attached to TFIIH, since the CAK is anchored via XPD to core TFIIH [32, 33]. However, similar results were also obtained for TFIIH complexes containing XP (XP6BE) and XP/CS (XPCS2) mutated XPD proteins [21, 23, 24].

Effect of reduced CAK association

Although, each of the XPD mutations appeared to affect the stability of TFIIH [34], the TTD-causing mutations might cause a more pronounced reduction of CAK anchoring. The overall fragility of TFIIH, resulting in a reduction of TFIIH level, was

shown to be a general feature within TTD cells [35, 36]. Interestingly, in cells from a particular group of TTD individuals (TTD-A), where no mutation has been found in any of the TFIIH subunits, the cellular features also seem to result from sub-limiting amounts of the complex [37]. Also in cells from this group, a strong reduction of CAK accumulation was observed (Table 2), further pointing into a direct relationship between TTD features, CAK-anchoring and possibly TFIIH levels.

Since TFIIH is not only required for NER, but also plays a pivotal role in transcription initiation, it was suggested that additional non NER-related features (from neuro-developmental origin, mainly displayed by XP/CS and TTD) was in part due to an affected transcription function of the complex [38, 39]. This hypothesis was supported by a number of different studies that show impeded transcription function in crude and (partially) purified cell lysates from TFIIH-mutated cells [34, 40, 41]. Further evidence for this repair/transcription syndrome was provided by a TTD mouse-model (mimicking a TTD-patient mutation in XPD, *i.e.* arg722trp), in which diminished transcription levels of the skin-specific *SPRR2* gene in terminally differentiating cells was observed [42]. Very recently, additional support for transcription alterations as a consequence of TTD-specific mutations was obtained from studies in tissue from TTD-individuals. First, reduced levels of β-globin synthesis have been reported in TTD patients with β-thalassaemia [43]. Secondly, alterations in T-cells and dendritic cells in a TTD individual with severe immunodeficiency have been described, suggesting a subtle transcription defect in a set of genes involved in maturation and function of these cells [44]. We postulate that not only reduced levels of TFIIH, but also the weakened association of CAK to core TFIIH, may contribute to altered gene-specific transcription. Reduced kinase activity, due to destabilized CAK association, in a cell line carrying an XPD mutation caused a severe effect on nuclear receptor-responsive transcription [24].

Function of CAK in NER

How can a decreased CAK association specifically affect CPD removal and or TC-NER function? The main observed function of CAK is its phosphorylating activity of a number of different substrates, including M-phase promoting complexes and the C-terminal domain (CTD) of the largest subunit of RNA polymerase II (RNAP2) [3, 45]. A likely role for CAK, whenever implicated in NER, is of course the phosphorylation of NER factors. Several NER factors carry potential phosphorylation sites. The phosphorylation status of a number of these factors differentially influences the *in vitro* NER activity [19 , 46]. A more specific role for CAK in TC-NER can be envisaged by its kineting activity of CTD. Lesion-stalled RNAP2 recruits TFIIH, possibly including CAK, for repair. The kinase complex can subsequently phosphorylate the CTD in the vicinity of the repair site. The CTD of RNAP2 becomes hypo-phosphorylated upon transcriptional arrest, likely also after lesion stalling. Hyper-phosphorylation of the CTD by recruited TFIIH may stimulate transcription progression after repair.

Consequently, kinase activity possibly affects transcription resumption rather than repair, thereby promoting the release of TFIIH, which in turn increases the pool of free TFIIH.

Reduced levels of TFIIH in TTD [35, 36] cells could also explain our obtained data, where (6-4)PPs are repaired, but at a slower rate (Table 2) and virtually no removal of CPDs lesions. A reduced level of TFIIH will mainly affect repair of poorly recognized lesions, since most TFIIH will be recruited to (6-4)PP sites and simply exhaust the available TFIIH pool. Future live cell kinetic experiments, using GFP-tagged CAK components in combination with different NER-deficient backgrounds (such as TC-NER defect or different TFIIH mutations) will show whether repair at the cross-road with transcription obeys the rules of chemical reaction kinetics. In a previous study [8] we have shown that at least participation of core TFIIH in NER and transcription is a stochastic process governed by diffusion, random collision and available target sites.

Material and Methods

Cell lines and culture conditions

Primary fibroblasts (C5RO (wild type), XP6BE (XP-D), XP1NE (XP-D), XPCS2 (XP-D/CS), TTD1BEL (TTD(XPD)), TTD1RO (TTD(XPD), TTD1BR (TTD-A), TTD6VI (TTD(XPB), XP131MA (XP-B/CS), XP21RO (XP-C) and CS1AN (CS-B) were cultured under standard conditions at 37°C and 5% CO_2 in Ham's F10 medium supplemented with 12% FCS and antibiotics.

UV-irradiation treatment

Before UV irradiation cells were rinsed with PBS and covered with an isopore polycarbonate filter (Millipore) containing 5 μm diameter pores before UV-irradiation with a Philips TUV lamp (254 nm) at a dose rate of ~ 0.8 $J.m^2/s$. In total a UV-dose of 48 J/m^2 is given and cells were put back into medium for 15 minutes, 4 or 8 hours.

UV-induced unscheduled DNA synthesis

At different time points after local UV-irradiation the cells were cultured in Ham's F10 medium supplemented with 12% dialyzed FCS, antibiotics and 20 μCi/ml of ^{3}H-thymidine for 1 hour (Amersham; 120 Ci/mM). Excess of radioactive nucleotides is removed by PBS washing and consequently fixation. Incorporation of ^{3}H-thymidine was visualized by microscopic autoradiography. Slides were dipped into a radiography emulsion (Ilford K2) and exposed for 3 days before photographic development. DNA repair was quantified by counting the autoradiographically-induced silver grains above nuclei in locally damaged sites. The mean number of grains of mutant cell lines is compared to wild-type amounts (set to 100%).

Immunofluorescence

Where stated cells were labeled with latex beads as described by [37]. Cells were fixed with 2% paraformaldehyde and 0.2% Triton X-100 and subsequently washed twice with PBS containing 0.1% Triton X-100. Antibodies were incubated in PBS^+ (containing 0.15% glycine and 0.5% BSA) for 90 minutes at room temperature at the following concentrations: α-XPC (1:500) [47], α-p62 (3C9, 1:2000), α-CDK7 (2F8, 1:5000), α-cyclinH (2D4, 1:1000), α-(6-4)PP (64Mz, 1:500) and α-CPD (TDMz, 1:500). All TFIIH-component monoclonals were kindly provided by J.M. Egly (IGMC, Illkirch, France) and the monoclonals against the UV-induced lesions were kindly provided by O. Nikaido (Kanazawa University, Japan). Afterwards cells were washed twice with PBS containing 0.1% Triton X-100. The secondary antibodies, goat-anti-mouse Cy3-conjugated (Jackson Laboratory) and goat-anti-rabbit Alexa-594-conjugated (Molecular Probes) were diluted 800 times in PBS^+ and incubated for 1 hour at room temperature. After two washing steps with PBS containing 0.1% Triton X-100 the coverslip was mounted in Vectashield mounting medium (Vector Laboratory) containing 1.5 μg/μl DAPI. Epifluorescent and phase-contrast images were generated on a Leitz Aristoplan microscope equipped with a 3-CCD camera (DXC-950P Sony).

References

1. **Gerard, M., et al.**, *Purification and interaction properties of the human RNA polymerase B(II) general transcription factor BTF2.* J. Biol. Chem., 1991. 266(31): p. 20940-20945.
2. **Conaway, R.C. and J.W. Conaway**, *General initiation factors for RNA polymerase II. Annu. Rev. Biochem.*, 1993. 62: p. 161-190.
3. **Egly, J.M.**, *The 14th Datta Lecture. TFIIH: from transcription to clinic.* FEBS Lett, 2001. 498(2-3): p. 124-8.
4. **Schaeffer, L., et al.**, *DNA repair helicase: a component of BTF2 (TFIIH) basic transcription factor.* Science, 1993. 260: p. 58-63.
5. **Schaeffer, L., et al.**, *The ERCC2/DNA repair protein is associated with the class II BTF2/TFIIH transcription factor.* EMBO J., 1994. 13(10): p. 2388-2392.
6. **Roy, R., et al.**, *The MO15 cell cycle kinase is associated with the TFIIH transcription-DNA repair factor.* Cell, 1994. 79: p. 1093-1101.
7. **Iben, S., et al.**, *TFIIH Plays an Essential Role in RNA Polymerase I Transcription.* Cell, 2002. 109(3): p. 297-306.
8. **Hoogstraten, D., et al.**, *Rapid Switching of TFIIH between RNA Polymerase I and II Transcription and DNA Repair In Vivo.* Mol Cell, 2002. 10(5): p. 1163-74.
9. **Drapkin, R., et al.**, *Dual role of TFIIH in DNA excision repair and in transcription by RNA polymerase II.* Nature, 1994. 368: p. 769-772.
10. **Van Vuuren, A.J., et al.**, *Correction of xeroderma pigmentosum repair defect by basal transcription factor BTF2 (TFIIH).* EMBO J., 1994. 13(7): p. 1645-1653.
11. **de Laat, W.L., N.G. Jaspers, and J.H. Hoeijmakers**, *Molecular mechanism of nucleotide excision repair.* Genes Dev., 1999. 13(7): p. 768-785.

12. **Hanawalt, P. and G. Spivak**, *Transcription-coupled DNA repair, in Advances in DNA damage and repair*, Dizdaroglu and Karakaya, Editors. 1999, Kluwer Academic/Plenum Publishers: New York.
13. **Sugasawa, K., et al.**, *Xeroderma pigmentosum group C protein complex is the initiator of global genome nucleotide excision repair*. Mol. Cell, 1998. 2(2): p. 223-232.
14. **Hoeijmakers, J.H.**, *Genome maintenance mechanisms for preventing cancer*. Nature, 2001. 411(6835): p. 366-74.
15. **Evans, E., et al.**, *Mechanism of open complex and dual incision formation by human nucleotide excision repair factors*. EMBO J., 1997. 16(21): p. 6559-6573.
16. **Rossignol, M., I. Kolb-Cheynel, and J.M. Egly**, *Substrate specificity of the cdk-activating kinase (CAK) is altered upon association with TFIIH*. Embo J, 1997. 16(7): p. 1628-37.
17. **Svejstrup, J.Q., et al.**, *Different forms of TFIIH for transcription and DNA repair: holo-TFIIH and a nucleotide excision repairosome*. Cell, 1995. 80(1): p. 21-28.
18. **Wood, R.D., M. Biggerstaff, and M.K.K. Shivji**, *Detection and measurement of nucleotide excision repair synthesis by mammalian cell extracts in vitro*. Methods, a companion to methods in enzymology., 1995. 7: p. 163-175.
19. **Araujo, S.J., et al.**, *Nucleotide excision repair of DNA with recombinant human proteins: definition of the minimal set of factors*, active forms of TFIIH, and modulation by CAK. Genes Dev., 2000. 14(3): p. 349-359.
20. **Tijsterman, M., et al.**, *Defective Kin28, a subunit of yeast TFIIH, impairs transcription-coupled but not global genome nucleotide excision repair*. Mutat Res, 1998. 409(3): p. 181-8.
21. **Coin, F., J.C. Marinoni, and J.M. Egly**, *Mutations in XPD helicase prevent its interaction and regulation by p44, another subunit of TFIIH, resulting in Xeroderma pigmentosum (XP) and trichothiodystrophy (TTD) phenotypes*. Pathol Biol (Paris), 1998. 46(9): p. 679-80.
22. **Coin, F., et al.**, *Mutations in the XPD helicase gene result in XP and TTD phenotypes, preventing interaction between XPD and the p44 subunit of TFIIH* [see comments]. Nat Genet, 1998. 20(2): p. 184-8.
23. **Sandrock, B. and J.M. Egly**, *A yeast four-hybrid system identifies Cdk-activating kinase as a regulator of the XPD helicase, a subunit of transcription factor IIH*. J Biol Chem, 2001. 276(38): p. 35328-33.
24. **Keriel, A., et al.**, *XPD mutations prevent TFIIH-dependent transactivation by nuclear receptors and phosphorylation of RARalpha*. Cell, 2002. 109(1): p. 125-35.
25. **Mone, M.J., et al.**, *Local UV-induced DNA damage in cell nuclei results in local transcription inhibition*. EMBO Rep, 2001. 2(11): p. 1013-1017.
26. **Volker, M., et al.**, *Sequential Assembly of the Nucleotide Excision Repair Factors In Vivo*. Molecular Cell, 2001. 8(1): p. 213-224.
27. **Mitchell, D.L., C.A. Haipek, and J.M. Clarkson**, *(6-4)Photoproducts are removed from the DNA of UV-irradiated mammalian cells more efficiently than cyclobutane pyrimidine dimers*. Mutat Res, 1985. 143(3): p. 109-12.
28. **van Hoffen, A., et al.**, *Cells from XP-D and XP-D-CS patients exhibit equally inefficient repair of UV-induced damage in transcribed genes but different capacity to recover UV-inhibited transcription*. Nucleic Acids Res, 1999. 27(14): p. 2898-904.
29. **Eveno, E., et al.**, *Different removal of ultraviolet photoproducts in genetically related xeroderma pigmentosum and trichothiodystrophy diseases*. Cancer Res, 1995. 55(19): p. 4325-32.

30. **Marionnet, C., et al.**, *Cyclobutane pyrimidine dimers are the main mutagenic DNA photoproducts in DNA repair-deficient trichothiodystrophy cells.* Cancer Res, 1998. 58(1): p. 102-8.
31. **Houtsmuller, A.B., et al.**, *Action of DNA repair endonuclease ERCC1/XPF in living cells.* Science, 1999. 284(5416): p. 958-961.
32. **Chang, W.H. and R.D. Kornberg**, *Electron crystal structure of the transcription factor and DNA repair complex, core TFIIH.* Cell, 2000. 102(5): p. 609-13.
33. **Schultz, P., et al.**, *Molecular structure of human TFIIH.* Cell, 2000. 102(5): p. 599-607.
34. **Satoh, M.S. and P.C. Hanawalt**, *Competent transcription initiation by RNA polymerase II in cell-free extracts from xeroderma pigmentosum groups B and D in an optimized RNA transcription assay.* Biochim Biophys Acta, 1997. 1354(3): p. 241-51.
35. **Vermeulen, W., et al.**, *A temperature-sensitive disorder in basal transcription and DNA repair in humans.* Nat Genet, 2001. 27(3): p. 299-303.
36. **Botta, E., et al.**, *Reduced level of the repair/transcription factor TFIIH in trichothiodystrophy.* Hum Mol Genet, 2002. 11(23): p. 2919-2928.
37. **Vermeulen, W., et al.**, *Sublimiting concentration of TFIIH transcription/DNA repair factor causes TTD-A trichothiodystrophy disorder.* Nat Genet, 2000. 26: p. 307-313.
38. **Bootsma, D. and J.H.J. Hoeijmakers**, *Engagement with transcription.* Nature, 1993. 363: p. 114-115.
39. **Vermeulen, W., et al.**, *Three unusual repair deficiencies associated with transcription factor BTF2(TFIIH): evidence for the existence of a transcription syndrome.*, in Cold-Spring-Harb-Symp-Quant-Biol. 1994. p. 317-329.
40. **Hwang, J.R., et al.**, *A 3' to 5' XPB helicase defect in repair/transcription factor TFIIH of xeroderma pigmentosum group B affects both DNA repair and transcription.* The Journal of Biological Chemistry, 1996. 271: p. 15898-15904.
41. **Dianov, G.L., et al.**, *Reduced RNA polymerase II transcription in extracts of cockayne syndrome and xeroderma pigmentosum/Cockayne syndrome cells.* Nucleic Acids Res, 1997. 25(18): p. 3636-42.
42. **de Boer, J., et al.**, *A mouse model for the basal transcription/DNA repair syndrome trichothiodystrophy.* Mol. Cell, 1998. 1(7): p. 981-990.
43. **Viprakasit, V., et al.**, *Mutations in the general transcription factor TFIIH result in beta-thalassaemia in individuals with trichothiodystrophy.* Hum Mol Genet, 2001. 10(24): p. 2797-802.
44. **Racioppi, L., et al.**, *Defective dendritic cell maturation in a child with nucleotide excision repair deficiency and CD4 lymphopenia.* Clin Exp Immunol, 2001. 126(3): p. 511-8.
45. **Harper, J.W. and S.J. Elledge**, *The role of Cdk7 in CAK function, a retro-retrospective.* Genes Dev, 1998. 12(3): p. 285-9.
46. **Winkler, G.S., et al.**, *Novel functional interactions between nucleotide excision DNA repair proteins influencing the enzymatic activities of TFIIH, XPG, and ERCC1- XPF.* Biochemistry, 2001. 40(1): p. 160-5.
47. **Van der Spek, P.J., et al.**, *XPC and human homologs of RAD23: intracellular localization and relationship to other nucleotide excision repair complexes.* Nucleic Acids Res., 1996. 24(13): p. 2551-2559.

Chapter 8

DNA-damage sensing in living cells by xeroderma pigmentosum group C

manuscript in preparation

DNA-damage sensing in living cells by xeroderma pigmentosum group C

Deborah Hoogstraten[1], Alex L. Nigg[2], Gert W.A. van Cappellen[3], Jan H. J. Hoeijmakers[1], Adriaan B. Houtsmuller[2] and Wim Vermeulen[1]

[1]Department of Cell Biology and Genetics (Medical Genetics Center, CBG), Erasmus University, P.O.Box 1738, 3000 DR Rotterdam, the Netherlands,
[2]Department of Pathology (Josephine Nefkens Institute), Erasmus University, the Netherlands,
[3]Department of Endocrinology and Reproduction, Erasmus University, P.O.Box 1738, 3000 DR Rotterdam, the Netherlands.

Summary

The global genome nucleotide excision repair (GG-NER) pathway removes numerous helix-distorting lesions from the genome, including UV-induced injuries. The initiator of GG-NER, XPC-hHR23B has an intrinsic high affinity for DNA, which is even greater for damaged DNA. The mechanism by which XPC-hHR23B locates DNA damages in the genome is not clear. Here, we report a study on the behavior of XPC in living cells. We generated a cell line that stably expresses at physiological level fully functional GFP-tagged XPC. High resolution confocal imaging uncovered that XPC-GFP had an inhomogeneous distribution and a high probability to be located at DNA. Photobleaching experiments revealed that the fusion protein is slowed down in its nuclear movement, by constantly dissociating and re-associating from an immobile nuclear component, likely DNA. Upon induction of UV-damages XPC-GFP was bound to DNA for a period of ~1-2 minutes, surprisingly shorter than other NER factors (ERCC1/XPF, TFIIH, XPA) that were bound in one single repair event for ~ 4 minutes. This suggests that XPC-GFP leaves the transient NER accumulation prior to other NER factors.

Introduction

DNA is constantly under attack by various metabolic and external factors, such as UV-light [1]. The integrity of DNA is ensured by multiple interwoven DNA repair systems. Nucleotide excision repair (NER) is one of the most versatile repair pathways, which removes a variety of lesions including UV-induced cyclobutane pyrimidine dimers (CPD) and pyrimidine (6-4) pyrimidone photoproducts ((6-4)PP) [2]. The biological significance of a functional NER is evident from the severity of clinical features seen in patients, suffering from inherited NER-deficient syndrome xeroderma pigmentosum (XP). Individuals carrying a mutation in one of the seven XP-genes (*XPA* to *XPG*) mainly exhibit cutaneous symptoms, including extreme UV-sensitivity and

sun-induced pigmentation anomalies and most importantly an >2000 fold increase in skin-cancer [3].

The highly conserved NER-pathway, is a multistep 'cut-and-patch' process involving the concerted action of about 30 polypeptides. Two sub-pathways exist within NER, differing in mode of damage recognition [2]. The transcription-coupled nucleotide excision repair (TC-NER), focuses on transcription-blocking lesions located in the transcribed strand of active genes. An RNA polymerase II stalled at a lesion efficiently triggers the NER pathway to quickly eliminate this cytotoxic blockage of transcription [4]. The global genome nucleotide excision repair (GG-NER) eliminates lesions located anywhere in the genome, where the XPC-hHR23B heterodimer serves as a damage detector assisted (for specific types of damage) by the UV-DDB complex [5, Chu, 1988 #571, 6]. Both sub-pathways funnel into the 'core'-NER', which comprises three additional steps, (i) open complex formation and verification, (ii) incision and (iii) DNA synthesis and ligation. The DNA helix around the lesion is melted by the transcription factor IIH (TFIIH) and this open DNA structure is stabilized by the replication protein A. After damage verification by XPA, the two endonucleases ERCC1/XPF and XPG will cut the damaged strand at some distance from the damage. The pre-incision complex was shown to contain TFIIH, XPA, RPA and the two endonucleases, but not XPC-hHR23B [7]. The last events in this multi-step repair procedure are filling of the gap by conventional DNA synthesis and ligation [8]. XPC-hHR23B is the first factor within the GG-NER pathway to bind to lesions, as was shown both *in vitro* and *in vivo* [5, 9]. Purified XPC-hHR23B complex displays high affinity for undamaged single and double stranded DNA [10, 11]. However, competition experiments revealed a preferential binding of the isolated complex to DNA with various induced lesions [12]. Recently, it was shown that XPC-hHR23B even binds to small bubble structures with or without a lesion [13]. However, dual incision in an *in vitro* NER assay was only observed when damage was present in the bubble. Suggesting that after binding of the XPC-hHR23B complex to a helix distorted site, the presence of the injured base is verified by additional NER-specific factors prior to dual excision. This multistep procedure ensures a high safety level within the GG-NER pathway, allowing the NER reaction only to proceed when the proper (NER-specific) lesions are encountered.

It has been suggested that the early NER factors, such as XPC-hHR23B are capable of sensing sites that exhibit unfavorable configuration in terms of free energy [14], e.g. helical distortions due to DNA damage. XPC-hHR23B might thus be probing the DNA helix for these (thermodynamic) instabilities. The XPC-hHR23B heterodimer has been shown to be able to induce a bend in DNA upon binding both at undamaged and damaged sites [15]. The helix of damaged DNA might accommodate the configuration that is induced by binding of XPC-hHR23B, more easily and thereby stabilizing the binding of the heterodimer to the lesion containing DNA. However, the manner in which XPC-hHR23B finds a lesion in the genome, is not clear. DNA binding proteins are thought to locate target sites by two possible mechanisms (reviewed in [16]), (i)

proteins could slide along the DNA, i.e. a one-dimensional linear diffusion along the DNA contour, otherwise (ii) translocation of proteins might also occur through three-dimensional space, via diffusion and multiple dissociation/re-association events on the genome.

The GG-NER pathway has been shown to remove the different UV-induced lesion ((6-4)PPs and CPDs) in a distinct way. (6-4)PPs are eliminated very rapidly after UV-irradiation throughout the entire genome including non-transcribed regions, whereas the CPDs persist for a longer period [17]. Purified XPC-hHR23B exhibited higher affinity for (6-4)PPs than CPDs. Although XPC-hHR23B does not preferentially bind CPDs, the excision of these lesions depends on the complex, since CPDs are not removed from the entire genome in cells of XP-C individuals, only from the transcribed strand [18]. The UV-damaged DNA binding protein (UV-DDB complex, [19, 20]) was shown to enhance the excision of CPDs in an *in vitro* NER reaction up to 17 fold, possibly by assisting XPC-hHR23B in damage recognition of these lesions. In contrast, the excision of 6-4PPs was hardly stimulated in this defined NER system [21]. Since UV-DDB was shown to interact with CBP/p300 histone-acetyltransferase, it is not unlikely that this complex facilitates repair in more compact chromatin structures.

In order to study the behavior, dynamics and reaction kinetics of the XPC-hHR23B complex within living cells we tagged XPC with the green fluorescent protein (GFP). Using confocal microscopy and applying various photobleaching techniques we investigated XPC-GFP mobility in untreated cells. We were also able to follow the kinetics of the fusion protein within the GG-NER pathway upon damage induction by UV-light, as was previously done for the core NER components XPA (Rademakers, *et al.*, submitted), TFIIH [22] and ERCC1/XPF [23]. However, both the mobility parameters and kinetic engagement of XPC-GFP in NER differs dramatically from the other core NER factors.

Results

Generation of stably XPC-GFP expressing cell line

In order to study the dynamic nuclear distribution in time and space of the XPC protein and to determine how this protein is targeted to DNA lesions in the most relevant context, the living cell nucleus, we tagged protein with life cell marker GFP. The cDNA encoding the GFP was fused in frame to the C-terminus of the XPC cDNA. Prior to the generation of a cell line expressing the fusion protein, the hybrid was first checked for its functionality by microinjection into XPC-deficient primary fibroblast and analysis of the repair capacity of the injected cells (Ng, *et al.*, submitted). After transfection of the fusion construct to XP4PA SV cells (SV-40 immortalized fibroblasts derived from a XP group C patient with a 2 bp deletion in the *XPC* gene, creating a frameshift at position 1483 and the introduction of a stopcodon [24, 25]), an NER-proficient population was selected by three rounds of 4 J/m^2 UV-light with 48 hours intervals. As shown by immunoblot analysis (Figure 1A), the expression of the GFP-

tagged XPC in the NER-proficient population is comparable to the wild type expression levels (compare lane 1 and 3).

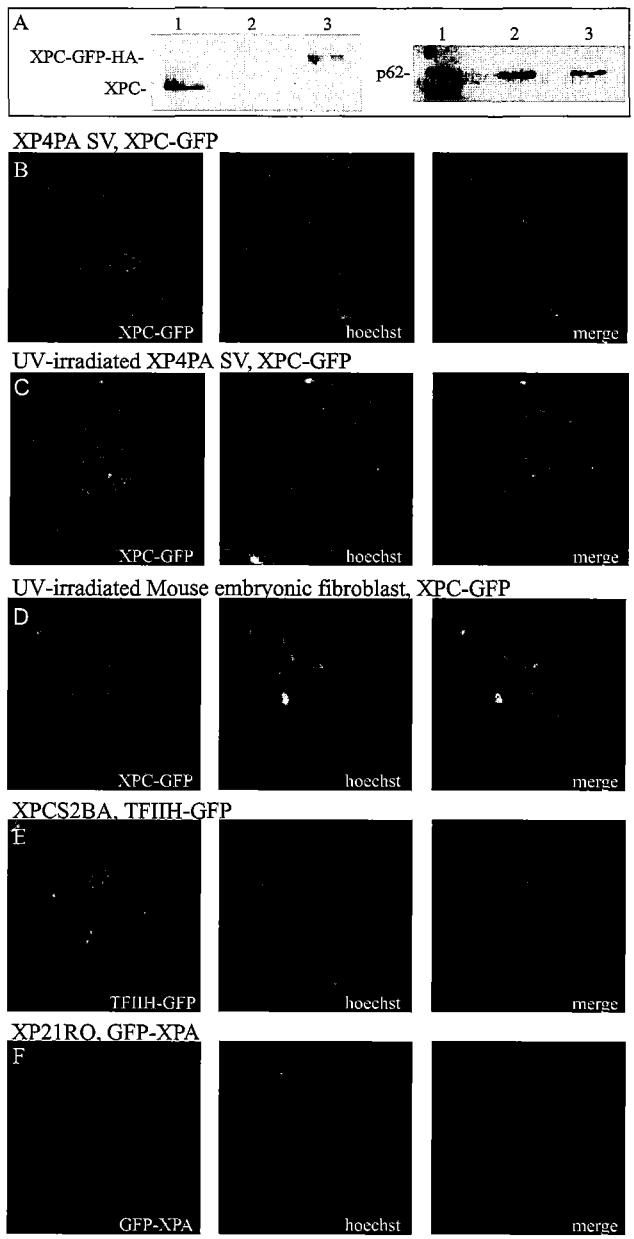

Figure 1. Characterization of the nuclear distribution of GFP tagged XPC, XPA and TFIIH in living cells.
(A) Immunoblot probed with anti-XPC polyclonal (left panel) and anti-p62 monoclonal (right panel) of WCE of MRC5 (lane 1), XP4PA (lane 2) and population of XP4PA cells stably expressing XPC-GFP (lane 3). (B) Confocal image of a living XPC-GFP expressing cell. (C) Confocal image of XPC-GFP expressing cell treated with $8J/m^2$ of UV-light. (D) Confocal image of a living mouse embryonic fibroblast expressing XPC-GFP treated with $8J/m^2$ of UV-light. (E) Confocal image of a living XPB-GFP (TFIIH-GFP) expressing cell. (F) Confocal image of a living cell expressing GFP-XPA. Left panel: GFP-fluorescence, Middle; hoechst staining of DNA, Right: merged image.

Distribution of XPC-GFP in mammalian nuclei

The distribution of XPC-GFP in living human fibroblasts was studied by using confocal laser scanning microscopy at high-resolution. The GFP tagged XPC had a strictly nuclear localization (Figure 1B, left panel), as was previously shown by immunofluorescence labeling with antibodies against endogenous XPC [26]. Close observation of the high resolution images revealed that in virtually all XPC-GFP expressing cells the internuclear distribution of the fusion protein was heterogeneous. This pronounced inhomogeneity was not observed with cell-lines stably expressing other GFP tagged core-NER factors, such as XPA (Rademakers, *et al.*, in prep), ERCC1/XPF [23] and TFIIH [22], which all showed a homogenous distribution, with TFIIH having additional nucleolar accumulations.

Interestingly, staining of the genomic DNA by Hoechst 33258 in these living cells uncovered a similar heterogeneous distribution of this DNA dye (Figure 1B, middle panel). The merged image of the DNA, which is characteristically observed as dense and less densely stained areas, and the XPC-GFP distribution showed a high level of co-localization of the two signals (Figure 1B, right panel). This indicates that XPC-GFP is located near or at the site of DNA. Moreover, XPC-GFP is located at both low and highly concentrated areas of DNA. Even with highly condensed DNA in M-phase, XPC-GFP appeared to be associated with mitotic chromosomes (data not shown), as was previously shown in fixed cells using antibodies raised against XPC [26]. XPC-GFP is the first NER-factor that displays this distribution pattern. The localization of the core-NER components XPA and TFIIH tagged with GFP is shown in Figure 1E and F. The XPC-GFP localization does not seem to be an over-expression artifact, since nearly all XPC-GFP expressing cells (very low to very high levels of XPC-GFP expression) exhibit this particular distribution pattern. Moreover, expression of the fusion protein in mouse embryonic fibroblasts resulted in similar XPC-DNA co-localization pattern (Figure 1D).

Nuclear mobility of XPC-GFP

The above data suggests that a large fraction of XPC-hHR23B is located at or even bound to DNA. In order to investigate whether the majority of XPC-GFP molecules are steadily bound to DNA, or if a large fraction is in a dynamic equilibrium in which a large fraction is transiently bound and a relatively smaller pool freely mobile, we have determined the nuclear mobility of the fusion protein. To that aim we applied fluorescence recovery after photobleaching (FRAP) on XPC-GFP expressing cells [27]. Briefly, a narrow strip spanning the nucleus is bleached by a high intensity laser pulse. Subsequently, the fluorescence redistribution within this strip is monitored in time. The relative fluorescence, (*i.e.* fluorescence after divided by fluorescence before bleaching) is plotted as a function of time. The diffusion coefficient (D) of a possible freely mobile fraction can be calculated from the first two seconds of recovery. Note that, the obtained diffusion coefficient is composed of both free diffusing molecules and

transiently bound molecules, resulting in an effective diffusion coefficient (D_{eff}). Surprisingly, the XPC-GFP fusion protein moved much slower than would be expected of a freely diffusing protein with a molecular size of ~230 kDa when in complex with hHR23B and Cen2 [28], including the GFP tag (Figure 2A). As a reference also the diffusion of XPA-GFP is shown, which clearly redistributed faster than XPC-GFP. In Figure 2B, the effective diffusion rates of various proteins, GFP, GFP-XPA, ERCC1-GFP/XPF and TFIIH-GFP are plotted against their expected molecular size on a logarithmic scale. Comparing the fluorescence recovery of XPC-GFP with ERCC1-GFP/XPF, a heterodimer with a molecular weight of the same order (185 kDa), revealed that complete recovery of fluorescence was significantly delayed for XPC-GFP than for ERCC1-GFP/XPF. XPC-GFP appeared to move even slower through the nucleus, than TFIIH-GFP, a complex twice its size (~500 kDa) (Figure 2B).

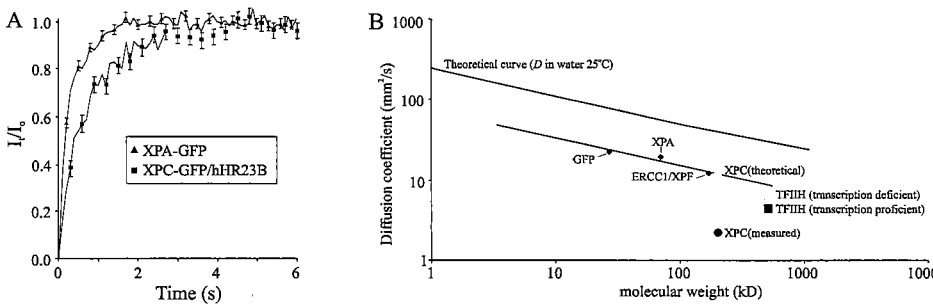

Figure 2. Temporal FRAP analysis of XPC-GFP dynamics in untreated cells.
(A) Temporal FRAP analysis of untreated XPA-GFP and XPC-GFP expressing cells. (B) Calibration curve, log of the effective diffusion rate of several GFP tagged proteins is plotted against the log of predicted molecular weight. The predicted and experimentally obtained diffusion coefficients (D) of XPC-GFP are shown.

The overall mobility of TFIIH-GFP appeared to be retarded by transcription-dependent transient interactions [22]. By inhibiting transcription the transient interactions of TFIIH with the transcription machinery were abrogated, resulting in an increased rate of fluorescence recovery. In the absence of transcription, the dynamical characteristics of the nuclear distribution of TFIIH-GFP favor a model of free diffusion, identical to a few other NER factors ([23], Rademakers, *et al.*, submitted). Extrapolation of the determined effective diffusion rate of XPC-GFP to a molecular size as in Figure 2B, would result in an improbable size of more than 2 GDa. Although incorporation of the heterodimer XPC/hHR23B into such an enormous complex cannot be excluded, the slower mobility could also be explained by short-term bindings to nuclear structures, as was found for TFIIH. Whatever model would be favored, it is at least clear that XPC displayed a complete different mode of dynamic distribution through the nucleoplasm as compared to other tested NER factors.

To further investigate this slow mobility phenomenon of XPC-GFP we used a modified FRAP application, simultaneous FRAP and FLIP (fluorescence recovery after photobleaching and fluorescence loss in photobleaching) [22]. Briefly, a strip at one side of the nucleus is bleached and subsequently fluorescence is monitored in both the bleached strip (FRAP) and at the opposite pole of the nucleus (FLIP). The difference in relative fluorescence intensities between the FRAP and the FLIP area is plotted against time and the time it takes to obtain full redistribution (>90%) ($t_{0.9}$) is determined as a measure for mobility. After ~70 seconds (including bleach time) 90% redistribution of bleached and non-bleached XPC-GFP molecules was reached (Figure 3A).

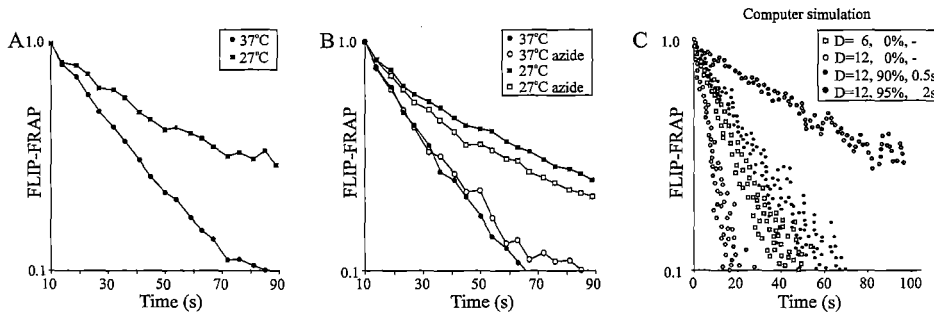

Figure 3. Simultaneous FRAP/FLIP of XPC-GFP dynamics in untreated cells.
(A) Simultaneous FRAP/FLIP analysis of untreated cells at 37 and 27 °C (closed circles and closed squares respectively). (B) Simultaneous FRAP/FLIP analysis of ATP depleted cells at 37 and 27 °C (open circles and open squares respectively). The curves of untreated cells at 37 and 27 °C (closed circles and closed squares respectively) are shown as a reference. (C) Computer simulation curves. Open squares and circles represent molecules with a diffusion rate of 6 and 12, respectively. Closed circles are a diffusion rate of 6, where 90% of the molecules are immobilized for 0.5 second. Similarly the gray circles, where 95% of the molecules are immobilized for 2 seconds.

In similar experiments, a $t_{0.9}$ of ~40 seconds was found for freely mobile TFIIH-GFP in transcriptionally inactive cells. These data are in agreement with the previous discussed FRAP data and clearly show that XPC-GFP mobility is much slower than expected. To distinguish if XPC-GFP is reduced in its mobility by incorporation into a larger complex or by short-term binding, we performed the simultaneous FRAP/FLIP analysis at 27 °C. At lower temperatures (10 K) the overall mobility of passive diffusing molecules is hardly effected [29, 30]. However, temperature-sensitive processes, such as enzymatic reactions are strongly affected by a decrease in temperature of 10 K, as was shown for TFIIH-GFP when engaged in RNA transcription initiation [22]. XPC-GFP exhibited a strongly reduced mobility at 27 °C compared to 37 °C, with a $t_{0.9}$ of ~ 140 seconds (Figure 3A). This suggests that the overall mobility of XPC-GFP is composed of traveling (in part) through a temperature-dependent process rather than simply free diffusion as part of a large complex. To check if XPC-GFP is slowed down due to involvement in an ATP-dependent process, we depleted ATP from the XPC-GFP expressing cells by adding Na-azide to deoxyglucose-containing glucose-free medium. The depletion of ATP from the cells

hardly effected the mobility of XPC-GFP both at 27 and 37 °C (Figure 3B), indicating that under unchallenged conditions XPC-GFP is not involved in an ATP-dependent process. In conclusion, these results suggests that XPC-GFP is not freely mobile in the nucleus, but its mobility is affected by a temperature-sensitive and ATP-independent event, most likely by frequently binding to DNA. The *in vivo* obtained mobility plots were compared to virtual mobility plots resulting from Monte Carlo computer simulation. Protein dynamics fitted best to simulated scenario in which a large fraction of XPC-GFP molecules (90%) was transiently immobilized for a relative short period (0.5 second) (Figure 2C). The mobility at 27 °C fitted best to a model in which a similar fraction was bound for a period of 2 s (4 times longer than at 37 °C). This suggests that binding to a nuclear structure is largely influenced by temperature.

Effects of the presence of UV-damage on the XPC-GFP mobility

To investigate the engagement of XPC-GFP in NER and the effect of NER-specific lesions in the genome have on the mobility properties, we exposed the XPC-GFP expressing cells to a UV-dose of 16 J/m^2 and performed FRAP experiments within the next 30 minutes. High resolution imaging revealed that the inhomogeneity of XPC-GFP was hardly affected in UV-treated cells compared untreated cells (Figure 1C). After UV irradiation XPC-GFP still co-localizes with genomic DNA.

In strip-FRAP studies, the effective diffusion coefficient is determined by normalizing the post-bleach fluorescence to zero and the maximum level of fluorescence reached after bleaching to one [27]. The D_{eff} of the unbound fraction of XPC-GFP of UV-damaged cells is similar to XPC-GFP from unchallenged cells, suggesting that the induction of UV-damage does not alter the mobility of XPC-GFP (Figure 4A). However, when the same strip-FRAP data is normalized differently and the pre-bleach fluorescence is normalized to one and the post-bleach fluorescence to zero, the decreased recovery of fluorescence can be used to determine the fraction of molecules that are immobile for a relatively long period [27]. This revealed a significant reduction in fluorescence recovery in the strip of XPC-GFP in UV-damaged cells (16 J/m^2) compared to non-UV-damaged cells (Figure 4B). With this high UV-dose of UV-C light a significant fraction (~40%) of XPC-GFP molecules was immobilized for a relatively long period. In addition, the fraction of immobilized XPC-GFP molecules appeared to be proportional to the amount of damage induced (applied UV-dose), and was saturated around 16 J/m^2 (Figure 4C). Surprisingly, two hours after applying 8 J/m^2 the immobilized fraction was decreased to background levels (Figure 4D). Similar kinetics are found for the removal of (6-4)PPs and the remaining immobilized fraction of XPC-GFP might be involved in the removal of CPDs which is a much slower process [31]. Together these results suggest that the observed binding of XPC-GFP molecules after UV induction mainly monitors the immediate targeting of the XPC-GFP to the most helix-distorting UV-lesion, i.e. (6-4)PPs. Also other NER-factors, such as TFIIH-GFP (Hoogstraten, *et al.*, in prep.) and ERCC1-GFP/XPF [23] revealed similar repair

kinetics, where the UV-induced immobile fraction was greatly reduced within 4 hours. In conclusion, the dose-dependent immobilization of XPC-GFP in combination with the time-dependent decay of immobilization, suggests that this immobilization of XPC-GFP reflects the binding of this protein into NER intermediates (DNA lesion/repair factor complexes).

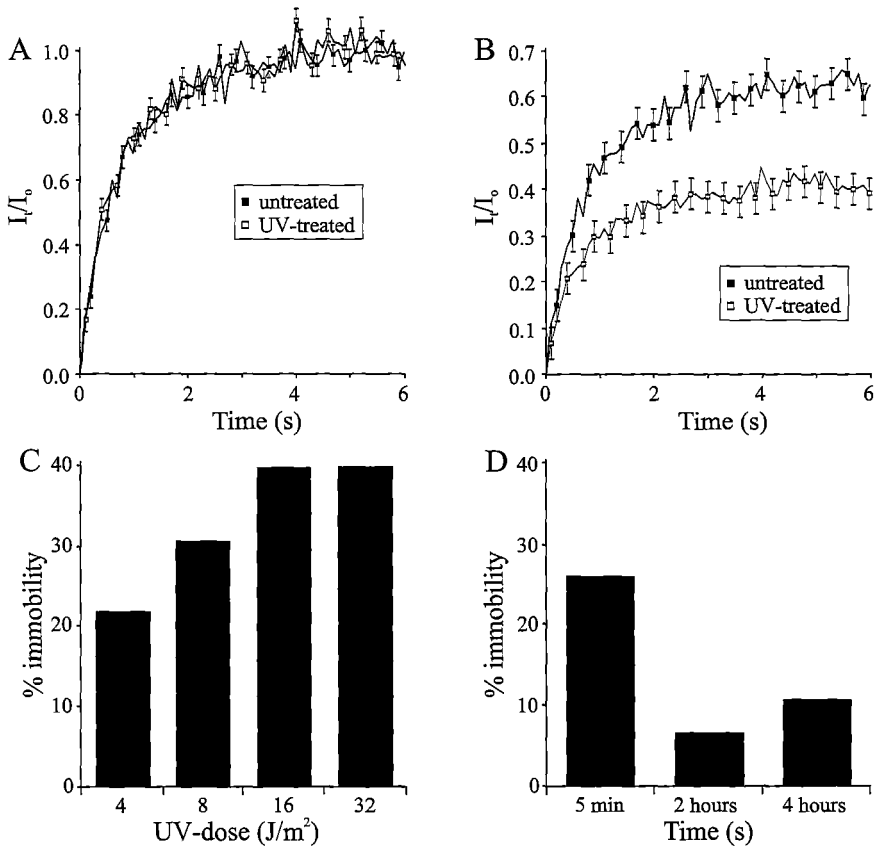

Figure 4. Temporal FRAP analysis of the alteration in DNA damage induced XPC-GFP dynamics.
(A) Temporal FRAP analysis of untreated and UV-irradiated cells. For evaluation of the effective diffusion rate the relative fluorescence is plotted against time, where the postbleach intensity is set to zero and the maximum reached intensity is set to one. (B) To determine the immobile fraction, in the same set of data as in (A) the post-bleach intensity is set to zero and the pre-bleach intensity is set to one. (C) UV-dose dependent immobilization of XPC-GFP. Percentage of immobilization is plotted against UV-dose. (D) UV-induced immobilized fraction plotted against time.

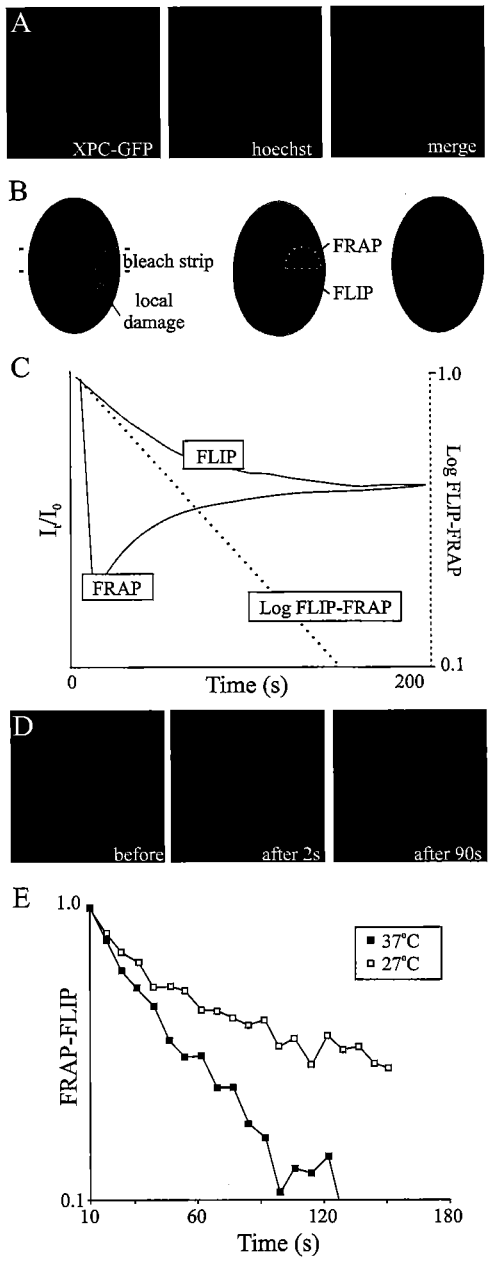

Figure 5. FRAP/FLIP application to determine the binding time of XPC-GFP molecules on damaged DNA.
(A) Confocal image of a locally irradiated cell expressing XPC-GFP (5 μm pore filter). Left panel: GFP-fluorescence, middle: hoechst staining of DNA, right: merged image. (B) Scheme of the FRAP/FLIP procedure on locally damaged areas. A small strip covering half of the local damage and spanning the entire nucleus is bleached at relatively low laser intensity for a period of 2 seconds. Subsequently fluorescence is monitored at regular time intervals in the bleached (FRAP) and non-bleached (FLIP) half of the local damage. (C) The relative fluorescence of the FRAP and FLIP area are shown in time. The log of fluorescence redistribution difference between FLIP and FRAP areas are plotted against time (dotted line). (D) Confocal image of a locally irradiated cell expressing XPC-GFP (8 μm pore filter). Left panel: before bleaching, middle panel: directly after bleaching and right panel: 90 seconds after bleaching. (E) Simultaneous FRAP/FLIP analysis of local damage at 37 °C and 27 °C.

Residence time of XPC-GFP at a NER site

To further study the dynamic involvement of XPC-GFP at NER sites, we visualized the repair process in living cells by inducing DNA damage at restricted areas of the nucleus [9, 32]. Within approximately one minute after applying local damage to XPC-GFP expressing cells, the fusion protein is accumulated into bright fluorescent areas, which remain visible up to 1 to 1.5 hours (Figure 5A). In addition to accumulation at the locally damaged site, XPC-GFP remains mainly localized to DNA in the undamaged areas of the nucleus. To determine the residence time of XPC-GFP at a local damaged site, we applied simultaneous FRAP and FLIP on the accumulation of XPC-GFP at the local damage. Briefly, a strip spanning the entire nucleus and covering half of the locally damaged site is bleached (Figure 5B). Subsequently, the fluorescence at the bleached (FRAP) and non-bleached area (FLIP) of the local damage is monitored (Figure 5B and C). The difference in relative fluorescence between the FRAP and FLIP area of the local damage is plotted against time. The time required to obtain full redistribution (>90%) of bleached and non-bleached molecules ($t_{0.9}$) is a measure for the mean residence time of XPC-GFP molecules at NER sites (Figure 5C). For XPC-GFP a $t_{0.9}$ of ~100 seconds was found at locally damaged sites (Figure 5D). This indicates that XPC-GFP was associated with the local damaged site for ~1-2 minutes and contrasts to other 'core'-NER factors like XPA, TFIIH and ERCC1/XPF which were shown to reside at the local damage for a longer period (4-6 minutes). When the equivalent experiment was performed at 27 °C, a residence time of ~220 seconds was observed for XPC-GFP at the locally damaged site (Figure 5D). Accordingly, a larger fraction of XPC-GFP molecules (150%) accumulated at the site of local damage at 27 °C compared to 37 °C. This indicates that the interaction of XPC-GFP with a lesion is temperature-dependent.

Discussion

The tagging of the XPC protein with the life cell marker GFP and stable expression (at physiologically relevant levels) of the fusion protein in living cells allowed us to study the *in vivo* functioning and reaction kinetics of XPC-GFP under various conditions using high resolution confocal microscopy and photobleaching techniques.

XPC-GFP is localized at DNA

In contrast to many of the other XP-proteins (Figure 1B to F), the XPC-GFP expressing cells revealed an inhomogeneous nuclear distribution. XPC-GFP is the only tagged NER factors thus far that exhibited this heterogeneous arrangement. XPA (Rademakers, *et al.*, submitted), ERCC1/XPF [23], TFIIH [22] XPG (A. Zotter, personal communication) and CSB (Van den Boom, *et al.*, in prep) all distributed homogeneously with the exception that TFIIH is also accumulated in the nucleolus and CSB displays irregularly distributed foci. Remarkably, this specific distribution of

XPC-GFP has escaped attention before in immunofluorescence studies, probably due to the fixation procedure involved and the high resolution imaging procedure applied in this study [26]. Comparison with the localization of chromosomal DNA by Hoechst staining revealed a striking correlation of the two signals, with XPC-GFP staining in DNA dense areas (Figure 1B to D). This suggests that the fusion protein has a preference to associate with DNA. In addition, the relatively high level of XPC-GFP fluorescence colocalizing with highly concentrated DNA , indicates that XPC-GFP is not only able to access the condensed part of the genome, like TFIIH and XPA, but in contrast to these other NER proteins is also retained there. The association with condensed DNA was further corroborated by the observation that the protein was co-localized even with chromatin at the highest level of condensation, i.e. mitotic chromosomes.

FRAP and simultaneous FRAP and FLIP analysis revealed that XPC-GFP was not freely diffusing according to its molecular size (D_{eff} = 4 $\mu m^2/s$), since a ~ 230 kDa protein in our set-up would have a diffusion coefficient of ~ 14 $\mu m^2/s$. This also contrasts to the other NER factors tested in a similar fashion and appeared to diffuse freely through the nucleus. This surprisingly slow mobility of XPC-GFP could be explained by a constant association/dissociation equilibrium with a less mobile nuclear component. As most likely candidate for this platform of binding is of course the chromosomal DNA, for which XPC has an intrinsically high affinity *in vitro* [10, 11]. And indeed, using computer simulation modeling our data fitted best to a model where at any time a very large fraction of the molecules is immobilized for a short time (best fit was at 90% for half a second at 37 °C). Note that the overall mobility of XPC-GFP is severely retarded by a 10 °C temperature decrease, suggesting that nuclear locomotion of this polypeptide is somehow regulated or influenced by a temperature-sensitive process likely enzymatic. Surprisingly, the dynamics of XPC-GFP do not respond to ATP depletion, suggesting that the energy requiring mobility is not an ATP-dependent process.

Dynamic action of XPC-GFP within NER

In unchallenged cells the XPC-GFP molecules are in an equilibrium where a large fraction of the heterodimer is bound and a smaller fraction freely diffusing. Upon UV-irradiation this equilibrium is shifted even more to the bound status when lesions are encountered, where XPC-GFP is bound significantly longer. Applying local damage to XPC-GFP expressing cells (Figure 5) showed that the fusion protein, can rapidly locate the lesions in the genome (< 2 minutes). and since XPC-GFP showed a prevalent accumulation at locally damaged sites, this suggests that it associates with the DNA damages for longer periods than with undamaged DNA, as was also shown for other NER proteins. Similarly, FRAP of total UV-irradiated cells showed that XPC-GFP molecules were immobilized shortly (within two minutes) after induction of DNA damage. This immobilization was dose-dependent with a saturation-dose of ~16 J/m^2

UV. Biochemical experiments showed that XPC-hHR23B not only preferentially binds to DNA lesions, but also binds to helix distorted sites with or without a lesion [5, 13, 33]. However, dual incision in an *in vitro* NER assay was only observed when damage was present in the bubble, ensuring a high safety level within the GG-NER pathway by allowing the NER reaction only to proceed when a NER-specific lesions is present. It was suggested that the preference for XPC-hHR23B binding to the damaged site might in part be due to damaged DNA more easily accommodating the distortion of the DNA induced by binding of the heterodimer to the injury [15].

Two hours after an UV-dose of 8 J/m^2 only a quarter of the bound fraction of XPC-GFP observed directly after UV, was found immobilized. This indicates that no more than 6% of the total XPC-GFP pool (versus 26% directly after UV) is engaged in repair two hours after UV-irradiation. The observed repair kinetics of XPC-GFP resembles the repair rate of (6-4)PPs. The majority of which are removed within 4 hours after $10J/m^2$ of UV [31]. The affinity of the purified XPC-hHR23B for the two main UV induced photoproducts, (6-4)PPs and CPDs were shown to be distinct. The complex appeared to preferentially bind (6-4)PPs, whereas CPDs were not favored by XPC-hHR23B. It was suggested that the DDB might aid the XPC-hHR23B in the recognition of CPDs [20]. Thus, the remaining immobilized fraction of XPC-GFP most likely represents the fraction of XPC-GFP proteins involved in the elimination of CPDs from the genome.

Model of NER mechanism

We have shown that XPA-GFP (Rademakers, *et al.*, submitted), ERCC1-GFP/XPF [23] and TFIIH-GFP [22] are not incorporated into a large preassembled repair holocomplex ('repairosome'), since each exhibited a for that factor specific diffusion rate. Although XPC is exceptional for its low mobility arguing for either incorporation in a large complex or reduced mobility by multiple transient interactions, it also argues against a model being part of a complex containing XPA, ERCC1/XPF or TFIIH. In addition, immunofluorescence studies on local damages in different NER-backgrounds further showed that NER was a process of sequential assembly of the different factors involved [9]. Various FRAP techniques uncovered that XPA-GFP, ERCC1-GFP/XPF and TFIIH-GFP display comparable binding times of ~4 minutes at a locally damaged site. This suggests that they form a stable assembly that exists on average for 4 minutes, possibly corresponding to the estimated average time of a single NER repair event [23]. In this context it is surprising to note that XPC-GFP revealed a much shorter residence time of ~1-2 minutes at the locally damaged site. This points to a scenario where this initiator of GG-NER is not present throughout the entire NER process, but releases from the NER DNA-protein complex in an early stage. It may be speculated that XPC-GFP leaves after one of the subsequent components, *e.g.* TFIIH, XPG or XPA have entered the complex. This model has been suggested previously, based on *in vitro* studies showing that XPC-hHR23B is not present in the pre-incision

complex [7]. In addition, recent *in vitro* studies showed that XPC-hHR23B, XPA and RPA do not form a stable three-protein complex at the damaged DNA. A scenario where the interaction of XPA and RPA on the damaged DNA might lead to the displacement of XPC-hHR23B from the DNA lesion, was suggested [34].

Material and methods

Cell culture conditions and specific treatments

Cell strains used are XP4PA SV stably expressing XPC-GFP, XPCS2BA SV stably expressing XPB-GFP [22], XP21RO SV stably expressing GFP-XPA (Rademakers, *et al.*, submitted), and Rad23A$^{-/-}$ Rad23B$^{-/-}$ double knock out mouse embryonic fibroblasts stably expressing XPC-GFP (Ng, *et al.*, submitted). All cell strains used in this study were cultured in RPMI + hepes (Life technologies) supplemented with 10% fetal calf serum and antibiotics, and maintained in a humidified 5% CO_2, 37 °C incubator. For DNA staining cells were incubated with 10 μg/ml Hoechst 33258 for 2 hours. Prior to UV irradiation with a Philips TUV lamp (254 nm) at a dose rate of ~ 0.8 J.m^2/s cells were rinsed with PBS. In the cases when cells are locally damaged, an isopore polycarbonate filter (Millipore) containing either 5 or 8 μm diameter pores was used to cover the cells before UV-irradiation [9, 32]. After irradiation cells were put back into medium and microscopically examined. For the azide-treatments, cells were incubated for 15 minutes in glucose-free medium (Gibco), with 60 mM deoxyglucose (Sigma) and 0.2% Na-azide (Sigma).

Generation of XPC-GFP-his$_6$HA fusion construct

Full length human XPC cDNA was cloned in frame in an eukaryotic expression vector pEGFP-N3 (Clonetech) (Kindly provided by J. Ng). A 3' histidine$_6$-hemaglutinine tag was added by insertion of a doublestranded oligo in SspBI-NotI site.

Generation of a stably expressing XPC-GFP cell line

The XPC-GFP fusion construct was transfected to XP4PA SV cells and the cells were selected with 250 μg/ml G418 (Sigma). An UV-resistant population that survived three UV-exposures (4 J/m^2) was isolated.

Confocal Microscopy

Three days prior to microscopic experiments, cells were seeded onto 24 mm diameter coverslips. Imaging and FRAP were performed on a Zeiss confocal laser scanning microscope LSM510 and LSM 410 (Zeiss, Oberkochen, FRG), equipped with a heatable scan stage (37 °C) respectively. Images were recorded with a 488nm Ar-laser and a 515-540 nm bandpass filter. Lateral resolution was 104 nm.

Fluorescence Recovery after Photobleaching

Diffusion measurements were performed by FRAP analysis at high time resolution (strip-FRAP). A strip spanning the nucleus was photobleached for 200 ms at 100% laser intensity. Recovery of fluorescence in the strip was monitored with 100 ms intervals at 1% laser intensity. The effective diffusion coefficient (D_{eff}) of TFIIH-GFP was obtained by calculating relative intensity $FR_{diff}(t) = (I_t-I_0)/(I_\infty-I_0)$, where I_∞ is fluorescence intensity (FI) after complete recovery, I_0 is FI immediately after bleaching, and I_t is FI during monitoring. D_{eff} was estimated by minimizing $\sum[FR_{diff}(t)-FT(t)]$, where FT is a theoretical equation for one-dimensional diffusion: $FT(t) = 1 - (w^2 * [w^2 + 4\pi t D_{\text{eff}}]^{-1})^{-½}$. Immobile fractions were calculated as $N_{\text{immobile}}/N_{\text{tot}} = 1 - FR_{imm}(\infty) * (1-N_{\text{mobile, bleached}}/N_{\text{tot}})^{-1}$, where $FR_{imm} = (I_t-I_0)/(I_{t<0}-I_0)$ and $I_{t<0}$ is fluorescence before bleaching and $N_{\text{mobile, bleached}}/N_{\text{tot}}$ is the fraction of mobile molecules bleached by the pulse. The latter is ~30% in our set-up as determined by bleaching experiments on free GFP. In simultaneous FRAP/FLIP experiments a strip at one side of a nucleus was bleached at 20% laser intensity for 8 s. Fluorescence was then monitored in the bleached and unbleached side of the nucleus and the difference was plotted against time [27].

Simultaneous FRAP/FLIP

Simultaneous FRAP/FLIP analysis to determine the mobility of fluorescent molecules in cell nuclei [22]. A small area at one side of a nucleus is bleached at relatively low laser intensity for a relatively long period of time (10 s) (Figure 5B). Subsequently fluorescence is monitored at regular time intervals (4 s) in the bleached area and in a region at the opposite side of the nucleus. The (log) of fluorescence redistribution (relative fluorescence) difference between FRAP and FLIP area is plotted against time (s) (Figure 5C). The steepness of the line determines the mobility of the fluorescent molecules.

References

1. **Lindahl, T.**, *Instability and decay of the primary structure of DNA.* Nature, 1993. 362: p. 709-715.
2. **Hoeijmakers, J.H.**, *Genome maintenance mechanisms for preventing cancer.* Nature, 2001. 411(6835): p. 366-74.
3. **Bootsma, D., et al.**, *Nucleotide excision repair syndromes: xeroderma pigmentosum, Cockayne syndrome and trichothiodystrophy.*, in *The genetic basis of human cancer*, B. Vogelstein and K.W. Kinzler, Editors. 2001, McGraw-Hill: New York. p. 677-703.
4. **Leadon, S.A.**, *Transcription-coupled repair of DNA damage: unanticipated players, unexpected complexities.* Am. J. Hum. Genet., 1999. 64(5): p. 1259-1263.
5. **Sugasawa, K., et al.**, *Xeroderma pigmentosum group C protein complex is the initiator of global genome nucleotide excision repair.* Mol. Cell, 1998. 2(2): p. 223-232.

6. **Wakasugi, M., et al.**, *Damaged DNA-binding protein DDB stimulates the excision of cyclobutane pyrimidine dimers in vitro in concert with XPA and replication protein A.* J Biol Chem, 2001. 276(18): p. 15434-40.
7. **Wakasugi, M. and A. Sancar**, *Assembly, subunit composition, and footprint of human DNA repair excision nuclease.* Proc Natl Acad Sci U S A, 1998. 95(12): p. 6669-74.
8. **de Laat, W.L., N.G. Jaspers, and J.H. Hoeijmakers**, *Molecular mechanism of nucleotide excision repair.* Genes Dev., 1999. 13(7): p. 768-785.
9. **Volker, M., et al.**, *Sequential Assembly of the Nucleotide Excision Repair Factors In Vivo.* Molecular Cell, 2001. 8(1): p. 213-224.
10. **Masutani, C., et al.**, *Purification and cloning of a nucleotide excision repair complex involving the xeroderma pigmentosum group C protein and a human homolog of yeast RAD23.* EMBO J., 1994. 13(8): p. 1831-1843.
11. **Shivji, M.K., A.P. Eker, and R.D. Wood**, *DNA repair defect in xeroderma pigmentosum group C and complementing factor from HeLa cells.* J Biol Chem, 1994. 269(36): p. 22749-57.
12. **Reardon, J.T., D. Mu, and A. Sancar**, *Overproduction, purification, and characterization of the XPC subunit of the human DNA repair excision nuclease.* J Biol Chem, 1996. 271(32): p. 19451-6.
13. **Sugasawa, K., et al.**, *A multistep damage recognition mechanism for global genomic nucleotide excision repair.* Genes Dev, 2001. 15(5): p. 507-21.
14. **Gunz, D., M.T. Hess, and H. Naegeli**, *Recognition of DNA adducts by human nucleotide excision repair. Evidence for a thermodynamic probing mechanism.* J Biol Chem, 1996. 271(41): p. 25089-98.
15. **Janicijevic, A., et al.**, *DNA bending by the human damage recognition complex XPC-HR23B.* DNA Repair (Amst), 2003. 2(3): p. 325-36.
16. **Halford, S.E. and M.D. Szczelkun**, *How to get from A to B: strategies for analysing protein motion on DNA.* Eur Biophys J, 2002. 31(4): p. 257-67.
17. **Mitchell, D.L. and R.S. Nairn**, *The biology of the (6-4) photoproduct.* Photochem. Photobiol., 1989. 49(6): p. 805-819.
18. **Venema, J., et al.**, *Xeroderma pigmentosum complementation group C cells remove pyrimidine dimers selectively from the transcribed strand of active genes.* Mol Cell Biol, 1991. 11(8): p. 4128-34.
19. **Chu, G. and E. Chang**, *Xeroderma pigmentosum group E cells lack a nuclear factor that binds to damaged DNA.* Science, 1988. 242: p. 564-567.
20. **Tang, J.Y., et al.**, *Xeroderma pigmentosum p48 gene enhances global genomic repair and suppresses UV-induced mutagenesis.* Mol Cell, 2000. 5(4): p. 737-44.
21. **Wakasugi, M., et al.**, *DDB accumulates at DNA damage sites immediately after UV irradiation and directly stimulates nucleotide excision repair.* J Biol Chem, 2002. 277(3): p. 1637-40.
22. **Hoogstraten, D., et al.**, *Rapid Switching of TFIIH between RNA Polymerase I and II Transcription and DNA Repair In Vivo.* Mol Cell, 2002. 10(5): p. 1163-74.
23. **Houtsmuller, A.B., et al.**, *Action of DNA repair endonuclease ERCC1/XPF in living cells.* Science, 1999. 284(5416): p. 958-961.
24. **Daya-Grosjean, L., et al.**, *An immortalized xeroderma pigmentosum, group C, cell line which replicates SV40 shuttle vectors.* Mutat Res, 1987. 183(2): p. 185-96.

25. **Li, L., et al.**, *Characterization of molecular defects in xeroderma pigmentosum group C.* Nature Genetics, 1993. 5: p. 413-417.
26. **Van der Spek, P.J., et al.**, *XPC and human homologs of RAD23: intracellular localization and relationship to other nucleotide excision repair complexes.* Nucleic Acids Res., 1996. 24(13): p. 2551-2559.
27. **Houtsmuller, A.B. and W. Vermeulen**, *Macromolecular dynamics in living cell nuclei revealed by fluorescence redistribution after photobleaching.* Histochem Cell Biol, 2001. 115(1): p. 13-21.
28. **Araki, M., et al.**, *Centrosome protein centrin 2/caltractin 1 is part of the xeroderma pigmentosum group C complex that initiates global genome nucleotide excision repair.* J Biol Chem, 2001. 276(22): p. 18665-72.
29. **Politz, J.C., et al.**, *Movement of nuclear poly(A) RNA throughout the interchromatin space in living cells.* Curr Biol, 1999. 9(6): p. 285-91.
30. **Phair, R.D. and T. Misteli**, *High mobility of proteins in the mammalian cell nucleus.* Nature, 2000. 404(6778): p. 604-9.
31. **Van Hoffen, A., et al.**, *Transcription-coupled repair removes both cyclobutane pyrimidine dimers and 6-4 photoproducts with equal efficiency and in a sequential way from transcribed DNA in xeroderma pigmentosum group C fibroblasts.* EMBO J., 1995. 14(2): p. 360-367.
32. **Mone, M.J., et al.**, *Local UV-induced DNA damage in cell nuclei results in local transcription inhibition.* EMBO Rep, 2001. 2(11): p. 1013-1017.
33. Kusumoto, R., et al., *Diversity of the damage recognition step in the global genomic nucleotide excision repair in vitro.* Mutat Res, 2001. 485(3): p. 219-27.
34. **You, J.S., M. Wang, and S.H. Lee**, *Biochemical analysis of damage recognition process in nucleotide excision repair.* J Biol Chem, 2002. 13: p. 13.

Chapter 9

Dynamics of the xeroderma pigmentosum group A DNA repair protein in living cells

Manuscript submitted

Dynamics of the xeroderma pigmentosum group A DNA repair protein in living cells

Suzanne Rademakers[1], Deborah Hoogstraten[1], Marcel Volker[2], Alex L. Nigg[3], Martijn Moné[4], Jan H.J. Hoeijmakers[1], Adriaan B. Houtsmuller[3, *] and Wim Vermeulen[1, *]

CBG, MGC-Dept. Cell Biology and Genetics, P.O. Box 1738, 3000 DR Rotterdam, The Netherlands.
MGC- Department of Toxicogenetics, Leiden University Medical Center, Wassenaarseweg 72, 2333 AL, Leiden, The Netherlands.
Dept. of Pathology (Josephine Nefkens Institute) Erasmus University Rotterdam, P.O. Box 1738, 3000 DR Rotterdam, The Netherlands.
Swammerdam Institute for Life Sciences, University of Amsterdam, The Netherlands.
* Authors contributed equally to this work.

Corresponding author: W. Vermeulen, e-mail: vermeulen@gen.fgg.eur.nl

Abstract

Nucleotide Excision Repair (NER) is the main DNA repair pathway in mammals to remove UV-induced lesions. NER involves the concerted action of more than 25 polypeptides in a coordinated fashion. The xeroderma pigmentosum group A protein (XPA) is recognized as a central organizer and damage verifier in NER. How XPA reaches DNA lesions and how the protein is distributed in time and space in living cells is unknown. Here we studied XPA *in vivo* using a cell-line stably expressing physiological levels of functional XPA fused to GFP and quantitative fluorescence microscopy. The majority of XPA moves rapidly through the nucleoplasm with a different diffusion rate as other NER-factors tested, arguing against a pre-assembled XPA-containing NER complex. DNA damage induced a transient (~ 5 minutes) immobilization of maximally 30% of XPA. Immobilization depends on XPC, indicating that XPA is not the initial lesion recognition protein *in vivo*. Moreover, loading of RPA on NER lesions did not dependent on XPA. Thus, XPA participates in NER by incorporation of free diffusing molecules in XPC-dependent NER/DNA complexes. These studies support a model for a rapid consecutive assembly of free NER factors, and a relatively slow simultaneous disassembly, after repair.

Introduction

DNA-damaging agents continuously challenge the integrity of DNA. DNA lesions directly affect transcription and replication leading to cell death and contributing to aging, and in addition induce mutations eventually causing carcinogenesis (12). Various repair mechanisms have evolved to prevent the consequences of DNA injuries and to preserve genetic integrity (20, 26). In mammals, the nucleotide excision repair (NER) process is the most important repair pathway to remove UV-light induced lesions including cyclobutane pyrimidine dimers (CPD) and 6-4 photoproducts and a wide range of helix-distorting chemical adducts. The significance of a functional NER system is apparent from the severe clinical features expressed by individuals suffering from the hereditary disorder xeroderma pigmentosum (XP), Cockayne syndrome (CS) and trichothiodystrophy (TTD) (7). Patients, suffering from the prototype repair disorder XP are extremely sensitive to solar (UV) exposure, have an increased risk for skin cancer and frequently exhibit neurological symptoms.

Detailed biochemical studies have shown that >25 polypeptides are required for *in vitro* NER (4, 14, 36). Two distinct NER sub-pathways operate within mammals: transcription-coupled repair (TCR) and global genome repair (GGR) each addressing a specific genome compartment and category of damages (9, 24). The distinction between these originates from the first steps of the mechanism, *i.e.* lesion detection. Lesions that block RNA polymerase II transcription elongation are preferentially repaired by TCR and require the CSA, CSB and XAB2 proteins (43). TCR allows rapid resumption of the vital process of RNA synthesis and is particularly important for lesions that are inefficiently repaired by GG-NER (such as CPDs). Injuries anywhere in the genome are targeted by the slower operating GGR. Damage sensing in this process is performed by the XPC/hHR23B/centrin2 heterotrimeric complex (2, 49, 50, 56). In addition, the DNA Damage Binding (UV-DDB) protein complex (8, 32) helps identifying CPDs in GGR (30, 34, 50, 53). On the other hand, a complex consisting of XPA and the ssDNA binding protein (RPA) has been suggested to be the primary lesion detector in GG-NER (57), this finding was recently challenged by the same group, claiming that only RPA is the initial damage sensor (45).

The next in NER step is performed by the nine-subunit TFIIH complex (56, 60), containing the XPB and XPD helicases. TFIIH locally opens the DNA double helix around the lesion (19, 21), likely in the presence of XPG. Subsequently, XPA and RPA play an essential, but as yet not fully understood role in the core of the reaction. XPA and RPA are necessary for further assembly and proper orientation of the incision proteins ERCC1/XPF and XPG (13). The latter are structure-specific endonucleases incising the damaged strand around the lesion (5' and 3', respectively) leaving an excised stretch of ~ 30 nucleotides. DNA polymerase δ/ε and auxiliary factors fill the remaining gap and is sealed by ligase 1 (14, 26, 36).

Despite detailed knowledge on the *in vitro* NER mechanism, little is known about how this process operates in living cells. Different models for the organization of NER

have been proposed, ranging from an ordered assembly of factors (1, 36, 42, 56), or 4 defined subcomplexes (22, 45, 57) to a pre-assembled NER holocomplex (51). Recently, we provided evidence that some of the NER constituents roam through the nucleoplasm by diffusion and were transiently bound to complexes actively engaged in NER (27, 28). The XPA protein plays a crucial role within NER, since in the absence of this protein NER is completely abrogated. Multiple interactions of XPA with other NER factors have been reported, suggesting a central role in complex assembly (13). These include the XPA/RPA complex exhibiting a higher specificity and affinity for damaged DNA than XPA alone, ERCC1/XPF/ XPA ternary complex, as well as an association with TFIIH (summarized in)(5, 14). In addition, a link between XPA and TCR was suggested by the observed association of CSB with the core NER factors XPA, XPG and TFIIH (31, 48) and between XPA and XAB2 (43).

In order to provide further insight into the molecular interactions of XPA in living cells, we tagged this central NER factor with the green fluorescent protein (GFP) and studied its distribution and mobility in living cells. We applied fluorescence based imaging and bleaching (Fluorescence Redistribution After Photobleaching, hereafter: FRAP) methods, using confocal laser scanning microscopy (28, 29) in cells containing local UV-damage (41, 56). In previous, similar studies on the NER factors ERCC1 and TFIIH (27, 28), we provide evidence that at least these proteins do not reside in large NER-holo-complexes. Here we present the dynamic properties of XPA-GFP, the NER reaction kinetics, and mode of complex assembly in living cells.

Results

Construction and characterization of GFP-XPA

The XPA cDNA was fused to the enhanced green fluorescent protein (eGFP) cDNA, containing a Histidine-, and HA- tag at it's N-terminus of eGFP (see M&M), resulting in a His_9-HA-eGFP-XPA hybrid gene (here after GFP-XPA) (Figure 1A). To verify whether the GFP tag did not interfere with the XPA function, the fusion gene was microinjected into nuclei of XPA-deficient human fibroblasts. One day after microinjection a bright fluorescent signal within the nuclei of injected cells was observed (Figure 1B). Fluorescent cells were recorded and assayed for their repair capacity by determining UV-induced unscheduled DNA synthesis (UDS). As shown in Figure 1C, the cells with green fluorescent nuclei (Figure 1B) were also corrected (up to wild type levels) for the severe UDS-defect, present in XP-A cells (non-injected neighboring cells). Both nuclear targeting and the complete restoration of UDS, indicate that the His_9-HA-eGFP tag does not interfere with the proper function of XPA, when transiently expressed in XP-A cells.

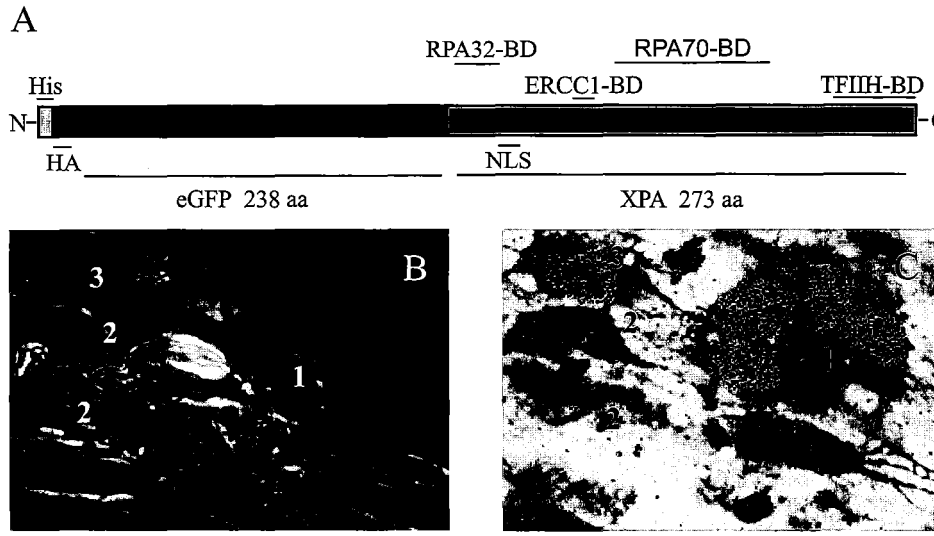

Figure 1. Functionality of GFP-XPA.
(A) Schematic representation of the His_9-HA-eGFP-XPA fusion gene with the different binding domains indicated. NLS, nuclear localization signal; BD, binding domain. (B) Fluorescence image of XP-A cells injected with GFP-tagged XPA cDNA. Only the multi-nucleated cell microinjected with GFP-XPA cDNA showed a homogeneous nuclear expression (nr.1), surrounding cells are not injected (nr.2). (C) Measurement of the repair capacity of cells with fluorescent nuclei by means of UV-induced UDS (see M & M). The amount of silver grains above nuclei of the injected cells (1) was comparable to wild-type cells (not shown), whereas the surrounding XP-A fibroblasts (2) show a low level of DNA synthesis typical for UV-exposed XP-A cells. The cell indicated with number 3 is in S-phase.

Generation and characterization of cells expressing GFP-XPA

To investigate the *in vivo* distribution of GFP-XPA in time and space, the fusion gene was stably expressed in an XPA-deficient human SV40-immortalized fibroblast. Immunoblot analysis of the clones selected indicated that clone 40 expressed near normal levels of GFP-XPA (Figure 2). As observed before, wild type XPA migrates as two distinct bands in PAGE (40 and 42 kDa)(16, 40, 46), the fusion protein is also present in two forms, migrating at the expected position of ~68 and ~70 kDa. Immunostaining with anti-GFP (data not shown) revealed that there was no detectable free GFP present in the crude-extracts. UV-survival experiments demonstrated that tagged XPA restores the extreme UV-sensitive phenotype of XP-A cells to the wild-type range (Figure 2B). This confirms the UDS results of the microinjection at physiological protein levels in stably expressing transformants.
GFP-XPA appeared homogeneously distributed in living nuclei (Figure 2C,D) including the nucleoli. In approximately 40% of the cells a few (1-5), bright fluorescent spots were observed. GFP signal in fixed cells (Figure 2E) and immunofluorescence (anti-XPA) (Figure 2E) displayed a similar distribution as in living cells (Figure 2D)

except that nucleoli seemed devoid of XPA after immunofluorescence (Figure 2F), similar to previous reports (40). The lack of nucleolar staining by immunofluorescence might be caused by the fixation procedure rendering this highly condensed organelle less permeable for antibodies (59). Although UV-C irradiation slightly reduced the number of cells containing spots, the overall distribution pattern did not change (not shown). Currently, the nature and significance of these foci remains unknown. Similar structures were found in ERCC1-GFP expressing cells (28).

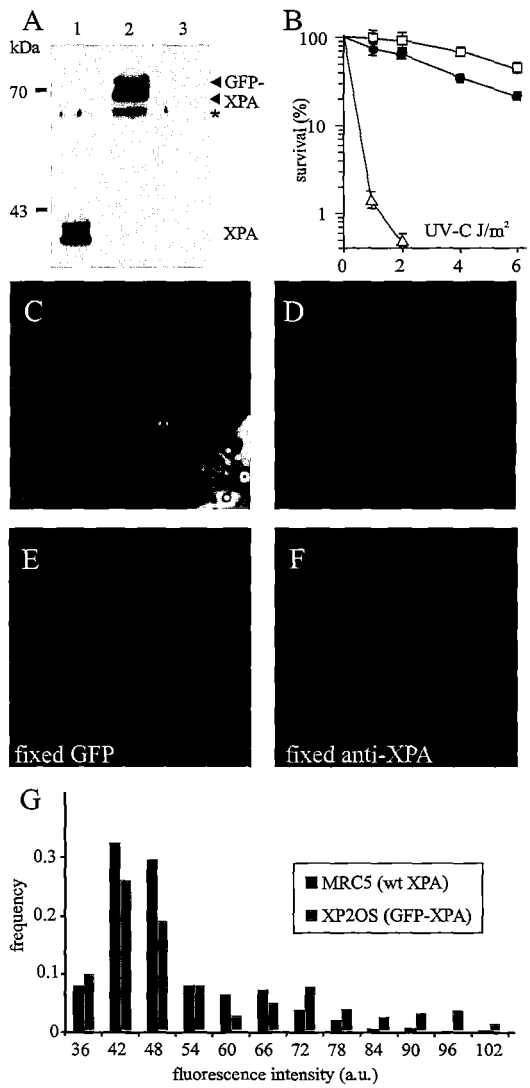

Figure 2. Expression and characterization of XP2OS cells stably expressing GFP-tagged XPA.
(A) Immunoblot of 30 μg whole-cell extract (WCE) from MRC5 (wild type), GFP-XPA transfected XP2OS and XP2OS (XP-A) cells respectively, probed with polyclonal anti-XPA. Molecular weight of protein markers is indicated in kilo-Dalton (kDa). No XPA protein is detected in XP2OS, because of a G-C transversion in the splicing acceptor site in intron 3 of the XPA gene. XPA protein: open triangles, GFP-XPA: filled triangles, and asterisk: specific cross-reacting band. (B) UV-survival of repair proficient MRC5 cells (□), GFP-XPA expressing cells (•) and XP2OS cells (...) (see M & M). The transfected cell-line shows a wild type correction of the XP-A specific UV-sensitivity. (C) Phase-contrast image of a living cell expressing GFP-XPA. (D) Epi-fluorescence GFP image of the same cell as in (C), showing a homogeneous nuclear distribution. (E) Fluorescence-image after fixation of GFP-XPA expressing cells, showing a similar distribution as in (D). (F), Immunofluorescence of the same cell as in (E), incubated with anti-XPA serum, showing a similar XPA distribution as with GFP fluorescence, except for the nucleoli. (G), Expression profile of XPA (black bars) and GFP-XPA (grey bars) in MRC5 and XP2OS respectively after immuno-fluorescence staining with XPA-antibodies. GFP-XPA cells exhibiting a similar expression level as the major peak of XPA expression in MRC5 were used in further experiments.

Diffusion of GFP-tagged XPA

Prior to mobility studies of GFP-XPA in living cells we first analyzed the expression level of individual cells in clone 40. Immunofluorescence with anti-XPA serum was performed on a (1:1) mixed population of wild-type (MRC5) and clone 40 cells. The frequency distribution (Figure 2G) shows that both the level of expression and the inter-cellular variation are comparable, with the exception of a small fraction of overexpressing GFP-XPA cells. Only cells with a modal expression level equivalent to wild-type cells were used in further quantitative fluorescent experiments, unless stated otherwise.

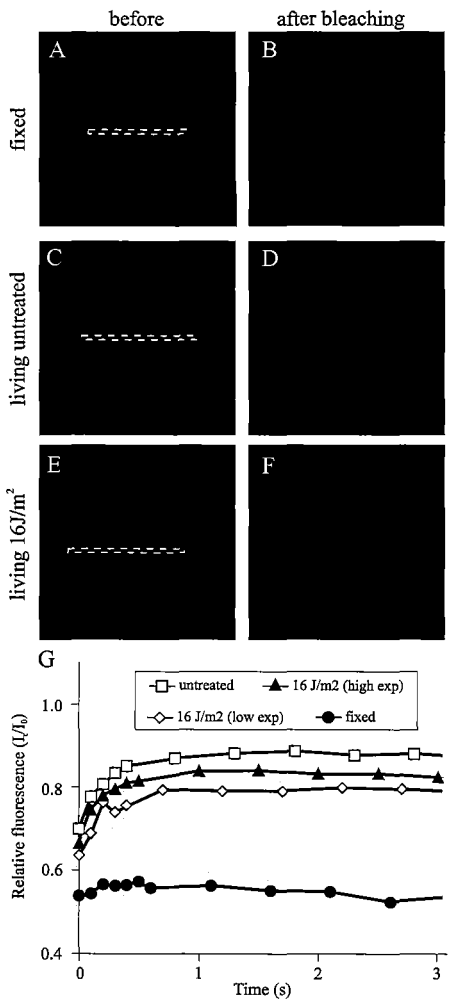

Figure 3. Temporal FRAP analysis applied on GFP-XPA expressing cells to determine the immobile fraction after UV-irradiation. Confocal images and corresponding FRAP profiles. The dotted line indicates the position of the photobleaching strip. To determine a potential immobile fraction the mean intensity immediately before bleaching was set to one and the fluorescence intensity immediately after bleaching was set to zero. (A) and (B) Pre- and postbleach images of fixed cells, showing complete immobilization of GFP-XPA. (C) and (D) Images of living cells monitored during FRAP, showing a homogeneous bleaching throughout the nucleus 4 s after the bleach pulse in D. (E) and (F) Images of living cells irradiated with 8 J/m^2 UV-C. Note that the UV-irradiated cell (F) shows an intermediate pattern between untreated (D) and fixed cells (B). (G) Fluorescence recovery profile expressed as relative fluorescence plotted against time after bleaching. Each plot is the mean value of at least 50 cells. Fixed cells (●), untreated living cells (□), UV-irradiated cells expressing relatively low levels of GFP-XPA (◆), and UV-irradiated high GFP-XPA expressing cells (▲). The immobile fraction can be calculated by measuring the reduction of fluorescence recovery compared to un-irradiated cells.

Mobility measurements to determine whether GFP-XPA molecules are mobile or bound to nuclear structures were performed by applying FRAP (fluorescence recovery after photobleaching). Here we used Strip-FRAP (see Methods and Houtsmuller 2001 for detailed information) to measure the mobility. Briefly, GFP-XPA molecules were photobleached in a defined narrow strip spanning the nucleus (Strip-FRAP). The speed of recovery is a measure for the diffusion rate of the molecules and the degree of fluorescence recovery indicates whether (part of) the GFP-XPA molecules are mobile. For chemically fixed cells no recovery is observed, as expected (Figure 3A, B). In contrast, in living cells the vast majority of GFP-XPA appeared mobile (Fig 3C, D). The kinetics of recovery yielded an effective diffusion coefficient (D_{eff}) for GFP-XPA of 15 ± 2 $\mu m^2/s$. This D_{eff} is much higher than XPB-GFP, part of TFIIH (6 ± 1 $\mu m^2/s$), and reproducibly, but not significantly, higher than ERCC1-GFP/XPF (12 ± 2 $\mu m^2/s$) that were assayed in parallel. These data suggest that in undamaged cells the majority (>95%) of XPA is not incorporated into a stable large complex, and diffuses freely as single molecules (or part of small transient sub-complexes) throughout the nucleoplasm.

DNA repair-dependent immobilization of GFP-XPA

To investigate the effect of the presence of DNA damage on XPA mobility we performed FRAP analysis on cells exposed to UV-C (16 J/m^2, an NER-saturating dose) (Figure 3E, F). The reduced fluorescence recovery, visible 2 seconds after bleaching (Figure 3F, compared to non-treated cells in 3D) and the lower recovery of the diffusion-plot (Figure 3G) are indicative for an immobilized fraction. The relative amount of binding (maximally ~35%) depends on the expression level, since high expressing cells show a proportionally smaller immobilized fraction compared to cells expressing a moderate amounts of GFP-XPA (Figure 3G). This suggests that at a given UV dose the total number of molecules participating in the DNA repair reaction (*i.e.* immobilization) is roughly the same in all cells independent of the expression level. The D_{eff} of the free fraction of GFP-XPA molecules did not change after damage induction (13 ± 2 $\mu m^2/s$) (Figure 3G), indicating that the free molecules were not incorporated into larger (mobile) complexes.

To more precisely quantify the DNA damage-induced immobilization of GFP-XPA we used a different FRAP procedure, designated FRAP-FIM (FRAP for immobilization measurements), as described previously (28, 29). FRAP-FIM measurements (the mean of at least 30 cells) and typical examples of cells are shown in Figure 4. In accordance to the strip-FRAP analysis, these measurements showed a UV-dose dependent (and maximally ~35%) immobilization of GFP-XPA (Figure 4G-J). These results indicate that the number of immobilized molecules depends on the number of lesions. In addition, the total amount of immobilized molecules, as shown above, does not depend on the amount of available GFP-XPA molecules, suggesting that XPA is not the rate-determining factor of NER in the cell line investigated.

The fraction of bound GFP-XPA molecules (~35%) remained more or less unaltered over a period of a few (2-4) hour's post UV. Subsequently, a gradual decrease of immobilized molecules was observed with no significant binding 24 h after UV (data not shown). Previous studies have shown that 24 h after UV most UV-induced lesions have been removed by NER, suggesting full release of bound molecules when repair is completed. This UV-induced immobilization is specific for NER proteins, as previously reported for ERCC1-GFP (28) and not observed in cells expressing single GFP or GFP-tagged RAD52 group proteins (18). In summary, the above findings are consistent with the idea that after DNA damage GFP-XPA molecules become transiently immobilized by engagement in NER.

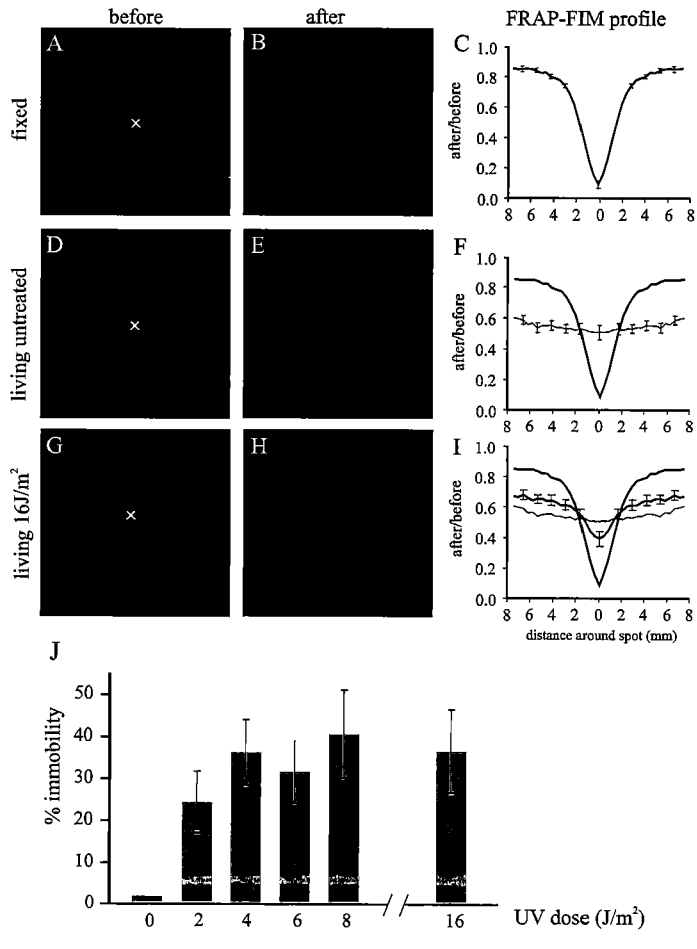

Figure 4. FRAP-FIM method applied on GFP-XPA expressing cells. Confocal images and corresponding fluorescence ratio profiles (FRP) of 50 cells. (A) and (B) Pre- and postbleach images respectively of cells fixed with 2% paraformaldehyde, displaying the immobilization of GFP-XPA molecules after fixation, visualized by the intense bleached spot and high fluorescent intensity outside the bleached spot (B). (C) FRP of fixed cells. (D) and (E) Images of living untreated cells, showing an overall reduction of fluorescence after the bleach pulse (E). (F) FRP of untreated cells. (G) and (H) Image of 8 J/m^2 UV-C irradiated cells. The UV-irradiated cell (H) displays a distribution pattern intermediate of untreated (B) and fixed (E). The X in A, D and G represents the position of the bleach pulse (I) FRP of UV-irradiated cells. (J) Response of GFP-XPA immobilization to different UV doses.

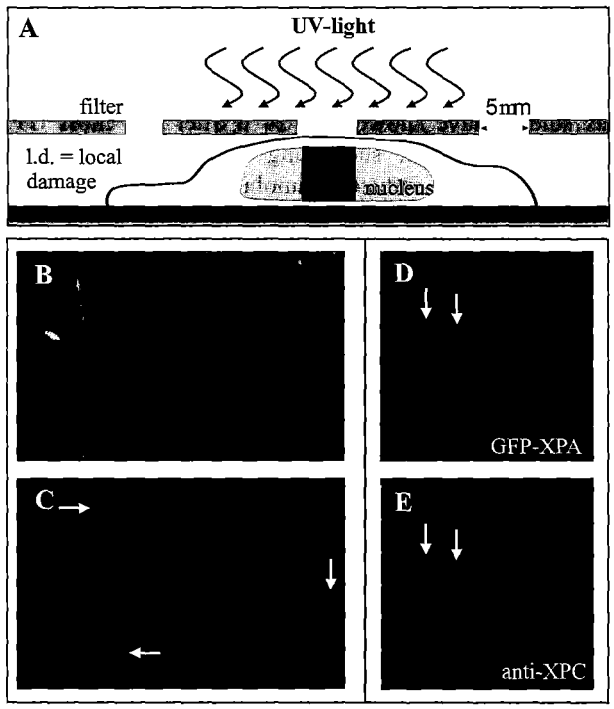

Figure 5. Accumulation of GFP-XPA within restricted nuclear areas after local UV-irradiation. (A) Schematic presentation of local UV-damage infliction on living cultured cells. (B) and (C) micrograph of living cells expressing GFP-XPA and UV-irradiated through a filter with small (here 5 μm) pores, phase-contrast image (B) and fluorescence image (C). The arrows in (C) point to the local accumulations of GFP-XPA. (D) and (E) GFP-XPA accumulations (arrows) in (D) clearly co-localizes with endogenous XPC (E) concentrations, as determined with anti-XPC antibodies, in fixed cells.

Local damage in GFP-XPA cells

To monitor the translocation of GFP-XPA molecules to damaged DNA in living cells and to determine the transient binding (or residence) time within NER complexes, we applied a novel technique for introducing UV-damage to a restricted area of the nucleus (41, 56). Cells were covered with a polycarbonate filter that shields UV-light and contains (5 μm) pores (Figure 5A), causing DNA damage after UV-exposure only at the position of the pores. Shortly after UV irradiation (< 5 min., *i.e.* the first time point analyzed) a clear accumulation of GFP-XPA molecules in restricted parts of living cell nuclei was observed (arrows, Figure 5B-C). These GFP-XPA accumulations, co-localize with XPC (Figure 5D-E) and with CPDs (Figure 7D-E) and confirm that XPA preferentially localizes to sites of DNA damage (56). These observations suggest a model, in which (free) diffusing GFP-XPA molecules bind rapidly to damaged DNA/NER-complexes in which they were transiently entrapped. To determine the residence time of GFP-XPA within these locally damaged areas, we applied FLIP (fluorescence loss in photobleaching)(see M & M). At a position opposite to the damaged domain a single pulse was used to bleach a small region in the nucleus (Figure 6B inset). Both bleached and non-bleached molecules will distribute and mix resulting in an overall decrease in fluorescence intensity. The time required to establish the initial (pre-bleach) fluorescence difference between damaged area and the

nucleoplasm is a measure for the mean residence time of molecules in that area. A typical series of images of this FLIP measurement is shown in Figure 6A. The determined residence time for GFP-XPA was approximately 4-6 min (Figure 6B). This residence time indicates the average binding period (or time of participation) of GFP-XPA molecules within a single NER event.

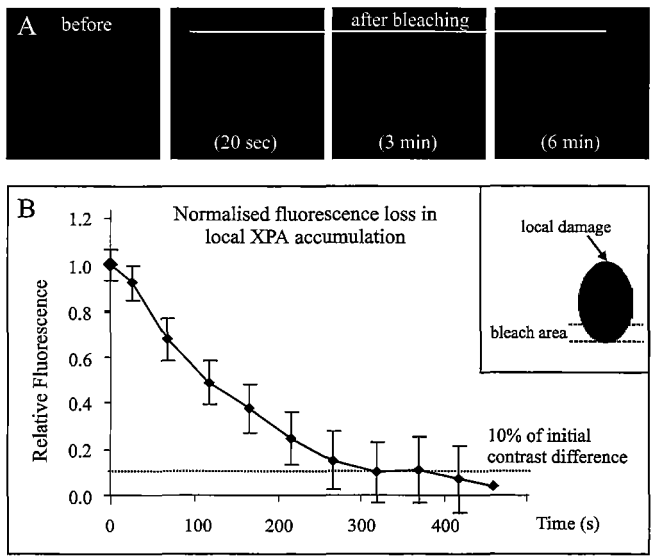

Figure 6. Application of FLIP to determine the binding time of GFP-XPA molecules on damaged DNA, using locally damaged cells.
(A) Confocal images of a locally UV-damaged GFP-XPA expressing cell. Images before applying a bleach-pulse and 20 s, 3 min and 6 min after bleaching. (B) Fluorescence profile as a function of time, residence time was estimated to be ~ 4 to 6 minutes, the time at which the relative fluorescence difference between damaged area and background is established to (< 10%) of the initial (prebleach) situation. Inset in B, FLIP procedure in local damaged cells, a laser beam is focused (between dotted lines) at opposite to the damaged area (light spot, arrow) (typical example shown in A).

GFP-XPA mobility in a XP-C deficient background

To obtain further evidence that immobilization is caused by actual engagement in NER we studied the dynamic properties of GFP-XPA in a mutant NER background: an XPC-deficient (XP20MA-SV) cell-line. Using FACS and Immunoblot analyses (data not shown) a clone was selected that expresses a relatively low level of GFP-XPA, approximately a 1:1 ratio with endogenous non-tagged XPA.

FRAP-FIM measurements revealed that even after a high UV dose of 16 J/m^2 no significant immobilization of GFP-XPA was observed in XP-C cells (Figure 7A-B). To study the inability of immobilization in XPC-deficient background in more detail, local damage was applied to GFP-XPA expressing, XPA-, and XPC-deficient cells. GFP-XPA accumulates at locally damaged areas (using CPD-antibodies) (Figure 7C-E) only in the presence of XPC (compare with Figure 7F-H, absence of XPC). These observations clearly show that binding and transient immobilization of XPA molecules to damaged regions depend on the presence of functional XPC. Since XPC is only involved in GGR, it further suggests that with the applied FRAP methods (and GFP-

XPA), predominantly GGR is monitored, at least in the analyzed time periods after UV. In conclusion, in living cells, XPC precedes XPA in NER complex assembly ruling out that XPA is the initial damage sensor.

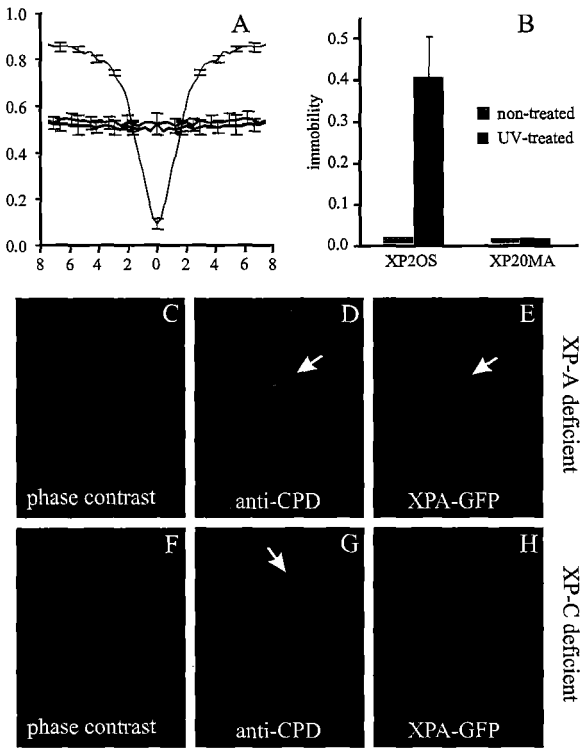

Figure 7. Effect of XPC on damage-induced XPA im-mobility analysed by FRAP-FIM and local damage induction.
(A) FRAP-FIM profile of GFP-XPA expression in XP20MA (XP-C). Un-irradiated cells (green line), 16 J/m^2 irradiated cells (blue line) and fixed cells (black line). UV-exposed XP20MA cells do not show any GFP-XPA immobilization. (B) Quantification of immobilization of GFP-XPA in XP20MA and XP2OS cells, with and without UV irradiation. (C-E) GFP-XPA expressing XP2OS cells. (C) Phase-contrast image. (D) anti-CPD immuno-staining in, the arrow indicates the site of the damage. (E) GFP image of the same cell, showing enrichment of GFP-XPA at the damaged site. (F-H) GFP-XPA expressing XP20MA cells. (F) Phase-contrast image (G) anti-CPD immuno-staining, indicated by the arrow. (H) GFP image, showing no enrichment of GFP-XPA molecules.

Loading of XPA and RPA in the NER preincision complex

Our studies indicated that incorporation of XPA into the NER preincision complex depends on the presence of XPC and that the XPA molecules get access to these lesions as a free diffusing entity. These dynamic studies do however not allow determining whether (part) of the XPA molecules are complexed to other (small) nuclear factors, such as RPA. It has been suggested that XPA is bound to the hetero-trimeric replication protein A (RPA) (25, 37). Moreover, it was claimed that these proteins bind as a complex to DNA damage (57, 58). This XPA-RPA complex has a higher and more lesion discriminative binding capacity than each of the separate proteins (39). To further investigate whether XPA gets access to the pre-incision complex as a single protein or in conjunction with RPA, we investigated the loading of RPA on UV-lesions in a number of different NER factor-deficient cells.

In accordance with our previous findings for other NER proteins (56), we found an accumulation of RPA in normal cells shortly after the introduction of local UV-damage in the cell (fig 8A-C). The recruitment of XPA to the NER complex is not impaired in XP-G/CS (56), despite the virtual absence of XPG protein. Here we show that also the relocalization of RPA to locally induced UV-damage is not impaired in these cells (fig 8D-F). This observation suggests that the recruitment of XPA and RPA is independent of XPG, or alternatively, that the XP-G/CS cells investigated might still express small amounts of truncated XPG protein that are sufficient to support recruiting of XPA and RPA

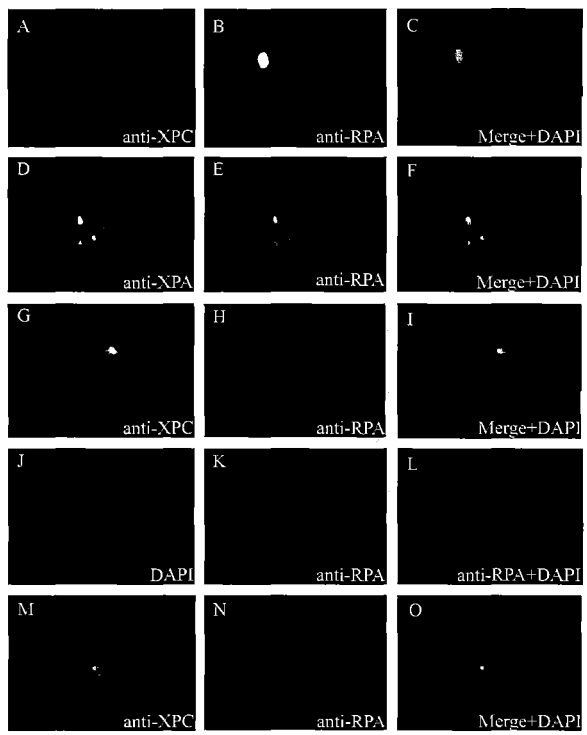

Figure 8. Relocalization of RPA to the NER complex 30' after local irradiation with 25J/m^2 UV. (A-C) VH25 cells.
(A) anti-XPC and (B) anti-RPA immunostaining, (C) merge of immunostainings with DAPI nuclear DNA staining. (D-F) XPCS1RO cells. (D) anti-XPA and (E) anti-RPA immunostaining, (F) merge of immunostainings with DAPI nuclear DNA staining. (G-I) XP25RO cells. (G) anti-XPC and (H) anti-RPA immunostaining, (I) merge of immunostainings with DAPI nuclear DNA staining. (J-L) XP21RO cells. (J) DAPI nuclear DNA staining, (K) anti-RPA staining, (L) overlay of (J) and (K). (M-O) XP8BR cells. (M) anti-XPC and (N) anti-RPA immunostaining, (O) merge of immunostainings with DAPI nuclear DNA staining. A yellow color in the merged images (C), (F), (I) and (O) indicates colocalization of NER proteins at sites of locally induced DNA damages.

Surprisingly however, when we tested cells lacking XPA we observed also relocalization of RPA to the UV-damaged area of the nucleus with similar efficiency as in wildtype cells (fig 8G-I). This suggests that RPA is recruited to the NER complex on the basis of its affinity for ssDNA, which is formed after the helix-unwinding action of TFIIH, or that other (protein-protein) interactions than those with XPA are sufficient to recruit RPA to the NER complex. These findings are in accordance with recent observations by Patrick and Turchi (2002), who presented evidence that initial binding of RPA to the damaged DNA is subsequently further stabilized by an interaction with

XPA. Whether XPA will be incorporated in the NER complex *in vivo* in the absence of RPA remains to be determined.

Furthermore, it was suggested by Wakasugi and co-workers that the DDB protein complex might be responsible for the direct recruitment of XPA and RPA to sites of damage, without the need for the XPC/hHR23B complex (Wakasugi et al. 2001). However, when we investigated XPC-deficient cells (that contain normal functional DDB complex) we found no accumulation of RPA in sites of local UV-damage (Figure 8J-L), in accordance with our previous findings that no NER proteins were found at sites of locally induced UV-damage in XP-C cells, including XPA. This observation together with our current and previous observations (56) support the notion that the visible assembly of the NER complex on a DNA lesion strictly depends on functional XPC protein and cannot be bypassed by 'alternative accumulation pathways' mediated by DDB. Importantly, our observations are in contrast with the very recently suggested new order of assembly by Reardon and Sancar (45), who describe a model in which RPA loading precedes XPC.

Discussion

The XPA protein plays an essential role in mammalian NER that until now has largely been assessed using biochemical and genetic means. In this study we have applied different variants of FRAP (29) on living cells stably expressing (at a biological relevant level) functional GFP-XPA. These analyses provide insight into the hitherto unexplored *in vivo* spatio-temporal organization of this central NER factor.
The following observations indicate that the GFP-XPA expressing cells accurately reflect the *in vivo* involvement of XPA in NER: 1) Expression in XPA-deficient cells established that the GFP-XPA protein is fully functional in NER in terms of UV survival and repair synthesis, despite the presence of the GFP tag almost doubling the size of the protein. 2) GFP-XPA is expressed at physiological levels, which is critical when analyzing the biologically active fraction of the protein. 3) The subnuclear distribution is similar to wild type, endogenous XPA (Figure 1 and 2). 4) As discussed below the protein shows a consistent, direct and specific response to NER-type DNA injury. Therefore, we consider this cell line as a *bona fide* tool to study the characteristics of XPA in living cells.

Organization of NER in living cells

Diffusion measurements in living cells indicated that the majority of GFP-XPA molecules are not part of a large, stable pre-assembled NER-complex. Obviously we can not exclude that a small fraction of XPA is incorporated into a larger functional NER (holo)complex. However, it is hard to envisage that such a small amount would be sufficient to account for the observed biological activity that involves a substantial fraction (>30%) of the XPA proteins actually participating in NER (Figure 4). The absence of (significant quantities of) pre-assembled NER holocomplexes containing

XPA (as determined here) in living cells, contrast to earlier biochemical studies in *S. cerevisiae* in which a completely assembled NER-complex was identified (51). It is, however, not excluded that part of the XPA molecules are present in smaller (transient) complexes, as reported previously (3, 15, 22, 57). Several explanations may account for these differences. First, during cell-lysis and extract preparation ionic-strength and local concentrations are different from the *in vivo* situation. In addition competing factors, or natural substrates, such as DNA and/or chromatin, are absent. This will affect (and may even enhance) associations between proteins with an intrinsic affinity for each other, influencing co-purification and immunoprecipitation behavior. Second, many reported interactions between NER factors are based on two-hybrid screens or immobilized factors on column matrices (reviewed by (5, 14)). In both these cases, high local concentrations of one NER factor will artificially shift the association-dissociation equilibrium to the side of binding. Finally, the process of an ordered repair complex assembly in mammalian nuclei (56) might differ from the situation in yeast cells due to differences in genome size and nuclear structure.

Transient immobilization of GFP-XPA in DNA repair

Here we provide evidence that GFP-XPA immobilization is linked to actual repair and involves sequential NER-complex assembly on DNA lesions in living cells. Immobilization of GFP-XPA is likely due to either, direct sequestration to damaged DNA, or entrapment into NER-reaction intermediates. First, free diffusing GFP-XPA became partially immobilized when DNA damage is inflicted by UV-light. Our *in vivo* results are consistent with previously reported binding of XPA to nuclear structures after UV-irradiation as determined by reduced Triton X-100 extractability on fixed cells (52). Second, the UV-induced immobilization is found specifically for NER factors, and is not noted with other proteins, such as transcription activators and proteins implicated in other repair pathways (Houtsmuller et al. 1999, Essers et al. 2002). Third, the fraction of immobilized GFP-XPA appears to depend on the number of lesions induced by UV irradiation. Fourth, we observe a time-dependent reduction of the amount of trapped GFP-XPA after UV-irradiation, with no significant binding 24-h. post UV. This is in agreement with the notion that when DNA repair proceeds, fewer target sites are available for binding GFP-XPA. Fifth, as discussed below XPA immobilization does not occur in an XPC-deficient background. Finally, we visualized a fast recruitment of GFP-XPA to locally UV-damaged areas in nuclei of living cells. FLIP measurements indicated that GFP-XPA molecules reside for approximately 4-6 minutes within these locally damaged sites.

The transient UV-dose dependent immobilization of GFP-tagged ERCC1 in CHO cells and GFP-XPA analyzed here in human cells show comparable kinetics in terms of the maximum fraction of molecules that become immobilized, and the UV dose at which both reach a plateau. The rate at which both proteins accumulate in damaged regions of nuclei (data not shown) and their residence-time at these areas are quite

similar as well. The observed comparable reaction kinetics, on-rate, binding time and substrate (UV-damage) dependency, suggest that both factors enter the NER-complex, stay bound and are subsequently released from the DNA-lesion/NER-complex at about the same time. A marked difference, however, is that in the CHO cell line expressing ERCC1-GFP the total repair time (*i.e.* time after UV-irradiation where no notable immobilization of ERCC1-GFP is observed anymore) is significantly shorter than in the case of GFP-XPA. This difference is likely due to the virtually absence of CPD removal of non-transcribed DNA (GG-NER) in rodent cells, in contrast to the more complete repair of CPDs in human cells (30).

Order of NER-factor assembly

Both UV-dependent immobilization (Figure 7A-B) and accumulation of GFP-XPA at locally UV-damaged nuclei depend on the presence of XPC (Figure 7C-H). These findings provide *in vivo* evidence for previous biochemical studies that indicate that the action of XPC/hHR23B precedes the XPA involvement in NER (6, 49, 50, 60). They are also in line with our immuno-cytochemistry analysis (56) indicating that assembly of various NER factors (XPA, TFIIH, ERCC1/XPF and XPG) at a local damaged area is dependent on XPC.

The major (and perhaps only) difference between TCR and GGR is based on the (initial) recognition step. It is therefore also likely that the factors that are different in the two pathways, *i.e.* XPC/hHR23B (and for some lesions UV-DDB (or XPE) (53)) and the CS factors, respectively for GGR and TCR, are the respective damage sensors for both NER subpathways. In addition, XP group A cells are deficient in both GGR and TCR, whereas XP-C and CS cells are selectively defective in respectively GGR and TCR, argues against an initial damage-sensing role for XPA. Since XPC only accounts for GGR, it is surprising that in XP-C cells, no local accumulation of GFP-XPA is observed whereas these cells have a normal functional TCR. Apparently, the contribution of TCR in these cells is too low to be detected by the currently applied immuno-cytochemistry procedure using 'local' irradiation or FRAP-FIM techniques.

Surprisingly, we also found that RPA is localized to UV-damaged sub-nuclear regions in the absence of XPA, suggesting that at least for loading of RPA into the NER pre-incision complex association to XPA is not required. In addition, to the observed diffusion rates of GFP-XPA it is therefore conceivable that the majority of XPA and RPA are not complexed prior to binding to the NER lesion. In view of the multiple roles of RPA it is also plausible that association of RPA to its interacting partners, here XPA, only occurs after entrance to the specific site of action.

Furthermore, local accumulation of RPA to UV-damaged areas seemed to depend on functional XPC, whereas XPA and XPG appeared to be dispensable for this relocalization. However, it cannot be excluded that the severely truncated XPG protein present in XP-G/CS cells is sufficient to (make it possible to) recruit RPA to the NER complex. These findings raise the question as to what causes the entry of RPA into the

NER complex, i.e. which protein(s) or protein function(s) is (are) necessary and indispensable for RPA to be recruited to the NER complex, and the timing of this entry. Theoretically, given our findings, it is possible that RPA enters the NER complex as the third protein (complex) in order to be incorporated into the NER incision complex, after XPC/hHR23B/centrin2 and TFIIH. Currently however, we cannot exclude that the XPG protein precedes this step.

Advantages of a sequential assembly model for NER

This work combined with our previous study (28), shows that repair factors XPA and ERCC1/XPF participate in NER by a temporary entrapment of free diffusing proteins into NER/DNA-lesion complexes. These results favor an 'assembly on the spot' model for individual NER-factors, rather than a model of preassembled NER complexes. Pre-assembled 'repairosomes' might be considered as efficient 'machines' ready to act on demand. On the other hand, dynamic assembly and disassembly of molecular complexes, allows a more combinatorial flexibility of the reaction constituents that participate in other mechanisms. This is particularly relevant for NER, since almost all NER factors, except XPA, are known to participate also in other DNA-metabolizing processes. TFIIH and CSB are involved in transcription (47, 54), ERCC1/XPF functions also in recombination repair (44), XPG plays an additional role in BER (11, 35) and the single-stranded DNA binding protein hRPA acts in almost every DNA transaction. The latter is perhaps the prototype of a multilateral factor, since this hRPA functions in at least replication, NER, base excision repair (BER) and homologous recombination (33, 38). The different repair proteins (from BER, NER, and double strand break repair) interact with a common small domain of this protein arguing for a competitive association with RPA, rather than divers pre-assembled sub-complexes including RPA specific for each cellular function. A distributive, diffusion driven model has the advantage of permitting efficient usage and quick switching of proteins or protein complexes between distinct nuclear processes. An additional important advantage of sequential assembly of NER factors is that it allows regulation at multiple levels.

The involvement of many NER factors in other processes may imply that the basic rules learned here for NER are also applicable to those other systems, at least when shared NER factors are concerned. Nuclear processes, such as replication and transcription, are scheduled and confined or initiated at specific loci in the genome. These mechanisms may require structural nuclear elements that co-ordinate their specific spatial and temporal action. High local concentrations of specific factors have indeed been found and models have been put forward in whom DNA is pulled through these 'factories' (10). However, such a spatio-temporal regulation might be less beneficial for repair than for replication and transcription, since repair has to act at any location in the genome at any moment in the cell cycle. Free diffusion of repair factors and binding when affinity is increased by a structural change (lesion) seems more

efficient than tracking along relatively crowded DNA stretches or chromatin fibers by large complexes over long distances before they encounter injuries. However, a partial scanning mode of action is not excluded for all NER factors. Lesion detection within TCR is by definition performed by a DNA tracking RNA polymerase II elongation complex. A similar scenario for the initial step in GGR can be envisaged.

Materials and methods

Cell-lines

Cell-lines used in this study were the SV40-immortalized fibroblasts MRC5 (wild type), XP2OS (XP-A), XP12RO (XP-A), and XP20MA (XP-C), these were cultured in $RPMI^+$-Hepes medium, supplemented with antibiotics and 10% fetal calf serum at 37°C, 5% CO_2. Primary fibroblasts used for micro-needle injection, C5RO (wild type) and XP25RO (XP-A), and used for immunofluorescence studies, VH25 (wild type), XP25RO (XP-A), XP21RO (XP-C), XPCS1RO and XPCS1LV (XP-G/CS), XP1DU (XP-D) and XP8BR (XP-D/CS) were cultured in Ham's F10, supplemented with antibiotics and 15% fetal calf serum.

Generation of GFP tagged XPA

GFP-tagged XPA was generated by in-frame ligation of *XPA* cDNA fragment (nt.9 – nt.863) encoding the entire XPA, except for the first three amino acids, into pEGFP-C1 (Clontech). His_9 and HA tags were both added to the N-terminus of eGFP. The His_9-HA encoding sequence was introduced via ligation of a double-stranded oligo-nucleotide at the N-terminus of eGFP after *Nhe*I-*Nco*I digestion (5' CTAGCAAC ATG GGC CAC CAC CAT CAC CAT CAT CAC CAC CAC GGC TAC CCA TAC GAT GTT CCA GAT TAC GCA AGC GC 3') resulting in a fusion gene under the control of a CMV-promoter, encoding a 9-histidine stretch (underlined) - HA tag (bold) - eGFP – XPA hybrid polypeptide.

Microneedle injection and UDS

Microinjection of cDNA into cultured, multi-nucleated primary XP-A (XP25RO) fibroblasts was performed as described previously (55). After injection, cells were incubated for 24-hrs at 37° C in standard medium to allow expression of the cDNA. Fluorescent (GFP) images were obtained with an Olympus IX70 microscope (excitation with 455-490 and long pass emission filter >510 nm). DNA repair capacity was determined by measuring unscheduled DNA synthesis (UDS). Fibroblasts were UV-irradiated with 16 J/m^2 (254 nm), pulse-labeled for 2-hrs using [^{3}H]thymidine (20μCi/ml) and fixed for *in situ* autoradiography. Autoradiographic grains above the nuclei of injected polykaryons were counted and compared with the amount of grains above nuclei of wild type primary fibroblasts (C5RO) treated in parallel.

Transfection of human fibroblasts

XP-A and XP-C deficient human SV40-transformed fibroblasts were transfected with the His_9-HA-eGFP-XPA fusion expression plasmid, containing the *NEO* gene, using SuperFect (Qiagen). Cells were diluted 24-hrs after transfection and medium containing 0.3 mg/ml G418 (Gentamycin) was added. Gentamycin resistant XP-A cells were subsequently selected for UV resistance by irradiating three times (with a one-day interval) with 4 J/m^2 UV-C. Surviving clones were further selected for the presence and proper expression level of nuclear fluorescence by cell sorting, using FACS-Vantage cell sorter (Becton Dickinson). eGFP fluorescence was excited at 488 nm with a 20 mW Ar-laser and eGFP emission was detected using a 525 nm dichroic shortpass mirror and a 530/30 nm bandpass filter.

Immunoblot analysis and UV-survival

Whole-cell extracts (WCE) prepared by sonication were separated on 11% SDS-PAGE and transferred to Nitro-cellulose membranes. Expression of the fusion gene was analyzed by hybridizing the membranes with a polyclonal anti-XPA antibody (Santa-Cruz), followed by a secondary antibody goat anti Rabbit conjugated with Horseradish peroxidase (Biosourche Int.) and detected using enhanced chemoluminescence (ECL; Amersham).
For UV-survival experiments, cells were plated and exposed to different UV doses 2 days after plating. Survival was determined 3 days after UV-irradiation by incubation at 37°C with [^{3}H]thymidine pulse labeling as described elsewhere (23).

Immunofluorescence

Cells were grown on glass coverslips and fixed with 2% paraformaldehyde at 37°C. Coverslips were washed with PBS containing 0.1% TritonX-100, 3 times for 5 minutes and subsequently washed with PBS^+ (PBS containing 0.15% glycine and 0.5% BSA). Cells were incubated at R.T. with primary antibody for 1.5 hrs in a moist chamber. Subsequently, coverslips were 3 times washed with PBS/TritonX-100 and PBS^+, 1 hr. incubated with secondary antibody at R.T. and again 3 times washed in PBS/TritonX-100. Samples were embedded in Vectashield mounting medium (Vector) containing 0.1 mg/ml DAPI (4'-6-diamino-2-phenylindole). Primary antibodies used for immunolabeling were: rabbit polyclonal anti-XPA antibodies (1:1000, kindly provided by Dr. K. Tanaka, Osaka University, Osaka, Japan)), mouse anti-CPD (TDM2) monoclonals (1:2000, gift from Dr. O. Nikaido (Kanazawa University, Kanazawa, Japan)), or mouse monoclonal anti-RPA70 (1:200). Secondary antibodies were: Alexa-594 conjugated goat anti-rabbit antiserum (Molecular Probes) and Cy2- and Cy3-conjugated goat anti-mouse antiserum (Jackson ImmunoResearch Laboratories). Fluorescent microscopy images were obtained with a Leitz Aristoplan microscope equipped with epi-fluorescence optics and a PLANAPO 63x/1.40 oil immersion lens,

or with a Zeiss Axioplan 2 microscope equipped with epi-fluorescence optics. Quantification of fluorescence signal was determined using macro-controlled digital image analysis software (KS-400, Zeiss).

Confocal microscopy

Digital images of GFP-expressing living cells were obtained using a Zeiss LSM 410 microscope equipped with a 60 mW Ar-laser (488nm) and a 40x, 1.3 n.a. oil immersion lens. Images of single nuclei were taken at a sample interval of 100 nm. For analysis of GFP-XPA expression levels confocal planes were scanned at relatively low resolution (625 nm sample interval). A computer controlled acousto-optic transmission filter (AOTF) was used to vary the intensity of the line of an Ar-laser. GFP fluorescence was detected using a dichroic beamsplitter (488/543nm) and an additional 515-540-nm bandpass emission filter.

UV irradiation

For total UV DNA damage induction, cultured cells were rinsed with PBS and UV-irradiated on coverslips with a Philips TUV lamp (254 nm) at a dose rate of ~ 0.8 $J/m^2/s$. In order to apply local UV-damage on living fibroblasts, cells were UV-irradiated through an isopore polycarbonate filter (Millipore) containing pores of 5 μm in diameter as described previously (41, 56). Subsequently, after filter removal cells were either cultured or microscopically examined, or fixed with paraformaldehyde and further processed for immuno-cytochemistry as described above.

Fluorescence recovery after photobleaching (FRAP) and fluorescence loss in photobleaching (FLIP)

FRAP experiments were used to determine the effective diffusion coefficient (D_{eff}) of GFP-labeled XPA (under various experimental conditions) (28, 29). Briefly, a narrow strip spanning the entire nucleus was bleached for 200 ms at high laser intensity (100% of the 488nm line of a 60 mW Ar-laser). Subsequently, the recovery of fluorescence in the strip was monitored at intervals of 100 ms at 5% of the laser intensity applied for bleaching. The effective diffusion coefficient (D_{eff}) was estimated by calculating relative fluorescence intensities given by equation 1: $FR_t = (I_t-I_0)/(I_\infty-I_0)$, where I_∞ is the fluorescence intensity measured after complete recovery, I_0 is the fluorescence intensity immediately after bleaching and I_t is the fluorescence intensity measured at different time points (at 100ms intervals). The resulting curves were fit to a theoretical diffusion model as described (17) (1-D diffusion). In this model, fluorescence recovery (FT) is defined by equation 2: $FT_t = 1 - (w^2 * (w^2 + 4D\pi t)^{-1})^{½}$, where w is the width of the bleached strip, D is the diffusion coefficient and t is time. The optimal fit was found by minimising $\Sigma(FR_t - FT_t)^2$ (ordinary least squares, OLS) for both the diffusion coefficient D and the fluorescence intensity immediately after bleaching I_0. The immobile fraction (FR) was calculated from equation 3: $FR = 1 - (I_\infty-$

$I_0)/(I_{t<0}-I_0)$ - $N_{mobile,bleached}/N_{tot}$, where N represents number of molecules. $I_{t<0}$ and I_0 are the fluorescence intensities immediately before and after bleaching and I_∞ is the fluorescence intensity measured after complete recovery. $N_{mobile,bleached}/N_{tot}$ is subtracted to correct for the fraction of mobile molecules in the relatively small volume of the nucleus that were bleached by the high intensity laser pulse.

The immobilization measurements of GFP-labeled molecules were performed using a modified FRAP assay as described previously, designated FRAP-FIM (for: FRAP for immobilization measurements) (28, 29). With this method quantitative fluorescence over a confocal plane of the entire nucleus is measured. Briefly, a small spot in the center of the nucleus is bleached with low laser intensity for a relatively long period (4 s at relatively low laser intensity (15% of a 60 mW Ar-laser)) with the aim to bleach a significant proportion of the GFP-tagged molecules in the nucleus. Subsequently, after an additional 4 seconds a post-bleach image is made and compared with a pre-bleach image of the same focal plane. The fluorescence intensity ratio (I_{post}/I_{bleach}) was plotted as a function of distance to the laser-bleach spot, generating a "fluorescence ratio profile" (FRP) (Figure 4). Chemically immobilized molecules (paraformaldehyde fixation) (Figure 4A-B) were used as 100% immobilization controls.

FLIP experiments were used to determine the residence time of GFP-tagged XPA molecules in local UV-irradiated areas (see above). For this, a strip at a relatively long distance from the local damage was photobleached for 4 seconds at relatively low laser intensity. Subsequently, fluorescence intensity was monitored in the local damage, in the bleached area and in an undamaged control region at the same distance from the bleached area as the local damage. The difference between fluorescence in the damage and in the control region was plotted and the time at which 10% of the initial difference was reached was taken as estimate for the residence time of individual molecules associated with the local damage.

Acknowledgements

The authors would like to thank Drs. Bert van Zeeland, Leon Mullenders and Roel van Driel for support and stimulating discussion and Drs. K. Tanaka (Osaka, Japan) and O. Nikaido (Kanazawa, Japan) for kindly providing polyclonal XPA antisera and anti-CPD monoclonals respectively. This work was supported by the Netherlands Organization for Scientific Research grants (NWO-ALW) 805-33-441-P, (investment grants NWO GB-MW) 903-68-370 and 901-01-229, The Dutch Cancer Society (KWF) EUR 1999-2004 and by the Louis Jeantet Foundation.

References

1. **Aboussekhra, A., M. Biggerstaff, M. K. K. Shivji, J. A. Vilpo, V. Moncollin, V. N. Podust, M. Protic, U. Hubscher, J.-M. Egly, and R. D. Wood** 1995. *Mammalian DNA nucleotide excision repair reconstituted with purified components*. Cell. 80:859-868.

2. **Araki, M., C. Masutani, M. Takemura, A. Uchida, K. Sugasawa, J. Kondoh, Y. Ohkuma, and F. Hanaoka** 2001. *Centrosome protein centrin 2/caltractin 1 is part of the xeroderma pigmentosum group C complex that initiates global genome nucleotide excision repair* J Biol Chem. 276:18665-72.
3. **Araujo, S. J., E. A. Nigg, and R. D. Wood** 2001. *Strong functional interactions of TFIIH with XPC and XPG in human DNA nucleotide excision repair, without a preassembled repairosome* Molecular and Cellular Biology. 21:2281-2291.
4. **Araujo, S. J., F. Tirode, F. Coin, H. Pospiech, J. E. Syvaoja, M. Stucki, U. Hubscher, J. M. Egly, and R. D. Wood** 2000. *Nucleotide excision repair of DNA with recombinant human proteins: definition of the minimal set of factors, active forms of TFIIH, and modulation by CAK* Genes Dev. **14:349**-359.
5. **Araujo, S. J., and R. D. Wood** 1999. *Protein complexes in nucleotide excision repair* Mutat Res. 435:23-33.
6. **Batty, D., V. Rapic'-Otrin, A. S. Levine, and R. D. Wood** 2000. Stable binding of human XPC complex to irradiated DNA confers strong discrimination for damaged sites J Mol Biol. 300:275-90.
7. **Bootsma, D., K. H. Kraemer, J. E. Cleaver, and J. H. J. Hoeijmakers** 2001. *Nucleotide excision repair syndromes: xeroderma pigmentosum, Cockayne syndrome and trichothiodystrophy.*, p. 677-703. *In* B. Vogelstein, and K. W. Kinzler (eds), The genetic basis of human cancer, 8th ed. McGraw-Hill, New York.
8. **Chu, G., and E. Chang** 1988. *Xeroderma pigmentosum group E cells lack a nuclear factor that binds to damaged DNA* Science. 242:564-567.
9. **Citterio, E., W. Vermeulen, and J. H. J. Hoeijmakers** 2000. *Transcriptional healing* Cell. 101:447-450.
10. **Cook, P. R.** 1999. *The organization of replication and transcription* Science. 284:1790-5.
11. **Cooper, P. K., T. Nouspikel, S. G. Clarkson, and S. A. Leadon** 1997. *Defective transcription-coupled repair of oxidative base damage in Cockayne syndrome patients from XP group G* Science. **275:**990-993.
12. **de Boer, J., and J. H. Hoeijmakers** 2000. *Nucleotide excision repair and human syndromes* Carcinogenesis. 21:453-60.
13. **de Laat, W. L., E. Appeldoorn, K. Sugasawa, E. Weterings, N. G. Jaspers, and J. H. Hoeijmakers** 1998. *DNA-binding polarity of human replication protein A positions nucleases in nucleotide excision repair* Genes Dev. 12:2598-2609.
14. **de Laat, W. L., N. G. Jaspers, and J. H. Hoeijmakers** 1999. *Molecular mechanism of nucleotide excision repair Genes* Dev. 13:768-785.
15. **Drapkin, R., J. T. Reardon, A. Ansari, J. C. Huang, L. Zawel, K. Ahn, A. Sancar, and D. Reinberg** 1994. *Dual role of TFIIH in DNA excision repair and in transcription by RNA polymerase II* Nature. 368:769-772.
16. **Eker, A. P., W. Vermeulen, N. Miura, K. Tanaka, N. G. Jaspers, J. H. Hoeijmakers, and D. Bootsma** 1992. *Xeroderma pigmentosum group A correcting protein from calf thymus* Mutat Res. 274:211-24.
17. **Ellenberg, J., E. D. Siggia, J. E. Moreira, C. L. Smith, J. F. Presley, H. J. Worman, and J. Lippincott-Schwartz** 1997. *Nuclear membrane dynamics and reassembly in living cells: targeting of an inner nuclear membrane protein in interphase and mitosis* J. Cell. Biol. 138:1193-1206.

18. **Essers, J., A. B. Houtsmuller, L. van Veelen, C. Paulusma, A. L. Nigg, A. Pastink, W. Vermeulen, J. H. Hoeijmakers, and R. Kanaar** 2002. *Nuclear dynamics of RAD52 group homologous recombination proteins in response to DNA damage* Embo J. 21:2030-7.
19. **Evans, E., J. G. Moggs, J. R. Hwang, J. M. Egly, and R. D. Wood** 1997. *Mechanism of open complex and dual incision formation by human nucleotide excision repair factors* EMBO J. 16:6559-6573.
20. **Friedberg, E. C., G. C. Walker, and W. Siede** 1995. *DNA repair and mutagenesis.* ASM Press, Washington D.C.
21. **Frit, P., E. Bergmann, and J. M. Egly** 1999. *Transcription factor IIH: a key player in the cellular response to DNA damage* Biochimie. 81:27-38.
22. **Guzder, S. N., P. Sung, L. Prakash, and S. Prakash** 1996. *Nucleotide excision repair in yeast is mediated by sequential assembly of repair factors and not by a pre-assembled repairosome* J Biol Chem. 271:8903-10.
23. **Hamel, B. C., A. Raams, A. R. Schuitema-Dijkstra, P. Simons, I. van der Burgt, N. G. Jaspers, and W. J. Kleijer** 1996. *Xeroderma pigmentosum--Cockayne syndrome complex: a further case* J Med Genet. 33:607-10.
24. **Hanawalt, P., and G. Spivak** 1999. *Transcription-coupled DNA repair. In* Dizdaroglu, and Karakaya (eds), Advances in DNA damage and repair. Kluwer Academic/Plenum Publishers, New York.
25. **He, Z., L. A. Henricksen, M. S. Wold, and C. J. Ingles** 1995. *RPA involvement in the damage-recognition and incision stepa of nucleotide excision repair.* Nature. 374:566-569.
26. **Hoeijmakers, J. H.** 2001. *Genome maintenance mechanisms for preventing cancer* Nature. 411:366-74.
27. **Hoogstraten, D., A. L. Nigg, H. Heath, L. H. F. Mullenders, R. van Driel, J. H. J. Hoeijmakers, W. Vermeulen, and A. B. Houtsmuller** 2002. *Rapid switching of TFIIH between RNA polymerase I and II transcription and DNA repair in vivo.* Mol Cell. 10(5):1163-74.
28. **Houtsmuller, A. B., S. Rademakers, A. L. Nigg, D. Hoogstraten, J. H. J. Hoeijmakers, and W. Vermeulen** 1999. *Action of DNA repair endonuclease ERCC1/XPF in living cells* Science. 284:958-961.
29. **Houtsmuller, A. B., and W. Vermeulen** 2001. *Macromolecular dynamics in living cell nuclei revealed by fluorescence redistribution after photobleaching* Histochem Cell Biol. 115:13-21.
30. **Hwang, B. J., J. M. Ford, P. C. Hanawalt, and G. Chu** 1999. *Expression of the p48 xeroderma pigmentosum gene is p53-dependent and is involved in global genomic repair* Proc. Natl. Acad. Sci. USA. 96:424-428.
31. **Iyer, N., M. S. Reagan, K.-J. Wu, B. Canagarajah, and E. C. Friedberg** 1996. *Interactions involving the human RNA polymerase II transcription/nucleotide excision repair complex TFIIH, the nucleotide excision repair protein XPG, and Cockayne syndrome group B (CSB) protein.* Biochemistry. 35:2157-2167.
32. **Keeney, S., G. J. Chang, and S. Linn** 1993. *Characterization of human DNA damage binding protein implicated in xeroderma pigmentosum E.* The Journal of Biological Chemistry. 268:21293-21300.
33. **Kowalczykowski, S. C.** 2000. *Some assembly required* Nat Struct Biol. 7:1087-9.

34. **Kusumoto, R., C. Masutani, K. Sugasawa, S. Iwai, M. Araki, A. Uchida, T. Mizukoshi, and F. Hanaoka** 2001. *Diversity of the damage recognition step in the global genomic nucleotide excision repair in vitro* Mutat Res. 485:219-27.
35. **Le Page, F., E. E. Kwoh, A. Avrutskaya, A. Gentil, S. A. Leadon, A. Sarasin, and P. K. Cooper** 2000. *Transcription-coupled repair of 8-oxoguanine: requirement for XPG, TFIIH, and CSB and implications for Cockayne syndrome* Cell. 101:159-171.
36. **Lindahl, T., and R. D. Wood** 1999. *Quality control by DNA repair* Science. 286:1897-905.
37. **Matsuda, T., M. Saijo, I. Kuraoka, T. Kobayashi, Y. Nahatssu, A. Nagai, T. Enjoji, C. Masutani, K. Sugasawa, F. Hanaoka, A. Yasui, and K. Tanaka** 1995. *DNA repair protein XPA binds to replication protein A (RPA).* J. Biol. Chem. 270:4152-4157.
38. **Mer, G., A. Bochkarev, R. Gupta, E. Bochkareva, L. Frappier, C. J. Ingles, A. M. Edwards, and W. J. Chazin** 2000. *Structural basis for the recognition of DNA repair proteins UNG2, XPA, and RAD52 by replication factor RPA* Cell. 103:449-56.
39. **Missura, M., T. Buterin, R. Hindges, U. Hubscher, J. Kasparkova, V. Brabec, and H. Naegeli** 2001. *Double-check probing of DNA bending and unwinding by XPA-RPA: an architectural function in DNA repair* Embo J. 20:3554-64.
40. **Miura, N., I. Miyamoto, H. Asahina, I. Satokata, K. Tanaka, and Y. Okada** 1991. *Identification and characterization of XPAC protein, the gene product of the human XPAC (xeroderma pigmentosum group A complementing) gene* Journal of Biological Chemistry. 266:19786-19789.
41. **Mone, M. J., M. Volker, O. Nikaido, L. H. Mullenders, A. A. van Zeeland, P. J. Verschure, E. M. Manders, and R. van Driel** 2001. *Local UV-induced DNA damage in cell nuclei results in local transcription inhibition* EMBO Rep. *2*:1013-1017.
42. **Mu, D., C. H. Park, T. Matsunaga, D. S. Hsu, J. T. Reardon, and A. Sancar** 1995. *Reconstitution of human DNA repair excision nuclease in a highly defined system* J. Biol. Chem. 270:2415-8.
43. **Nakatsu, Y., H. Asahina, E. Citterio, S. Rademakers, W. Vermeulen, S. Kamiuchi, J. P. Yeo, M. C. Khaw, M. Saijo, N. Kodo, T. Matsuda, J. H. Hoeijmakers, and K. Tanaka** 2000. *XAB2, a novel tetratricopeptide repeat protein involved in transcription-coupled DNA repair and transcription* J Biol Chem. 275:34931-7.
44. **Niedernhofer, L. J., J. Essers, G. Weeda, B. Beverloo, J. de Wit, M. Muijtjens, H. Odijk, J. H. Hoeijmakers, and R. Kanaar** 2001. *The structure-specific endonuclease Ercc1-Xpf is required for targeted gene replacement in embryonic stem cells* Embo J. 20:6540-9.
45. **Reardon, J. T., and A. Sancar** 2002. *Molecular anatomy of the human excision nuclease assembled at sites of DNA damage* Mol Cell Biol. 22:5938-45.
46. **Robins, P., C. J. Jones, M. Biggerstaff, T. Lindahl, and R. D. Wood** 1991. *Complementation of DNA repair in xeroderma pigmentosum group A cell extracts by a protein with affinity for damaged DNA* EMBO J. 10:3913-3921.
47. **Schaeffer, L., R. Roy, S. Humbert, V. Moncollin, W. Vermeulen, J. H. J. Hoeijmakers, P. Chambon, and J. Egly** 1993. *DNA repair helicase: a component of BTF2 (TFIIH) basic transcription factor* Science. 260:58-63.
48. **Selby, C. P., and A. Sancar** 1997. *Human transcription-repair coupling factor CSB/ERCC6 is a DNA-stimulated ATPase but is not a helicase and does not disrupt the ternary transcription complex of stalled RNA polymerase II.* J. Biol. Chem. 272:1885-1890.

49. **Sugasawa, K., J. M. Ng, C. Masutani, S. Iwai, P. J. van der Spek, A. P. Eker, F. Hanaoka, D. Bootsma, and J. H. Hoeijmakers** 1998. *Xeroderma pigmentosum group C protein complex is the initiator of global genome nucleotide excision repair* Mol. Cell. 2:223-232.
50. **Sugasawa, K., T. Okamoto, Y. Shimizu, C. Masutani, S. Iwai, and F. Hanaoka** 2001. *A multistep damage recognition mechanism for global genomic nucleotide excision repair* Genes Dev. 15:507-21.
51. **Svejstrup, J. Q., Z. G. Wang, W. J. Feaver, X. H. Wu, D. A. Bushnell, T. F. Donahue, E. C. Friedberg, and R. D. Kornberg** 1995. *Different forms of TFIIH for transcription and DNA repair: holo-TFIIH and a nucleotide excision repairosome* Cell. 80:21-28.
52. **Svetlova, M., A. Nikiforov, L. Solovjeva, N. Pleskach, N. Tomilin, and P. C. Hanawalt** 1999. *Reduced extractability of the XPA DNA repair protein in ultraviolet light-irradiated mammalian cells* FEBS Lett. 463:49-52.
53. **Tang, J. Y., B. J. Hwang, J. M. Ford, P. C. Hanawalt, and G. Chu** 2000. *Xeroderma pigmentosum p48 gene enhances global genomic repair and suppresses UV-induced mutagenesis* Mol Cell. 5:737-44.
54. **Van Gool, A. J., G. T. J. Van der Horst, E. Citterio, and J. H. J. Hoeijmakers** 1997. *Cockayne syndrome: defective repair of transcription?* EMBO J. 16:4155-4162.
55. **Vermeulen, W., A. J. Van Vuuren, M. Chipoulet, L. Schaeffer, E. Appeldoorn, G. Weeda, N. G. Jaspers, A. Priestley, C. F. Arlett, A. R. Lehmann, M. Stefeanini, M. Mezzina, A. Sarasin, D. Bootsma, J.-M. Egly, and J. H. J. Hoeijmakers** 1994. *Three unusual repair deficiencies associated with transcription factor BTF2(TFIIH): evidence for the existence of a transcription syndrome.*, p. 317-329, Cold-Spring-Harb-Symp-Quant-Biol., vol. 59.
56. **Volker, M., M. J. Moné, P. Karmakar, A. Hoffen, W. Schul, W. Vermeulen, J. H. J. Hoeijmakers, R. van Driel, A. A. Zeeland, and L. H. F. Mullenders** 2001. *Sequential Assembly of the Nucleotide Excision Repair Factors In Vivo* Molecular Cell. 8:213-224.
57. **Wakasugi, M., and A. Sancar** 1999. *Order of assembly of human DNA repair excision nuclease* J Biol Chem. 274:18759-68.
58. **Wakasugi, M., M. Shimizu, H. Morioka, S. Linn, O. Nikaido, and T. Matsunaga** 2001. *Damaged DNA-binding protein DDB stimulates the excision of cyclobutane pyrimidine dimers in vitro in concert with XPA and replication protein A* J Biol Chem. 276:15434-40.
59. **Wansink, D. G., W. Schul, I. van der Kraan, B. van Steensel, R. van Driel, and L. de Jong** 1993. *Fluorescent labeling of nascent RNA reveals transcription by RNA polymerase II in domains scattered throughout the nucleus* J. Cell. Biol. 122:283-293.
60. **Yokoi, M., C. Masutani, T. Maekawa, K. Sugasawa, Y. Ohkuma, and F. Hanaoka** 2000. *The xeroderma pigmentosum group C protein complex XPC-HR23B plays an important role in the recruitment of transcription factor IIH to damaged DNA* J Biol Chem. 275:9870-5.

Chapter 10

Concluding remarks and future directions

Concluding remarks and future directions

In the last few decades substantial biochemical data has been published which provide insight into the molecular mechanisms of complex and multistep DNA-transacting processes, such as RNA polymerase II (RNAP2) gene transcription [1], DNA replication and nucleotide excision repair (NER) [2]. Most relevant factors within these pathways have been identified and isolated, and their functions have been characterized. Both NER and RNAP2 transcription initiation have been reconstituted *in vitro* from purified proteins and often non-chromatinized templates. However, many questions are still unanswered, including (i) what is the nuclear organization of these processes in time and space, (ii) do the proteins involved reside in subnuclear structures, (iii) are these proteins immobilized to nuclear structures or moving freely, (iv) are these proteins incorporated into functional repair and transcription 'holo'complex or are they sequentially assembled and, (v) is there crosstalk between these processes and/or with other nuclear mechanisms? These kind of issues can not readily be uncovered biochemically and require an *in vivo* approach. The combined recent developments in several disciplines, have opened an entire new field in biological research. These proceedings include: (i) the possibility to genetically tag cellular proteins with the life cell marker green fluorescence protein (GFP) and its spectral variants, (ii) the technical development to adapt microscopes to be able to culture and simultaneously image fluorescence in life specimen, (iii) development of spectroscopic procedures to study the kinetic behavior of fluorescent molecules in living cells (fluorescence recovery after fluorescence (FRAP), fluorescence resonance energy transfer (FRET), fluorescence correlation spectrometry (FCS) and fluorescence life-time imaging microscopy (FLIM)), (iv) digital image analysis software to quantitatively analyze time-resolved spatial fluorescence distribution, and (v) computer modeling.

10.1 RNAP2 transcription

Biochemical studies revealed that transcription initiation by RNAP2 is an elaborate multistep process that requires as a minimum the five basal transcription factors, TFIIB, D, E, F and H. The mechanisms of assembly of the pre-initiation complex and the ATP-dependent open complex formation have been described extensively (for review see, [3, 4]). In addition, the subsequent steps, promoter escape and early elongation and the novel roles for TFIIE, F and H in these course of actions, are emerging (for review see [1]). Obtained knowledge on the molecular structure, biochemical properties and enzymatic functions have contributed to a tremendous detailed insight into the molecular mechanism of this process. However, fundamental issues as are these proteins incorporated into transcription 'holo'complexes, bound to promoter sites or is transcription rather a stochastic assembly of the various

polypeptides, cannot be addressed in a test-tube. One facet in facilitating the elucidation of the transcription process is to study the dynamic behavior of factors involved in the various events of transcription. In chapter 5, the dynamical interaction of GFP tagged TFIIH with RNAP2 transcription is described. Experiments based on fluorescence recovery after photobleaching (FRAP) revealed a very short association (2-10 s) of TFIIH with the transcription machinery, where the involvement of TFIIH in the transcription process is likely a 'hit and run' type of mechanism. The GFP technology has also been applied to other factors of the RNAP2 transcription machinery, including the RNAP2 itself [5], TBP (TFIID) [6], the nuclear hormone receptor glucocorticoid receptor (GR) and its cofactor GRIP-1 [7, 8]. Photobleaching experiments revealed that all these components are mobile within the nucleus of living cells and appeared to assemble and associate with each other on a promoter to form an initiation complex and consequently, activate transcription. Each of the individual interactions of RNAP2, TFIIH, TBP, GR and GRIP-1 with the promoter are of a transient nature, albeit each with their own duration. Transcription factors involved in early events of transcription, such as GR and TFIIH, were only entrapped in the process for a short period in time. As expected, RNAP2 as the prime elongation factor was involved in transcription for a relative long period. In addition, it was calculated that only a fraction of TFIIH interactions with the RNAP2 transcription machinery led to the successful completion of a transcription initiation event. Very early RNAP2 elongation intermediates were shown to be very unstable and susceptible to transcriptional arrest *in vitro* or abortive transcription resulting in unstable short RNA molecules.

Based on the live cell dynamic studies, it has been suggested that transcription is driven by a series of probabilistic events. This further lead to the speculative model at which transcription factors collide at random with promoters to bind and dissociated immediately. Only occasionally transcription factors collide in the appropriate sequence, where they assemble onto the DNA and form a functional preinitiation complex [5, 9]. After each transcription cycle the transcription machinery is disassembled and all components are released. This transient dynamic interaction of various components during the action of transcription is not unique for RNAP2, since recent live cell dynamic studies also suggested a similar mechanism for RNAP1 transcription [10].

10.2 Nucleotide excision repair

The study on GFP tagged TFIIH, XPC and XPA (Rademakers, *et al.*, in prep), presented in chapters 5, 6, 8 and 9, combined with studies on ERCC1/XPF [11] revealed that these repair factors participate in NER via a transient engagement of free diffusing factors with the pre-incision NER complex. These results suggest an 'on the spot assembly' model for individual NER-factors, rather than a model of large preassembled NER 'repairosomes'. These data are in line with previous immuno-

cytochemistry analysis [12], indicating an ordered assembly of NER factors at damaged sites. In addition, ERCC1/XPF, XPA, TFIIH and XPG (A. Zotter, personal communication) resided in NER complexes bound to lesions for similar times (~4 minutes), suggesting that they form one stable assembly in a relatively short time and that after a relatively long period all factors are simultaneously released, possibly when repair has been completed. The NER binding time of ~4 minutes corresponds very well with the average calculated time of a single NER event [11]. The shorter residence time of XPC in NER suggests that this protein is less stably incorporated into this assembly (chapter 8), but rather dissociates from the NER complex before other factors, such as ERCC1/XPF, XPA and TFIIH, detach from the NER assembly. These *in vivo* observations are in line with studies showing that XPC-hHR23B is not present in the ultimate dual excision complex [13].

To study the association of XPC-hHR23B at a NER assembly in more detail, various *in vivo* and *in vitro* approaches can be employed. It would be of interest to study the localization, behavior and dynamic interaction with a NER site of XPC-hHR23B and another NER factor such as TFIIH, XPA and ERCC1 simultaneously within one nucleus. When two proteins are differentially tagged with either yellow fluorescent protein (YFP) or cyan fluorescent protein (CFP), both tagged proteins can be monitored simultaneously. Another advantage of differentially labeling two proteins is that the interaction between the two hybrid proteins can be monitored, by using a technique called fluorescence resonance energy transfer (FRET). When two CFP and YFP tagged proteins are in close proximity (< 100Å), efficient energy transfer from the excited CFP (donor) to YFP (acceptor) will result in emission of the acceptor. By differentially tagging XPC and for instance TFIIH, XPA or ERCC1 with these donor and acceptor couples, FRET experiments could be performed to identify, monitor and measure possible interactions of e.g. XPC with other NER factors. This might reveal the interaction partners of XPC-hHR23B at a damaged site. A drawback of this technique is that a negative FRET signal does not necessarily mean that the two proteins are not interacting, but could also be due to incorrect orientation of the two chromophores. Also Fluorescence lifetime imaging microscopy (FLIM), where the mean lifetime of a chromophore is measured at different sites in a microscope image, can be used to study possible interactions, where the lifetime of a certain fluorophore (donor) will be influenced by the proximity of an acceptor.

Another option to study the dissociation of XPC-hHR23B from the NER assembly in living cells is to examine the accumulation features of XPC at locally damaged sites, in various NER-deficient backgrounds. If XPC requires the presence of TFIIH, XPA or ERCC1 to detach from the NER complex, the residence time of XPC at NER sites would be altered when these factors are absent. Various strategies can be considered to perform studies on NER-factors in different NER-deficient backgrounds, (i) expression of GFP-tagged NER proteins in mouse embryonic fibroblasts, that have two dysfunctional NER proteins (double knock-out MEFs) and thereby rescuing one function, (ii) introduction of small dsRNA (~20bp) into a cell will cause the

degradation of homologous mRNA molecules, resulting in a knock-out cell line (postreplicational gene-silencing or RNAi), or (iii) generation of a knock-in mouse, that expresses a GFP tagged NER protein under the endogenous promoter and consequently crossing this mouse with the available NER knock-out mice.

In addition, chromatin-immunoprecipitation (ChIP) experiments after a low dose of UV-irradiation using antibodies against XPC, might also reveal which proteins co-localize with XPC at the damaged DNA and can provide information on possible chromatin modifications at or near repair sites. Furthermore, the application of scanning force microscopy (SFM) using reconstituted NER intermediates and defined DNA substrates creates the possibility to look at the architecture of NER complexes at the single molecule level [14]. Recently Segers-Nolten *et al.* (2002) showed that NER can be analyzed on a single molecule level using combined scanning and confocal microscopy and purified GFP fusion proteins on fluorescently labeled DNA, which creates the possibility to study the dynamics of interactions between NER proteins and DNA on single molecules [15].

XPC-hHR23B is an interesting NER factor, since it is the initiator of GG-NER. The mechanism of how the heterodimer travels through the nucleus and how it discriminates lesions from the bulk of the genome is not clear. The experimental work in chapter 8 shows that XPC-GFP had a high probability to be located at DNA and biochemical experiments have previously shown an intrinsically high affinity for DNA with even increased binding at helix distorted regions. The presented FRAP experiments in combination with computer simulation suggested that the protein mobility is slowed down by constantly binding to and dissociating from DNA. However, in our experimental setup a one-dimensional sliding mechanism along the contours of the DNA cannot be excluded. To gain more insight into the diffusion of XPC-hHR23B through the nucleus with regard to DNA, a technique called fluorescence correlation spectroscopy (FCS) could be applied. With FCS the movement of single molecules can be monitored in living cells. If we also fluorescently label the DNA of the XPC-GFP expressing cells, the mobility of the fusion protein with respect to the DNA can be determined.

The above described FRAP experiments, showing the transient assembly of NER factors on damaged DNA, were performed in a NER-proficient wild-type background. Similar to the experiments suggested for GFP tagged XPC, also the behavior of XPA, ERCC1/XPF and TFIIH would be interesting to study in a NER-deficient background. This would mimic the situation in cells derived from XP, CS, XP/CS or TTD patients, where a mutation in a gene coding for one of the NER factors, can cause severe clinical abnormalities. One possibility is to study if an early NER factor, such as XPC, XPG or TFIIH, is assembled into indefinite steady NER complexes when a later component, like XPA or ERCC1/XPF, is missing or whether this interaction is still transient, where the complex is assembled and disassembled repeatedly. As described in chapter 9, GFP-XPA was not captured in a NER complex at a lesion in an XPC deficient cell after damage induction, but rather no effect was seen on the mobility of the fusion protein.

Another interesting extension of these studies is to analyze the behavior of mutant NER proteins, as found in XP, CS, XP/CS or TTD individuals, in the repair process in comparison to the wild-type protein.

10.3 Transcription factor IIH

One of the most intriguing nuclear factors is TFIIH. This multisubunit complex is essential for multiple vital processes, such as RNAP1 and RNAP2 transcription and NER. In order to study the nuclear organization of TFIIH and to understand how TFIIH accomplishes its multiple engagements and to examine the crosstalk between NER, TC-NER and transcription, an *in vivo* approach is required. The GFP and photobleaching technology has shown to add an extra dimension to current biochemical investigations on TFIIH.

Expression of the fully functional GFP tagged TFIIH in living cells, revealed that its localization was distinct from most of the other NER factors (chapter 5). TFIIH appeared homogeneously distributed through the nucleoplasm, with disperse clusters in nucleoli, which co-localized with RNAP1. This observation provided the first *in vivo* evidence for recently published data indicating that TFIIH is involved in RNAP1 transcription [16]. The interaction of TFIIH with RNAP1 transcription revealed to be sensitive to UV-irradiation. Within a few minutes after induction of UV-damage, the nucleolar accumulation of TFIIH was abolished and the complex was homogeneously distributed throughout the entire nucleoplasm. This abolishment of nucleolar accumulation is possibly caused by a transcriptional arrest of RNAP1, and moreover TFIIH is recruited into NER complexes. Four hours after UV-irradiation, TFIIH re-localizes into large bright foci at the periphery of the nucleolus, which co-localize with RNAP1. The nature and significance of these large TFIIH and RNAP1 containing nucleolar foci is not clear, but they might be essential for the recovery of RNAP1 transcription. However, the percentage of cells, which still exhibit TFIIH to be localized in peripheral nucleolar foci rather than disperse nucleolar clusters after repair has been completed, is similar to the percentage of cells not surviving the UV-treatment. In other words, these large perinucleolar accumulations could be an early marker for cells prone to die as a consequence of the large amount of lesions. Time-lapse studies, where with regular intervals high-resolution images are recorded, allows us to follow the localization of TFIIH-GFP in one nucleus in time. This might be of value to study the behavior of TFIIH after various treatments in time. Detailed immuno-cytochemistry analysis in combination with in situ studies to visualize nascent rRNA transcripts could also elucidate the biological importance of these nucleolar structures.

The question to what determines TFIIH to act in transcription versus repair has been a topic of research for a long time. Several models have been put forward to explain the activity of TFIIH, such as; (i) distinct complex composition for each process [17], or (ii) modifications of subunits [18], or (iii) large assemblies capable of

transcription and repair [19, 20]. Our *in vivo* data (chapter 5) support neither of those models, but rather a stochastic principle of participation of TFIIH in RNAP1 and RNAP2 transcription and NER. The complex is ubiquitously present, moves freely by diffusion and by random collisions TFIIH is transiently bound at places with high affinity, such as preinitiation complexes at promoters and precursor NER factors bound to lesions. When no or hardly any damage is present, TFIIH is mainly engaged in RNAP1 and RNAP2 transcription. However, when UV damages are introduced into the DNA, the bound/unbound equilibrium of TFIIH quickly shifts towards TFIIH being bound in NER. Thus, the available affinity sites and the strength of these sites to capture or withdraw TFIIH from the free-diffusing fraction primarily determine the participation of TFIIH in any of the three processes. The observed reaction kinetics of TFIIH favor a model of 'simple' chemical reaction kinetics, as was also determined for various components of the RNAP1 machinery by computational modeling of FRAP data by Dundr *et al.* (2002) [10].

There are several advantages conceivable for a stochastic principle of small freely diffusing constituents as compared to large bulky 'holo-complexes. Free diffusion of small subunits allows them to rapidly exchange between various processes. In addition, it warrants a quick response to changing conditions, such as induction of DNA damage. Moreover, small components have more efficient access to condensed areas in chromatin compared to bulky holo-complexes. Sequential assembly of individual factors also permits regulation of the process and creates possibilities for premature abortion of the reaction. A similar reasoning was forwarded to explain the multiple engagements of the replication protein A (RPA) in the diverse repair processes [21].

Additional GFP based studies on TFIIH might include, the analysis of the effect of mutations in one of the subunits on the dynamic interactions with RNAP1 and RNAP2 transcription and on NER. Numerous mutations are known for the *XPD* gene, that lead to the severe UV-hypersensitive human syndromes xeroderma pigmentosum (XP), XP combined with Cockayne syndrome (XP/CS) or trichothiodystrophy (TTD) and only a few mutations are identified in the *XPB* gene, leading to either XP/CS or TTD. Possible differential behavior of these defective proteins in RNAP1 and RNAP2 transcription and NER might help to provide an explanation for some of the observed clinical features in these patients. As described above, another interesting follow-up of these experiments is to study the behavior of TFIIH in different NER-deficient backgrounds, such XPA or ERCC1. In addition, the dynamical features of TFIIH in a CSB-deficient background, would provide another way to study the reaction kinetics of the GG-NER pathway as described in chapter 6, where TC-NER was excluded by the transcriptional inhibitors DRB and α-amanitin. In addition, the requirement of CSB to recruit TFIIH to the lesion-stalled RNAP2 can be investigated in these cells. The dynamic features of TFIIH after UV damage induction in an XPC-deficient background, enables us to examine the behavior of TFIIH specifically in TC-NER. Furthermore, the involvement of TFIIH in the TC-BER pathway and proposed general TCR pathway could be another

subject of investigation, by inducing BER and transcription-blocking lesions in the genome.

The experiments described in chapter 7, provides for the first time evidence that the ternary cyclin-activating kinase (CAK) sub-complex of TFIIH plays a role in NER *in vivo* but that it is not required for the removal of (6-4)PPs, that are mainly targeted by GG-NER. Additional experiments are in progress to study the requirement of the CAK complex in TC-NER and GG-NER. Moreover, live cell protein dynamics of GFP-tagged CAK components are in progress to reveal mobility parameters of this sub-complex in relation to the entire TFIIH. The dynamic behavior under different experimental conditions may provide clues for the possible differential engagement of CAK in repair and transcription. The possible dissociation of CAK from core-TFIIH at a GG-NER site could be studied *in vivo*, by differentially tagging a core-subunit and a CAK-subunit with either yellow fluorescent protein (YFP) or cyan fluorescent protein (CFP) and using FRET analysis at locally damaged sites. When these studies are performed in either a XPC- or CSB-deficient background, the association of CAK to core TFIIH could be examined in the TC-NER and GG-NER pathway, respectively. By using XPC or CSB antibodies in chromatin immunoprecipitation studies after UV-irradiation, the presence of core TFIIH components and CAK factors could be studied at GG-NER and TC-NER sites, respectively.

The experimental work described in chapter 7, in addition shows that eight hours after local UV-irradiation, XPC and TFIIH are still accumulated at the site of damage in XP-D and XP/CS type of cells, to the same extent as compared to directly after irradiation. It is not clear whether these NER factors are assembled into a steady NER complex, or whether they are binding and dissociating to the assembly repeatedly. In these patient cell lines, the dynamic behavior of TFIIH in NER could be studied by tagging one of the core components with GFP. FRAP analysis would subsequently reveal the residence time of the mutant TFIIH complex at the locally damages sites. In addition, a competition experiment in our immuno-cytochemistry settings on XP-D and XP/CS cells could also indicate the binding state of XPC and TFIIH at NER sites. An overall saturating UV-irradiation followed by local irradiation of nuclei, will not reveal accumulation of XPC and TFIIH at locally damaged sites, when these factors are indefinitely bound to an NER complex. But when these factors are binding and dissociating the NER assembly repeatedly, local accumulation of TFIIH and XPC should be visible.

1. **Dvir, A., J.W. Conaway**, and R.C. Conaway, *Mechanism of transcription initiation and promoter escape by RNA polymerase II.* Curr Opin Genet Dev, 2001. 11(2): p. 209-14.
2. **de Laat, W.L., N.G. Jaspers, and J.H. Hoeijmakers**, *Molecular mechanism of nucleotide excision repair.* Genes Dev., 1999. 13(7): p. 768-785.
3. **Conaway, R.C. and J.W. Conaway**, *General initiation factors for RNA polymerase II.* Annu. Rev. Biochem., 1993. 62: p. 161-190.
4. **Roeder, R.G.**, *The role of general initiation factors in transcription by RNA polymerase II.* Trends Biochem Sci, 1996. 21(9): p. 327-35.

5. **Kimura, H., K. Sugaya, and P.R. Cook**, *The transcription cycle of RNA polymerase II in living cells.* J Cell Biol, 2002. 159(5): p. 777-82.
6. **Chen, D., et al.**, *TBP dynamics in living human cells: constitutive association of TBP with mitotic chromosomes.* Mol Biol Cell, 2002. 13(1): p. 276-84.
7. **McNally, J.G., et al.**, *The glucocorticoid receptor: rapid exchange with regulatory sites in living cells.* Science, 2000. 287(5456): p. 1262-5.
8. **Becker, M., et al.**, *Dynamic behavior of transcription factors on a natural promoter in living cells.* EMBO Rep, 2002. 3(12): p. 1188-94.
9. **Vermeulen, W. and A.B. Houtsmuller**, *The transcription cycle in vivo. A blind watchmaker at work.* Mol Cell, 2002. 10(6): p. 1264-6.
10. **Dundr, M., et al.**, *A kinetic framework for a mammalian RNA polymerase in vivo.* Science, 2002. 298(5598): p. 1623-6.
11. **Houtsmuller, A.B., et al.**, *Action of DNA repair endonuclease ERCC1/XPF in living cells.* Science, 1999. 284(5416): p. 958-961.
12. **Volker, M., et al.**, *Sequential Assembly of the Nucleotide Excision Repair Factors In Vivo.* Molecular Cell, 2001. 8(1): p. 213-224.
13. **Wakasugi, M. and A. Sancar**, *Assembly, subunit composition, and footprint of human DNA repair excision nuclease.* Proc Natl Acad Sci U S A, 1998. 95(12): p. 6669-74.
14. **Janicijevic, A., et al.**, *DNA bending by the human damage recognition complex XPC-HR23B.* DNA Repair (Amst), 2003. 2(3): p. 325-36.
15. **Segers-Nolten, G.M., et al.**, *Scanning confocal fluorescence microscopy for single molecule analysis of nucleotide excision repair complexes.* Nucleic Acids Res, 2002. 30(21): p. 4720-7.
16. **Iben, S., et al.**, *TFIIH Plays an Essential Role in RNA Polymerase I Transcription.* Cell, 2002. 109(3): p. 297-306.
17. **Svejstrup, J.Q., et al.**, *Different forms of TFIIH for transcription and DNA repair: holo-TFIIH and a nucleotide excision repairosome.* Cell, 1995. 80(1): p. 21-28.
18. **van Oosterwijk, M.F., et al.**, *Lack of transcription-coupled repair of acetylaminofluorene DNA adducts in human fibroblasts contrasts their efficient inhibition of transcription.* J. Biol. Chem., 1998. 273(22): p. 13599-13604.
19. **Ossipow, V., et al.**, *A mammalian RNA polymerase II holoenzyme containing all components required for promotor-specific transcription initiation.* Cell, 1995. **83**: p. 137-146.
20. **Maldonado, E., et al.**, *A human RNA polymerase II complex associated with SRB and DNA-repair proteins.* Nature, 1996. 381(6577): p. 86-89.
21. **Kowalczykowski, S.C.**, *Some assembly required.* Nat Struct Biol, 2000. 7(12): p. 1087-9.

Summary

The carrier of our genetic information, DNA, is continuously susceptible to adverse changes, as a consequence of replication errors, intrinsic chemical instability or reactive metabolites. Also environmental factors, such as chemical compounds or the short-wave UV component of sunlight, can cause serious damage to DNA.

In **chapter 2**, the biological relevance of genome stability is described. Damages to the DNA can have detrimental consequence for the cell. Short-term effects include the inhibition of vital nuclear processes such as DNA replication, transcription and cell cycle progression. Whereas the long term effects of persisting lesions are alterations within the genetic code of the DNA. Depending on the location, these mutations can ultimately lead to cancer or inborn diseases. A complex network of genome surveillance processes, including several DNA repair mechanisms has evolved to counteract the harmful effects of DNA injuries. In this chapter the most relevant mammalian DNA repair pathways are summarized. Each repair mechanism removes structurally different types of damages. Nucleotide excision repair is one of the major DNA repair pathways, which eliminates a wide variety of DNA lesions, including the UV-induced photoproducts and bulky DNA adducts. In NER two subpathways exist, global genome NER (GG-NER) and transcription-coupled NER (TC-NER), each with a different damage recognition mode. Within GG-NER a specialized protein complex, XPC-hHR23B, surveys the entire genome for lesions. Damage recognition in TC-NER is performed by RNA polymerase II (RNAP2) when stalled at an injury during elongation and only acts on lesions in the transcribed strand of active genes. NER is a multistep procedure, which requires the concerted action of ~30 polypeptide for the excision of a short segment containing the damaged DNA and the restoration of the genetic information by copying the complementary strand. Briefly, after damage recognition and local unwinding of the DNA duplex, the damaged strand is excised at both sides of the lesion. The remaining gap is re-synthesized by the replication machinery.

DNA repair mechanisms as described in chapter 2 are usually portrayed as separate pathways, however most are linked to other vital nuclear processes, often due to the usage of shared components. For instance, transcription is connected to the transcription-coupled NER pathway. In addition, both transcription and NER require the activity of transcription factor IIH (TFIIH).

The various functions of the TFIIH complex are reviewed in **chapter 3**. The biochemical aspects for the requirement of TFIIH in RNAP1 and RNAP2 transcription, NER, and cell cycle regulation are discussed. TFIIH consists of nine subunits, of which five (XPB, p62, p52, p44 and p34) form a tight "core"-complex. The XPD protein is less tightly associated and serves as a bridge between the core and the ternary cyclin-activating kinase (CAK) complex, consisting of CDK7, MAT1 and cyclinH. The two subunits, XPB and XPD, encompass ATPase/helicase activities, which are required to unwind the DNA helix around the promoter start site or DNA damage. The CDK7 subunit is a kinase, which is able to phosphorylate the C-terminal domain of the large subunit of RNAP2. Mutations in the genes encoding the XPB and XPD subunits are associated with three hereditary syndromes: xeroderma pigmentosum (XP), a combined form of xeroderma pigmentosum and Cockayne syndrome (XP/CS), and a photosensitive variant of

trichothiodystrophy (TTD). The for these disorders characteristic UV-hypersensitivity can easily be explained by a NER defect. However, the developmental and neurological abnormalities seen in XP/CS and TTD patients, are not directly linked to NER-deficiency. The dual involvement of TFIIH in both NER and transcription suggested that a transcriptional defect may underlie some of the clinical symptoms seen in XP/CS and TTD individuals.

Chapter 4 focuses on the nuclear organization in time and space of DNA transacting processes like transcription, replication and various DNA repair pathways. The recently uncovered highly dynamical properties of these processes are discussed and evaluated with respect to the more classical view of static functional compartmentalization. The principal findings described in the experimental part of this thesis are integrated and discussed in this chapter.

In the subsequent **chapters 5 and 6**, experimental work is presented that addresses the dynamical features of TFIIH. The generation of a cell line stably expressing a fully functional TFIIH-green fluorescent protein (GFP) hybrid, allowed the study of nuclear organization and dynamical properties of the TFIIH complex in living cells. A surprising dispersed focal accumulation of TFIIH was observed by live cell confocal microscopy in nucleoli (referred to as NCs) on top of a homogenous distribution throughout the nucleus. These NCs co-localize with RNAP1. The accumulation of TFIIH into NCs appeared sensitive to RNAP1 and RNAP2 inhibition and UV damage. Within a few minutes after UV-irradiation the NCs disappeared, resulting in a homogeneous distribution of TFIIH-GFP. Two to four hours after UV damage irradiation, TFIIH re-localizes into large bright foci at the periphery of nucleoli. This distribution pattern of TFIIH is reminiscent of the localization of the complex after inhibition of RNAP1 transcription. In both instances, TFIIH co-localizes with RNAP1 in these large bright foci, suggesting that these structures are due to the repressed status of the RNAP1. When repair has been completed, TFIIH regains its original distribution pattern.

The nuclear mobility of TFIIH molecules was examined by quantitative photobleaching techniques. TFIIH diffuses through the nucleus with a diffusion rate according to its molecular size, suggesting that this repair/transcription factor is not incorporated into a large repair and/or transcription 'holo'-complex. Alterations in the mobility of TFIIH, after inhibition of transcription and UV damage induction, were used to study the engagement of the complex with transcription and repair processes. TFIIH interacts with both RNAP1 and RNAP2 transcription machineries in a highly dynamic manner. The time of involvement of TFIIH in RNAP1 and RNAP2 transcription is ~25 and ~6 seconds respectively. Whereas, TFIIH when engaged in both TC-NER and GG-NER is bound significantly longer (~4 minutes). In addition, by irradiating a subpart of the nucleus, we were able to show that TFIIH readily switches between transcription and repair sites without large-scale alterations in composition. Our findings support a model where TFIIH is moving freely through the nucleus by passive diffusion and gets assembled into RNAP1, RNAP2 transcription or NER-complexes by random collision, which permits a quick and versatile response to changing conditions.

In **chapter 7**, the presence and/or requirement for CAK within the NER process is investigated in both wild type and TFIIH mutant cell lines. The individual factors required for NER were visualized at the site of DNA damage, by irradiating a subpart of the nucleus. The

CAK components were shown to be present at the site of local damage in wild-type cells and displayed similar accumulation kinetics as core TFIIH factors. The accumulation of CAK was not observed in a CSB-deficient background, suggesting that the complex is not present at the sites of GG-NER. Similar experiments were performed on cells of individuals displaying XP, XP/CS or TTD features, with a mutation in the *XPB* or *XPD* gene. In contrast to cells from XP/CS and XP individuals, where a clear accumulation of CAK components was observed, the complex was not or hardly located at the site of local UV damage in cells from TTD patients. In XP/CS and XP-D cells no repair of the UV-induced (6-4)PPs and CPDs could be observed. Interestingly, TTD cells were able to repair (6-4)PPs, despite the reduced presence of CAK at a NER site. However, CPDs were not or hardly removed in these cells. These data indicate that XP/CS and XP-D individuals have an overall NER defect, whereas TTD individuals might have a TC-NER defect. In addition, the CAK complex does not seem to be required for the removal of (6-4)PP.

Chapter 8 describes the dynamic behavior of XPC in living cells. A cell line stably expressing functional XPC-GFP fusion protein was generated. High resolution confocal microscopy revealed a unique distribution pattern for XPC, not seen for any of the other NER factors. XPC-GFP appeared to be located at DNA, which did not alter upon the induction of UV damage. The nuclear mobility of XPC-GFP was determined by quantitative fluorescence redistribution after photobleaching (FRAP) techniques. XPC-GFP moved through the nucleus a rate slower than predicted by the size of the XPC-GFP/hHR23B heterodimer assuming free diffusion. In addition, the mobility of this hybrid protein was very temperature-sensitive. Together with the localization of XPC-GFP at DNA, this suggests that the protein complex is searching the DNA for lesions by constantly interacting with it, in a temperature-sensitive fashion. Induction of UV damage alters the mobility of XPC-GFP severely, where 40% of all molecules were immobilized at a saturating dose of 16 J/m^2. XPC-GFP was shown to reside at a NER site for ~90 seconds, whereas the average time for one single repair event was calculated to be in the order of ~4 minutes. The latter was also shown to the residence time of other NER factors, including TFIIH, at NER sites. This suggests that XPC is not incorporated into a stable NER assembly on the damaged DNA, but rather that XPC dissociates from this NER complex before repair has been completed and the other components detach from the DNA. In **chapter 9** the *in vivo* involvement of XPA in NER is described. GFP-XPA appeared to diffuse rapidly and freely through the nucleus and upon UV-irradiation a significant fraction was transiently immobilized for ~ 5 minutes. This immobilization was shown to dependent on a functional XPC protein, suggesting that in living cells XPC precedes XPA in the NER reaction. In addition, the loading of RPA is independent of XPA, but dependent of XPC.

Samenvatting

De structuur van DNA, de drager van genetische informatie, wordt continu beschadigd door replicatiefouten of intrinsieke chemische instabiliteiten. Eveneens, kunnen omgevingsfactoren, waaronder chemische verbindingen en UV stralen uit het zonlicht, beschadigingen in het DNA veroorzaken.

In **hoofdstuk 2** wordt het belang van genomische stabiliteit beschreven. Een direct gevolg van DNA schades is onder andere verstoring van essentiële processen zoals replicatie (verdubbeling van DNA), transcriptie (aanmaak van RNA) en progressie van de celcyclus. Op langer termijn veroorzaken DNA beschadigingen veranderingen in de genetische code. Deze mutaties kunnen uiteindelijk leiden tot kanker of erfelijke afwijkingen, afhankelijk van de locatie. Een uitgebreid netwerk van verschillende herstel mechanismen beschermen het genoom tegen de nadelige effecten van DNA schade. Dit hoofdstuk geeft een overzicht van de belangrijke herstel mechanismen in zoogdieren. Elk reparatie mechanisme verwijdert een ander type schade. Één van deze DNA herstel mechanismen is nucleotide excisie reparatie (NER). NER is verantwoordelijk voor de herkenning en verwijdering van een grote verscheidenheid aan DNA beschadigingen, waaronder die door UV-licht veroorzaakt worden. Binnen transcriptie gekoppeld NER (TC-NER) vindt schade herkenning plaats door actieve stremming van transcriberende RNA polymerase II moleculen. In Globaal genoom-NER (GG-NER) worden schades in het gehele genoom herkend door een gespecialiseerd eiwit dimeer, genaamd XPC-hHR23B, terwijl. NER is een multi-enzymatisch proces, dat de samenwerking van ongeveer 30 eiwitten vereist. In opeenvolgende stappen na de schade herkenning wordt vervolgens: de dubbele DNA helix plaatselijk geopend, waarna een kort fragment met de schade wordt verwijderd door specifieke knip-enzymen en het DNA wordt hersteld door de tegenoverliggende onbeschadigde streng te gebruiken als matrijs voor het opvullen van het ontstane gat door de replicatie-mechanismen.

De herstel mechanismen worden gewoonlijk beschreven als afzonderlijke processen, maar de meeste zijn verbonden met andere essentiële nucleaire systemen. Transcriptie is bijvoorbeeld verbonden met het TC-NER herstel mechanisme, waarbij beide processen gebruik maken van het eiwit complex, transcriptie factor IIH (TFIIH).

In **hoofdstuk 3** staan de verschillende functies van TFIIH centraal. De biochemische aspecten van TFIIH's functie in RNA polymerase I en II transcriptie, NER en de celcyclus regulatie worden beschreven. TFIIH bestaat uit negen eiwitcomponenten, waarvan vijf (XPB, p62, p52, p44, en p34) een compacte kern vormen. Het XPD eiwit is minder sterk gebonden en vormt een brug tussen de TFIIH kern en het drieledig cycline-activerend-kinase complex (CAK), bestaande uit CDK7, MAT1 en cycline H. De twee grootste componenten van TFIIH, XPB en XPD, zijn DNA helicases, waarmee de twee DNA strengen ontwonden worden rond promotoren en DNA schades. Het CDK7 eiwit is een kinase, dat het C-terminale deel van het grootste component van de RNA polymerase II kan fosforyleren.
Mutaties in de genen coderend voor de XPB en XPD eiwitten, kunnen leiden tot drie erfelijke ziektes: xeroderma pigmentosum (XP), XP gecombineerd met Cockayne syndroom (XP/CS) en trichothiodystrophy. Patiënten, die lijden aan deze syndromen hebben gemeen dat ze een extreme

overgevoeligheid voor zonlicht hebben. Deze eigenschap kan verklaard worden door een defect in het NER mechanisme. Echter, andere klinische symptomen, zoals neurologische afwijkingen en ontwikkelingsstoornissen voornamelijk manifest bij CS en TTD patiënten, , zijn moeilijker te verklaren door een NER-defect. De tweezijdige betrokkenheid van TFIIH in zowel transcriptie en NER doet vermoeden dat een defect in het transcriptieproces aan de basis van deze symptomen ligt.

Hoofdstuk 4 beschrijft hoe processen, zoals transcriptie, replicatie en DNA herstel mechanismen georganiseerd zijn in de kern van zoogdieren. De onlangs ontdekte, dynamische eigenschappen van deze processen worden besproken ten opzichte van de klassieke kijk op de organisatie van DNA metaboliserende mechanismen. De belangrijke waarnemingen die worden beschreven in het experimentele gedeelte van dit proefschrift zijn opgenomen en worden besproken in dit hoofdstuk.

In de **hoofdstukken 5 en 6** worden de dynamische eigenschappen van TFIIH en zijn organisatie in de kern in levende cellen beschreven. Met behulp van stabiele expressie van een functioneel gemarkeerd TFIIH met het groen fluorescent eiwit (GFP) in humane fibroblasten, was het mogelijk het eiwit complex in levende cellen te bestuderen. Confocale microscopie toonde aan dat TFIIH naast een homogene verdeling, is geconcentreerd in meerdere, kleine foci in de nucleolus, genaamd nucleolaire clusters (NC's). Deze nucleolaire ophopingen van TFIIH bevatten ook de RNA polymerase I en stellen waarschijnlijk transcriptie eenheden voor. Het ophopen van TFIIH in NC's bleek erg gevoelig te zijn voor zowel UV-bestraling als het onderdrukken van RNA polymerase I en II transcriptie door chemische stoffen. Binnen vijf minuten na het bestralen van de cellen met UV-licht, is TFIIH herverdeelt in een homogeen patroon in de kern, waarbij de nucleolaire ophopingen van het complex verdwenen zijn. Twee tot vier uur na bestraling, is TFIIH opnieuw opgehoopt in de nucleolus, maar nu in grote heldere foci aan de periferie van dit kernonderdeel. Deze verdeling van TFIIH doet denken aan het verdelingspatroon van dit complex na transcriptie-onderdrukking van RNA polymerase I. In beide gevallen, bevatten deze grote heldere foci van TFIIH ook RNA polymerase I, wat suggereert dat deze structuren het resultaat zijn van de geremde toestand van deze transcriptie factor. Wanneer het DNA gerepareerd is, krijgt TFIIH zijn oorspronkelijke verdelingspatroon terug.

De mobiliteit van TFIIH moleculen in de kern werd onderzocht door het kwantitatief meten van de redistributie van flourescentie na foto-bleking (fluorescence redistribution after photobleaching, FRAP). TFIIH diffundeert in de kern met een snelheid dat op grond van de grootte van het complex verwacht wordt. Dit betekent dat TFIIH niet in een groter reparatie of transcriptie complex ingelijft is. Veranderingen in de mobiliteit van TFIIH in de kern, na UV bestraling of transcriptie remming, werden gebruikt om de betrokkenheid van dit complex bij de transcriptie- en herstel processen te bestuderen. De interactie van TFIIH met deze processen bleek erg dynamisch te zijn. De tijd die TFIIH verbonden is met RNA polymerase I en II transcriptie is ongeveer 25 en 6 seconden, respectievelijk. Terwijl, TFIIH ongeveer 4 minuten betrokken is bij zowel TC-NER als GG-NER. Bovendien, konden we aantonen dat TFIIH probleemloos uitwisselt tussen transcriptie en herstel locaties in het DNA, zonder grootschalige compositie veranderingen. Onze bevindingen ondersteunen een model waarbij TFIIH zich vrij en

passief door kern beweegt en betrokken raakt in transcriptie of herstel processen door willekeurig te botsen en te binden wanneer het nodig is. Dit garandeert een snelle en veelzijdig respons op veranderingen in de omgeving.

In **hoofdstuk 7** is de aanwezigheid en betrokkenheid van het CAK complex in NER in zowel normale als cellijnen met een mutatie in één van de TFIIH componenten onderzocht. De individuele NER factoren werden zichtbaar gemaakt op het beschadigd DNA, door een deel van de kern te bestralen met UV-licht. De CAK factoren bleken aanwezig te zijn in de lokaal beschadigde gebieden in wild type cellen. Echter, de ophopingen van CAK componenten in UV beschadigde gebieden, waren niet aanwezig in TC-NER deficiënte cellen. Dit suggereert dat het CAK complex niet aanwezig is bij GG-NER substraten in het DNA. Soortgelijke experimenten zijn ook gedaan met cellen van XP, XP/CS en TTD patiënten met een mutatie in het *XPB* of *XPD* gen. In tegenstelling tot XP/CS en XP cellen, waar een duidelijke accumulatie van CAK componenten bij NER plaatsen te zien is, hoopt het complex zich niet of amper op in lokaal beschadigde gebieden in TTD cellen. In XP/CS en XP cellen werden beide UV-licht geïnduceerde beschadigingen, 6-4 fotoprodukten (6-4PP) en cyclobutaan pyrimidine dimeren (CPD), niet verwijderd uit het DNA. De cellen van TTD patiënten, daarentegen, bleken wel de (6-4)PP te repareren, ondanks de afwezigheid of nauwelijks aanwezigheid van het CAK complex in beschadigde gebieden. Dit suggereert dat het CAK complex niet nodig is bij het verwijderen van (6-4)PP uit het DNA.

In **hoofdstuk 8** worden de dynamische eigenschappen van XPC beschreven. Hierbij werd een cellijn gebruikt die een met GFP gemarkeerd XPC eiwit stabiel tot expressie brengt. Confocale microscopie toonde aan dat XPC een uniek distributie patroon vertoonde, dat voor geen van de andere NER factoren gezien is. XPC is met name op plaatsen met hoge DNA concentraties aanwezig, deze verdeling was onveranderlijk na het beschadigen van het DNA met UV-licht. De mobiliteit van XPC moleculen in de kern werd onderzocht door verschillende FRAP technieken. XPC diffundeert langzamer in de kern dan op grond van de grootte van het eiwit dimeer verwacht wordt. Daarnaast, was de mobiliteit van XPC erg temperatuur gevoelig. Tezamen met de lokalisatie van het eiwit, suggereert dit dat XPC zoekt naar DNA beschadigingen door constant (temperatuur-gevoelige) interacties aan te gaan met het DNA. Inductie van UV schade aan het DNA, vertraagde de mobiliteit van XPC uitermate, waarbij 40% van alle molekulen binnen een aantal minuten geïmmobiliseerd waren na een verzadigende dosis van 16 J/m^2. XPC was ongeveer 90 seconden betrokken bij het NER herstel proces, terwijl de berekende tijd voor één enkel herstel gebeurtenis circa 4 minuten is. De andere NER factoren bleken daarentegen allen gedurende 4 minuten gebonden te zijn in het NER proces. Dit suggereert dat XPC niet stabiel wordt geïncorporeerd in het NER incisie complex, maar dat het eiwit de schade verlaat voordat herstel heeft plaats gevonden en ook de andere componenten los komen van het DNA. In **hoofdstuk 9** wordt de betrokkenheid van XPA in NER in levende cellen beschreven. XPA diffundeert snel en vrij door de kern. Na inductie van UV-schades raakt een significante fractie transient geïmmobiliseerd voor een periode van ongeveer 5 minuten. Deze immobilisatie is afhankelijk van een functioneel XPC eiwit, wat suggereert dat XPC XPA voorgaat in de NER reactie. Daarnaast is het laden RPA onafhankelijk van XPA.

Curriculum Vitae

Naam:	Deborah Hoogstraten
Geboren:	5 juni 1972 te Stadskanaal
Juni 1989	Eindexamen HAVO, Winschoter scholen gemeenschap
September 1989- Juni 1993	HLO te Groningen, specialisatie biotechnologie Afstudeer stage op de afdeling Experimentele Hematologie, RUG
Juni 1993- Mei 1996	Doorstroom studie biotechnologie, RUG Stage op de afdeling Moleculaire Microbiologie, RUG Afstudeerstage aan de Max-Planck-Institut für Biochemie, Martinsried bei Munchen, Duitsland
Januari 1997- Juni 1998	Research assistant at the Department of Microbiology, Public Health Research Institute New York, USA
September 1998- December 2002	Promotie onderzoek, afdeling Celbiologie en Genetica, Erasmus Universiteit Rotterdam Promotor: Prof. Dr. J.H.J. Hoeijmakers Co-promotor: Dr. W. Vermeulen
Januari 2003- heden	Post-doc, afdeling, Celbiologie en Genetica, Erasmus MC

List of publications

de Wit H, Hoogstraten D, Halie RM, Vellenga E. (1996) *Interferon-gamma modulates the lipopolysaccharide-induced expression of AP-1 and NF-kappa B at the mRNA and protein level in human monocytes.* Exp Hematol. 24(2):228-35.

Houtsmuller AB, Rademakers S, Nigg AL, Hoogstraten D, Hoeijmakers JH, Vermeulen W. (1999) *Action of DNA repair endonuclease ERCC1/XPF in living cells.* Science. 284(5416):958-61

Mindich L, Qiao X, Qiao J, Onodera S, Romantschuk M, Hoogstraten D. (1999) *Isolation of additional bacteriophages with genomes of segmented double-stranded RNA..* J Bacteriol. 181(15):4505-8

Hoogstraten D, Qiao X, Sun Y, Hu A, Onodera S, Mindich L. (2000) *Characterization of phi8, a bacteriophage containing three double-stranded RNA genomic segments and distantly related to Phi6.* Virology. 272(1):218-24.

Iben S, Tschochner H, Bier M, Hoogstraten D, Hozak P, Egly JM, Grummt I. (2002) *TFIIH plays an essential role in RNA polymerase I transcription.* Cell. 109(3):297-306

Hoogstraten D, Nigg AL, Heath H, Mullenders LH, van Driel R, Hoeijmakers JH, Vermeulen W, Houtsmuller AB. (2002) *Rapid switching of TFIIH between RNA polymerase I and II transcription and DNA repair in vivo.* Mol Cell.10(5):1163-74.

Dankwoord

Eindelijk is het dan zover, de laatste pagina van mijn proefschrift, het dankwoord. Voor mij een gelegenheid om iedereen die op de een of andere manier (wetenschappelijk of persoonlijk) bij de totstandkoming ervan betrokken is geweest te bedanken.
Allereerst wil ik mijn promotor Prof.dr. Jan Hoeijmakers bedanken. Jan, ik wil je bedanken voor je aanstekelijke enthousiasme voor het GFP gebeuren en je kritische blik op het geheel. Mijn grootste dank gaat uit naar mijn copromotor Dr. Wim Vermeulen. Wim, ik heb het zeer gewaardeerd dat je altijd tijd voor mij wist vrij te maken, zeker de afgelopen maanden. Ik heb erg veel van je geleerd. Op deze plaats wil ook mijn tweede begeleider Dr. Adriaan Houtsmuller bedanken. Adriaan, ik zal onze werkbesprekingen nooit vergeten. Ze waren niet alleen zeer leerzaam, maar ook erg vermakelijk. I appreciate the collaboration with Prof.dr. J.M. Egly. Jean-Marc, thank you for introducing me to the *in vitro* world.
Natuurlijk wil ik alle mensen van lab 730, later 1053, bedanken voor alle gezelligheid de afgelopen vierenhalf jaar. Betty en Suzanne, mijn twee paranimfen c.q. jonge moeders. Dankzij jullie voelde ik me direct thuis op het lab. Ik heb jullie vriendschap, binnen en buiten het lab, altijd zeer gewaardeerd. Ik vind het dan ook erg leuk dat jullie mijn paranimfen willen zijn. Vincent, nu mag jij. Ik vond het prettig om een medebleker op het lab te hebben waarmee ik het wel en wee van confocale experimenten mee kon doornemen. Daarnaast vond ik dat weekend in Milaan erg gezellig. Nils, bedankt voor het vele pipetteren de afgelopen paar maanden. Ana, I really liked having you as a labmate. Ook dank aan de labgenoten voor kortere tijd, Ali, Angelika, Ambra, Arjan, Bas, Claire, Francesca, Nancy en Steven.
Jerome, thank you for your hospitality the weeks I was in Strasbourg. I am indebted to you for all your help and the nice experiments.
Alle andere leden van de afdeling celbiologie en genetica bedank ik voor de aangename sfeer op het lab. Anja, bedankt voor de gezelligheid in het kweekhok. Martijn, nogmaals bedankt voor al je hulp en ik vind het fijn dat je het leed van 7 mei met me wilt delen.
Mijn familie wil ik bedanken voor hun steun en interesse in mijn onderzoek. Pap en mam, jullie begrip voor mijn afwezigheid de laatste paar maanden waardeer ik in het bijzonder. Ik houd van jullie. Ook wil ik bij deze mijn schoonfamilie bedanken. Ondanks alle narigheden de laatste maanden, bleven jullie geïnteresseerd in mijn promotieonderzoek. Jan, jij bent mijn steun en toeverlaat en als geen ander weet jij wat deze periode in mijn leven inhoudt. De komende tijd gaan we het lekker rustig aan doen met z'n tweeën.

Bedankt voor alles,
Deborah